

CLASS GUIDELINE

DNVGL-CG-0129

Edition January 2018

Fatigue assessment of ship structures

The content of this service document is the subject of intellectual property rights reserved by DNV GL AS ("DNV GL"). The user accepts that it is prohibited by anyone else but DNV GL and/or its licensees to offer and/or perform classification, certification and/or verification services, including the issuance of certificates and/or declarations of conformity, wholly or partly, on the basis of and/or pursuant to this document whether free of charge or chargeable, without DNV GL's prior written consent. DNV GL is not responsible for the consequences arising from any use of this document by others.

The electronic pdf version of this document, available free of charge
from <http://www.dnvg.com>, is the officially binding version.

FOREWORD

DNV GL class guidelines contain methods, technical requirements, principles and acceptance criteria related to classed objects as referred to from the rules.

© DNV GL AS January 2018

Any comments may be sent by e-mail to rules@dnvgl.com

If any person suffers loss or damage which is proved to have been caused by any negligent act or omission of DNV GL, then DNV GL shall pay compensation to such person for his proved direct loss or damage. However, the compensation shall not exceed an amount equal to ten times the fee charged for the service in question, provided that the maximum compensation shall never exceed USD 2 million.

In this provision "DNV GL" shall mean DNV GL AS, its direct and indirect owners as well as all its affiliates, subsidiaries, directors, officers, employees, agents and any other acting on behalf of DNV GL.

CHANGES – CURRENT

This document supersedes the October 2015 edition of DNVGL-CG-0129.

Changes in this document are highlighted in red colour. However, if the changes involve a whole chapter, section or sub-section, normally only the title will be in red colour.

Changes January 2018, entering into force as from date of publication

Topic	Reference	Description
Update with regard to fatigue	Sec.1 [General]	Many editorial changes have been done to follow style guideline throughout the document.
	Sec.2 Table 2	Replaced edges "broken" with edges "chamfered". "Local" stress has been applied instead of "notch" stress.
	Sec.2 [4.2]	The application of mean stress effect is defined, including an important example where the mean stress effect factor cannot be applied.
	Sec.2 [5.2]	The parameter d , for thickness effect of butt welds and cruciform joints, has been changed.
	Sec.3 [2.3]	Rewritten subsection on environmental factor f_e with reference to DNVGL-RU-SHIP Pt.3 Ch.9 , where it has been introduced.
	Sec.3 [2.4]	Rewritten section on operational factor f_R with reference to DNVGL-RU-SHIP Pt.3 Ch.9 , where it has been introduced, and DNVGL-CG-0130 where it is described in more detail when used in direct hydrodynamic calculations.
	Sec.3 [3.6]	The calculation of predicted fatigue life, T_F , in third option in formula is corrected.
	Sec.3 [4]	The formula for f_N has been corrected and the reference to related S-N curves has been updated.
	Sec.4 [1.4]	It is clarified that main stress components (also in way of transverse bulkheads, see Sec.4 [1.1]) are hull girder loads and local loads unless ship specific requirements or additional class notations require more.
	Sec.4 [6.1]	A new subsection is removing local internal pressure on deck with air pipe ending just above the deck considered.
	Sec.4 [6.2] and Sec.4 [6.3]	The exponent of C has been changed in the formulas.
	Sec.4 [7.5]	The difference between simplified transverse bulkhead configuration and stiffeners with clamped ends has been clarified by describing it in different subsections.
	Sec.4 [7.7]	The formulas for C_a and C_f coefficients for local stiffener bending have been changed.

Topic	Reference	Description
	Sec.6 [1.5]	For hot spot principal stress in "1" direction, the misalignment effect is only related to the axial stress component. It is also clarified that the thickness effect can be different in "1" and "2" direction. Clarification is also made on the mean stress effect. The environmental factor f_e should be included in the calculation of the dynamic stress range in the calculation of the mean stress effect. Missing formula for calculation of mean stress is included for free plate edge. Introduction of coefficients f_s (effect of stress gradient along weld line) and f_{ws} (effect of supporting member) for flange of web stiffened cruciform joints has been made; aligned with CSR.
	Sec.6 [1.6]	Similar change has been made related to misalignment effect and additional factors f_s and f_{ws} as for prescriptive calculations in previous subsection Sec.6 [1.6] .
	Sec.6 [2.6]	Clarification is made on the use of truss and beam elements on free plate edges.
	Sec.6 [3.3]	The procedure for read out stresses based on stress components has been clarified.
	Sec.6 [5.2]	Editorial removal of "hot spot" stress, when referring to stress at shifted position. Clarification of which thickness that should be associated with the shifted position, i.e. the thickness of the plate, at which the hot spot is located. Correction related to extrapolation of stress components rather than principal stresses has been made; aligned with proposed correction of CSR. Clarifying that reduction of bending stress component is not relevant for shear stress component.
	Sec.6 [6.2]	The misalignment effect K_m has been introduced in the hot spot stress formula in order to avoid it being used twice when calculating the fatigue stress range.
	App.A [2.1]	The 0.9 factor times K_b has been removed for rolled angle bar and the use of the 1.12 factor relative to 8mm edge clearance has been clarified.
	App.A Table 1	Reduced stress concentration factor for axial loading in hot spot A, K_a , for tripping brackets with soft nose termination for detail id. 17-20 and 29; aligned with CSR.
	App.A Table 1	Change of arrow for parameter d on detail id. 1, 2 and 25, disregarding the thickness of the transverse frame.
	App.A [3]	Clarification of NDE and 100% NDE for butt welds, where large benefit can potentially be achieved.
	App.C [3]	The table for maximum allowable stress range at 10^{-4} probability level has been removed. Reference tables for S-N curves C1 and B for 10^{-2} and 10^{-8} levels have been added.
	App.D Fig.1 and App.D Fig.2	Editorial; symbols have been corrected.

<i>Topic</i>	<i>Reference</i>	<i>Description</i>
	App.D [1.2]	The formula for double side bending has been corrected with reduced and more realistic height, b , for calculation of bending stress, consistent with relative deflection, by introduction of parameter K_i , z_{b1} and z_{b2} . Introduction of missing formula for coefficient K_{c1} and K_{c2} replacing K_c . Limiting application to side and not bottom.
	App.D [1.3]	Similar changes for static double side bending as for dynamic double side bending in App.D [1.2] have been made.
	App.D [2.1] and App.D [2.2]	Reduction of relative bending stress due to reduced effective height, b , replacing D , and introduction of same K_i (distribution parameter) as for double side bending have been done. The relative deflection criteria have been limited to the side and not bottom.
	App.E [5]	Subsection on screening procedure is removed; specified within ship specific class guidelines when relevant. For CSR ships it is covered in CSR and not generally applicable.
	App.H [4.1]	The formula has been corrected and made more general (2 factor removed).

Editorial corrections

In addition to the above stated changes, editorial corrections may have been made.

CONTENTS

Changes – current.....	3
Section 1 General.....	10
1 Introduction.....	10
2 Symbols and abbreviations.....	10
3 Application.....	19
4 Methods for fatigue assessment.....	20
5 Fatigue approaches.....	22
6 Additional class notations.....	27
7 Definitions.....	28
Section 2 Fatigue capacity.....	31
1 Introduction.....	31
2 S-N curves.....	31
3 Corrosive environment.....	37
4 Mean stress effect.....	37
5 Thickness effect.....	39
6 Material factor.....	44
Section 3 Fatigue strength representation.....	45
1 Introduction.....	45
2 Fatigue stress range.....	45
3 Fatigue damage and fatigue life calculation.....	48
4 Permissible stress range.....	51
5 Permissible stress concentration factor and required FAT class.....	52
Section 4 Prescriptive fatigue strength assessment.....	53
1 Introduction.....	53
2 Wave induced loads.....	56
3 Fatigue stress range.....	56
4 Global hull girder stress.....	59
5 Stress due to bending of PSM.....	60
6 Local stiffener bending stress.....	60
7 Local relative deflection stress.....	64
8 Stress concentration factors.....	68
Section 5 Direct fatigue strength assessment.....	69
1 General.....	69

2 Fatigue strength assessment.....	70
3 Component stochastic analysis.....	70
4 Full stochastic analysis.....	74
Section 6 Finite element analysis.....	77
1 Introduction.....	77
2 Finite element modelling.....	82
3 Derivation of hot spot stress.....	85
4 Procedure for analysis of standard details.....	88
5 Procedure for analysis of hot spot stress of web-stiffened cruciform joints.....	89
6 Procedure for analysis of hot spot stress of simple cruciform joints.....	94
Section 7 Improvement of fatigue life by fabrication.....	96
1 Introduction.....	96
2 Grinding.....	96
Section 8 Detail design standard.....	100
1 Introduction.....	100
2 Detail design standard for longitudinal end connections without top stiffener.....	100
3 Detail design standard for different ship types.....	105
Section 9 References.....	106
1 References.....	106
Appendix A Stress concentration factors and FAT classes.....	108
1 General.....	108
2 Longitudinal end connections.....	109
3 Butt welds.....	124
4 Flange connections.....	129
5 Welded attachments.....	134
6 Simple cruciform joints.....	137
7 Scallops and block joints.....	139
8 Lower hopper knuckles.....	141
9 Pipe connections.....	143
10 Holes with edge reinforcements.....	143
11 Rounded rectangular, elliptical and oval holes.....	164
Appendix B Fatigue capacity.....	169
1 Failure criterion inherent in the S-N curves.....	169

2 Other S-N curves.....	169
3 Effect of fabrication tolerances.....	171
4 Design chart for fillet and partial penetration welds.....	171
Appendix C Fatigue damage calculations and fatigue stress design tables.....	173
1 Weibull long term stress distribution.....	173
2 Fatigue damage accumulation.....	173
3 Maximum allowable stress range.....	176
4 Guidance for omission of fatigue analysis.....	180
Appendix D Prescriptive fatigue strength assessment.....	182
1 Bending stress of PSM.....	182
2 Local relative displacement stress.....	185
3 Local plate bending stress.....	188
Appendix E Finite element analysis.....	190
1 FE modelling.....	190
2 Derivation of hot spot stress.....	190
3 Derivation of stress at read out points.....	192
4 Procedure for analysis of hot spot stress for tuned details.....	196
5 Derivation of stress concentration factors for alternative end connection designs.....	199
6 Verification of analysis methodology.....	200
Appendix F Workmanship and link to analysis procedures.....	201
1 Tolerance limits.....	201
2 Weld profiling by machining and grinding.....	202
3 TIG dressing.....	203
4 Hammer peening.....	203
5 Improvement factors for TIG dressing and Hammer peening.....	203
Appendix G Uncertainties in fatigue life predictions.....	205
1 Introduction.....	205
2 Probability of fatigue failure.....	206
3 Size of defects inherent in S-N data and requirements to non-destructive examination.....	209
Appendix H Low cycle fatigue.....	211
1 General.....	211
2 Number of static design cycles and fraction in different loading conditions.....	212
3 Loading conditions.....	213

4 Simplified calculations of stresses.....	219
5 Fatigue damage calculations for low cycle fatigue.....	224
6 Correction of the damage or stress.....	224
7 Combined fatigue damage due to high and low cycle fatigue.....	225
8 Example of application.....	225
Appendix I Wave induced vibrations for blunt vessels.....	229
1 Introduction.....	229
2 How to include the effect of vibration.....	230
3 Vibration factor for blunt vessels.....	230
4 Application of the vibration factor f_{vib}.....	231
5 Effect of the trade.....	232
6 Model tests procedure.....	233
7 Numerical calculation procedure.....	233
8 Full scale measurements.....	233
Appendix J Considerations of special details.....	234
1 Crane foundations and foundations for heavy top side loads.....	234
Changes – historic.....	235

SECTION 1 GENERAL

1 Introduction

This class guideline (CG) gives a transparent and detailed description of the fatigue assessment methods and procedures to support and satisfy the requirements given in the rules. The rules provides the requirements and is governing compared to this CG.

2 Symbols and abbreviations

2.1 Symbols

The symbols in [Table 1](#) are used in this CG. For symbols not defined in this CG, reference is made to [DNVGL-RU-SHIP Pt.3 Ch.1 Sec.4](#) and [DNVGL-RU-SHIP Pt.3 Ch.9](#).

Table 1 Symbol list

Symbol	Meaning	Unit
α	angular misalignment	degrees
$\alpha_{(j)}$	fraction of time in loading condition j compared to other loading conditions	-
α_h	angle between main plate and attachment plate of hopper knuckles	degrees
β	relative wave heading to bow direction	degrees
β_s	fraction of permissible still water bending moment	-
β_h	hot spot stress correction factor for hopper knuckles	-
γ	incomplete gamma function	-
$\Gamma(\cdot)$ $\Gamma(\cdot; \cdot)$	complete gamma function complementary incomplete gamma function	-
δ	standard deviation of S-N curve	-
$\delta_{Fwd,ik(j)} \delta_{Aft,ik(j)}$	relative deflection between transverse bulkhead and adjacent flange, aft and forward of the transverse bulkhead	mm
$\Delta\sigma$	stress range, S-N curve variable, nominal or local stress range	N/mm ²
$\Delta\sigma_0$	reference (largest) stress range value exceeded once out of n_0 cycles.	N/mm ²
$\Delta\sigma_{BS}$	local stress range at free plate edge from FE analysis or beam theory	N/mm ²
$\Delta\sigma_{FS,(j)}$	fatigue stress range for loading condition j, i.e. the stress range to enter into the S-N curve	N/mm ²
$\Delta\sigma_{FS1} \Delta\sigma_{FS2}$	fatigue stress range for stress normal and parallel to the weld	N/mm ²
$\Delta\sigma_{HS}$	hot spot stress range from FE analysis or beam theory	N/mm ²
$\Delta\sigma_{HS1} \Delta\sigma_{HS2}$	hot spot stress range for stress normal and parallel to the weld	N/mm ²

Symbol	Meaning	Unit
$\Delta\sigma_G$	global stress range	N/mm ²
$\Delta\sigma_L$	local stress range	N/mm ²
$\Delta\sigma_{loc}$	local stress range at based material or free plate edge	N/mm ²
$\Delta\sigma_h$	nominal stress range due to horizontal bending	N/mm ²
$\Delta\sigma_n$	nominal stress range (giving a total damage $D = 1$) at 10^{-2} probability level	N/mm ²
$\Delta\sigma_{perm}$	permissible stress range giving a total damage $D = 1$	N/mm ²
$\Delta\sigma_q$	reference stress range at knuckle of the S-N curve, i.e. at $N = 10^7$ cycles	N/mm ²
$\Delta\sigma_v$	nominal stress range due to vertical bending	N/mm ²
ξ	weibull shape parameter (ξ_i)	-
η	stress magnification factor	-
η	fatigue usage factor	-
$\eta_W, \eta_{Id}, \eta_{bd}$ $\eta_S, \eta_{Is}, \eta_{bs}$	pressure normal coefficients for dynamic sea, liquid and dry bulk cargo pressure. pressure normal coefficients for static sea, liquid and dry bulk cargo pressure.	-
θ	toe angle (relevant for soft toe definition)	degrees
q	angle between local finite element x-direction and local X-direction of principal stress	rad
q	roll angle	rad
μ	parameter in damage calculations accounting for change of inverse slope of S-N curve	-
ν	parameter in the incomplete gamma distribution	-
ν_0	average zero-crossing frequency of the stress (based on the wave bending moment)	Hz
ρ	density of liquid	tons/m ³
σ	stress amplitude; surface principal stress at hot spot	N/mm ²
$\sigma_{bending}$	stress amplitude from the bending component from FE analysis at the element surface	N/mm ²
σ_{comb}	combined transverse stress and shear stress of fillet welds on holes with reinforcements	N/mm ²
σ_d	local relative deflection stress between frames/bulkheads	N/mm ²
σ_{dD}	dynamic wave induced stress amplitude from relative deflection	N/mm ²
$\sigma_{dFwd-a,ik(j)}$ $\sigma_{dFwd-f,ik(j)}$ $\sigma_{dAft-a,ik(j)}$ $\sigma_{dAft-f,ik(j)}$	relative deflection stress at location 'a' or 'f' aft or forward of the transverse bulkhead for load case i, snap shot k and loading condition j	N/mm ²

Symbol	Meaning	Unit
σ_{dh}	stress amplitude due to bending of PSM, e.g. bending of double hull or frame/girder grillage system	N/mm ²
σ_{dhD}	dynamic wave induced stress amplitude from double hull bending	N/mm ²
σ_G	global hull girder stress amplitude	N/mm ²
σ_{GD}	dynamic wave induced stress amplitude from global loads	N/mm ²
σ_L	local stiffener bending stress amplitude	N/mm ²
σ_{LD}	dynamic wave induced stress amplitude from local loads	N/mm ²
σ_{dS}	static stress amplitude from relative deflection	N/mm ²
σ_{dhS}	static stress amplitude from double hull bending	N/mm ²
σ_{GS}	static stress amplitude from global loads	N/mm ²
σ_{HS}	hot spot stress to be used in fatigue assessment by hot spot stress approach	N/mm ²
σ_{LS}	static stress amplitude from local loads	N/mm ²
σ_{loc}	local stress from FE analysis, e.g. base material free plate edge of hatch corner, not excluding welded details	N/mm ²
σ_{mdD}	mean stress of dynamic wave induced stress from relative deflection	N/mm ²
σ_{mdhD}	mean stress of dynamic wave induced stress from bending of PSM	N/mm ²
σ_{mLD}	mean stress of dynamic wave induced stress from local loads	N/mm ²
σ_{mGD}	mean stress of dynamic wave induced stress from global loads	N/mm ²
σ_{mean}	mean stress amplitude	N/mm ²
$\sigma_{mean, i(j)pX}$ $\sigma_{mean, i(j)pY}$	mean stress amplitude corrected to the principal stress direction of the hot spot 'normal' and 'parallel' to the weld	N/mm ²
$\sigma_{membrane}$	stress amplitude from the membrane component from FE analysis at the mid layer of the element	N/mm ²
σ_{max}	maximum stress amplitude (positive is tension)	N/mm ²
σ_{min}	minimum stress amplitude (negative is compression)	N/mm ²
σ_n	nominal stress in N/mm ² to be used in fatigue assessment by nominal stress approach	N/mm ²
σ_{notch}	notch stress, which is implicitly included in the hot spot S-N curves.	N/mm ²
$\sigma_{n,a}$	nominal axial stress at from axial force at the stiffener flange	N/mm ²
$\sigma_{n,b}$	nominal bending stress from unit lateral pressure at the stiffener flange in way of the hot spot	N/mm ²
$\sigma_{HS,a}$	hot spot stress determined at the stiffener flange from the axial load	N/mm ²

Symbol	Meaning	Unit
$\sigma_{HS,b}$	hot spot stress determined fat the stiffener flange from unit pressure	N/mm ²
σ_{shift}	surface principal stress amplitude at shifted position from the FE analysis	N/mm ²
$\sigma_{surface}$	hot spot stress amplitude from the surface component from FE analysis	N/mm ²
σ_p	local plate bending stress amplitude	N/mm ²
σ_{px}	principal stress amplitude in local X-direction	N/mm ²
σ_{py}	principal stress amplitude in local Y-direction	N/mm ²
σ_2	secondary stress amplitude	N/mm ²
σ_3	tertiary stress amplitude produced by bending of plate elements between longitudinal and transverse frames/stiffeners	N/mm ²
τ	shear stress amplitude	N/mm ²
$\Delta\tau$	shear stress range	N/mm ²
ϕ	toe angle	degrees
ω	wave frequency	rad/s
ω_{i-n50}	net sectorial co-ordinate of the point being considered in the transverse cross section	m ²
A_k	stress to load ratio for load component k (unit depends on the load component)	-
b_{eff}	effective flange of attached plating at the end of the span	mm
b_{f-n50}	net flange width	mm
b_f	gross flange breath	mm
b_{g-n50}	eccentricity of the stiffener equal to the distance from the flange edge to the centre line of the web	mm
b_g	gross eccentricity	mm
c	correction coefficient for bending stress when relative deflection is included; c_a or c_f aft and forward of the bulkhead when the spans aft and forward differ	-
d	attachment length, or top stiffener breath	mm
d	weld width of butt welds, attachments and cruciform joints (including attachment thickness)	mm
d	burr grinding depth	mm
D	total predicted fatigue damage	-
$D_{(j)}$	damage during the design fatigue life in loading condition j assuming 100% time at sea	-
$D_{E,(j)}$	annual fatigue damage in air for loading condition j assuming 100% time at sea	-
D_{air}	annual fatigue damage for all loading conditions in air including port time	-
e	eccentric misalignment/deflection	mm

Symbol	Meaning	Unit
f_0	factor for fraction of time at sea	-
f_c	scantling approach factor for correction of stress according to net scantlings approach	-
f_d	reduction factor of wave fatigue moment for location x compared to maximum wave fatigue moment along hull girder	-
f_e	environmental reduction factor	-
$f_{material}$	correction factor for material strength	-
f_{mean}	mean stress reduction factor	-
f_N	correction factor for spectrum shape and number of load cycles	-
f_{NL}	correction factor for the effect on non-linearity	-
f_{thick}	factor for thickness effect ≥ 1	-
f_{vib}	correction factor for wave induced vibration	-
f_w	post-weld treatment factor reducing the fatigue stress	-
$FAT X_{req}$	required FAT class giving a total damage $D = 1$	N/mm^2
$h_{stf}, h_{stf-n50}$	stiffener height and net web height including face plate	mm
h_{toe}	height of bracket toe (relevant for soft nose definition)	mm
h_{HS}	height from plate to hot spot on stiffener without top stiffener on the stiffener flange	mm
h_w	water head equivalent to the pressure at waterline	m
h_{w-n50}	height of stiffener web without flange thickness	mm
h_{HS}	height from plate to hot spot on the stiffener web	mm
$I_{Fwd-n50}$ $I_{Aft-n50}$	area moment of inertia for longitudinal stiffeners aft or forward of the transverse bulkhead	cm^3
K	total stress concentration factor	-
K_a	geometrical stress concentration factor for axial loading	-
K_b	geometrical stress concentration factor for bending loading	-
K_d	factor for relative deflection	-
K_1	S-N curve parameter (mean); "crossing of x-axis", upper part	$(N/mm^2)^m$
K_2	S-N curve parameter (mean minus two standard deviations); "crossing of x-axis" upper part	$(N/mm^2)^m$
K_3	S-N curve parameter (mean minus two standard deviations); "crossing of x-axis" lower part	$(N/mm^2)^m$
K_g	geometric stress concentration factor	-
K_n	stress concentration factor due to shear bending of unsymmetrical stiffeners with lateral loading	-
K_p	stress reduction factor for stress parallel with weld direction	-

Symbol	Meaning	Unit
K_{perm}	permissible stress concentration factor based on the nominal stress approach giving $D = 1$	-
K_{ma}	stress concentration factor due to angular misalignment	-
K_{me}	stress concentration factor due to eccentric misalignment (normally plate connections)	-
K_m	stress concentration factor due to misalignment	-
K_w	weld shape factor normally taken as 1.5 and included in the hot spot S-N curve	-
ℓ_{Fwd}, ℓ_{Aft}	stiffener span aft and forward of the transverse bulkhead	m
$\ell_{bdg}\ell$	effective bending span of stiffener	m
$\log()$	10th logarithm	
$\ln()$	natural logarithm	
m	S-N curve parameter for inverse slope	-
Δm	S-N curve parameter; change of inverse slope for lower part of two slope S-N curve compared to upper part	-
m_{0inj}	zero spectral moment of stress response in short term condition (i,n) and loading condition j	N/mm ²
$M_{wvLC,ik}$	vertical wave bending moment for the load case i and snap shot k ($k = 1,2$)	kNm
$M_{wh-LC,ik}$	horizontal wave bending moment for the load case i and snap shot k ($k = 1,2$)	kNm
$M_{\sigma-wt-LC,ik}$	dynamic bi-moment related to warping stress for the load case i and snap shot k ($k = 1,2$)	kNm ²
M_{sw}	permissible still water bending moment	kNm
n	exponent in calculation of the thickness effect	-
n	number of load cycles at a given probability of exceedance	-
n	number of load components	-
n_0	total number of cycles corresponding to the reference stress range level $\Delta\sigma_0$	-
n_i	number of load cycles in stress range block i	-
n_{LC}	number of applicable loading conditions	-
n_{tot}	total number of stress range blocks i	-
N_D	number of stress cycles per year	-
N_R	average number of cycles between each exceedance at a given probability of exceedance, e.g. $N_R = 100$ for 10^{-2} probability of exceedance	-
N_i	number of cycles to failure in stress range block i according to the S-N curve	-
N	number of cycles to failure according to the S-N curve	-
$P_{bd,ik(j)}$	dynamic dry bulk cargo pressure for load case i, snap shot k and loading condition j	kN/m ²
$P_{bs,(j)}$	static dry bulk cargo pressure for loading condition j	kN/m ²

Symbol	Meaning	Unit
$P_{ld,ik(j)}$	dynamic liquid tank pressure for load case i, snap shot k and loading condition j	kN/m ²
$P_{ls,(j)}$	static liquid tank pressure for loading condition j	kN/m ²
$P_{S,(j)}$	static sea pressure for loading condition j	kN/m ²
P_w	dynamic wave pressure	kN/m ²
$P_{w,WL}$	dynamic wave pressure at water line	kN/m ²
$P_{w,ik(j)}$	dynamic wave pressure for load case i, snap shot k and loading condition j	kN/m ²
$P_{w,sz}$	dynamic wave pressure in the splash zone	kN/m ²
q	weibull scale parameter	N/mm ²
$Q(\Delta\sigma)$	probability level for exceedance of stress range $\Delta\sigma$	-
r_p	splash zone correction factor	-
r_{inj}	relative number of stress cycles in short term condition (i,n) for loading condition j	-
R	radius of free edge of rounded bracket	mm
R_{eH}	yield stress	N/mm ²
Ra	surface roughness	µm
r	radius of burr grinding disk	mm
t	thickness; either net thickness (t_{n50}) or gross thickness (t_{gr})	mm
t_a	thickness of transverse attachment	mm
t_d	doubling plate thickness	mm
t_{eff}	effective thickness for butt welds, attachments and cruciform joints	mm
t_{1-n50}	net thickness of main plate	mm
t_{2-n50}	net thickness of attachment plate	mm
t_{3-n50}	net thickness of supporting girder/frame	mm
t_{p-n50}	plate thickness	mm
t_{f-n50}	flange net thickness	mm
t_{f-gr}	flange gross thickness	mm
t_{gr}	gross thickness	mm
t_{w-n50}	net web thickness	mm
t_{w-gr}	gross web thickness	mm
t_{n50}	net thickness for fatigue assessment with half corrosion addition deducted	mm
t_{n25}	net thickness with 25% corrosion addition deducted	mm
t_{bkt-gr}	gross thickness of bracket	mm
T_c	time in corrosive environment during the design fatigue life	years

<i>Symbol</i>	<i>Meaning</i>	<i>Unit</i>
T_{C25}	time in corrosive environment during the design life	years
T_D	design life = 25 years	years
T_{DF}	design fatigue life to be specified in the design brief	years
T_{DF-C}	corrected design fatigue life converting time in corrosive environment to time in air	years
T_F	predicted fatigue life	years
T_{LC}	draft of actual loading condition	m
V	vessel speed at 15% sea margin, 85% MCR and design draft	knots
V_d	vessel contract speed at y% sea margin, x% MCR and design draft	knots
W	width of groove	mm
X_{eFwd} X_{eAft}	distance from closest end of stiffener span to hot spot; forward and aft of the transverse bulkhead	m
X_{wt}	external fillet weld length	mm
x	longitudinal coordinate in the ship's coordinate system at the load calculation point; positive forward	m
x_s	longitudinal distance from liquid surface centre to load point	m
x_{shift}	shifted distance from intersection point to read out point	mm
X	stress at 2 000 000 cycles of the FAT class S-N curve	N/mm ²
y	transverse coordinate in the ship's coordinate system at the load calculation point; positive to port side	m
y_s	transverse distance from liquid surface centre to load point	m
z	vertical coordinate value in the ship's coordinate system at the load calculation point relative to base line; positive upwards	m
z_s	vertical distance from liquid surface centre to load point	m
$Z_{eff-n50}$ $Z_{Aft-n50}$ $Z_{Fwd-n50}$	net section modulus of stiffener based on effective flange (or hot spot at stiffener web in case of no top stiffener); aft or forward of the transverse bulkhead	cm ³
Z_{n50}	net section modulus of stiffener based on attachment plate with breadth equal to the stiffener spacing	mm
(i)	suffix which denotes dynamic load case HSM, FSM, BSR-P, BSR-S, BSP-P, BSP-S, OST-P or OST-S specified in the rules DNVGL-RU-SHIP Pt.3 Ch.4 . 'i1' denotes dynamic load case (snap shot) HSM-1, FSM-1, BSR-1P, BSR-1S, BSP-1P, BSP-1S, OST-1P or OST-1S. 'i2' denotes dynamic load case (snap shot) HSM-2, FSM-2, BSR-2P, BSR-2S, BSP-2P, BSP-2S, OST-2P or OST-2S.	
(j)	suffix which denotes loading condition relevant according to the rules	

2.2 Abbreviations

The abbreviations in [Table 2](#) is used in this class guideline.

Table 2 Abbreviation list

FE	Finite element
FEA	Finite element analysis
FEM	Finite element model
CG	Class guideline
RP	Recommended practice
CSR	Common structural rules
COG	Centre of gravity
EDW	Equivalent design wave
LCF	Low cycle fatigue (implying frequencies from changes in the loading conditions)
HCF	High cycle fatigue (implying wave frequencies)
$H(\omega, \beta)$	Transfer function
LF	Low frequency (implying slow drift forces or changes to loading conditions)
WF	Wave frequency
HF	High frequency (implying frequencies from vibration)
NA	North atlantic
WW	World wide
PSM	Primary supporting member, e.g. frames, girders, stringers and floors
RAO	Response amplitude operator
TRF	Transfer function
STR	Short term response
LTR	Long term response
A-E	Normal strength (mild) steel
A-E32/36	High tensile steel with yield stress of 315/355 N/mm ²
VBM	Vertical bending moment
HBM	Horizontal bending moment
VSF	Vertical shear force
HSF	Horizontal shear force
AF	Axial force
NDE	Non-destructive examination

2.3 Coordinate system and sign conventions

The origin of the “right hand” coordinate system has co-ordinates (L aft of the foremost end, centre line, base line), see [Figure 1](#). x , y and z are longitudinal, transverse and vertical distance from origin to the load point of the considered structural member. A similar coordinate system is given in the rules to define positive motions, relevant to define inertia loads or internal pressure loads, but the origin is defined at COG instead. Positive global hull girder loads is also defined in the rules and could refer to origin located at the neutral axis. The software may refer to the origin as located at FE minus the rule length. Care should be used when estimating the fatigue stress based on these different definitions.

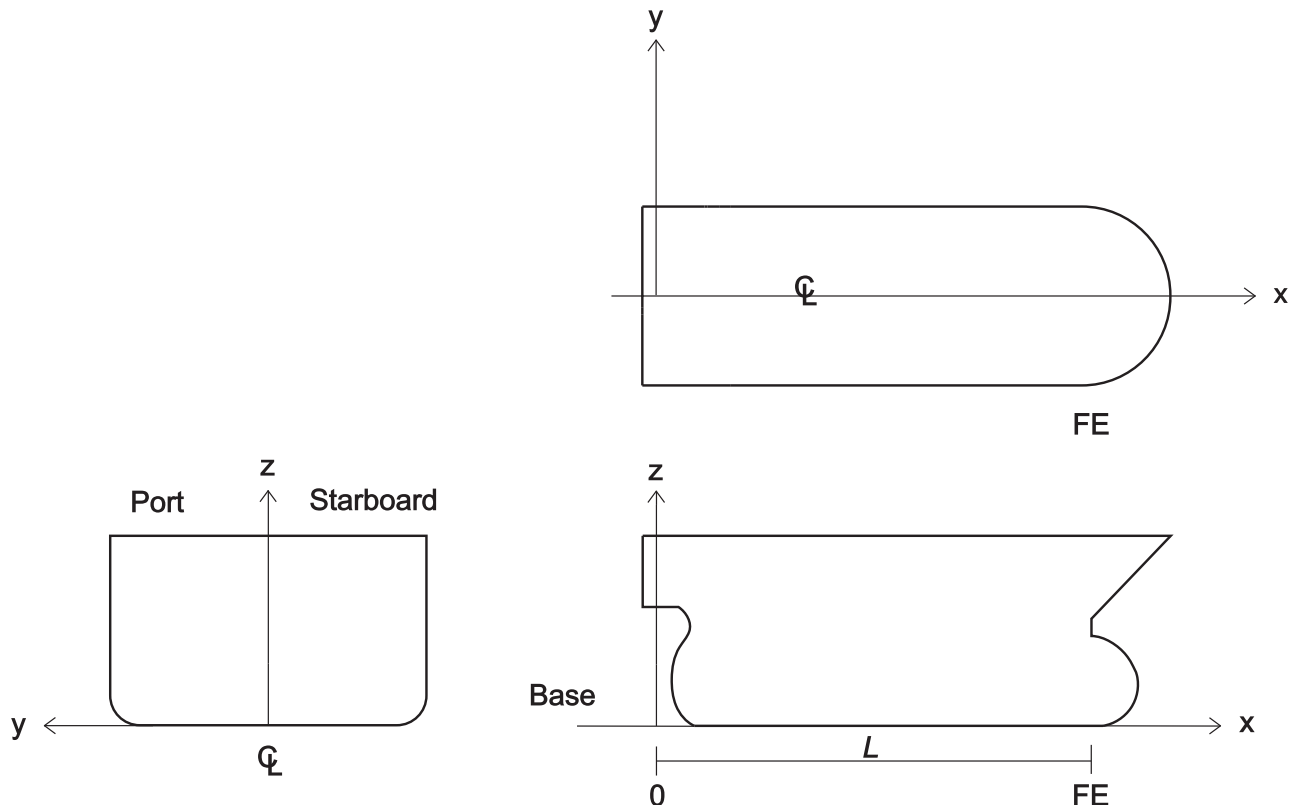


Figure 1 Coordinate system

Tension is defined as positive stress and compression as negative stress, e.g. the hogging wave bending moment is defined as positive, which gives tension in deck which is consistent with positive z at a hot spot above the neutral axis.

3 Application

3.1 General

This CG includes procedures for evaluation of fatigue strength based on cyclic stresses from wave loads and ship motions for the following, but not limited to:

- steel ship structures

- foundations welded to hull structures
- any other areas designated as primary structures
- connections in way of attachments and outfitting details welded to primary ship structures, such as doubling plates.

This CG may be adapted for modification of existing ship structures, subject to the limitations imposed by the original material and fabrication techniques.

This CG is valid for C-Mn steels, duplex and super duplex steels and austenitic steels with yield stress less than 500 N/mm².

Fatigue capacity for aluminium is not included, but reference is given to IIW, ref [9.10].

3.2 Calculated and observed fatigue strength

Real fatigue performance may differ from design calculations due to influence from important parameters like workmanship related to fabrication, corrosion protection, maintenance and the actual encountered fatigue loading. To achieve a good correlation between calculated and the actual fatigue strength, the assumptions in the calculations need to reflect the expected conditions.

3.3 Vibrations

The procedures do not take into account the effect of wave induced hull girder vibrations. Guidance on how to take into account the fatigue effect of wave induced vibrations for full body vessels (tankers, bulk carriers and ore carriers) is presented in App.I and for container ships in DNVGL-CG-0153, *Fatigue and Ultimate Strength Assessment of Container Ships Including Whipping and Springing*. Wave induced vibrations may contribute to fatigue damage also on other ship types.

The procedures do not include methods for other vibratory effects such as engine or propeller induced vibrations.

3.4 Low cycle fatigue

The procedures do not take into account the effect of low cycle fatigue. Low cycle fatigue, e.g. as occurring during the loading-unloading cycles or during high utilisation of crane capacity during operation, is presented in App.H.

4 Methods for fatigue assessment

4.1 Stress types used for fatigue assessment

Depending on the stress calculation method and the model representing the ship structure, the fatigue assessment may be done for nominal stresses, hot spot stresses, or local stresses at free plate edge. Fatigue life based on nominal and local stresses can be assessed from nominal stress S-N curves (FAT classes). Hot spot stresses can be calculated based on direct calculations or based on nominal stress times tabulated stress concentration factors (K). The fatigue assessment in the two latter cases should be done using hotspot stress S-N curves.

4.2 Methods for stress calculation

The long term stress range distribution is fundamental for comparing the fatigue loading with the fatigue capacity, represented by the S-N curve. This CG outlines three methods for stress range calculation:

- 1) A rule load assessment of the long-term stress range distribution, represented by a dynamic stress range at a specific probability level and a straight line spectrum.

- 2) A direct design wave approach calculated for the ship to represent the wave loading and use of a straight line spectrum.
- 3) A spectral method for calculation of the long-term dynamic stress range distribution considering the wave.

In the first method, the loads are based on the equivalent design waves, EDW, prescribed by the rules and applied to beam or FE models. The load components are combined by prescriptive formulations.

In the second method, ship specific design waves are established to represent the loading from the rules. The design waves may be applied to beam models and various types of finite element models. The load components are combined considering phase relations.

In the third method the long-term stress range distribution is calculated based on directly calculated hydrodynamic loads for a specific ship and specific wave scatter diagram. The loads may be applied to beam models and various types of finite element models. The load components are combined accurately considering the phase relations.

The different methods are illustrated in [Figure 2](#).

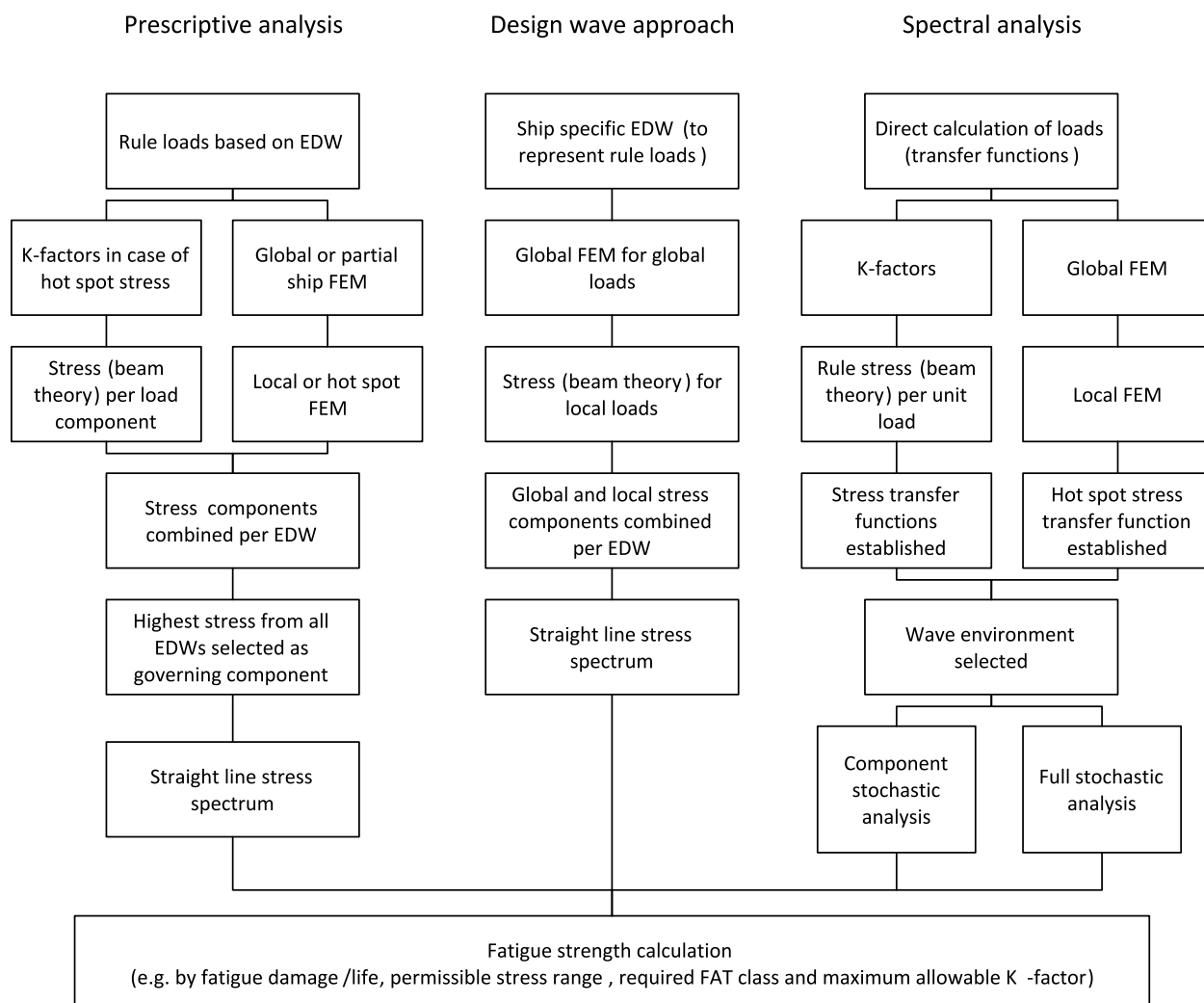


Figure 2 Flow diagram over possible fatigue analysis procedures

4.3 Selection of prescriptive or direct methods for calculation of stresses

Methods to be used for the standard ship types are given by the rules.

Refined analysis may be applied based on:

- experience with the methods applied to similar structural details
- experience of cracks on similar details
- consequences of a fatigue damage.

In general, the prescriptive method for fatigue assessment gives a good representation of the fatigue strength. The reliability of the calculated fatigue lives is, however, assumed to be improved by refined design analysis.

5 Fatigue approaches

5.1 General

Different approaches are used depending on efficiency and applicability. The following approaches can be applied for welded joints:

- nominal stress S-N curves referred to as FAT classes in [Sec.2 \[2\]](#)
- hot spot stress S-N curve as described in [Sec.2 \[2\]](#)
- weld notch stress S-N curve, which is not used in this CG, reference is made to [DNVGL-RP-C203](#).

For base material (free plate edges) the following approach is applicable:

- Base material S-N curves for local stress at free plate edge depending on the surface conditions, as described in [Sec.2 \[2\]](#).

Nominal stress, [Figure 4](#), can be derived by beam theory using sectional forces and moments or from coarse FE models. In a simple plate specimen with an attachment as shown in [Figure 3](#) the nominal stress is the membrane stress. An example of fatigue design using this procedure could be the transverse butt welds in a deck.

Hot spot stress, [Figure 5](#), is the structural stress, which in addition to the nominal stress, also contains the part of the stress increase caused by structural discontinuities and presence of attachments. The weld notch stress due to the local weld geometry is excluded from the stress calculation as it is accounted for in the corresponding hot spot S-N curve.

The weld notch stress, [Figure 5](#), is defined as the total stress resulting from the geometry of the detail and the non-linear stress field due to the notch at the weld toe. The notch stress approach is also applicable to the weld root. The local stress at free plate edge, [Figure 4](#), is defined as the stress resulting from the geometry of the detail at the free plate edge, such as a cut-out or hatch corner. The local stress needs to be assessed with finite element analysis for more complex geometries. The selection of S-N curve may depend on the amount and type of inspection during fabrication. The size of defects inherent the S-N data are described in [App.G](#).

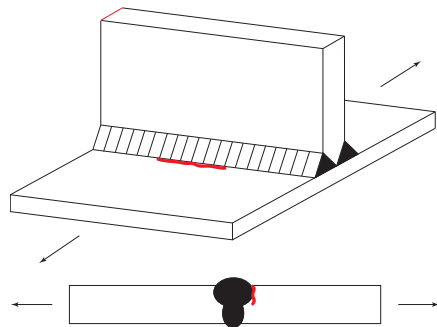
It should be noted that in welded joints, there may be several locations at which fatigue cracks can develop, e.g. at the weld toes, at the weld roots and in the weld itself. Each potential location may need to be considered separately.

5.2 Crack failure modes

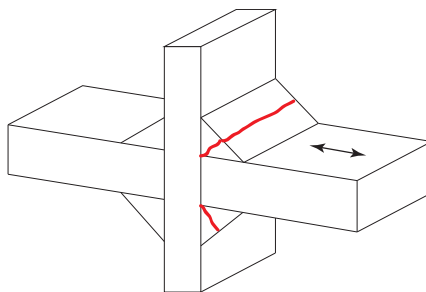
The following fatigue cracking failure modes are considered, see also [Figure 3](#):

- *Weld toe cracking into the base material*, see [Figure 3](#) a) In welded structures fatigue cracking from weld toes into the base material is a frequent failure mode. The fatigue crack is initiated at small defects or undercuts at the weld toe where the stress is highest due to the weld notch geometry.

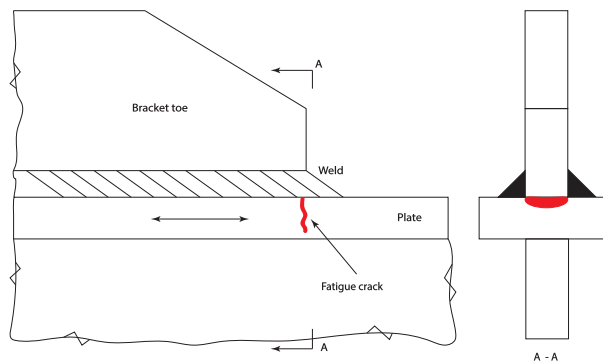
- *Weld root cracking through the fillet weld*, see [Figure 3 b\)](#) Fatigue cracking from root of fillet welds with crack growth through the weld is a failure mode that can lead to significant consequences. Use of fillet welds should be avoided in highly stressed cruciform joints. Non-destructive examination (NDE) is less reliable in this type of connection compared with a full penetration weld as crack propagation from the root is difficult detect before the crack reach the surface. To avoid root failure a sufficient weld throat thickness or partial/full penetration weld is needed, see also [Figure 2](#) and [Figure 3](#).
- *Weld root cracking into the section under the weld*, see [Figure 3 c\)](#) Fatigue crack growth from the weld root into the section under the weld has been experienced. The number of cycles until failure for this failure mode may be of similar magnitude as fatigue failure from the weld toe. However, it is difficult to improve the fatigue strength except by using alternative types of welds locally, e.g. improvement of the weld toe may make the root become the critical location, and improvement for the root becomes necessary. This can be obtained by partial or full penetration weld instead of fillet weld close to the termination of the weld connection.
- *Crack growth from a surface irregularity, notch or thermal cutted edge into the base material*, see [Figure 3 d\)](#) Fatigue cracking in the base material is a failure mode that is relevant in areas with high stress range. Then the fatigue cracks often initiate from notches or grooves in the components or from small surface defects/irregularities. Examples of such details of concern are cut-outs and hatch corners.



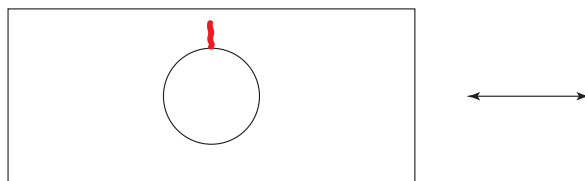
a) Fatigue crack growth from the weld toe into the base material



b) Fatigue crack growth from the weld root through the fillet weld



c) Fatigue crack growth from the weld root into the section under the weld



d) Fatigue crack growth from a surface irregularity or notch into the base material

Figure 3 Failure modes

5.3 Assessment using local and nominal stress approach

In cases where nominal stresses are well defined, the nominal stress approach can be applied using related S-N curves. The joint classification and corresponding FAT classes takes into account the local stress concentrations created by the joints themselves and by the weld profile. The design stress is the nominal stress, σ_n , which is acting adjacent to the weld under consideration. However, if the joint is situated in a region of gross stress concentration, K_g , resulting from the geometry of the structure, this need to be taken into account as illustrated in [Figure 4](#) and derived as:

$$\sigma_{loc} = K_g \cdot \sigma_n$$

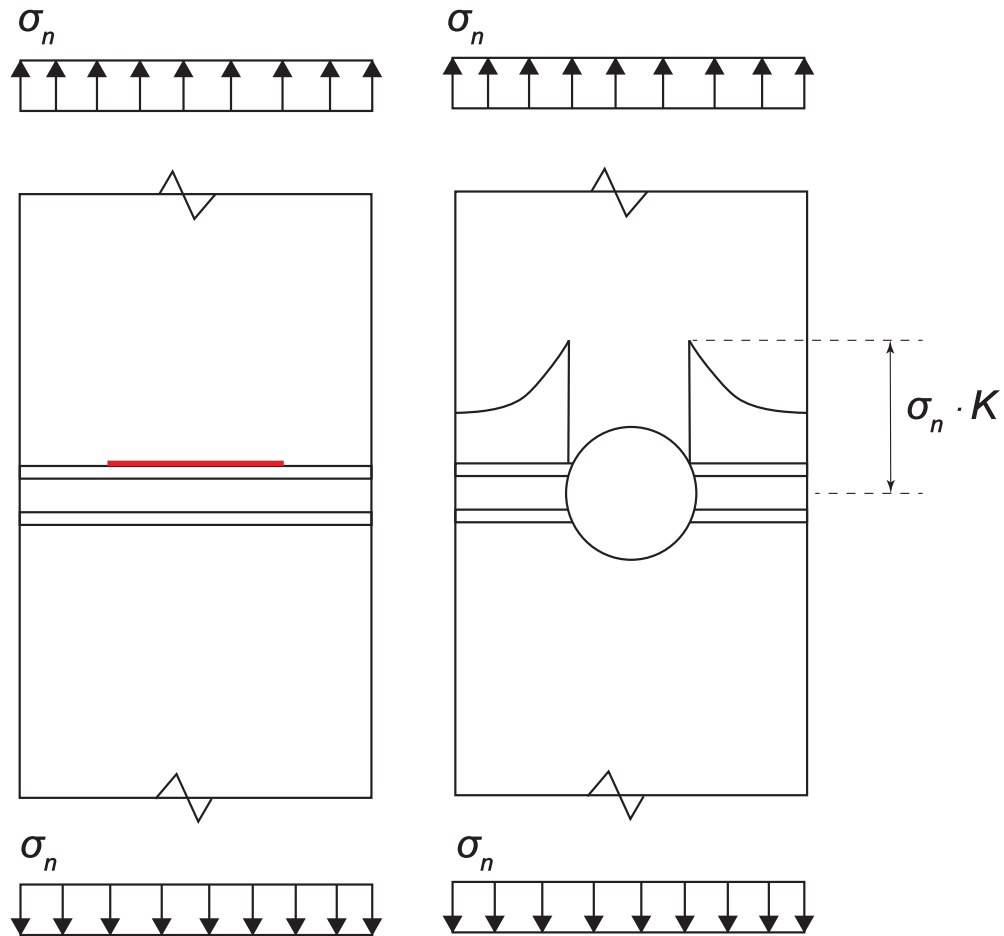


Figure 4 Nominal stress, σ_n , and local stress, σ_{loc}

5.4 Assessment using hot spot stress approach

The relevant hot spot stress in the parent material at the weld toe is the range of maximum principal stress adjacent to the potential crack location using stress concentration due to the geometry of the structure. As an example, for the welded connection shown in [Figure 5](#), the relevant stress is the hot spot stress, σ_{hs} . For

the weld shown in [Figure 3](#), the stress concentration factors need to include both the local geometry of the transverse attachment and the hole.

For details, e.g. longitudinal end connections, or for other details where the stress concentration factor depends on the load component or where there are more than one hot spot, it is recommended to use the hot spot stress approach. The hot spot stress is then established by the following relation between nominal stress and hot spot stress:

$$\sigma_{HS} = K \cdot \sigma_n$$

where K is the structural stress concentration factor, which can be tabulated for standard details and load components. Hot spot stress may also be calculated by use of local FEA.

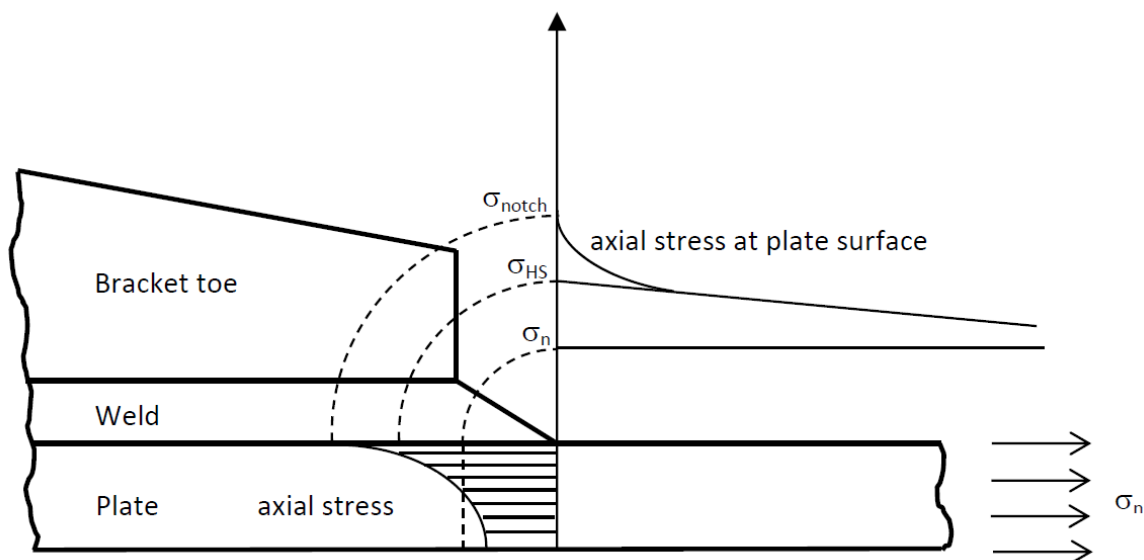


Figure 5 Hot spot stress, σ_{HS} , and notch stress, σ_{notch}

5.5 Stress range

Dynamic stress variations are referred to as either *stress range* ($\Delta\sigma$) or *stress amplitude* (σ). For linear responses with zero mean stress, the following relation applies:

$$\Delta\sigma = 2\sigma$$

Alternatively, if the mean stress differs from zero, the stress range can be estimated as:

$$\Delta\sigma = \sigma_{max} - \sigma_{min}$$

The stress range, $\Delta\sigma$, is being used as the reference in the S-N curves.

6 Additional class notations

6.1 General

DNVGL-RU-SHIP Pt.6 specify different class notations. This subsection contains an overview of the class notations which are related to fatigue assessment or damage.

6.2 CSA

CSA requires that specified structural details should be assessed by directly calculated loads. This includes typically longitudinal end connections, plates between stiffeners and specified details in the rules. For some details local FE analysis is required, and these local models are sub-models in global FE models.

6.3 RSD

RSD requires a direct wave load analysis and global FE model for container ships. Typical structural details subject to fatigue assessment are hatch corners, end connections of longitudinals and welded details of upper part of hull girder.

6.4 PLUS

PLUS requires extended assessment for specified structural details based on prescriptive loads in the rules. It typically includes hot spots at the crossing of longitudinals and web frames (e.g. slots and lugs) and specified details in the rules. The procedure is based on local FE analysis and these local models are sub-models in partial ship models or global FE models.

6.5 HMON

HMON refers to an approved Hull Monitoring System. A hull monitoring system, including strain sensors, is a decision support system (DSS) which gives guidance to the officer on watch on the fatigue (and extreme) loading of the hull structure in general and for specific structural details. The measurements capture also the fatigue (and extreme) contribution from wave induced vibrations like springing and whipping. The change of the fatigue loading due to change of the course and speed are displayed on board and measurement data can further be inspected on shore.

6.6 VIBR and COMF(V)

High cycle fatigue damage may also be a result of vibration. Hull structure, e.g. frames, vibrating due to engine or propeller excitation may give fatigue cracks at odd places. Also other equipment may contribute to the excitation. For tank structures, added mass from the fluid reduces the natural frequencies of the structural members, which then may be excited in resonance. The two class notations **VIBR** and **COMF(V)** have the objective of limiting the level of vibration and thereby directly or indirectly will reduce the risk of fatigue damage.

6.7 NAUT and routing

Weather routing will have a significant impact on wave load level, both with respect to extreme loads as well as fatigue loading. There is currently no class notation for weather routing, although there are some requirements to resolution of data from weather information system of weather surveillance system within the **NAUT** notation. A **HMON** system may also be a part of a routing system.

6.8 WIV

Wave induced vibrations, typically designated as whipping and springing, cause additional high-frequent dynamic stress in the ship hull structure superimposed to the wave-induced stress. The additional stress has impact on the fatigue loading. Class notation **WIV** can be assigned if additional strength assessment is carried out with explicit consideration of hull girder vibrations.

7 Definitions

A list of definitions is given in the following.

<i>classified structural detail</i>	= structural detail containing a structural discontinuity including a weld or welds, also referred to as a standard structural detail for which the nominal stress approach is applicable. Each classified detail is defined to belong to one S-N curve. This means that the <i>K</i> -factor for this detail is included in the S-N curve.
<i>constant amplitude loading</i>	= type of loading causing a regular stress fluctuation with constant magnitudes of stress maxima and minima
<i>crack growth rate</i>	= increase of crack length, in m, per loading cycle
<i>eccentricity</i>	= misalignment of plates at welded connections measured in the plate thickness direction
<i>effective notch stress</i>	= notch stress calculated for a notch with a certain effective notch radius
<i>fatigue</i>	= deterioration of a component caused by crack initiation and/or by the growth of cracks
<i>fatigue action</i>	= load effect causing fatigue
<i>fatigue damage ratio</i>	= for constant amplitude stress, it is the ratio of the number of stress cycles to the number of cycles to failure from the S-N curve. For a stress spectrum, it is the sum of the individual fatigue damage ratio for the different stress range levels
<i>fatigue life</i>	= for constant amplitude loading, it is the number of stress cycles at a particular stress range required to cause fatigue failure of a component. For a stress spectrum, it is the total number of stress cycles until failure
<i>fatigue limit</i>	= fatigue strength under constant amplitude loading corresponding to a high number of cycles large enough to be considered as infinite by a design code. The fatigue limit may be used for screening and it is illustrated in Figure 1 .
<i>fatigue rate</i>	= fatigue damage calculated for a certain time interval divided by the budget damage for the same time interval. The time interval is typical five minutes, half an hour or one hour. The budget damage is estimated as the ratio of the time interval to the target fatigue life. This is used to demonstrate the instant fatigue loading of critical details compared to the design requirement.
<i>fatigue resistance</i>	= structural detail's resistance against fatigue actions in terms of S-N curve or crack propagation properties
<i>fatigue strength</i>	= magnitude of stress range leading to a particular fatigue life. Good fatigue strength then implies low stress level or long fatigue life
<i>fatigue stress</i>	= stress including corrections, for e.g. mean stress, thickness effect, surface finishing and material factor, relevant for fatigue assessment purpose, i.e.: <ul style="list-style-type: none"> — nominal stress for welded details — hot spot stress for welded details — local stress at free plate edge.
<i>fracture mechanics</i>	= assessment of fatigue by crack propagation analysis until unstable fracture occur
<i>geometric stress</i>	= see hot spot stress

<i>hot spot</i>	= location in the structure where fatigue cracks may initiate due to the combined effect of nominal structural stress fluctuation and stress raising effects due to the weld geometry. Hot spots may be located at: <ul style="list-style-type: none"> — weld toes — weld root of partial penetration or fillet welds.
<i>hot spot stress</i>	= value of stress on the surface at the hot spot (also known as geometric stress or structural stress). Hot spot stress is e.g. the stress at the weld toe taking into account the stress concentration due to structural discontinuities and presence of welded attachments but disregarding the non-linear stress caused by the notch at the weld toe. The hot spot stresses to be considered correspond to the two principal stresses on the plate surface at the weld toe. The first principal stress acts within $\pm 45^\circ$, perpendicular to the weld and the second principal stress acts outside $\pm 45^\circ$. The hot spot stress should be obtained by multiplying the nominal stress by tabulated stress concentration factor (K) or directly by FE hot spot analysis.
<i>local notch</i>	= notch such as the local geometry of the weld toe, including the toe radius and the angle between the base plate surface and weld reinforcement. The local notch does not alter the structural stress but generates non-linear stress peaks.
<i>local stress at free edge</i>	= stress at a free plate edge derived using finite element analysis or tabulated stress concentration factors (K)
<i>macro-geometric discontinuity</i>	= global discontinuity, the effect of which is usually not taken into account in classified structural details, such as large openings, a curved part in a beam, a bend in a flange, and eccentricity in lap joints
<i>macro-geometric effect</i>	= stress raising effect due to macro-geometry in the vicinity of the welded joint, but not due to the welded joint itself
<i>membrane stress</i>	= average normal stress across the thickness of a plate
<i>miner sum</i>	= summation of individual fatigue damage ratios caused by each stress cycle or stress range block according to the Palmgren-Miner rule
<i>misalignment</i>	= axial and angular misalignments caused either by detail design or by fabrication
<i>nominal stress</i>	= stress in a structural component taking into account macro-geometric effect including effective breadth of flanges, but disregarding the stress concentration due to structural discontinuities and the presence of welds. Nominal stress should be obtained either using coarse or fine mesh FE analysis or using analytical calculation based on beam theory with effective breadth of flanges included.
<i>non-linear stress peak</i>	= stress component of a notch stress which exceeds the linearly distributed structural stress at a local notch
<i>notch stress</i>	= total stress of a notch at a free plate edge, weld root or weld toe, taking into account the stress concentration caused by the local notch. Thus, for welds the notch stress consists of the sum of structural stress and the non-linear stress peak.
<i>notch stress concentration factor</i>	= ratio of notch stress to the nominal stress
<i>Paris' law</i>	= experimentally determined relation between crack growth rate and stress intensity factor range (fracture mechanics)
<i>Palmgren-Miner rule</i>	= linear damage accumulation for variable amplitude loading using S-N curves. Fatigue failure is expected when the Miner sum reaches unity.
<i>Rainflow counting</i>	= standardised procedure for stress range counting
<i>shell bending stress</i>	= bending stress in a shell or plate-like part of a component, linearly distributed across the thickness as assumed in the theory of shells
<i>S-N curve</i>	= graphical presentation of the dependence of fatigue life (N) on fatigue strength (S)

<i>stress cycle</i>	= part of a stress history containing a stress maximum and a stress minimum
<i>SCF</i>	= stress concentration factor
<i>stress intensity factor</i>	= factor used in fracture mechanics to characterise the stress at the vicinity of a crack tip
<i>stress range</i>	= difference between stress maximum and stress minimum in a stress cycle
<i>stress range block</i>	= part of a total spectrum of stress ranges which is discretised in a certain number of blocks
<i>stress range exceedance</i>	= tabular or graphical presentation of the cumulative frequency of stress range exceedance, i.e. the number of ranges exceeding a particular magnitude of stress range in stress history. Here frequency is the number of occurrences.
<i>stress ratio</i>	= ratio of minimum to maximum value of the stress in a cycle
<i>structural discontinuity</i>	= geometric discontinuity due to the type of welded joint, usually found in tables of classified structural details. The effects of a structural discontinuity are (i) concentration of the membrane stress and (ii) formation of secondary bending stress.
<i>structural stress</i>	= stress in a component, resolved taking into account the effects of a structural discontinuity, and consisting of membrane and shell bending stress components. Also referred to as geometric stress or hot spot stress.
<i>structural stress concentration factor</i>	= ratio of hot spot (structural) stress to nominal stress, also referred to as geometrical stress concentration factor. In this document the shorter notation: stress concentration factor due to geometry (K) is used.
<i>variable amplitude loading</i>	= type of loading causing irregular stress fluctuation with stress ranges (and amplitudes) of variable magnitude
<i>weld shape factor</i>	= ratio between the notch stress and the structural (hot spot) stress describing the effect of the weld contour. This is part of the notch stress concentration factor. The weld shape factor, K_w , is included in the hot spot S-N curve.

SECTION 2 FATIGUE CAPACITY

1 Introduction

The main principles for fatigue capacity are described in this section. The basis is the design S-N curves in [2], but the following should be considered in assessment of the fatigue strength:

- Corrosive environment or in air environment, [3].
- Mean stress effect, [4].
- Thickness effect, [5].
- Material effect, [6].
- Post-weld treatment, Sec.7.

Additional stresses resulting from fabrication tolerances of butt welds and cruciform joints should be considered when the fabrication tolerances exceed that inherent in the S-N data. See App.A.

2 S-N curves

2.1 General

The fatigue capacity of welded joints and base material is defined by S-N curves, which are obtained from fatigue tests. The design S-N curves are based on the mean-minus-two-standard-deviation curves, which are associated with a 97.5% probability of survival. A failure refers to a through thickness crack with reference to App.B.

The S-N curves are applicable for normal and high strength steels used in construction of hull structures up to 500 N/mm². Other S-N curves are given in App.B.

The S-N curves for welded joints include the effect of the local weld notch for the hot spot approach. This also means that if a butt weld is machined or ground flush without weld overfill a better S-N curve can be used. For the nominal stress approach, i.e. FAT class S-N curves, also the detail itself is included.

2.2 S-N curves and detail classification

For practical fatigue design, welded details and base material can be divided into several classes, each with a corresponding design S-N curve. Typical details may fall in one of the classes specified in Table 1 and Table 2, depending upon:

- the geometry of the detail
- the direction of the fluctuating stress relative to the detail
- the method of fabrication (misalignment/defects and surface condition) and inspection of the detail.

Each detail at which fatigue cracks may potentially develop should, where possible, be classified in accordance with tables given in App.A for welded joints and in accordance with Table 2 for base material. Each potential crack location should be classified separately.

The basic design S-N curve is given as

$$\log N = \log K_2 - m \log \Delta\sigma$$

with S-N curve parameters given in Table 1 and where:

- | | | |
|----------------|---|---|
| N | = | predicted number of cycles to failure for stress range $\Delta\sigma$ |
| $\Delta\sigma$ | = | stress range, in N/mm ² |
| m | = | Negative inverse slope of S-N curve |

$\log K_2$ = intercept of log N-axis by S-N curve

$$\log K_2 = \log K_1 - 2\delta$$

where:

- K_1 = constant of mean S-N curve (50% probability of survival)
- K_2 = constant of design S-N curve (97.5% probability of survival)
- δ = standard deviation of $\log N$:
- = 0.20

2.3 S-N curves for in-air environment

S-N curves for in-air environment are given in [Table 1](#) and in [Figure 2](#) up to 10^8 cycles.

The reference stress ranges at $2 \cdot 10^6$ and 10^7 cycles are included, and also the structural stress concentration factor as derived from the hot spot method is included for reference. For welded details, the D-curve is the reference curve for the hot spot stress method. For base material, the B1 curve is used as the reference. The B, B2, C, C1 and C2 curves are applicable for local stress at free plate edges according to [Table 2](#). The parameterized S-N curve designated with *FAT X* (where *X* is the stress range at $2 \cdot 10^6$ cycles, see [Figure 1](#)) is used for welded details assessed with the nominal stress approach, and should not be used in relation to the free plate edges.

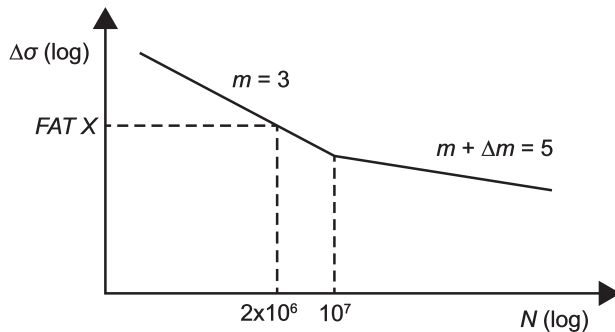


Figure 1 Illustration of FAT class S-N curves with FAT X number.

The B1 curve forms the upper limit of all other curves at very low number of cycles, i.e. for well below 10000 cycles. This is regarded relevant for certain details for low cycle fatigue.

Table 1 S-N parameters for air

<i>S-N Curve</i>	Reference stress at $2 \cdot 10^6$ cycles (<i>FAT</i>)	Reference stress at 10^7 cycles (knuckle), $\Delta\sigma_q$	Structural stress concentration embedded in the detail and taken at $2 \cdot 10^6$ (10^7) cycles	$N \leq 10^7$		$N > 10^7$	
				$\log K_2$	<i>m</i>	$\log K_2$	$m + \Delta m$
B1	160	107.00	0.56 (0.49)	15.118	4	19.176	6

S-N Curve	Reference stress at $2 \cdot 10^6$ cycles (FAT)	Reference stress at 10^7 cycles (knuckle), $\Delta\sigma_q$	Structural stress concentration embedded in the detail and taken at $2 \cdot 10^6$ (10^7) cycles	$N \leq 10^7$		$N > 10^7$	
	N/mm^2	N/mm^2	-	$\log K_2$	m	$\log K_2$	$m + \Delta m$
B	150	100.31	0.60 (0.52)	15.005	4	19.008	6
B2	140	93.62	0.64 (0.56)	14.886	4	18.828	6
C	125	78.92	0.72 (0.67)	13.640	3.5	17.435	5.5
C1	112	70.72	0.80 (0.74)	13.473	3.5	17.172	5.5
C2	100	63.14	0.90 (0.83)	13.301	3.5	16.902	5.5
D	90	52.63	1.00 (1.00)	12.164	3	15.606	5
E	80	46.78	1.13 (1.13)	12.010	3	15.350	5
F	71	41.52	1.27 (1.27)	11.855	3	15.091	5
FAT	X	$0.585 \cdot X$	$90/X$ ($90/X$)	$6.301 + 3 \cdot \log(X)$	3	$7 + 5 \cdot \log(0.585 \cdot X)$	5

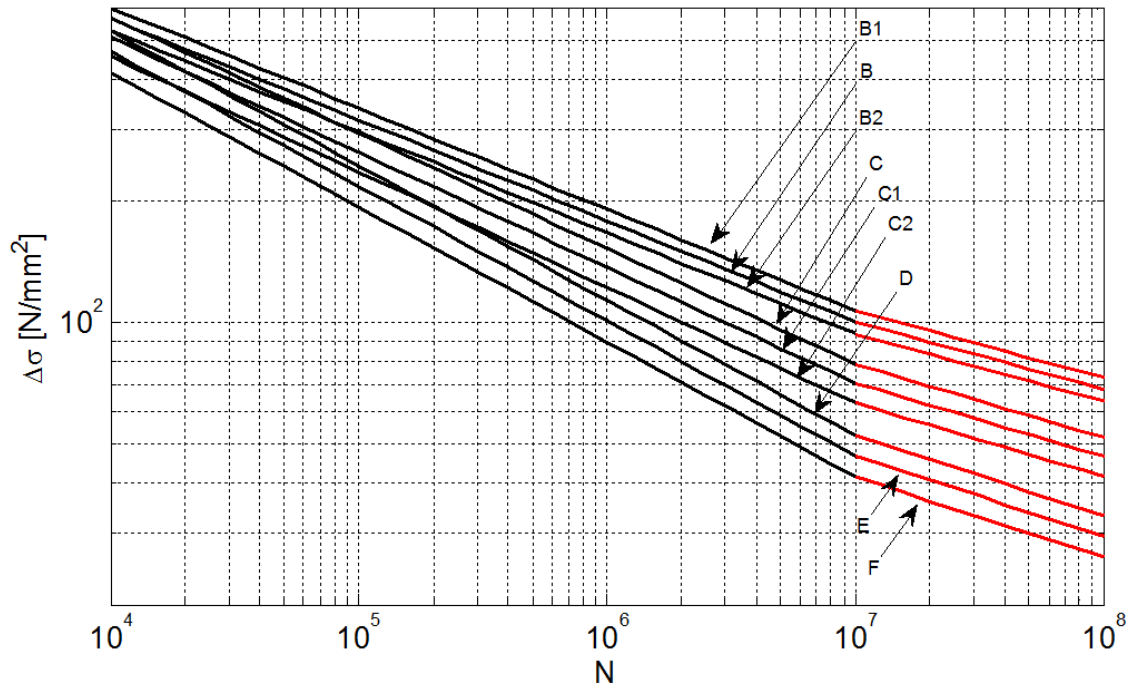
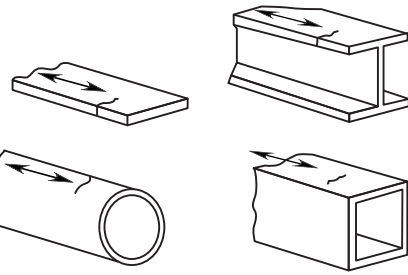
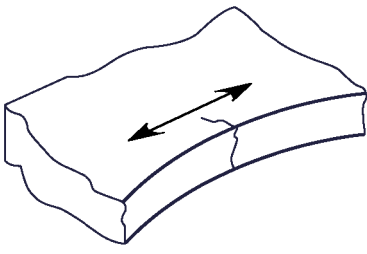
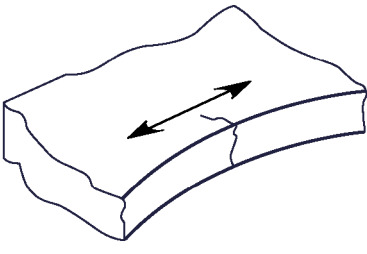
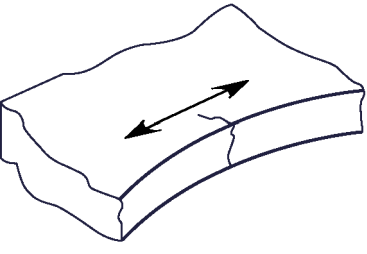
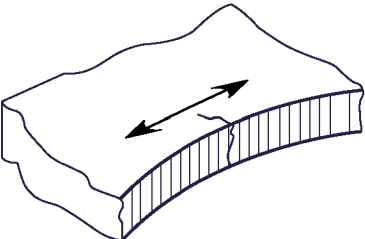
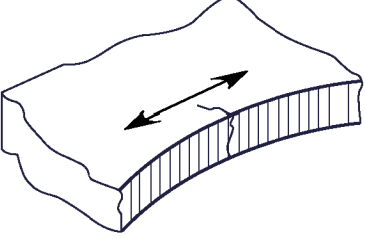


Figure 2 S-N curves in air

Table 2 S-N-curve depending on surface finishing for base material and free plate edge

<i>Joint configuration, fatigue crack location and stress direction</i>	<i>Description of joint</i>	<i>S-N curve</i>	<i>FAT class N/mm²</i>
1 	Base material. Rolled or extruded plates and sections as well as seamless pipes. No surface or rolling defects	B1	160
2 	Free plate edge. Machine cutting e.g. by a thermal process or shear edge cutting. Smooth surface free of cracks and notches. Cutting edges chamfered or rounded by means of smooth grinding, groove direction parallel to the loading direction. Stress increase due to geometry of cut-outs to be considered by means of direct numerical calculation of the appertaining maximum local stress range	B	150
3 	Free plate edge. Machine cutting e.g. by a thermal process or shear edge cutting. Smooth surface free of cracks and notches. Cutting edges chamfered or rounded.	B2	140
4 	Free plate edge. Machine cutting e.g. by a thermal process or shear edge cutting. No edge treatments. Surface free of cracks and severe notches.	C	125

<i>Joint configuration, fatigue crack location and stress direction</i>		<i>Description of joint</i>	<i>S-N curve</i>	<i>FAT class N/mm²</i>
5		Free plate edge. Manually thermally cut e.g. by flame cutting. With edge treatments. Surface free of cracks and severe notches.	C1	112
6		Free plate edge. Manually thermally cut e.g. by flame cutting. No edge treatments. Surface free of cracks and severe notches.	C2	100

Note 1: Stress increase due to geometry of cut-outs to be considered.

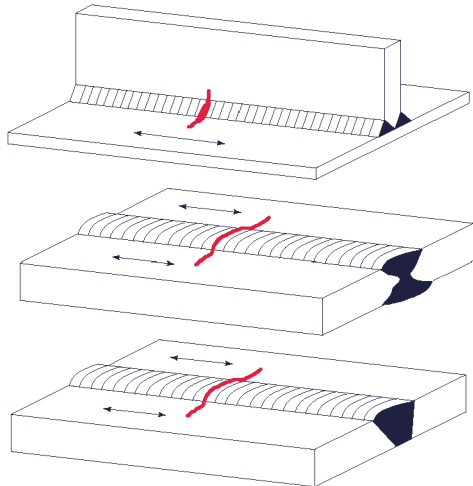
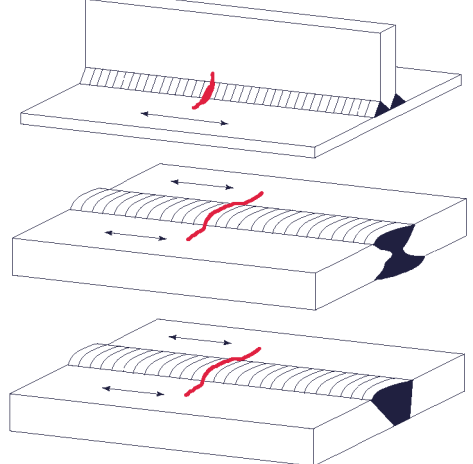
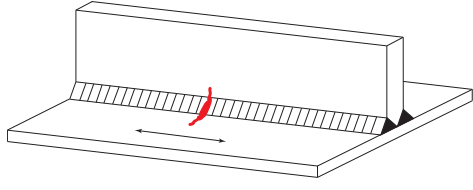
2.4 S-N curves for stress along the welds

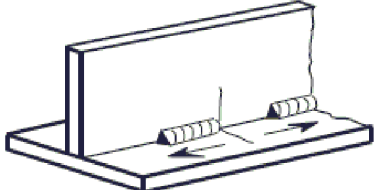
The S-N curves given in [Table 1](#) are developed for principal stresses acting normal to the weld and should be used together with the maximum stress range within $\pm 45^\circ$ of the normal to the weld as explained in [Sec.6 \[1.3\]](#).

If the governing stress direction is parallel with the weld direction a stress reduction factor K_p should be used on the principal stress range before entering stress into the S-N curve D. The stress reduction factor will depend on the quality of the weld, [Table 3](#). K_p is by default 1.0 for stress direction normal to the weld. Instead of using stress reduction factor, K_p , for the hot spot stress approach also alternative S-N curves can be applied as given in [Table 3](#). Alternatively, the procedure of effective hot spot stress described in [Sec.6 \[1.3\]](#) and [App.E](#) may be used.

The correction needs to be applied for the nominal stress approach if a parametrized FAT X class is chosen, which is applicable to a governing stress direction parallel to the weld direction.

Table 3 Stress reduction factor K_p and FAT classes for longitudinally loaded welds

K_p/FAT N/mm^2	Figure	Description	Requirement
0.72/125		1. Automatic welds carried out from both sides.	1. No start-stop position is permitted except when the repair is performed by a specialist and inspection carried out to verify the proper execution of the repair.
0.80/112		2. Automatic fillet or butt welds carried out from both sides, but containing stop-start positions. 3. Automatic butt welds made from one side only, with a backing bar, but without start-stop positions.	3. When the detail contains start-stop positions use $K_p = 0.90$ or FAT 100
0.90/100		4. Manual fillet or butt welds. 5. Manual or automatic butt welds carried out from one side only, particularly for box girders. 6. Repaired automatic or manual fillet or butt welds.	5. A very good fit between the flange and web plates is essential. Prepare the web edge such that the root face is adequate for the achievement of regular root penetration with out brake-out. 6. Improvement methods that are adequately verified may restore the original category.

K_p/FAT N/mm^2	Figure	Description	Requirement
1.13/80		Intermittent longitudinal fillet weld (based on stress range in the flange at weld ends)	In presence of shear stress, τ , the FAT class and K_p factor should be downgraded by the factor $1 - \Delta\tau/\Delta\sigma$, but not below FAT 36 or K_p of 2.5.

2.5 Nominal stress S-N curves

For welded details of which the fatigue capacity does not strongly depend on the type of loading, i.e. axial or bending, the nominal stress approach can be used based on S-N curves from [Table 1](#) designated as *FAT X*. In [App.A](#) the FAT classes are included in parallel with stress concentration factors, K , for various details.

FAT class curves are not given for the structural stress concentration factors referring to typical end connections, since for these there are separate geometrical stress concentration factor for axial loading, K_a , and bending, K_b .

2.6 Other steel types

For Duplex, Super Duplex and austenitic steel one may use the same S-N curve as for C-Mn steels.

3 Corrosive environment

3.1 General

Fatigue life of steel structures in freely corroding condition, e.g. submerged in sea water, is shorter than in-air environment. For coated or cathodically protected steel in sea water, approximately the same fatigue life as in dry air is obtained.

The fraction of time in-air and in corrosive environments depends on the location of the detail and is specified by the rules. For details being partly in air and partly in corrosive environment, the fatigue damage may be calculated according to [\[3\]](#).

The general principle is that all details should be protected from freely corroding conditions, which means that the dominating part of the design fatigue life is associated with the in-air environment, while a minor part is considered as corrosive.

3.2 Fatigue assessment in corrosive environment

For details in corrosive environment like sea water the S-N curves for in-air environment can be used, but the fatigue damage in corrosive environment should be multiplied with a factor of 2.0. The same effect is achieved if the increase of the fatigue design life is assumed, as described in [Sec.3 \[3\]](#).

4 Mean stress effect

For fatigue analysis the stress range may be reduced dependent on whether the cycling stress is in tension or in compression.

The basis for the mean stress effect is the variable amplitude stress range, $\Delta\sigma$, at a 10^{-2} probability level of exceedance for the specific wave environment. This implies that $\Delta\sigma$ should include the environmental factor, f_e , when the prescriptive loads are used.

4.1 Base material and free plate edges

Mean stress, σ_{mean} , refers to the static stress. If the stress concentration factor is included, it needs to be included consistently in the mean stress and the dynamic stress range. The calculated stress range should be multiplied with the mean stress reduction factor, f_{mean} , illustrated in [Figure 3](#) and given as:

$$f_{mean} = \begin{cases} \min\left[1.0; \left(0.8 + 0.4 \frac{\sigma_{mean}}{2 \cdot \Delta\sigma}\right)\right] & \text{for } (\sigma_{mean} \geq 0) \\ \max\left[0.6; \left(0.8 + 0.4 \frac{\sigma_{mean}}{2 \cdot \Delta\sigma}\right)\right] & \text{for } (\sigma_{mean} < 0) \end{cases}$$

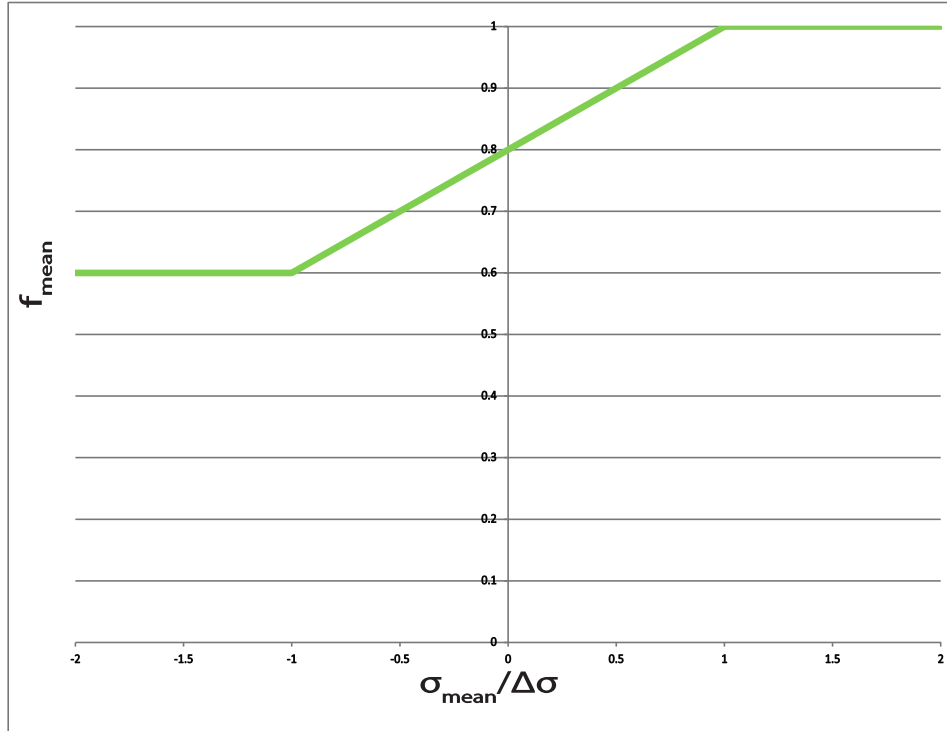


Figure 3 The stress range reduction factor for base material and free plate edges

4.2 Welded joints

The mean stress reduction factor, f_{mean} , for welded details is illustrated in [Figure 4](#) and given as:

$$f_{mean} = \begin{cases} \min\left[1.0; \left(0.9 + 0.2 \frac{\sigma_{mean}}{2 \cdot \Delta\sigma}\right)\right] & \text{for } (\sigma_{mean} \geq 0) \\ \max\left[0.7; \left(0.9 + 0.4 \frac{\sigma_{mean}}{2 \cdot \Delta\sigma}\right)\right] & \text{for } (\sigma_{mean} < 0) \end{cases}$$

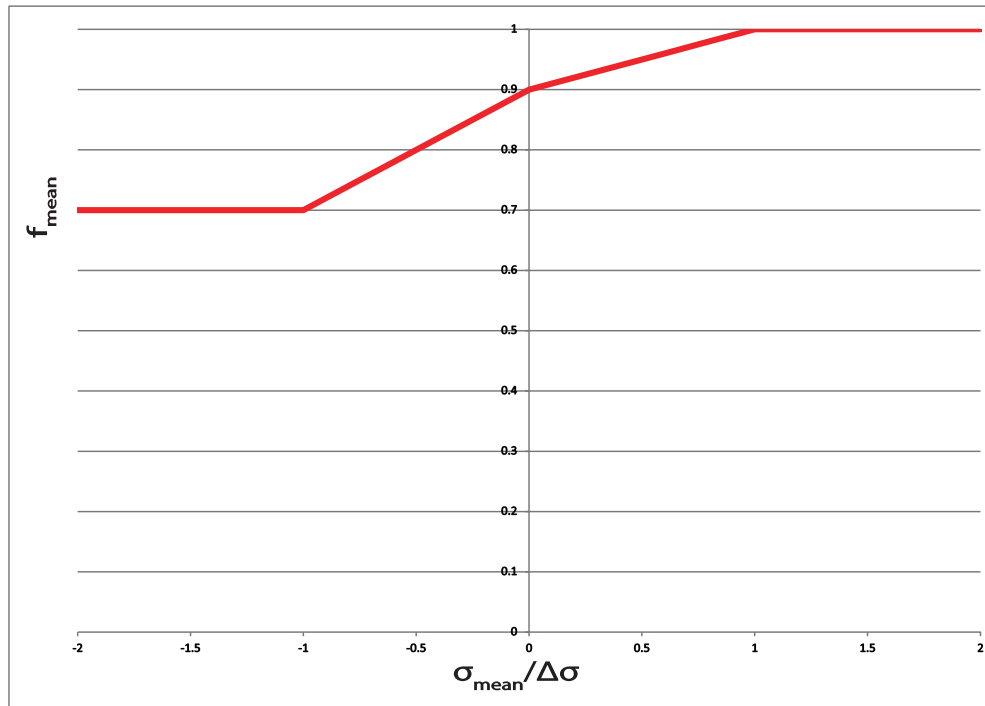


Figure 4 The stress range reduction factor for welded details

For welded details, the mean stress effect is applicable when the loading process causes high tensile stress in yield at the hot spot, reducing the residual stresses from the welding process. Without yield occurring due to tensile stresses, the mean stress effect should be disregarded. One example is side shell plating with sea pressure externally and void space internally and no significant hull girder loads. Then, only sea pressure is acting causing only compressive stresses in the weld toe.

5 Thickness effect

5.1 General

The fatigue strength of welded joints depends to some extent on the plate thickness. This effect is due to the local geometry of the weld toe in relation to thickness of the adjoining plates, e.g. weld profiling may affect the thickness effect as given in App.F. It is also dependent on the stress gradient over the thickness, i.e. it can differ between axial and bending loading.

The correction factor, f_{thick} , of the stress range is given as:

$$f_{thick} = \left(\frac{t_{eff}}{25} \right)^n \quad \text{for } t_{eff} > 25 \text{ mm}$$

$$f_{thick} = 1 \quad \text{for } t_{eff} \leq 25 \text{ mm}$$

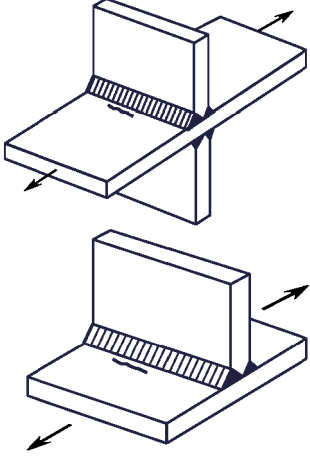
where:

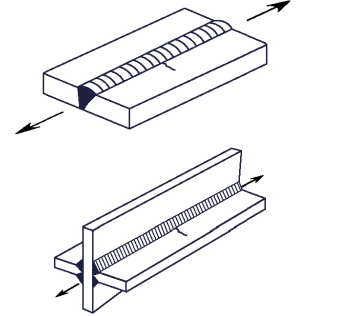
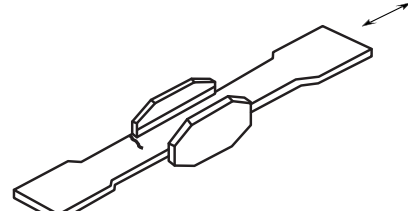
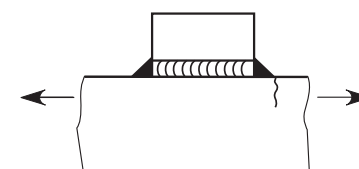
n = Thickness exponent

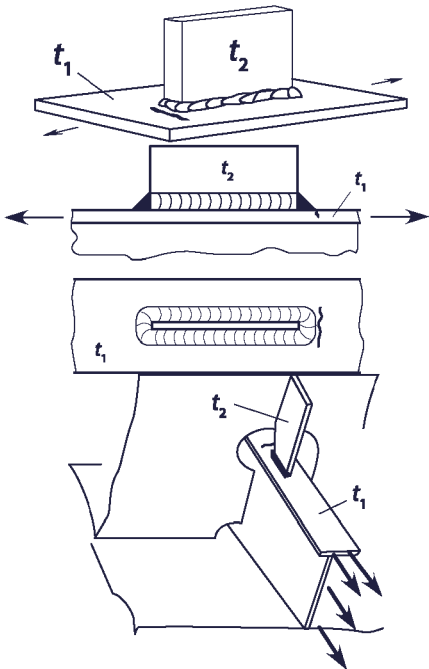
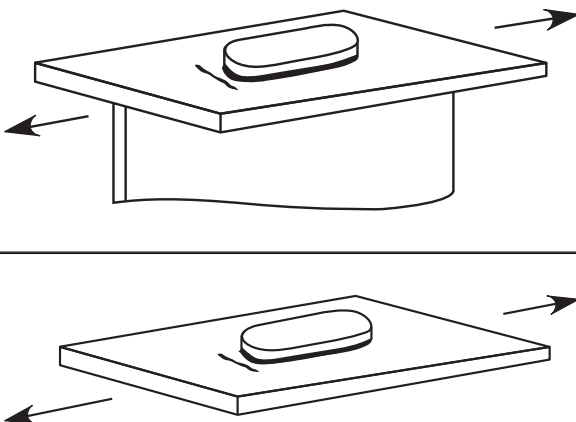
t_{eff} = Effective thickness according to [5.2]. If nothing else is specified t should be used.

The thickness exponent, n , on the fatigue strength is given in [Table 4](#) for specific details. If nothing else is stated, an exponent of 0.20 may be used for welded details.

Table 4 Welded details; thickness exponents

No	Detail category description	Geometry	Condition	n
1	Cruciform joints, transverse T-joints, plates with transverse attachments		As-welded	0.2
			Weld toe treated by post-weld improvement method	0.2
2	Transverse butt welds		As-welded	0.2
			Ground flush or weld toe treated by post-weld improvement method	0.1

No	Detail category description	Geometry	Condition	n
3	Longitudinal welds or attachments to plate edges	 	Any	0.1
			Weld toe treated by post-weld improvement method	0.1
4	Longitudinal attachments on the flat bar or bulb profile		Any	0.0
			Weld toe treated by post-weld improvement method ¹⁾	0.0

No	Detail category description	Geometry	Condition	n
5	Longitudinal attachments unsupported and supported longitudinally		As-welded $t_2 \geq 0.33 t_1$ else	0.1 0.0
6	Doubling plates, unsupported and supported		As-welded	0.1
			Weld toe treated by post-weld improvement method ¹⁾	0.0

¹⁾ No benefit applicable for post-weld treatment of longitudinal end connections

5.2 Effective thickness of welds

The thickness exponent is considered to account for the size of the plate, through which a crack will most likely grow. To some extent it also accounts for local geometry at the weld toe. However, the equation in [5.1] does not account for the weld width.

The thickness effect depends also on the weld width, d , of butt welds and attachment length of cruciform connections as illustrated in [Figure 5](#). For butt welds, where d may differ on the two plate sides, the width d for the considered hot spot side should be used. The thickness effect is lower for short lengths of d . Thus the thickness t for butt welds and cruciform joints should be replaced by an effective thickness, in mm, which can be derived as:

$$t_{eff} = \min(14 + 0.66d; t)$$

where the parameters d and t are measured in mm and are defined in [Figure 5](#).

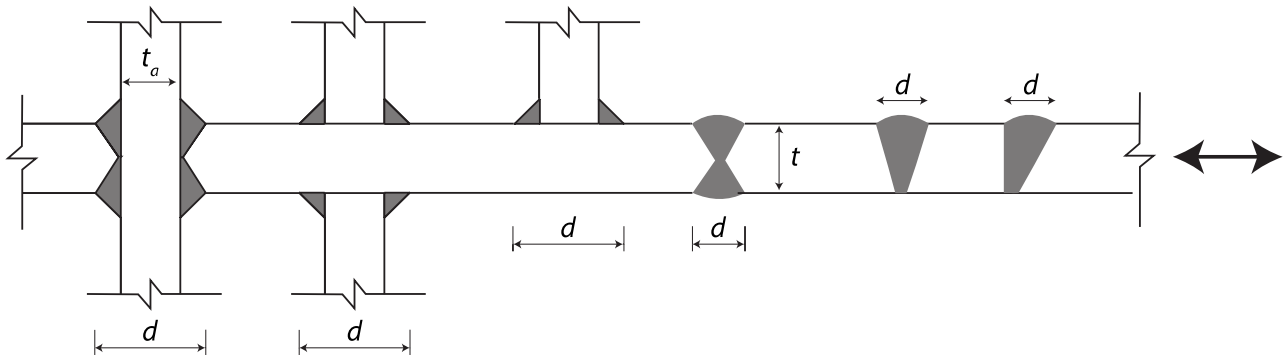


Figure 5 Definition of attachment length of cruciform joints and weld width for butt welds

If the details of the weld are not shown on the structural drawings, an estimate of the width, in mm, can be taken as:

$$d = 1.15 t + 5 \quad \text{for butt welds}$$

$$d = 3 \cdot t_a \quad \text{for transverse attachments and cruciform joints.}$$

5.3 Thickness effect of welds in prescriptive analysis of longitudinal end connections

For prescriptive stress analysis, the following effective thickness should be considered:

- Flat bar and bulb profile: no thickness effect.
- Angle bar and T-bar: flange thickness, $t_{eff} = t_{f-n50}$, and a thickness exponent $n = 0.1$ when the hot spot is located on the stiffener flange.

5.4 Thickness effect of welds in FE analysis

For FE analysis, the effective thickness to be considered is the thickness of the member where the crack is likely to initiate and propagate.

5.5 Thickness effect of base material

The thickness effect is not regarded applicable for base material and free plate edges assuming good workmanship practise (S-N curve B1, B, B2 and C) and when adequate protective measures are taken against wear, tear and corrosion, e.g. from friction from cargo or cargo handling appliances.

The thickness exponent of $n = 0.1$ can be assumed if the above is not fulfilled (S-N curve C1 and C2).

6 Material factor

The fatigue stress range, $\Delta\sigma$, should include a correction factor for the material strength, $f_{material}$, taken as:

$$f_{material} = \frac{1200}{965 + R_{eH}} \quad \text{for base material and free plate edges}$$

$$f_{material} = 1 \quad \text{for welded details}$$

where the specified minimum yield stress, R_{eH} , is in N/mm².

SECTION 3 FATIGUE STRENGTH REPRESENTATION

1 Introduction

The basis for the fatigue assessment is an estimate of the stress range (hot spot, nominal or local at free plate edge) which is described in [2]. When assessing the fatigue strength the time in corrosive and in-air environment, the time in different loading conditions and the time in port need to be accounted for as described in [3]. The results of the fatigue assessment can be presented in different ways depending on what is found convenient:

- Calculated fatigue damage versus allowable fatigue damage, [3]
- Calculated fatigue life versus design fatigue life, [3]
- Actual stress range (calculated) versus permissible peak stress range (calculated), [4]
- Given stress concentration factor versus permissible stress concentration factor (calculated), [5]
- Given FAT class versus required FAT class (calculated), [5].

The scope and extent of the fatigue assessment, the loading conditions and related parameters to consider and the time at sea are given in the rules for the standard ship types.

2 Fatigue stress range

2.1 General

The calculated stress range should follow the net scantling approach, t_{n50} , for prescriptive fatigue assessment and net or gross, t , based on FE analysis, where net or gross scantlings is defined in the rules for the specific ship types. Since there is a difference on how the corrosion affects the global and local stress, a correction factor f_c needs to be included. In addition, the calculated stress depends on the wave environment which is represented by the environmental factor f_e .

Before performing fatigue strength assessment, the calculated stress entered into the S-N curve needs to be corrected for other fatigue capacity effects such as:

- Mean stress
- Thickness
- Material
- Post-weld treatment.

Results from performed fatigue analyses are presented in App.C in terms of allowable stress ranges as function of the Weibull shape parameter. The basis for the allowable stress ranges is that long term stress ranges can be described by a two parameter Weibull distribution.

2.2 Scantlings approach factor, f_c

The global stress is less affected by the corrosion than the local stress due to the probabilistic nature of corrosion, which gives less average corrosion on a global level compared to at a local level. Thus, the local stress should be based on t_{n50} while the global stress should be based on t_{n25} .

For prescriptive fatigue assessment using a beam model based on t_{n50} , the correction factor f_c only applies to the global stresses. When using a global FE model based on t_{n50} or t_{gr} , the same correction factor applies to both the global and local stresses, i.e. directly on the stress.

The correction factor should be taken as:

- a) Prescriptive fatigue strength assessment
 - $f_c = 1.0$ for local plate and stiffener bending based on t_{n50}
 - $f_c = 0.95$ for hull girder stresses based on t_{n50}

b) FE based fatigue strength assessment

- $f_c = 1.0$ for stresses based on t_{gr}
- $f_c = 0.95$ for stresses based on t_{n50}

Since FE models may be based on either t_{n50} or t_{gr} , the notation t is used for the thickness in relation to FE analysis. However, prescriptive assessment should be based on t_{n50} .

2.3 Environmental factor, f_e

The environmental factor f_e is covering World Wide and North Atlantic wave environment for merchant vessels. The f_e factor for prescriptive approach is listed in DNV GL Pt.3 Ch.9 Sec.4 [4.2].

In direct hydrodynamic calculations based on a specific scatter diagram, the f_e factor is set to 1.0 or can be omitted.

2.4 Operational factor, f_R

While the environmental factor f_e refers to the operational area, the operational factor f_R relates to how the vessel operates in the operational area regarding weather routing. The operational factor for prescriptive loads is defined in DNV GL Pt.3 Ch.9 Sec.4 [4.3].

In direct hydrodynamic calculations, the operational factor, f_R , and possibly also the fatigue coefficient, f_{fa} , and the vibration factor, f_{vib} , depending on the scatter diagram used, are multiplied with the directly calculated stress range, $\Delta\sigma_{FS}^{dir}$, as explained in DNV GL CG 0130 Sec.2 [7] Wave loads to find the fatigue stress range:

$$\Delta\sigma_{FS} = f_R \cdot f_{fa} \cdot f_{vib} \cdot \Delta\sigma_{FS}^{dir}$$

For site specific operation the f_{vib} is reduced to 1.05. For site specific scatter diagram and trade specific scatter diagram with full effect of routing the f_{fa} and f_R are omitted.

2.5 Post-weld treatment

Reference is made to the rules for the application of the post-weld treatment. There are several limitations for the benefit of post-weld treatment. This factor should preferably not be considered in the initial design phase. For burr grinding the stress range can be multiplied with the following factor:

$$f_w = \left(\frac{1}{f_T} \right)^{\frac{1}{3.5}}$$

where:

f_T = Fatigue life factor as given in Sec.7 [2.3].

2.6 Fatigue stress range

The fatigue stress range $\Delta\sigma_{FS}$ in N/mm² to be used in the assessment is based on the calculated stress range $\Delta\sigma$ times the corrections for mean stress effect, thickness effect, material factor, scantlings approach factor, the environmental factor and the post-weld treatment factor:

$$\Delta\sigma_{FS} = f_{mean} \cdot f_{thick} \cdot f_{material} \cdot f_w \cdot f_c \cdot f_e \cdot \Delta\sigma$$

The stress range should be estimated at a 10^{-2} probability level of exceedance.

The straight line spectrum, i.e. 2-parameter Weibull distribution with Weibull slope $\xi = 1.0$, is displayed in [Figure 1](#) where it can also be seen that in this case the permissible stress range at a probability level of 10^{-2} is 25% of the stress range at a probability level of 10^{-8} . In [Figure 2](#) the distribution of the damage is illustrated at different probability levels based on the straight line spectrum, suggesting that most of the fatigue damage comes from smaller stress ranges close to a probability level of 10^{-2} .

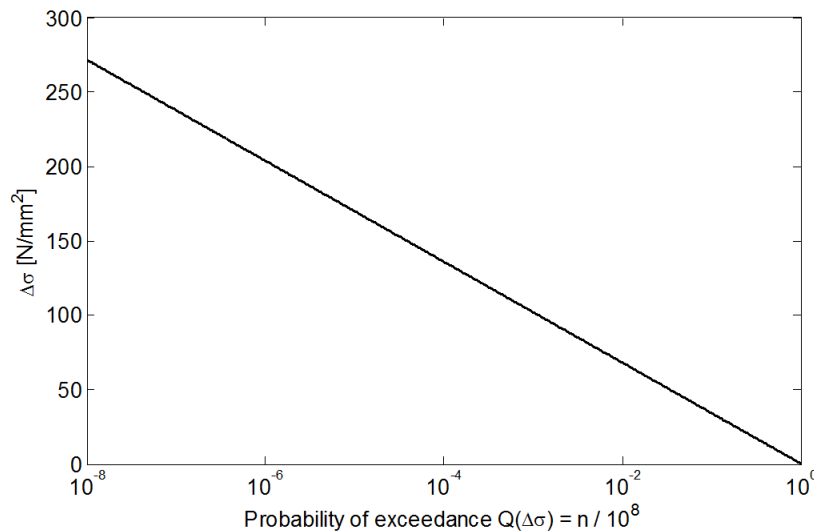


Figure 1 Straight line spectrum giving a damage of 1.0 based on S-N curve D/FAT 90.

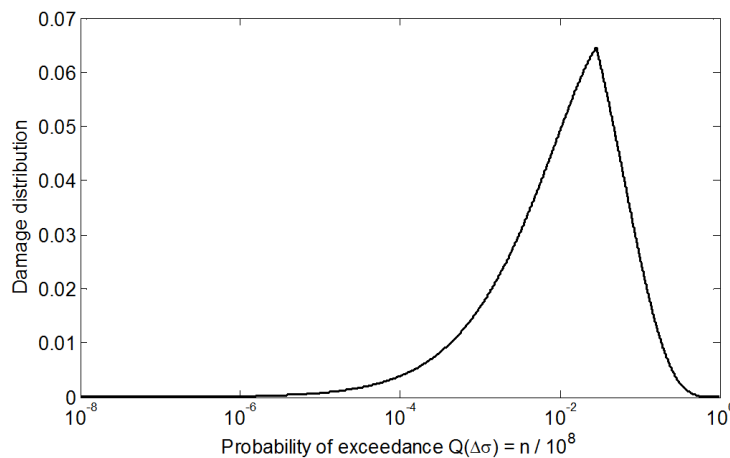


Figure 2 Damage distribution for a straight line spectrum based on S-N curve D/FAT 90.

3 Fatigue damage and fatigue life calculation

3.1 Fatigue damage accumulation with Palmgren - Miner's rule

Fatigue assessment may be carried out by estimating the linear cumulative fatigue damage D by using Palmgren-Miner's rule formulated as:

$$D = \sum_{i=1}^{n_{tot}} \frac{n_i}{N_i}$$

where:

- n_i = Number of cycles at stress range $\Delta\sigma_i$
- N_i = Number of cycles to failure at stress range $\Delta\sigma_i$
- n_{tot} = Total number of stress range blocks
- i = Stress range block index.

The number of load cycles, n_i , is determined by the long term stress distribution, e.g. represented by the Weibull distribution, while the number of cycles to failure, N_i , is represented by the S-N curve.

The acceptance criteria to the damage D is given by the rules.

3.2 Time in air and corrosive environment

The design fatigue life is divided into two time periods due to limitation of the corrosion protection. It is assumed that the corrosion protection (i.e. coating system) is only effective for a limited number of years during which the structural details are exposed to in-air environment. During the remaining part of the design life, T_C , as specified in the rules, the structural details are unprotected i.e. exposed to corrosive environment.

3.3 Annual fatigue damage

The annual fatigue damage is the damage in-air accumulated during a specific loading condition (j) assumed 100% time at sea. The annual fatigue damage, can be based on the fatigue stress range obtained from the predominant load case (EDW giving the highest and thereby the most representative fatigue stress range, $\Delta\sigma_{FS}$) in the prescriptive fatigue assessment. This can be calculated based on a closed form formulation as:

$$D_{E(j)} = \frac{N_D}{K_2} \frac{\Delta\sigma_{FS, (j)}^m}{(\ln N_R)^{m/\xi}} \cdot \mu_{(j)} \cdot \Gamma\left(1 + \frac{m}{\xi}\right)$$

$$N_D = \frac{31.557 \cdot 10^6}{4 \log L}$$

$$\mu_{(j)} = 1 - \frac{\left\{ \gamma\left(1 + \frac{m}{\xi}, v_{(j)}\right) - v_{(j)}^{-\Delta m/\xi} \cdot \gamma\left(1 + \left(\frac{m + \Delta m}{\xi}\right), v_{(j)}\right) \right\}}{\Gamma\left(1 + \frac{m}{\xi}\right)}$$

$$v_{(j)} = \left(\frac{\Delta\sigma_q}{\Delta\sigma_{FS,(j)}} \right)^{\xi} \ln N_R$$

where:

- N_D = Total number of stress cycles possible per year, where $1/(4\log L)$ is assumed as the zero up-crossing frequency
- $\Delta\sigma_{FS,(j)}$ = Fatigue stress range from the predominate load case at the reference probability level of exceedance of 10^{-2} , in N/mm^2
- N_R = Number of cycles corresponding to the reference probability of exceedance of 10^{-2} . $N_R = 100$.
- ξ = Weibull shape parameter, $\xi = 1$
- $\Gamma(\xi)$ = Complete Gamma function
- K_2 = Constant of the design S-N curve, as given in [Table 1](#) for in-air environment
- $\mu(j)$ = Coefficient taking into account the change of inverse slope of the S-N curve, m
- $\gamma(a, \xi)$ = Incomplete Gamma function
- $\Delta\sigma_q$ = Stress range, in N/mm^2 , corresponding to the intersection of the two segments of design S-N curve at $N = 10^7$ cycles, as given in [Table 1](#)
- Δm = Change in inverse slope of S-N curve at $N = 10^7$ cycles.
 $\Delta m = 2$

3.4 The combined fatigue damage

The combined fatigue damage is the damage accumulated in both in-air and in corrosive environment for a specific loading condition (j) during a specified design fatigue life, T_{DF} , with 100% time at sea. The combined fatigue damage for the design fatigue life, T_{DF} , for each loading condition (j) can be calculated as:

$$D_{(j)} = D_{E(j)} \cdot (T_{DF} + T_C)$$

$$T_C = T_{C,25} \cdot \frac{T_{DF}}{T_D}$$

where:

- $T_{C,25}$ = Time in corrosive environment, in years, within the duration of the design life, T_D

T_D = Design life, in years, taken as $T_D = 25$ years.

$D_{E,(j)}$ = The annual fatigue damage for in-air environment for loading condition (j).

3.5 The total fatigue damage from multiple loading conditions

Total fatigue damage within the design fatigue life, T_{DF} , is the sum of the combined fatigue damages obtained for all loading conditions and accounting for the fraction of the time at sea and the fraction in each loading condition. The total fatigue damage for all applicable loading conditions is calculated as:

$$D = f_0 \cdot \sum_{j=1}^{n_{LC}} \alpha_j \cdot D_{(j)}$$

where:

f_0 = Factor taking into account time in seagoing operations given in the rules

α_j = Fraction of time in each loading condition given in the rules

n_{LC} = Total number of loading conditions given in the rules

$D_{(j)}$ = Combined fatigue damage for each applicable loading condition.

3.6 Fatigue life

The predicted fatigue life, T_F , is based on different part times in-air and corrosive environment. For short fatigue lives less than $T_D - T_{C,25}$ years, the predicted fatigue life is based on in-air environment. For predicted fatigue lives between T_D and $T_{C,25}$, the time after $T_D - T_{C,25}$ is based on corrosive environment. For predicted fatigue lives above T_D , it is assumed that the predicted fatigue life is based on a regular maintenance intervals from the delivery of the vessel. This may be approximated by a constant annual damage rate which also reflects a relative amount of corrosive environment. The predicted fatigue life above $T_D = 25$ years is independent on design fatigue life T_{DF} (which is equal or longer than T_D). If the design fatigue life is changed at a later time due to the need for life time extension, the predicted fatigue life for the same operation area does not change. The formulation is illustrated in [Figure 3](#). The predicted fatigue life is calculated as:

$$T_F = \frac{1}{D_{air}} \quad \text{for} \quad \frac{T_{DF}}{D} \leq T_D - T_{C,25}$$

$$T_F = \frac{1}{2} \cdot \left(T_D - T_{C,25} + \frac{1}{D_{air}} \right) \quad \text{for} \quad T_D - T_{C,25} < \frac{T_{DF}}{D} \leq T_D$$

$$T_F = \frac{T_{DF}}{D} \quad \text{for} \quad \frac{T_{DF}}{D} > T_D$$

where:

$$D_{air} = f_0 \cdot \sum_{j=1}^{n_{LC}} \alpha_j \cdot D_{E,(j)}$$

and where:

D = Total damage given by [3.5]

$D_{E,(j)}$ = The annual fatigue damage for in-air environment for loading condition (j).

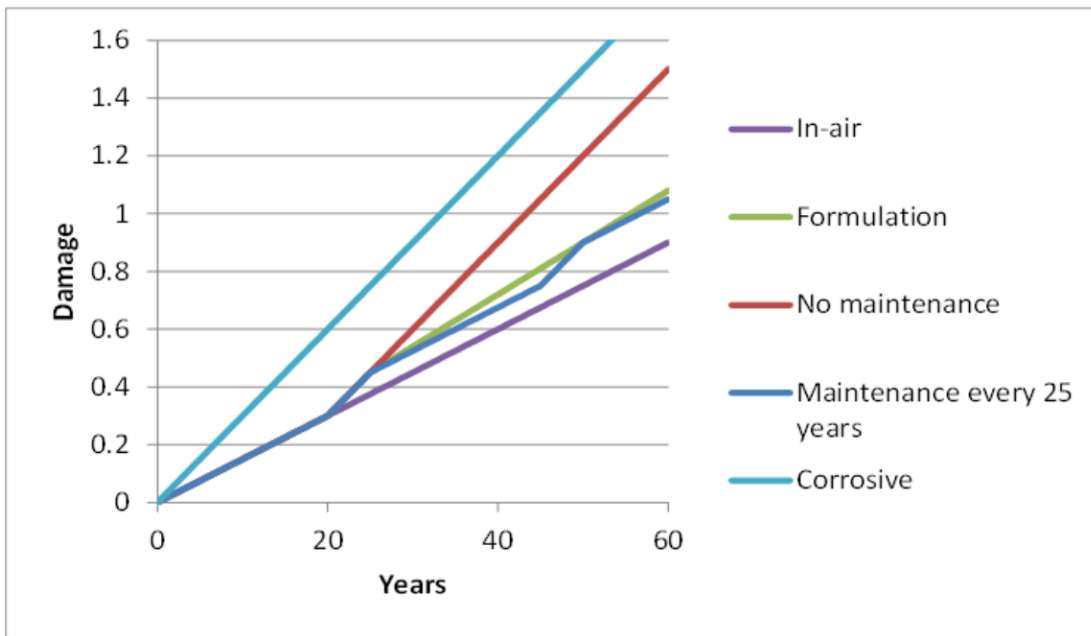


Figure 3 Illustration of fatigue damage accumulation for different assumptions of time in corrosive environment

4 Permissible stress range

The stress range should be less or equal to the permissible stress range:

$$\Delta\sigma \leq \Delta\sigma_{perm}$$

In general, the permissible stress range, $\Delta\sigma_{perm}$, can be assessed iteratively as the stress range which yields a total damage $D = 1$. However, the assessment of $\Delta\sigma_{perm}$, is limited to cases where there is only one loading condition applicable for the whole design fatigue life. However, it can be used on several loading conditions, to see which is worst. The permissible stress range at 10^{-2} probability level can be calculated as:

$$\Delta\sigma_{perm} = \frac{FAT}{f_N \cdot f_{mean} \cdot f_{thick} \cdot f_{material} \cdot f_w \cdot f_c \cdot f_e}$$

FAT	=	Reference stress, in N/mm ² , range of the S-N curve at $2 \cdot 10^6$ load cycles (FAT class), in N/mm ²
	=	Factor for the spectrum's shape (straight-line) and the number of load cycles
	=	$0.786 \log(N_D \cdot f_0 \cdot T_{DF-C}) - 4.966$ for welded details with S-N curves D, E, F and FAT according to Sec.2 Table 1
f_N	=	$0.681 \log(N_D \cdot f_0 \cdot T_{DF-C}) - 4.188$ for free plate edges with S-N curves C, C1 and C2, Sec.2 Table 1
	=	$0.6007 \log(N_D \cdot f_0 \cdot T_{DF-C}) - 3.578$ for base material with S-N curve B1 and free plate edges with S-N curves B and B2, Sec.2 Table 1.

To reflect the part time in the different environments (protected or corrosive), for the determination of f_N , the design fatigue life should be taken as:

$$T_{DF-C} = T_{DF} + T_{C,25} \cdot \frac{T_{DF}}{T_D}$$

5 Permissible stress concentration factor and required FAT class

In general, the permissible stress concentration factor or required FAT class can be estimated iteratively, yielding a total damage $D = 1$. In cases where there is only one loading condition applicable for the whole design fatigue life, the permissible stress concentration factor, K_{perm} , can be estimated as:

$$K_{perm} \leq \frac{FAT}{\Delta\sigma_n \cdot f_N \cdot f_{mean} \cdot f_{thick} \cdot f_{material} \cdot f_w \cdot f_c \cdot f_e}$$

where:

$$\Delta\sigma_n = \text{Nominal stress range of a straight-line spectrum at } 10^2 \text{ load cycles, in N/mm}^2.$$

The required reference stress range of the S-N curve at $2 \cdot 10^6$ load cycles, FAT_{req} , can be estimated as:

$$FAT_{req} \geq \Delta\sigma \cdot f_N \cdot f_{mean} \cdot f_{thick} \cdot f_{material} \cdot f_w \cdot f_c \cdot f_e$$

for nominal stress, where:

$$\Delta\sigma = \text{Nominal stress range or local stress range at free plate edge of a straight-line spectrum at } 10^2 \text{ load cycles, in N/mm}^2.$$

The estimation of K_{perm} or FAT_{req} should be limited to cases where all load components refer to the same stress concentration factor. As the stress concentration factors K for bending and axial loading of longitudinal end connections may differ, this method is not regarded applicable, or too conservative for these details. If different loading conditions should be assessed for fractions of the time of the design fatigue life, K_{perm} or FAT_{req} can only be estimated iteratively, yielding a total damage $D = 1$.

SECTION 4 PRESCRIPTIVE FATIGUE STRENGTH ASSESSMENT

1 Introduction

1.1 Stress approach for longitudinal end connections

This section outlines the prescriptive procedure to determine the stress ranges to be used in the fatigue life predictions of longitudinal end connections. The approach is based on the hot spot stress approach using equivalent design waves (EDW).

The stress ranges and mean stresses in way of each longitudinal end connection, as shown in [Figure 3](#), should be evaluated at the flange (for most details) at the following locations:

- at transverse web frames
- at transverse bulkheads (swash bulkheads or stools).

Stress concentration factors for unsymmetrical stiffener geometry and stiffener end connection geometry at two potential hot spots (point 'A' and 'B') should be applied according [App.A](#).

The hot spot stress approach uses the following:

- nominal stresses from beam theory
- stress concentration factors, K , for the different longitudinal end connections as specified in [App.A](#)
- loading conditions as specified in the rules.

1.2 Calculation procedure for longitudinal end connections

Assessment of the fatigue strength of structural members includes at least the following seven steps:

- a) Selecting type of longitudinal end connection.
- b) Calculation of wave induced loads from equivalent design waves (EDW).
- c) Calculation of stress ranges for global and local stress components for each EDW.
- d) Combination of global and local stress components for each EDW.
- e) Selection of predominate EDW, i.e. the EDW giving the highest stress range.
- f) Use of the S-N curve D.
- g) Calculation of the cumulative damage or the fatigue life.

A flow chart of the calculation procedure is given in [Figure 1](#), and includes also the case when other details than longitudinal end connections are covered by FE models. For description of FE analysis, reference is made to [Sec.6](#).

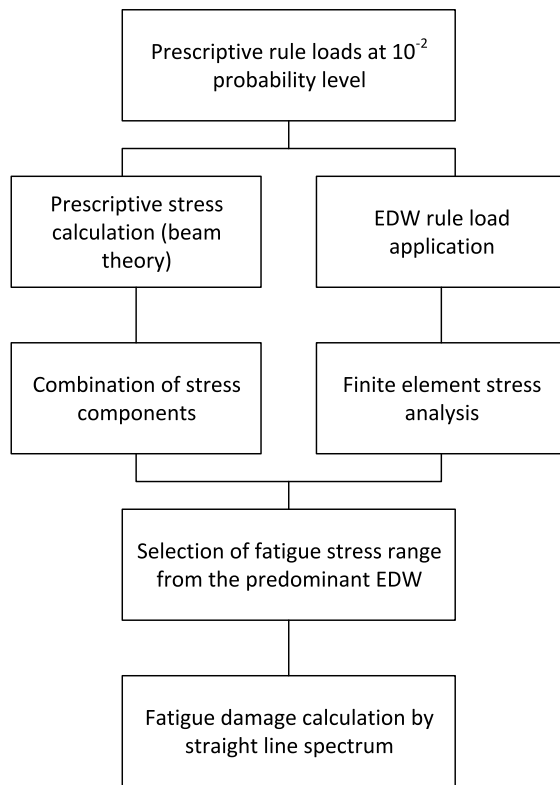


Figure 1 Flow diagram for prescriptive fatigue calculations

1.3 Definition of stress components

A schematic illustration of different stress components is given in [Figure 2](#). It shows four levels of stress components which may be relevant, i.e. from global hull girder loads, bending of primary supporting members (PSM), local stiffener bending and plate bending.

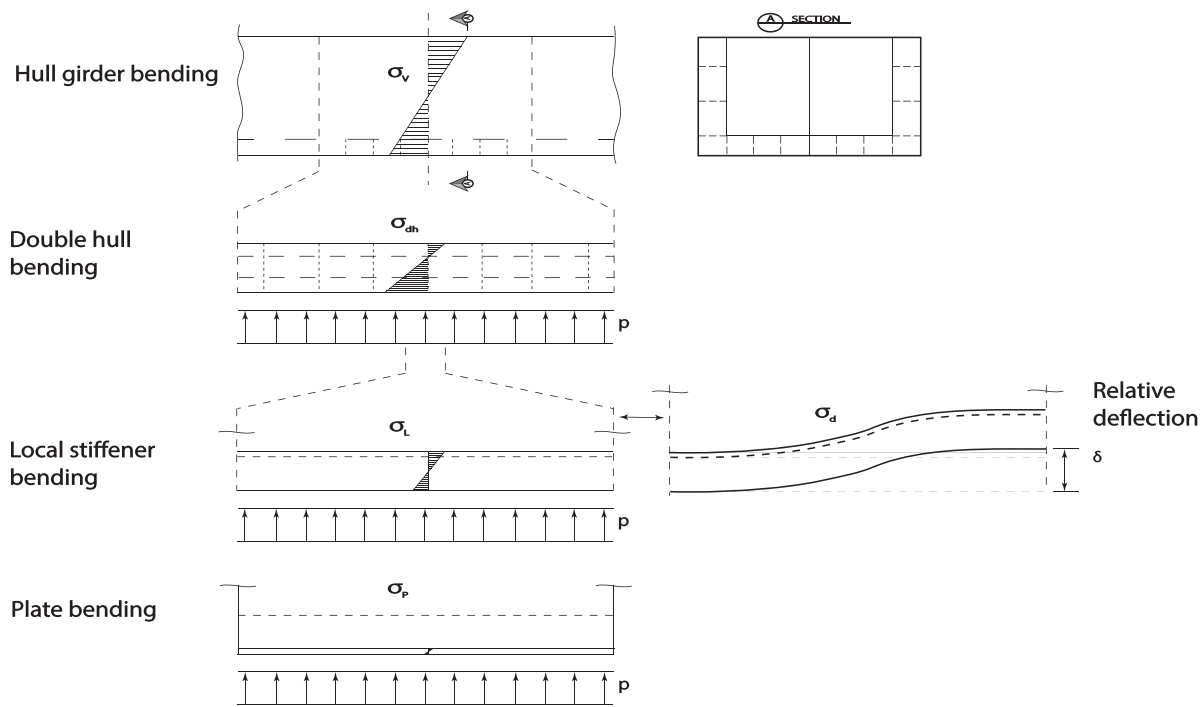


Figure 2 Definition of stress components

The dynamic global hull girder stress amplitude, in N/mm², is denoted

σ_G = wave induced hull girder stress amplitude from global loads as vertical bending, horizontal bending, torsion (warping) and axial force (the latter is neglected in prescriptive assessment).

The dynamic stress amplitude due to bending of PMS is denoted

σ_{dh} = bending stress amplitude of PSM, e.g. double hull or frame/girder grillage system, due to dynamic external and/or internal pressure loads on any side.

The dynamic local bending stress amplitudes are denoted

σ_L = local stiffener bending stress amplitude between two frames/bulkheads due to pressures/loads on any side

σ_d = local relative deflection stress between two frames/bulkheads from bending of PSM due to pressure/loads on any side

σ_p = local plate bending stress between frames or stiffeners due to pressure/loads on any side.

1.4 Calculation of stress components

The stress response in stiffeners and plating subjected to axial loading due to hull girder bending and local bending due to lateral pressures can be calculated based on beam theory combined with tabulated values of stress concentration factors. Tabulated stress concentration factors are listed in App.A. For details with a more complex stress response and/or where tabulated values of stress concentration factors are not available, the stress response should be calculated by FE analyses as described in App.E.

In general, fatigue life may be calculated based on stress induced by hull girder bending, σ_G , and stresses induced by bending of stiffeners due to lateral pressure, σ_L . Ship specific class notations, [DNVGL-RU-SHIP Pt.5](#), or additional class notations, [DNVGL-RU-SHIP Pt.6](#), may in addition require consideration of stress due to bending of primary support members and/or stresses due to relative deflection between end support of stiffeners.

For the nominal stress approach, instead of stress concentration factors, detail specific FAT classes need to be applied.

The stress formulas may be combined with prescribed loads derived according to the rules or serve as basis for determination of stress component factors for a component stochastic fatigue analysis as described in [Sec.5](#).

2 Wave induced loads

Specification of the prescriptive wave induced loads for vertical and horizontal bending, torsion (warping), external and internal pressures are given in the rules. The prescriptive wave induced loads are based on the Equivalent Design Wave (EDW) approach with loads referring to a 10^{-2} probability level of exceedance.

The prescriptive wave induced loads are used in the prescriptive fatigue analysis based on beam theory, but the EDWs may also be used for FE analysis of cargo hold, partial ship or global FE models.

3 Fatigue stress range

3.1 Hot spot stress or nominal stress

The equations in [\[3.2\]](#), [\[3.3\]](#) and [\[3.4\]](#) reflect the hot spot stress approach. This is however also applicable for the nominal stress approach. In the latter case the stress concentration factors K_a (for axial stress) and K_b (for bending stress) in the formulas in [\[4\]](#), [\[5\]](#), [\[6\]](#) and [\[7\]](#) need to be omitted. Further, the calculated stress $\Delta\sigma_{HS}$ and $\Delta\sigma_{BS}$ in [\[3.2\]](#) is replaced by the nominal stress range $\Delta\sigma_n$ and local stress range at free plate edge $\Delta\sigma_{loc}$, respectively.

3.2 Prescriptive fatigue stress range

The fatigue stress range for each load case of each loading condition needs to be determined. The stress range of each loading condition (j) to be considered is the stress range obtained from the predominant load case, according to the rules. The stress to be considered for the fatigue assessment is:

$$\Delta\sigma_{FS, (j)} = \max_i (\Delta\sigma_{FS, i(j)})$$

where:

$\Delta\sigma_{FS, i(j)}$ = fatigue stress range, in N/mm², for load case (i) of loading condition (j).

The fatigue stress range $\Delta\sigma_{FS, i(j)}$, in N/mm², corrected for mean stress effect, thickness effect, material factor, post-weld treatment and environmental factor, is taken as:

$$\begin{aligned}\Delta\sigma_{FS, i(j)} &= f_{mean, i(j)} \cdot f_{thick} \cdot f_{material} \cdot f_w \cdot f_e \cdot \Delta\sigma_{HS, i(j)} \\ \Delta\sigma_{FS, i(j)} &= f_{mean, i(j)} \cdot f_{thick} \cdot f_{material} \cdot f_e \cdot \Delta\sigma_{BS, i(j)}\end{aligned}$$

where:

$\Delta\sigma_{FS,i(j)}$	= calculated fatigue stress range for load case i in loading condition (j) , in N/mm ²
$\Delta\sigma_{HS,i(j)}$	= hot spot stress range for load case i in loading condition (j) , in N/mm ²
$\Delta\sigma_{BS,i(j)}$	= local stress range at free plate edge for load case i in loading condition (j) , in N/mm ²
$f_{mean,i(j)}$	= correction factor for mean stress for load case i in loading condition (j)
f_e	= environmental factor, see Sec.3 [2.3]
f_{thick}	= thickness effect, see Sec.2 [5]
$f_{material}$	= material factor, see Sec.2 [6]
f_w	= post-weld treatment factor, see Sec.3 [2.4].

The correction factor for the mean stress effect for welded joints is calculated as:

$$f_{mean,i(j)} = \begin{cases} \min\left[1.0; \left(0.9 + 0.2 \frac{\sigma_{mean,i(j)}}{2 \cdot f_e \cdot \Delta\sigma_{HS,i(j)}}\right)\right] & \text{for } (\sigma_{mean,i(j)} \geq 0) \\ \max\left[0.7; \left(0.9 + 0.4 \frac{\sigma_{mean,i(j)}}{2 \cdot f_e \cdot \Delta\sigma_{HS,i(j)}}\right)\right] & \text{for } (\sigma_{mean,i(j)} < 0) \end{cases}$$

where

$$\sigma_{mean,i(j)} = \text{fatigue mean stress for the welded joints for load case } i \text{ in loading condition } (j), \text{ in N/mm}^2.$$

For the application of mean stress effect for welded joints, see Sec.2 [4.2].

For the base material free plate edge, then the mean stress effect is estimated as:

$$f_{mean,i(j)} = \begin{cases} \min\left[1.0; \left(0.8 + 0.4 \frac{\sigma_{mean,i(j)}}{2 \cdot f_e \cdot \Delta\sigma_{BS,i(j)}}\right)\right] & \text{for } (\sigma_{mean,i(j)} \geq 0) \\ \max\left[0.6; \left(0.8 + 0.4 \frac{\sigma_{mean,i(j)}}{2 \cdot f_e \cdot \Delta\sigma_{BS,i(j)}}\right)\right] & \text{for } (\sigma_{mean,i(j)} < 0) \end{cases}$$

3.3 Stress range

The stress range, in N/mm², due to dynamic (wave induced) loads for load case (i) of loading condition (j) is obtained from the following formula:

$$\Delta\sigma_{HS,i(j)} = |-(\sigma_{GD,i2(j)} + \sigma_{LD,i2(j)} + \sigma_{dD,i2(j)} + \sigma_{dhD,i2(j)}) + (\sigma_{GD,i1(j)} + \sigma_{LD,i1(j)} + \sigma_{dD,i1(j)} + \sigma_{dhD,i1(j)})|$$

where:

$$\sigma_{GD,i1(j)}, \sigma_{GD,i2(j)} = \text{stresses due to wave induced hull girder loads, in N/mm}^2, \text{ as defined in [4.1]}$$

$$\sigma_{LD,i1(j)}, \sigma_{LD,i2(j)} = \text{stresses due to wave induced local bending, in N/mm}^2, \text{ as defined in [6.1]}$$

$\sigma_{dD,i1(j)}, \sigma_{dD,i2(j)}$ = stresses due to wave induced relative displacement, in N/mm², as defined in [7.7]

$\sigma_{dhD,i1(j)}, \sigma_{dhD,i2(j)}$ = stresses due to wave induced bending of PSM, in N/mm², as defined in [5.1].

3.4 Mean stress

The mean stress, in N/mm², due to static and dynamic loads for load case (*i*) of loading condition (*j*) is obtained from the following formula:

$$\sigma_{mean, i(j)} = \sigma_{GS, (j)} + \sigma_{LS, (j)} + \sigma_{dS, (j)} + \sigma_{dhS, (j)} + \sigma_{mGD, i(j)} + \sigma_{mLD, i(j)} + \sigma_{mdD, i(j)} + \sigma_{mdhD, i(j)}$$

$$\sigma_{mGD, i(j)} = \frac{\sigma_{GD, i1(j)} + \sigma_{GD, i2(j)}}{2}$$

$$\sigma_{mLD, i(j)} = \frac{\sigma_{LD, i1(j)} + \sigma_{LD, i2(j)}}{2}$$

$$\sigma_{mdD, i(j)} = \frac{\sigma_{dD, i1(j)} + \sigma_{dD, i2(j)}}{2}$$

$$\sigma_{mdhD, i(j)} = \frac{\sigma_{dhD, i1(j)} + \sigma_{dhD, i2(j)}}{2}$$

where:

- $\sigma_{GS, (j)}$ = stress due to still water hull girder bending moment, in N/mm², as defined in [4.3]
- $\sigma_{LS, (j)}$ = stress due to still water local bending, in N/mm², as defined in [6.2]
- $\sigma_{dS, (j)}$ = stress due to still water relative displacement, in N/mm², as defined in [4.3]
- $\sigma_{dhS, (j)}$ = stress due to still water bending of PSM, in N/mm², as defined in [5.2]
- $\sigma_{mLD, i(j)}$ = mean stress contribution due to wave induced local bending, in N/mm², as defined above
- $\sigma_{LD, i1(j)}, \sigma_{LD, i2(j)}$ = stresses due to wave induced local bending, in N/mm², as defined in [6.1]
- $\sigma_{mGD, i(j)}$ = mean stress contribution due to wave induced hull girder loads, in N/mm², as defined above
- $\sigma_{GD, i1(j)}, \sigma_{GD, i2(j)}$ = stresses due to wave induced hull girder loads, in N/mm², as defined in [4.1]
- $\sigma_{mdD, i(j)}$ = mean stress contribution due to relative deflection, in N/mm², as defined above
- $\sigma_{dD, i1(j)}, \sigma_{dD, i2(j)}$ = stresses due to wave induced relative deflection, in N/mm², as defined in [7.5]
- $\sigma_{mdhD, i(j)}$ = mean stress contribution due to bending of PSM, in N/mm², as defined above

$\sigma_{dhD,i1(j)}$, $\sigma_{dhD,i2(j)}$ = stresses due to wave induced bending of PSM, in N/mm², as defined in [5].

4 Global hull girder stress

4.1 Stress due to wave induced hull girder loads

The hull girder hot spot stress (or nominal stress with $K_a = 1$), in N/mm², for maximum and minimum load component $i1$ and $i2$ (load case i) of loading condition (j) is obtained from the following formula:

$$\sigma_{GD, ik(j)} = f_c \cdot K_a \left(\frac{M_{wv-LC, ik}}{I_{y-n50}} (z - z_n) - \frac{M_{wh-LC, ik}}{I_{z-n50}} y + \frac{M_{\sigma-wt-LC, ik} \cdot \omega_{i-n50}}{I_{\omega-n50}} \right) 10^{-3}$$

where:

- $M_{wv-LC, ik}$ = vertical wave bending moment, in kNm, for load case i in loading condition (j) for maximum and minimum load component k (i.e snap shot 1 or 2)
- $M_{wh-LC, ik}$ = horizontal wave bending moment, in kNm, for load case i in loading condition (j) for maximum and minimum load component k
- $M_{\sigma-wt-LC, ik}$ = dynamic bi-moment related to warping stresses, in kNm², for load case i in loading condition (j) for maximum and minimum load component k
- $I_{\omega-n50}$ = net sectional moment of inertia, in m⁶, of the hull transverse cross section
- ω_{i-n50} = net sectorial coordinate, in m², of the point being considered in the transverse cross section.

$M_{\sigma-wt-LC, ik}$ is only relevant for vessels with large deck openings according to definition in the rules, and may apply to container vessels, general cargo vessels, multi purpose vessels and bulk carriers.

4.2 Hull girder vibrations

In addition to the wave induced hull girder stresses, the waves induced hull girder vibrations cause additional hull girder stresses. Guidance on the how to account for the effect of wave induced vibration for blunt ships (e.g. tankers, bulk carriers and ore carriers) is given in App.I and for container vessels in DNVGL-CG-0153, *Fatigue and ultimate strength assessment of container ships including the effect of whipping and springing*.

4.3 Stress due to still water hull girder bending moment

The hull girder hot spot stress or nominal stress (with $K_a = 1$) due to still water bending moment, in N/mm², in loading condition (j) is obtained from the following formula:

$$\sigma_{GS, (j)} = \frac{f_c \cdot K_a \cdot \beta_{(j)} \cdot M_{sw} \cdot (z - z_n)}{I_{y-n50}} 10^{-3}$$

where:

- M_{sw} = permissible still water vertical bending moment, in kNm
- $\beta_{(j)}$ = fraction of permissible still water vertical bending moment for loading condition (j) .

The fraction of permissible still water vertical bending moment, $\beta_{(j)}$, for standard ship types are given in the rules.

Static warping stresses are neglected for vessels with large deck openings, like container vessels, since the still water torsion moment can either be positive or negative and in average zero, thereby giving zero static warping stress in average. Zero stress from horizontal static bending moment is also assumed in even keel condition.

5 Stress due to bending of PSM

5.1 General

Stresses in PSM are the results of bending of single skin or double hull structures between transverse bulkheads and due to lateral pressure or loads, see [Figure 2](#). The bending stress should be determined by FE analysis or 3(2)-dimensional grillage analysis. Prescriptive (analytical) methods cover a limited amount of structural configurations.

The stresses in PSM should be calculated for external and internal loads. The loads to be used should be determined at the mid-position between the transverse bulkheads.

In the prescriptive assessment the bending stress of PSM may be included, where relevant, when relative deflection stress is included.

Prescriptive estimate of the stress of PSM from double hull bending based on analytical method is given in [App.D](#).

6 Local stiffener bending stress

6.1 General

Local stiffener bending should be included whenever lateral pressure is acting on one or both sides of the panel, with the following exception:

- for the external deck, longitudinal stiffeners with air pipe just above the same deck no internal tank pressure should be considered.

6.2 Wave induced stiffener bending stress

The hot spot stress, in N/mm², due to local dynamic pressure in maximum and minimum load component $i1$ and $i2$ (load case i) for loading condition (j) , $\sigma_{LD, ik(j)}$, is obtained from the following formula:

$$\sigma_{LD, ik(j)} = \frac{K_b K_n^{sc} \ell_{bdg}^2 \left(\eta_W f_{NL} P_W, ik(j) + \eta_{ld} P_{ld, ik(j)} + \eta_{bd} P_{bd, ik(j)} \right) \left(1 - \frac{6x_e}{\ell_{bdg}} + \frac{6x_e^2}{\ell_{bdg}^2} \right)}{12Z_{eff} - n50}$$

$$\begin{aligned}
f_{NL} &= 1 && \text{for } z > T_{LC} + 2h_w \\
f_{NL} &= 2.5 \frac{z - T_{LC}}{h_w} - 4 && \text{for } T_{LC} + 1.8h_w < z \leq T_{LC} + 2h_w \\
f_{NL} &= 0.5 \frac{z - T_{LC}}{h_w} - 0.4 && \text{for } T_{LC} + 1.6h_w < z \leq T_{LC} + 1.8h_w \\
f_{NL} &= 0.4 && \text{for } T_{LC} + 1.2h_w < z \leq T_{LC} + 1.6h_w \\
f_{NL} &= 0.7 - 0.25 \frac{z - T_{LC}}{h_w} && \text{for } T_{LC} + 0.6h_w < z \leq T_{LC} + 1.2h_w \\
f_{NL} &= 1 - 0.75 \frac{z - T_{LC}}{h_w} && \text{for } T_{LC} - 0.2h_w < z \leq T_{LC} + 0.6h_w \\
f_{NL} &= 0.1875 \frac{z - T_{LC}}{h_w} + 1.1875 && \text{for } T_{LC} - h_w < z \leq T_{LC} - 0.2h_w \\
f_{NL} &= 1 && \text{for } z \leq T_{LC} - h_w
\end{aligned}$$

$$b_{eff} = s \cdot \min \left(\frac{\frac{1.04}{3}; 1.0}{1 + \frac{\left(\frac{\ell_{bdg}}{s} \left(1 - \frac{1}{\sqrt{3}} \right) \cdot 10^3 \right)^{1.35}}{\left(\frac{\ell_{bdg}}{s} \left(1 - \frac{1}{\sqrt{3}} \right) \cdot 10^3 \right)^{1.35}}} \right) \quad \text{for } \frac{\ell_{bdg}}{s} \left(1 - \frac{1}{\sqrt{3}} \right) \times 10^3 \geq 1$$

$$b_{eff} = 0.26 \ell_{bdg} \left(1 - \frac{1}{\sqrt{3}} \right) \times 10^3 \quad \text{for } \frac{\ell_{bdg}}{s} \left(1 - \frac{1}{\sqrt{3}} \right) \times 10^3 < 1$$

where:

- $P_{W,ik(j)}$ = dynamic wave pressure, at the mid span, in kN/m^2 , for load case i in loading condition (j) for maximum and minimum load component k (i.e snap shot 1 or 2).
- $P_{ld, ik(j)}$ = dynamic liquid tank pressure, at the mid span, in kN/m^2 , for load case i in loading condition (j) for maximum and minimum load component k . Pressure from different tanks acting on both sides of the stiffener should be simultaneously considered if relevant in the loading condition.
- $P_{bd, ik(j)}$ = dynamic dry bulk cargo pressure at the mid span, in kN/m^2 , for load case i in loading condition (j) for maximum and minimum load component k .
- $\eta_w, \eta_{ld}, \eta_{bd}$ = pressure normal coefficients, taken as:
 $= 1$ when the considered pressure is applied on the stiffener side
 $= -1$ otherwise
- f_{NL} = correction factor for the non-linearity of the wave pressure as taken above
- h_w = water head equivalent to the pressure at waterline, in m
- x_e = distance, in m, to the hot spot from the closest end of the span ℓ_{bdg} , as defined in Figure 3

- ℓ_{bdg} = effective bending span of stiffener, in m
- $Z_{eff-n50}$ = net section modulus, in cm^3 , of the considered stiffener calculated considering an effective flange b_{eff} of attached plating. Z_{eff-50} is taken at the stiffener flange. however, for detail 32 in [App.A Table 1](#) the Z_{eff-50} should be calculated at a height h_{HS} above the plate flange as shown in [App.A Figure 1](#). The axial stress from the hull girder shall then also be estimated for this hot spot point rather than at the stiffener flange.
- b_{eff} = effective flange, in mm, of attached plating specified at the ends of the span and in way of end brackets and supports, taken as above
- c = c_a or c_f , according to [\[7.7\]](#), when hot spot is located aft or forward, respectively, of a bulkhead and when relative deflection is included, otherwise $c = 1.0$.

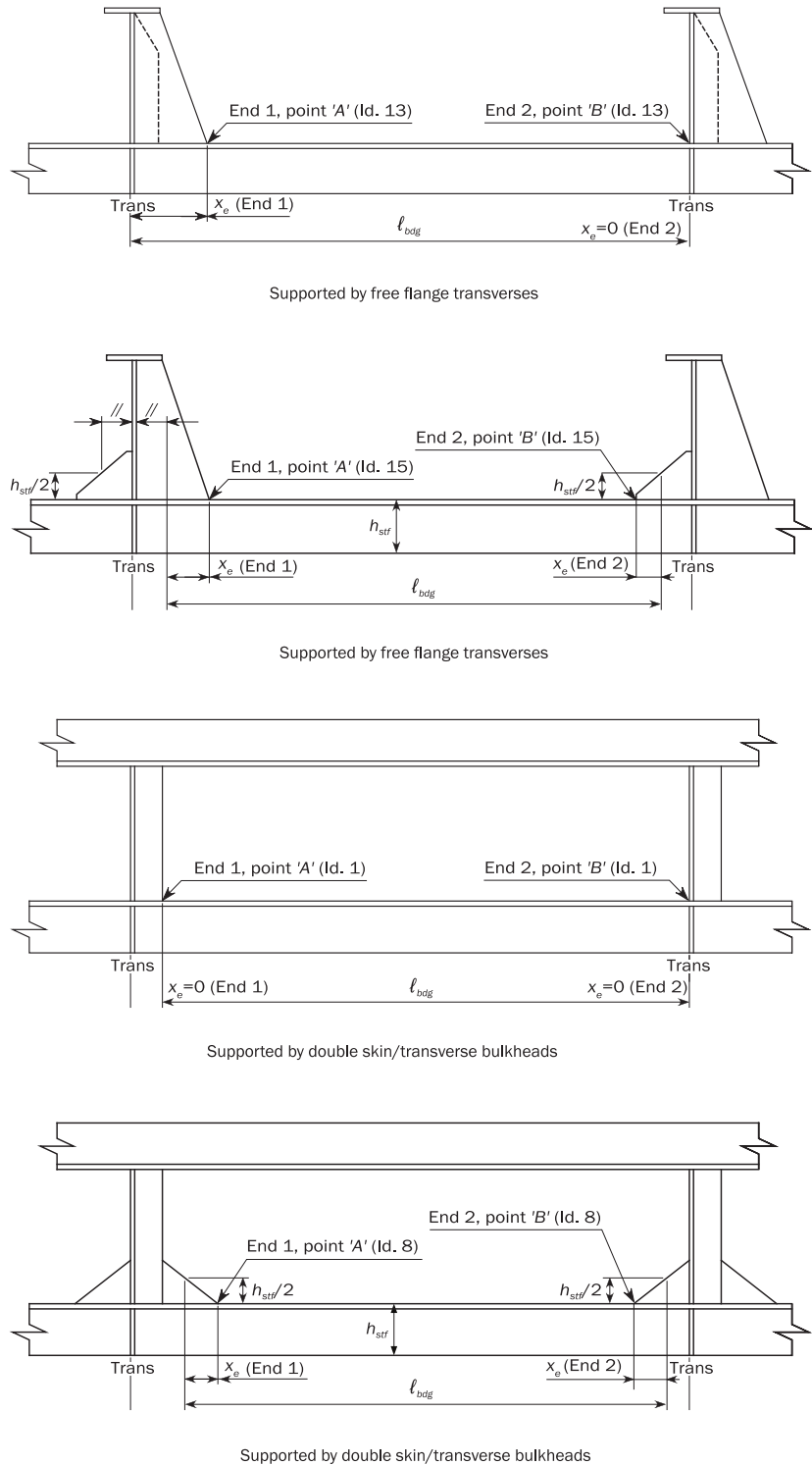


Figure 3 Definition of effective span and x_e for hot spot

6.3 Still water stiffener bending stress

The hot spot stress due to local static pressure, in N/mm², for loading condition (j), $\sigma_{LS,(j)}$, is obtained from the following formula:

$$\sigma_{LS,(j)} = \frac{K_b K_n^{sc} \ell_{bdg}^2 \left(\eta_S P_{S,(j)} + \eta_{ls} P_{ls,(j)} + \eta_{bs} P_{bs,(j)} \right) \left[1 - \frac{6x_e}{\ell_{bdg}} + \frac{6x_e^2}{\ell_{bdg}^2} \right]}{12Z_{eff} - n50}$$

where:

- $P_{S,(j)}$ = static external pressure, in kN/m², in loading condition (j)
- $P_{ls,(j)}$ = static liquid tank pressure, in kN/m², in loading condition (j). Pressure acting on both sides should be simultaneously considered if relevant in the loading condition
- $P_{bs,(j)}$ = static dry bulk cargo pressure, in kN/m², in loading condition (j)
- pressure normal coefficients, taken as:
- $\eta_S, \eta_{ls}, \eta_{bs}$ = $\eta = 1$ when the considered pressure is applied on the stiffener side,
 $\eta = -1$ otherwise.

7 Local relative deflection stress

7.1 General

For longitudinal end connections located at transverse bulkheads (or restrained frames), the additional stress due to the relative deflection should be considered.

7.2 Relative deflection definition

The relative deflection is defined as the lateral displacement of the stiffener measured at the frame forward (Fwd) or afterward (Aft) relative to the displacement at the transverse bulkhead (or restrained frame).

7.3 Sign convention

The sign of the relative deflection is positive when the stress at the hot spot is in tension. The hot spot is associated with the stress in the flange of the stiffener at the transverse bulkhead (or restrained frame).

7.4 Estimate of relative deflection

The relative deflection or stress from relative deflection can be estimated by prescriptive formulations or from FEM analysis, e.g.:

- from partial ship or cargo hold FE model where the relative deflection is derived and the stress is estimated by the formulation in [7.5]
- prescriptive method of relative deflection stress as described in App.D when applicable.

A FE model is generally more applicable and should be used when available.

7.5 Prescriptive stress due to relative deflection derived by FE analysis

The relative deflection stress can be calculated based on relative deflection derived from FE analysis. In the estimate of the relative deflection from FE analysis, the local rotation at the position of the hot spot needs to be accounted for.

7.5.1 Simplified transverse bulkhead configuration

For a simplified transverse bulkhead configuration as illustrated in [Figure 4](#), the stress due to relative deflection, in N/mm², for load case *i1* and *i2* of loading condition (*j*) for both locations 'a' and 'f' should be calculated directly using the following expression:

$$\sigma_{dD, ik(j)} = \begin{cases} K_b \sigma_{dFwd-a, ik(j)} + K_b \sigma_{dAft-a, ik(j)} & \text{for location "a"} \\ K_b \sigma_{dFwd-f, ik(j)} + K_b \sigma_{dAft-f, ik(j)} & \text{for location "f"} \end{cases} \quad (k = 1, 2)$$

$$\sigma_{dFwd-a, ik(j)} = \frac{3.9\delta_{Fwd, ik(j)} EI_{Aft-n50} I_{Fwd-n50}}{Z_{Aft-n50} \ell_{Fwd} (\ell_{Aft} I_{Fwd-n50} + \ell_{Fwd} I_{Aft-n50})} \left(1 - 1.15 \frac{|x_{eAft}|}{\ell_{Aft}} \right) 10^{-5}$$

$$\sigma_{dAft-a, ik(j)} = \left[\frac{3.9\delta_{Aft, ik(j)} EI_{Aft-n50} I_{Fwd-n50}}{Z_{Aft-n50} \ell_{Aft} (\ell_{Aft} I_{Fwd-n50} + \ell_{Fwd} I_{Aft-n50})} \left(1 - 1.15 \frac{|x_{eAft}|}{\ell_{Aft}} \right) \right] 10^{-5} - \left[\frac{0.9\delta_{Aft, ik(j)} EI_{Aft-n50} |x_{eAft}|}{Z_{Aft-n50} \ell_{Aft}^3} \right] 10^{-5}$$

$$\sigma_{dFwd-f, ik(j)} = \left[\frac{3.9\delta_{Fwd, ik(j)} EI_{Aft-n50} I_{Fwd-n50}}{Z_{Fwd-n50} \ell_{Fwd} (\ell_{Aft} I_{Fwd-n50} + \ell_{Fwd} I_{Aft-n50})} \left(1 - 1.15 \frac{|x_{eFwd}|}{\ell_{Fwd}} \right) \right] 10^{-5} - \left[\frac{0.9\delta_{Fwd, ik(j)} EI_{Fwd-n50} |x_{eFwd}|}{Z_{Fwd-n50} \ell_{Fwd}^3} \right] 10^{-5}$$

$$\sigma_{dAft-f, ik(j)} = \frac{3.9\delta_{Aft, ik(j)} EI_{Aft-n50} I_{Fwd-n50}}{Z_{Fwd-n50} \ell_{Aft} (\ell_{Aft} I_{Fwd-n50} + \ell_{Fwd} I_{Aft-n50})} \left(1 - 1.15 \frac{|x_{eFwd}|}{\ell_{Fwd}} \right) 10^{-5}$$

where:

- a, f = suffix which denotes the location as indicated in [Figure 4](#)
- Aft, Fwd = suffix which denotes the direction, afterward (Aft) or forward (Fwd), from the transverse bulkhead. as shown in [Figure 4](#)
- K_b = stress concentration factor due to bending for the location 'a' or 'f' which may correspond to points 'A' or 'B' as defined in [App.A](#)

- $\sigma_{dFwd-a,ik(j)}$ = additional stress at location 'a' and 'f', in N/mm², due to the relative displacement between the transverse bulkhead including swash bulkhead or floors in way of stool and the forward (Fwd) and afterward (Aft) transverse web or floor respectively for load case i1 and i2 of loading condition (j), taken as above:
- $I_{Fwd-n50}$ = net moment of inertia, in cm⁴, of forward (Fwd) and afterward (Aft) stiffener based on effective breadth according to DNVGL-RU-SHIP Pt.3 Ch.3 Sec.7 [1.3.1]
- $Z_{Fwd-n50}$ = net section modulus of forward (Fwd) and afterward (Aft) stiffener, in cm³.
- $Z_{Aft-n50}$
- ℓ_{Fwd}, ℓ_{Aft} = span, in m, of forward (Fwd) and afterward (Aft) stiffener, as shown in Figure 4
- x_{eFwd}, x_{eAft} = distance, in m, as shown in Figure 3, to the hot spot in location 'a' or 'f' from the closest end of ℓ_{Fwd} and ℓ_{Aft} respectively
- $\delta_{Fwd,ik(j)}, \delta_{Aft,ik(j)}$ = relative displacement in the direction perpendicular to the attached plate, in mm, between the transverse bulkhead (including swash bulkhead or floor in way of stools) and the forward (Fwd) or afterward (Aft) transverse web (or floor) as shown in Figure 4

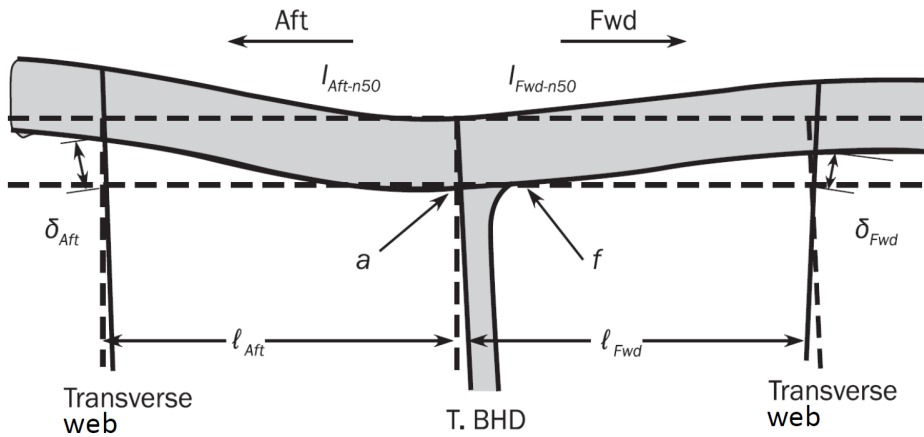


Figure 4 Definition of the relative displacement of a stiffener between transverse bulkhead and adjacent web frames

7.5.2 Stiffeners with clamped ends

When the stiffener is clamped by a stringer plate or by a bracket, as illustrated in Figure 5, causing the effective bending span ℓ_{bdg} of the adjoining stiffener to be less than 80% of its unsupported span ℓ , e.g. in way of the transverse bulkhead, the stress due to relative deflection, in N/mm², for load case i1 and i2 of loading condition (j) for locations 'a' and 'f' should be calculated using the following expression:

$$\sigma_{dD, ik(j)} = \begin{cases} K_b \sigma_{dAft - a, ik(j)} & \text{for location 'a'} \\ K_b \sigma_{dFwd - f, ik(j)} & \text{for location 'f'} \end{cases} \quad (k = 1, 2)$$

$$\sigma_{dAft - a, ik(j)} = \left[\frac{3.9 \delta_{Aft, ik(j)} EI_{Aft - n50}}{Z_{Aft - n50} \ell_{Aft}^2} \left(1 - 1.15 \frac{|x_{eAft}|}{\ell_{Aft}} \right) \right] 10^{-5}$$

$$\sigma_{dFwd-f, ik(j)} = \left[\frac{3.9\delta_{Fwd, ik(j)} EI_{Fwd} - n50}{z_{Fwd} - n50 \ell_{Fwd}^2} \left(1 - 1.15 \frac{|x_{eFwd}|}{\ell_{Fwd}} \right) \right] 10^{-5}$$

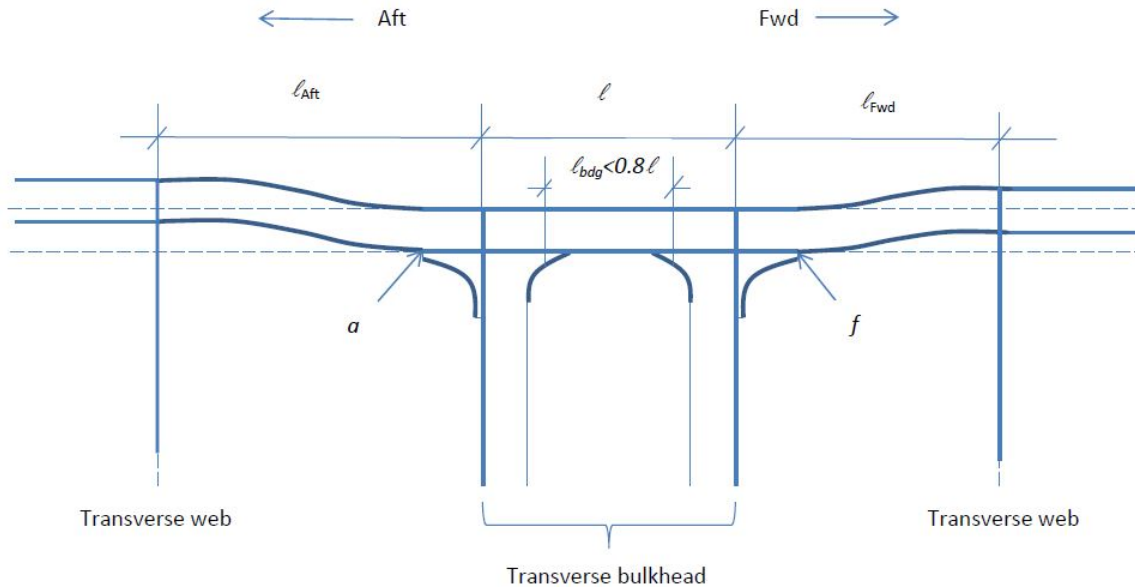


Figure 5 Definitions for the calculation of stress due to relative displacement for a stiffener clamped by a stringer plate or bracket

Hot spots on the stiffener at ends of brackets, leading to an effective bending span ℓ_{bdg} of the stiffener of less than 80% of its unsupported span ℓ , should not be assessed by the methods given in [7.5.1]. If such design cannot be avoided by, e.g. using stringer plates, the hot spot stress should be calculated using a hot spot FE model, see [Sec.6](#).

7.6 Stress due to relative displacement in still water

The additional hot spot stress, in N/mm², in still water, due to the relative displacement is obtained according to procedures in [7.5] or [7.7] replacing the dynamic local stress σ_{dD} and dynamic pressure with static local stress σ_{dS} and static pressure.

7.7 Correction of local stiffener bending stress

When the stiffener lengths (e.g. at the transverse bulkhead) differ within the range $0.25 \leq \ell_{bdg, Aft} / \ell_{bdg, Fwd} \leq 4$, the local stiffener bending stress in [6] needs to be corrected at the location where the additional stress from relative displacement is calculated. However, when the stiffener, e.g. in way of the transverse bulkhead, is clamped by a stringer plate or by a bracket causing the effective bending span ℓ_{bdg} of the adjacent stiffener to be less than 80% of its unsupported span ℓ , the local stiffener bending stress should not be corrected. The corrected stiffener bending stress due to local pressure can be calculated using correction factors, c_a , aft and, c_f , forward of the transverse bulkhead as follows:

$$c_a = \left(\frac{\ell_{bdg, Fwd}}{\ell_{bdg, Aft}} \right)^2 - \left(\frac{\ell_{bdg, Fwd}}{\ell_{bdg, Aft}} \right) + 1.0$$

$$c_f = \left(\frac{\ell_{bdg, Aft}}{\ell_{bdg, Fwd}} \right)^2 - \left(\frac{\ell_{bdg, Aft}}{\ell_{bdg, Fwd}} \right) + 1.0$$

8 Stress concentration factors

8.1 Longitudinal end connections

The stress concentration factors K_a and K_b are given in [App.A Table 1](#) for end connection of stiffeners subjected to axial and lateral loads, respectively.

The values for soft toe are valid provided the toe geometry complies with [App.A \[2.2\]](#). The stress concentration factor K_b given for lateral loads should be used also for stress due to relative displacements.

For end connections without top stiffener, e.g. detail 31 and 32, a recommended design is given by the design standard A and B in [Sec.8 \[2.2\]](#) and [Sec.8 \[2.1\]](#), respectively.

8.2 Other connection types and overlapped connections

When connection types other than those given in [App.A](#) are proposed, the fatigue strength for the proposed connection type may be assessed by a FE hot spot analysis as described in [Sec.6](#) to obtain directly the hot spot stress. Alternatively, the stress concentration factor can be calculated using FE analysis according to [App.E \[6\]](#).

Overlapped connection types for stiffeners, i.e. attachments welded to the web of the stiffeners (e.g. struts), are regarded as unconventional design. If it is used, a hot spot model is needed to establish the stress concentration factors, alternatively an additional stress concentration factor of 1.15 should be added to the K -factors in [App.A](#).

SECTION 5 DIRECT FATIGUE STRENGTH ASSESSMENT

1 General

1.1 Definition

Direct fatigue strength assessment is based on directly calculated wave loads for selected loading conditions and for a specific wave environment. The stress may be estimated by beam theory or finite element analysis.

Reference is made to the [DNVGL-CG-0130, Wave load analysis](#), for conditions to be used in the hydrodynamic analysis and to [DNVGL-CG-0127, Finite element analysis](#) for modelling and load application of global FE models.

1.2 Stress transfer functions

The linear hydrodynamic analysis in the frequency domain is referred to as spectral analysis. The aim of spectral fatigue calculations should establish complex stress transfer functions through direct wave load analysis combined with stress response analyses. The stress transfer functions express the relation between the wave heading and frequency and the stress response at a specific location in the structure. The stress transfer functions may be determined either by

- component stochastic analysis, see [3]
- full stochastic analysis, see [4].

1.3 Assumptions

Spectral fatigue calculations imply that the simultaneous occurrence of the different load effects are preserved through the calculations, and the uncertainties are reduced compared to prescriptive calculations. The fatigue strength assessment includes the following assumptions:

- wave climate represented by scatter diagram
- wave heading distribution relative to the ship
- a speed profile which may depend on the sea state and heading
- probability distribution of amplitudes (e.g. Rayleigh/Rice) applied to the stresses within each short term condition (sea state)
- cycle counting consistently with the probability distribution for the short term stress response
- linear cumulative summation of damage contributions from each sea state in the wave scatter diagram when the fatigue damage is calculated.

1.4 Hydrodynamic theory

The spectral method assumes linear load effects and responses. The hydrodynamic loads should be calculated using 3D potential theory, which gives a better estimate of flow field towards the ends of the ship ends. A benefit is also that the axial stress from the axial force component can be included.

Non-linear effects due to large amplitude motions and large waves can be neglected in the fatigue analysis, since the stress ranges at lower load levels dominate the fatigue damage. In order to determine the roll damping or intermittent wet and dry surfaces in the splash zone, the linearization should be performed at a load level which dominates the fatigue damage.

Hydrodynamic analysis is carried out to obtain transfer functions, $H(\omega, \beta)$, of the load components, which will be used in the component stochastic. For full stochastic analysis, the internal and external pressures and accelerations (inertia) are directly transferred to the FE model to establish directly the stress transfer function for each node or element, $H(\omega, \beta)$. In the transfer function ω refers to the encounter frequency and β refers to the relative heading angle between the ship and the incident waves. The procedures are explained more in

detail in DNVGL CG 0130, *Wave load analysis*, which covers the hydrodynamic analysis procedures and the wave environment conditions.

2 Fatigue strength assessment

2.1 Fatigue damage calculations

When the long term stress range distribution is defined through a short term Rayleigh distribution within each short term sea state, the fatigue damage for bi-linear S-N curves is given in App.C [2.5].

It should be noted that the stress in the direct calculations should account for different corrections as given in Sec.3 [2.5]. If the stress is directly estimated from the FE, then the K_m factor in Sec.6 [1.6] needs to be accounted for in the case of welded details.

Alternative fatigue strength representations can be useful for axially loaded details or where axial loads dominates, e.g.

- permissible peak stress range (for single loading condition)
- permissible stress concentration factor
- required FAT class

as explained in Sec.3 [4] and Sec.3 [5].

3 Component stochastic analysis

Component stochastic calculations can be used for fatigue assessment of all details exposed to well defined load components, in particular longitudinal end connections. The procedure is based on combining load transfer functions from wave load analysis with stress factors, i.e. stress per unit load. A flow diagram of the calculation procedure is given in Figure 1.

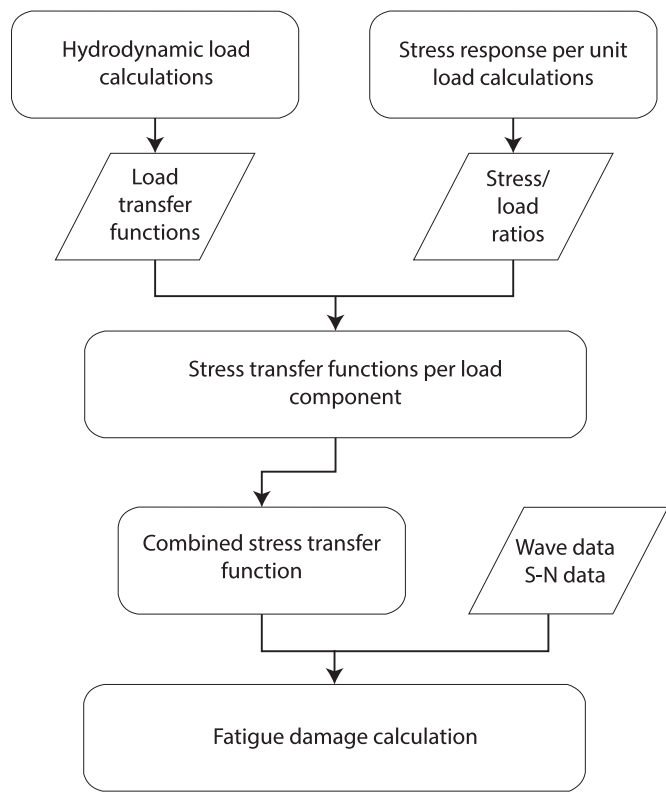


Figure 1 Flow diagram for component stochastic fatigue calculations

3.1 Load components

The load transfer functions to be considered can include:

- vertical hull girder bending moment
- horizontal hull girder bending moment
- hull girder axial force
- torsional moments
- external (panel) pressures
- internal pressure due to dynamic gravity components from vessel motions and due to inertia forces from accelerations.

Load transfer functions for internal cargo and ballast fluid pressures due to accelerations in x-, y- and z-direction are derived from the vessel motions:

$$\begin{aligned}
 H_{p,ax}(\omega|\beta) &= \rho \cdot x_s \cdot H_{ax}(\omega|\beta) \\
 H_{p,ay}(\omega|\beta) &= \rho \cdot y_s \cdot H_{ay}(\omega|\beta) \\
 H_{p,az}(\omega|\beta) &= \rho \cdot z_s \cdot H_{az}(\omega|\beta)
 \end{aligned}$$

where x_s , y_s and z_s is the distance from the centre of free liquid surface to the load point in x-, y- and z-direction defined by the coordinate of the free surface centre minus the coordinate of the load point.

The acceleration transfer functions should be determined in the tank centre of gravity and include the gravity component due to pitch and roll motions. The gravity components are expressed as:

$$H_{p,axg}(\omega|\beta) = -g\sin\varphi \approx -g\varphi$$

$$H_{p,ayg}(\omega|\beta) = g\sin\theta \approx g\theta$$

3.2 From load to stress transfer functions

For each load transfer function, the corresponding stress transfer function is determined as

$$H_{\sigma,k}(\omega|\beta) = A_k \cdot H_k(\omega|\beta)$$

where:

A_k = stress/load ratio for load component k

$H_k(\omega|\beta)$ = load transfer function for load component k .

The combined stress response is determined by a linear complex summation of the n number of stress transfer functions

$$H_{\sigma}(\omega|\beta) = \sum_{k=1}^n H_{\sigma,k}(\omega|\beta)$$

3.3 Stress factors per unit load

The following stress component factors may be relevant to determine the combined stress in stiffeners and plating:

A_1 = axial stress per unit vertical hull girder bending moment

A_2 = axial stress per unit horizontal hull girder bending moment

A_3 = axial stress per unit global axial force

A_4 = warping stress per unit bi-moment (from torsion) for vessels with open deck structure

A_5 = bending stress per unit local external pressure

A_6 = bending stress per unit local internal pressure (to be combined with accelerations in x-, y- and z-direction)

A_7 = axial stress due to double hull bending per unit external pressure

A_8 = axial stress due to double hull bending per unit internal pressure (to be combined with accelerations in x-, y- and z-direction)

A_9 = bending stress due to relative deflection per unit external pressure

A_{10} = bending stress due to relative deflection per unit internal pressure (to be combined with accelerations in x-, y- and z-direction)

The stress factors A_k may be either positive or negative depending on the position in the structure, type of loading and sign convention of sectional loads used in the wave load programme.

The warping stress factor A_4 is related to the bi-moment, which is a result of the torsional distribution. To establish the warping stress transfer function, the response from the torsional distribution needs to be assessed for each period and wave heading to establish the transfer function of the bi-moment.

Depending on the detail to be investigated the stress per load ratio is either calculated directly by finite element analyses or derived from the prescriptive formulas given in Sec.4 combined with stress concentration factors as given in App.A.

3.4 Splash zone correction

In the partly dry surface region of the ship hull (i.e. splash zone), as illustrated in Figure 2, the transfer function for external pressures should be corrected to account for intermittent wet and dry surfaces. The dynamic pressure in the splash zone region, $P_{W,SZ}$, in kN/m², is estimated as:

$$P_{W,SZ} = r_p \cdot P_W$$

where:

$$\begin{aligned} r_p &= 1.0 && \text{for } z < T_{LC} - h_W \\ r_p &= 0 && \text{for } z > T_{LC} + h_W \\ r_p &= \frac{T_{LC} + h_W - z}{2h_W} && \text{for } T_{LC} - h_W \leq z \leq T_{LC} + h_W \end{aligned}$$

$$h_W = \frac{P_{W,WL}}{\rho \cdot g}$$

h_W = water head equivalent to the pressure at waterline, in m

$P_{W,WL}$ = wave pressure at the water line, in kN/m²

P_W = wave pressure, in kN/m². Above the water line P_W is $P_{W,WL}$. Below the water line, P_W is taken as the linear hydrodynamic pressure at location z.

The dynamic pressure at the mean waterline at 10⁻⁴ probability of exceedance should be used to calculate $P_{W,WL}$ and thereby the splash zone extent. Since panel pressure refers to the midpoint of the panel, an extrapolation using the values for the two panels closest to the waterline has to be carried out to determine the dynamic pressure at the waterline.

Above the waterline the pressure should be stretched using the pressure transfer function for the pressure at the waterline combined with the r_p factor. Below the water line, but still within the splash zone, the panel pressure closest to the load point should be used, and this panel pressure needs to be corrected to the load point by interpolation, before multiplied with the r_p factor. Below the splash zone, the panel pressure closest to the load point should be used, but corrected to the load point by interpolation.

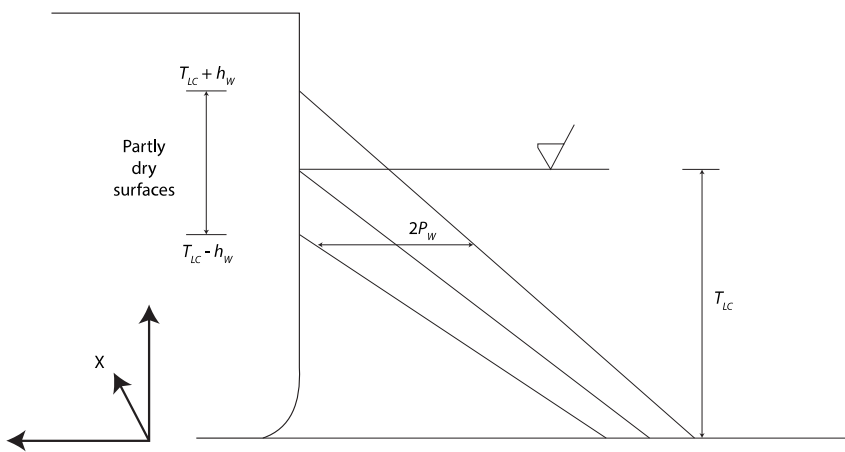


Figure 2 Reduced pressure range in the splash zone

3.5 Double hull and relative deflection stress

Stresses due to deformation of the main girder system, such as double hull bending and relative deflection, are a result of the pressure distribution over the frame and girder system. Consequently, the corresponding stress component factors should be calculated using reference panels representative for the pressure distribution over the hull section rather than the local pressure at the stiffener considered. In general, a panel at $B/4$ from the centre line (CL) may be used as reference panel for bottom structures and a panel at $2/3$ of the draught, T_{LC} , may be used for side structures.

Relative deflections (or double hull stresses) may be calculated by applying the directly calculated pressure distribution, based on 10^{-4} probability level of exceedance and including the splash zone correction, to the cargo hold FE analysis. This gives a relative deflection (or double hull stress) distribution. The relative deflection (or double hull stress) distribution per unit pressure at a specific position can then be established. Thereby the relative deflection (or double hull stress) transfer function for all positions can be defined based on the transfer function of the pressure in a single specific position. To achieve increased accuracy the pressure distribution can be divided into several pressure distributions with smaller extents, which can be added as load components due to linear theory.

4 Full stochastic analysis

4.1 Introduction

In full stochastic analysis, hydrodynamic loads are directly transferred from the wave load analysis program to FE models. Hydrodynamic loads include panel pressures, internal tank pressures and inertia forces due to rigid body accelerations. Full stochastic analysis can be applied to any kind of structure.

The analysis can be based on a global FE model of the vessel, which can be combined with local FE models as sub-models. As an alternative to the global model, a cargo hold or partial ship FE model can be used transferring sectional loads calculated by the wave load program to the forward and aft end of the cargo hold or partial ship model.

All load effects are preserved through the calculations, and hence the method is suitable for fatigue calculations of details with complex stress pattern and loading. Typical examples are panel knuckles, bracket terminations of the main girder system, larger openings and hatch corners.

A flow diagram of the calculation procedure is shown in [Figure 3](#).

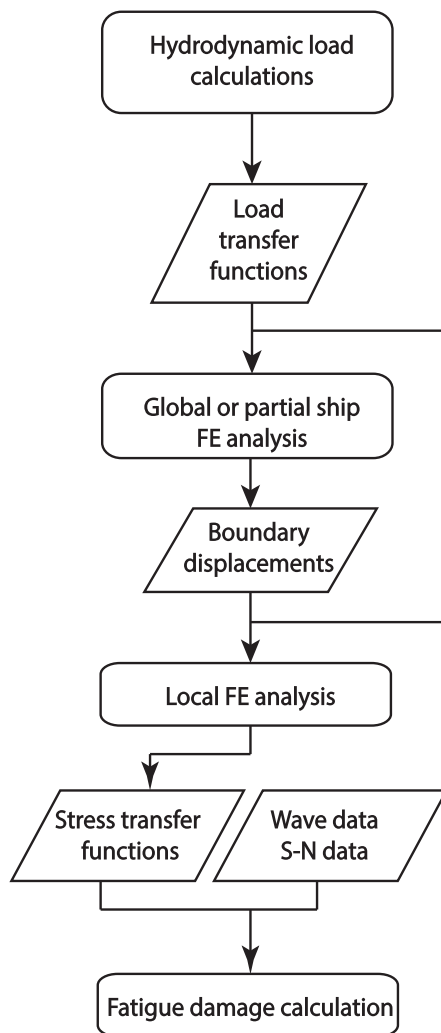


Figure 3 Flow diagram for full stochastic fatigue calculations

By direct load transfer the stress response transfer functions are implicitly described by the FE analysis results. All wave headings from 0 to 360° with an increment of maximum 30° should be included. For each wave heading a minimum of 20 wave frequencies should be included to properly describe the shape of the transfer functions.

A prerequisite for correct load transfer from the hydrodynamic program is sufficient compatibility between the hydrodynamic and the global FE model:

- if different masses are used, the mass distributions needs to be similar
- if different panel model is used, the buoyancy distribution needs to be similar.

Similar mass properties and buoyancy can be ensured by using the structural FE model as mass model and panel model in the hydrodynamic analysis.

Having performed the load transfer, the final load equilibrium should be checked by comparing transfer functions and longitudinal distribution of sectional forces, e.g. bending moment and shear forces, for different wave headings. Significant unbalanced forces will disturb the global response.

4.2 Assessment of local details

Local FE models can be used as sub models to the global model, and the displacements from the global model are automatically transferred to the local model as boundary displacements. In addition, the local internal and external pressure loads and inertia loads are transferred from the wave load analysis.

From the local FE models transfer functions of hot spot stress (or local stress at free plate edges) are determined, see [Sec.6](#).

For details dominated by axial loading, the nominal stress approach can be an efficient alternative to local FE models.

SECTION 6 FINITE ELEMENT ANALYSIS

1 Introduction

1.1 Thickness

The thickness to be used in FE analysis is required by the rules for the specific ship type and can be either t_{n50} or t_{gr} with the corresponding scantling approach factor, f_c , as given in [Sec.3 \[2.2\]](#). The net or gross thickness are thereby referred to as the thickness t in relation to FE analysis.

1.2 Application

This section describes the finite element (FE) method to be used for fatigue assessment. The methods are based on the hot spot stress approach as well as the local stress for free plate edge. The main aim of applying a FE model in the fatigue analysis should obtain a more accurate assessment of the stress response.

The methods described in this section is regarded applicable for many details using shell elements, but for certain details customized methods are regarded necessary. Alternative methods are also given in [App.E](#).

Three types of hot spots, denoted 'a', 'b' and 'c' are described in [Table 1](#). These are defined according to their location on the plate and their orientation to the weld toe as illustrated in [Figure 1](#). For shell elements 'a' and 'c' are for practical purposes the same, while for solid elements 'a' and 'c' differs.

Table 1 Types of hot spots

Type	Description
a	hot spot at the weld toe on plate surface at an ending attachment
b	hot spot at the weld toe around the plate edge of an ending attachment
c	hot spot at the weld toe of an attached plate (weld toes on both the plate and attachment surface)

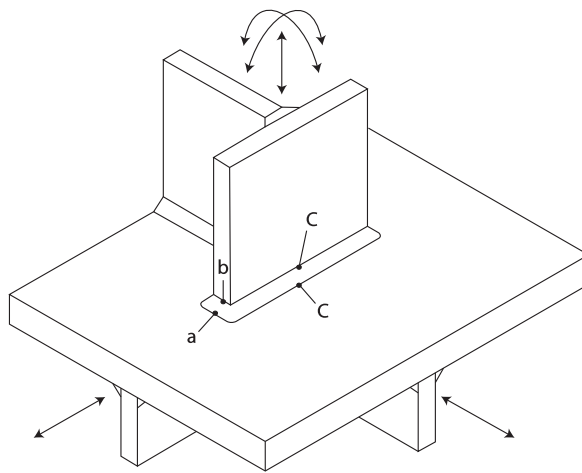


Figure 1 Types of hot spots

The method for calculation of hot spot stress at weld toe for any welded details is given in [\[4.1\]](#) except for web stiffened cruciform joints. The method for calculation of local stress of free plate edges is given in [\[4.2\]](#).

The method for calculation of hot spot stress at web stiffened cruciform joints such as hopper knuckle connection, transverse bulkhead lower stool to inner bottom connection and horizontal stringer heel is given in [5].

Limitations of the hot spot stress methodology for simple connections are given in [6].

1.3 Stress to be used from finite element analysis

The principal stress range within 45° of the normal to the weld toe should be used for the analysis as illustrated in Figure 2. It is assumed here that the crack is growing parallel to the weld.

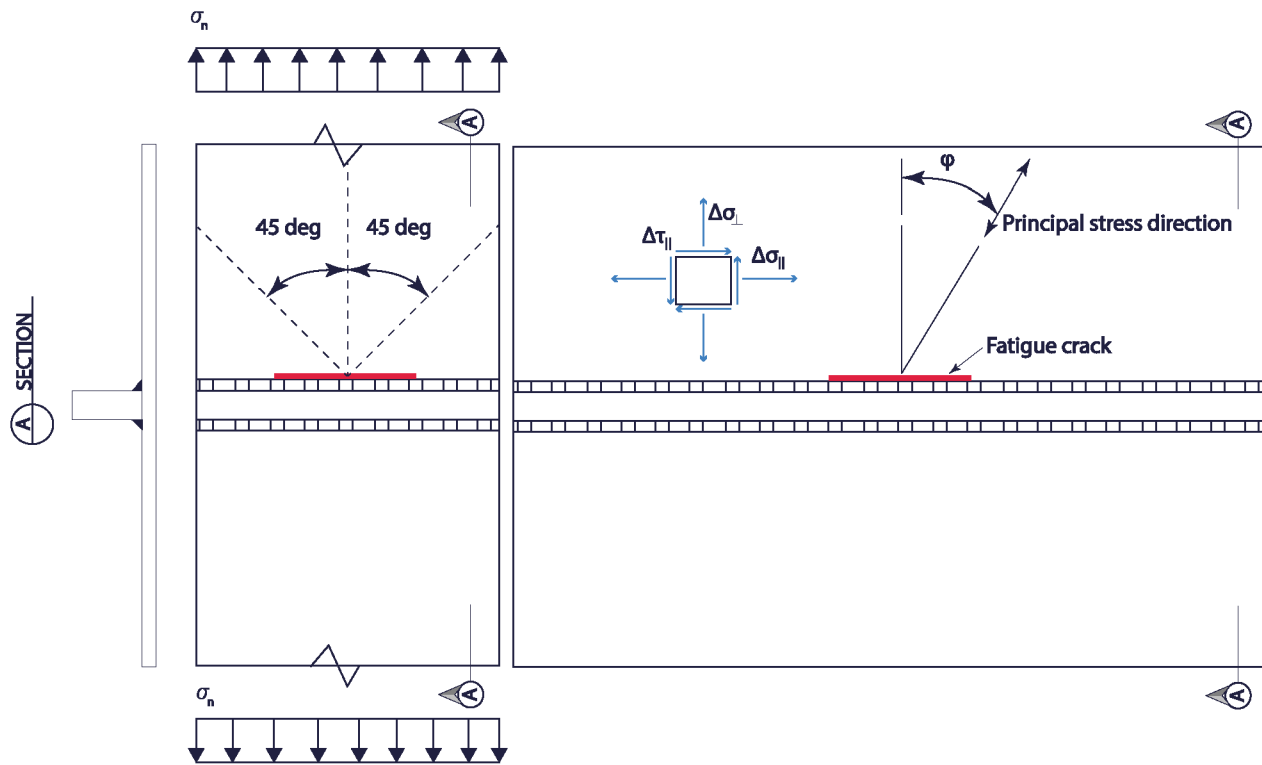


Figure 2 Principal stress to be used for cracks parallel to the weld

When the principal stress direction differs significantly from the normal to the weld toe, it becomes conservative to use the principal stress range as indicated in Figure 2. If the angle between the principal stress direction and the normal to the weld, Φ , is increased further, fatigue cracking may initiate in the weld and grow normal to the principal stress direction as shown in Figure 3. This means that the notch at the weld toe no longer significantly influences the fatigue capacity and a higher S-N curve or allowable hot spot stress applies for this stress direction. More guidance on this effect of stress direction relative to the weld toe as shown in Figure 2 and Figure 3 when using finite element analysis and hot spot stress S-N curves is presented in App.E.

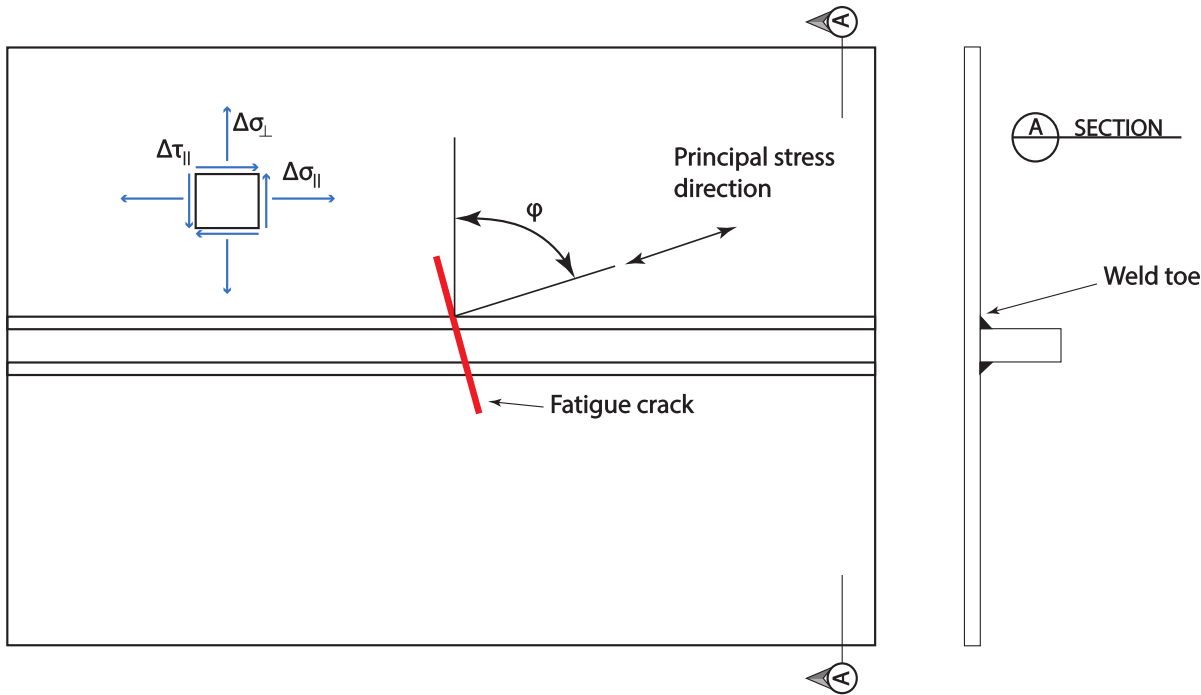


Figure 3 Fatigue cracking when principal stress direction is more parallel with weld toe

1.4 Stress field at a welded detail

Figure 5 illustrated the stress increase due to the structural geometry and the notch. Based on the stress field at the surface the hot spot stress needs to be established. The notch effect due to the weld is included in the S-N curve, and the hot spot stress can be derived by extrapolation of the structural stress as in [2.1] to the hot spot, but this Section includes the simplified method in [3.3].

1.5 Fatigue stress range based on EDW approach

The stress range to be used for each loading condition (j) is the stress range obtained from the predominant load case.

$$\Delta\sigma_{FS,(j)} = f_s \cdot f_{ws} \cdot \max_i(\Delta\sigma_{FS,i(j)})$$

where:

$\Delta\sigma_{FS,i(j)}$ = fatigue stress range, in N/mm², for load case (i) of loading condition (j)

f_s = correction factor for the effect of stress gradient along weld line given as 0.96 for hot spot at the flange of web stiffened cruciform joint, and otherwise 1.0 for web and other details

f_{ws} = correction factor for the effect of supporting member given as 0.95 for hot spot at the flange of web stiffened cruciform joint, and otherwise 1.0 for web and other details.

The fatigue stress range $\Delta\sigma_{FS,i(j)}$, in N/mm², for free plate edge corrected for mean stress effect, thickness effect, material factor and environmental factor, is taken as:

$$\Delta\sigma_{FS,i(j)} = f_{mean,i(j)} \cdot f_{thick} \cdot f_{material} \cdot f_c \cdot f_e \cdot \Delta\sigma_{BS,i(j)}$$

For local stress at free plate edge, the stress range is derived as:

$$\Delta\sigma_{BS,i(j)} = |\sigma_{BS,i1(j)} - \sigma_{BS,i2(j)}|$$

where:

$\Delta\sigma_{BS,i1(j)}$ = local stress in load case 'i1' and 'i2' of loading condition (j), in N/mm², obtained by local stress FE analysis.

For welded details, the fatigue stress range is derived as:

$$\Delta\sigma_{FS,i(j)} = \max(\Delta\sigma_{FS1,i(j)}, \Delta\sigma_{FS2,i(j)})$$

$$\Delta\sigma_{FS1,i(j)} = K'_m, i(j) \cdot f_{mean1,i(j)} \cdot f_{thick1} \cdot f_{material} \cdot f_w \cdot f_c \cdot f_e \cdot \Delta\sigma_{HS1,i(j)}$$

$$\Delta\sigma_{FS2,i(j)} = K_p \cdot f_{mean2,i(j)} \cdot f_{thick2} \cdot f_{material} \cdot f_w \cdot f_c \cdot f_e \cdot \Delta\sigma_{HS2,i(j)}$$

where:

$\Delta\sigma_{FS1,i(j)}$ = fatigue stress range due to the principal hot spot stress range $\Delta\sigma_{HS1,i(j)}$, in N/mm²

$\Delta\sigma_{FS2,i(j)}$ = fatigue stress range due to the principal hot spot stress range $\Delta\sigma_{HS2,i(j)}$, in N/mm²

K_p = stress reduction factor for stress along welds given in Sec.2 [2.4]

K'_m = $K'_m, i(j) = K_m - \Delta\sigma_{HS1,bending,i(j)} / \Delta\sigma_{HS1,i(j)} \cdot (K_m - 1)$

K_m = stress magnification factor due to misalignment (angular or due to eccentricity), as given in Appendix A

$f_{mean1,i(j)}$, $f_{mean2,i(j)}$ = correction factor for mean stress effect for the different principal stresses. The environmental factor, f_e , should be combined with the hot spot stress range (similar for free plate edge) in the estimate of the mean stress effect

f_{thick1} , f_{thick2} = thickness effect for the different principal stresses due to thickness effect exponent n in Sec.2 [5.1] Table 4

$f_{material}$ = material factor

f_w = post-weld treatment factor

f_c = scantlings correction factor

f_e = environmental factor

$\Delta\sigma_{HS1,i(j)}$ = principal hot spot stress ranges, in N/mm², due to the dynamic loads for load case i of loading condition (j) which acts within 45° of the perpendicular to the weld toe

$\Delta\sigma_{HS2,i(j)}$ = principal hot spot stress ranges, in N/mm², due to the dynamic loads for load case i of loading condition (j) which acts outside 45° of the perpendicular to the weld toe

$\Delta\sigma_{HS1,bending,i(j)}$ = bending part of the principal hot spot stress range, in N/mm², which acts within 45° of the perpendicular to the weld toe.

Mean stress for base material free plate edge, $\sigma_{mean,i(j)}$, in N/mm², due to static and dynamic load case 'i1' and 'i2' of loading condition (j) is calculated as:

$$\sigma_{mean,i(j)} = \frac{\sigma_{i1(j)} + \sigma_{i2(j)}}{2}$$

The hot spot mean stress for welded details for loading condition j in direction 1 and 2 corresponding to normal to weld, $\sigma_{mean,HS1,i(j)}$, and parallel to weld, $\sigma_{mean,HS2,i(j)}$, due to static and dynamic loads are estimated as:

$$\sigma_{mean,HS1,i(j)} = \frac{\sigma_{HS1,i1(j)} + \sigma_{HS1,i2(j)}}{2}$$

$$\sigma_{mean,HS2,i(j)} = \frac{\sigma_{HS2,i1(j)} + \sigma_{HS2,i2(j)}}{2}$$

where the index "1" and "2" after "HS" refers to direct normal to and parallel with the weld. The hot spot stress in these cases includes both the static and the dynamic loads.

1.6 Fatigue stress range based on direct calculations

The stress range for each loading condition (j) is obtained:

$$\Delta\sigma_{FS,(j)} = 2 \cdot \sigma_{FS,(j)}$$

where:

$\sigma_{FS,(j)}$ = fatigue stress amplitude of loading condition (j), in N/mm², obtained by hot spot FE analysis.

The fatigue stress $\sigma_{FS,i(j)}$, in N/mm², for welded details is given as:

$$\Delta\sigma_{FS,(j)} = f_s \cdot f_{ws} \cdot \max(\Delta\sigma_{FS1,(j)}, \Delta\sigma_{FS2,(j)})$$

$$\Delta\sigma_{FS1,(j)} = K'_{m,i(j)} \cdot f_{mean1,(j)} \cdot f_{thick1} \cdot f_{material} \cdot f_w \cdot f_c \cdot \Delta\sigma_{HS1,(j)}$$

$$\Delta\sigma_{FS2,(j)} = K_p \cdot f_{mean2,(j)} \cdot f_{thick2} \cdot f_{material} \cdot f_w \cdot f_c \cdot \Delta\sigma_{HS2,(j)}$$

where:

$\sigma_{FS1,(j)}$ = fatigue stress amplitude due to the principal hot spot stress $\sigma_{HS1,(j)}$, in N/mm².

$\sigma_{FS2,(j)}$ = fatigue stress amplitude due to the principal hot spot stress $\sigma_{HS2,(j)}$, in N/mm².

$f_{mean1,(j)}$, $f_{mean2,(j)}$ = correction factor for mean stress effect for the different principal stresses

- $\sigma_{HS1,(j)}$ = principal hot spot stress amplitude, in N/mm², due to the dynamic loads of loading condition (j) which acts within 45° of the perpendicular to the weld toe
 $\sigma_{HS2,(j)}$ = principal hot spot stress amplitude, in N/mm², due to the dynamic loads of loading condition (j) which acts outside 45° of the perpendicular to the weld toe.

The fatigue stress $\sigma_{FS,(j)}$, in N/mm², for free plate edge is taken as:

$$\sigma_{FS,(j)} = f_{mean,(j)} \cdot f_{thick} \cdot f_{material} \cdot f_c \cdot \sigma_{BS,(j)}$$

where:

- $\sigma_{BS,(j)}$ = fatigue stress amplitude due to the principal hot spot stress at the free plate edge, in N/mm², taken from the FE analysis.

Mean stress for base material free plate edge or welded details, $\sigma_{mean,(j)}$, in N/mm², is taken from the static loads only for loading condition (j). The mean stress should correspond to the respective stress component directions normal to, ' σ_x ', or parallel to, ' σ_y ', the weld for welded details and tangentially of the edge for free plate edges.

1.7 Hot spot S-N curve

The hot spot S-N curves to be used are described in Sec.2 [2.3]. For welded details S-N curve D (FAT 90) should be used. For the free plate edge, the S-N curve depends on the surface condition.

2 Finite element modelling

2.1 General

Hot spot stresses and stresses at free plate edges are calculated assuming linear material behaviour and using an idealized structural model with no fabrication-related misalignment. Effects caused by fabrication imperfections as e.g. misalignment of structural parts, must be separately accounted for.

Models with thin plate, plane stress elements, shell elements or solid elements can be used. The arrangement and type of elements have to allow for steep stress gradients and formation of plate bending, but only the linear stress distribution in the plate thickness direction needs to be evaluated with respect to the definition of hot spot stress. This section covers shell elements.

2.2 FE models

Three levels of FE models are commonly used:

- global model
- partial ship model, like cargo hold model for ships with cargo holds
- local models, like hot spot models for welded details and local stress models for free plate edges.

Description of the upper two FE models are included in the [DNVGL-CG-0127](#), *Finite element analysis*. Local models used for fatigue assessment are described in this section.

Hot spot and local stress models are used for fully stochastic fatigue analyses and prescriptive fatigue analysis. Hot spot models are also being used in component stochastic analyses when the structural stress concentration is unknown. Typical considered details are:

- bracket toe and flange terminations of stiffeners
- slots and lugs in the web frames at the intersection with stiffeners

- bracket and flange terminations of girder systems
- panel knuckles.

[2.7] gives examples of an end bracket and a hatch corner.

2.3 Load application

For prescribed fatigue calculations the loads are described by the rules. Direct calculated loads are described in Sec.5. For each loading condition the following dynamic and static loads (for mean stress effect) are relevant:

- internal and external pressure
- global hull girder loads for partial and local models
- inertia loads of the structure and cargo in case of direct analysis.

For a local model, the external loads like global hull girder loads are transferred through the boundary conditions. If local loads as lateral pressure are internal loads to the local model, these loads shall be included in the local model.

The various models have to be "compatible" meaning that the larger models should produce deformations and/or forces applicable as boundary conditions for the smaller models. This stiffness in the global and local part should be equivalent, especially in the case of load transfer. The extent of the local model has to be chosen such that effects due to the boundaries on the structural detail considered are sufficiently small and that reasonable boundary conditions can be formulated.

2.4 Mesh size

The evaluation of hot spot stress for 'a' type hot spot in Figure 1 should be based on shell element of mesh size $t \times t$, where t is the thickness of the plate in way of the considered hot spot.

The evaluation of hot spot stress for a 'b' type hot spot in Figure 1 should be based on shell element of mesh size 10×10 mm.

The aforementioned mesh size should be maintained within the hot spot mesh zone, extending over at least 10 elements in all directions from the fatigue hot spot position. The transition of element size between the coarser mesh and the hot spot mesh zone should be done gradually and an acceptable mesh quality should be maintained. This transition mesh should be such that a uniform mesh with regular shape gradually transitions from smaller elements to larger ones. An example of the mesh transition is shown in Figure 4. Mesh transitions should not be arranged close to the hot spot.

For efficient read out of element stresses a mesh density in the order of $t \times t$, where t is the plate thickness, is in general preferred at the hot spot region.

2.5 4-node or 8-node elements

Four-node shell elements with adequate bending and membrane properties should be used inside the hot spot mesh zone. The four node element should have a complete linear field of in-plane stresses and hence pure in-plane bending of the element can be exactly represented. Care should be given to possible stress underestimation especially at weld toes of type 'b' in Figure 1. Use of 4-node elements with improved in-plane bending modes is a good alternative. In case of steep stress gradients, 8-node thin shell elements should be used.

The shell elements should represent the mid plane of the plating, as indicated in Figure 7. For practical purposes, adjoining plates of different thickness may be assumed to be median line aligned, i.e. no staggering in way of thickness change is required. The geometry of the weld and construction misalignment is not required to be modelled.

The welds are usually not modelled except for special cases where the results are affected by high local bending, e. g. due to an offset between plates or due to a small free plate length between adjacent welds such as at lug (or collar) plates. Here, the weld may be included by transverse plate elements having

appropriate stiffness or by introducing constrained equations for coupled node displacements. A thickness equal to two times the thickness of the plates may be used for modelling of the welds by transverse plates.

All structure in close proximity to the hot spot mesh zones should be explicitly modelled with shell elements. Triangular elements close to the hot spot should be avoided where possible. Use of extreme aspect ratio (e.g. aspect ratio greater than 3) and distorted elements (e.g. element's corner angle less than 60° or greater than 120°) should be avoided.

2.6 Base material free plate edges

When stresses should be evaluated on a free plate edge, such as hatch corners, truss elements having a negligible cross sectional area should be used to obtain the required local edge stress values. In case of significant out-of-plane bending, beam elements having the same depth as the adjoining plate thickness and negligible width should be used instead.

2.7 Example: Hatch corners and hatch coaming end bracket

In addition to the general guidance in [2.1] to [2.6], examples of modelling a hatch corners and a hatch coaming end bracket are illustrated in the [Figure 4](#) and [Figure 5](#). The hatch corner area should be meshed using elements with a sufficiently small size to capture the local stress on the edge. The element edge dimension should not exceed $0.2R$ where R is the hatchway radius. In general, a minimum of 10 elements in a 90° arc is regarded sufficient to describe the curvature of the hatchway radius plating for a rounded corner, see [Figure 5](#). For an elliptical or parabolic corner, a minimum of 10 elements is regarded sufficient from the inboard radius end to a point on the edge located at half the longitudinal distance of the semi-major axis. A total of 15 elements is regarded sufficient at the elliptical edge of the hatch corner, see [Figure 6](#).

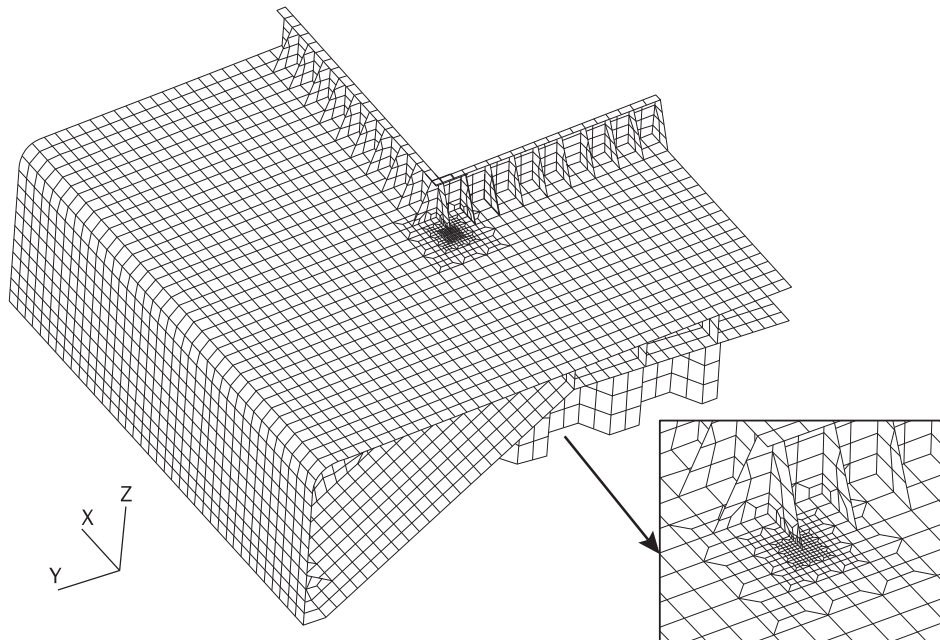


Figure 4 Local FE model of longitudinal hatch coaming end bracket to the deck plating with hot spot mesh zone, $t \times t$ mesh

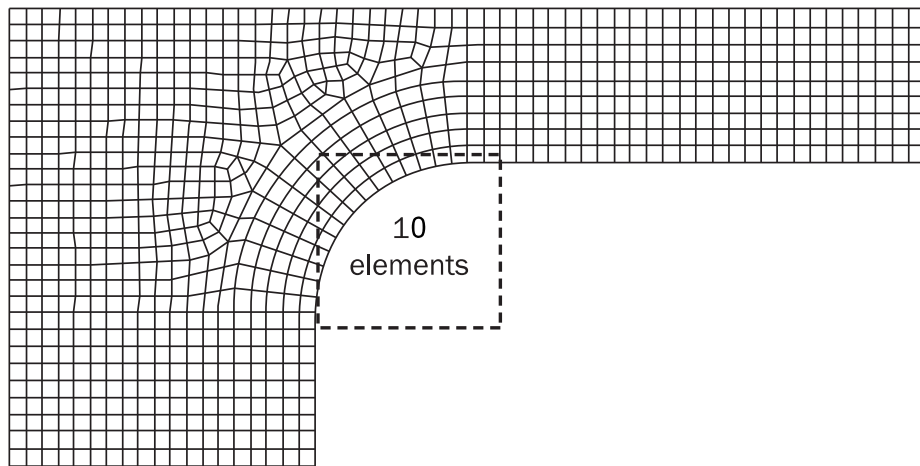


Figure 5 Example of mesh density for rounded hatch corner with 10 elements

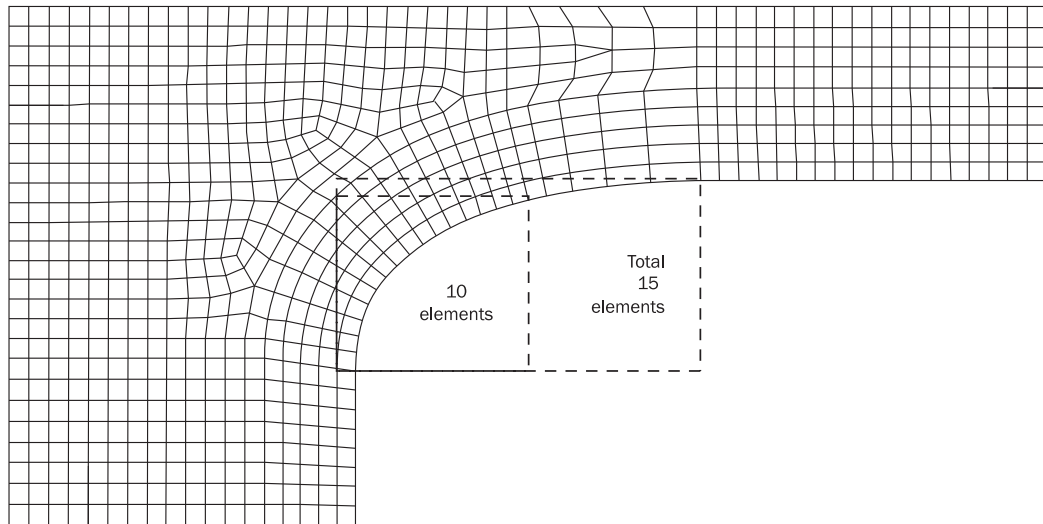


Figure 6 Example of mesh density for elliptical hatch corner with 15 elements

3 Derivation of hot spot stress

3.1 General

The S-N curve to be used needs to be consistent with the meshing and the way of hot spot stress determination, which is done by extrapolation, correction and/or tuning. The main method explained in this section is:

- derivation of stress at read out point $t/2$ from the hot spot times a coefficient. For hot spot 'b' in [Figure 1](#) read out would however be 5 mm from the hot spot.

The main method is widely applicable and convenient when using the right mesh size in combination with 8-node shell elements hot spots in [Figure 1](#). The following alternative methods can result in less conservative results:

- extrapolation from $t/2$ and $3t/2$ to the hot spot, see [App.D](#)
- the main method or extrapolation, but accounting for principal stress directions, see [App.D](#)
- reduction of bending stress component for hot spot of highly localized stress peaks, see [\[3.4\]](#)
- read out at shifted position for tuned details, see [\[5\]](#).

In any case, when shell elements are regarded non-conservative (point 'c' in [Sec.14](#)) and should have been replaced by a solid model, it can still be used provided a correction is made according to [Sec.6](#).

3.2 Read out point at $t/2$

The stress evaluation points are located at distances $t/2$ from the hot spot, where t is the plate thickness at the weld toe. This location is denoted as the stress read out point. For hot spot 'b' it would be 5 mm from the hot spot. For modelling with shell elements without any weld the hot spot stress is taken as the principal stress within an angle $\pm 45^\circ$ to the normal to the weld and at the read out point $t/2$ away from the intersection line. This 45° is not an issue for hot spot b as the shear at the surface is zero and the axial stress can be used.

The stress components on the plate surface, on which the weld is located, should be evaluated.

3.3 Derivation of stress at read out point, $t/2$

Depending on the element type, one of the following stress read out methods should be used:

- with 4-node shell element:

Element surface stress (surface where the weld is located) components at the centre points are linearly extrapolated to the line A-A as shown in [Figure 7](#) to determine the stress components at the stress read out point located at a distance $t/2$ from the intersection line for type 'a' and 'c' hot spots.

- with 8-node shell element:

With a $t \times t$ element mesh using 8-node element type, the element mid-side node is located on the line A-A at a distance $t/2$ for type 'a' and 'c' hot spots. This node coincides with the stress read out point. The element surface stress components can be used directly without extrapolation within each adjacent element located on each side (side L, side R) of the line A-A as illustrated in [Figure 8](#).

Common for both 4-node and 8-node shell elements is that the two principal hot spot stress ranges are determined at the stress read out point from the stress components tensor differences (between load case 'i1' and 'i2' in case of EDW approach) calculated from each side (side L, side R) of line A-A. The average of the component stresses from both sides of line A-A should be taken, and then the component stress difference ($\sigma_{x,i1} - \sigma_{x,i2}; \sigma_{y,i1} - \sigma_{y,i2}; \tau_{xy,i1} - \tau_{xy,i2}$) should be estimated prior to the two principal stresses with 90° relative angle. The angle θ between the direction x of the element co-ordinate system and the principal direction pX of the principal hot spot stress range co-ordinate system has to be determined.

For hot spot type 'b' the derivation is simpler. For fatigue assessment of type 'b' hot spots, a beam element shall be used to obtain the fatigue stress range at the read out point 5 mm from the hot spot. The stress range should be based on axial and bending stress in the beam element. The beam element should have the same depth as the connecting plate thickness while the in-plane width is negligible, i.e. it should not contribute to the strength and it should be compatible with the shell elements and read out the bending stress correctly.

The above read out procedure is based on element surface stresses. Generally, in FE software the element stresses are calculated at the Gaussian integration points located inside the element. Depending on the element type implemented in the FE software, it may be necessary to perform several interpolations in order to determine the actual stress at the considered stress read out point at the surface of the element mid-point or element edge.

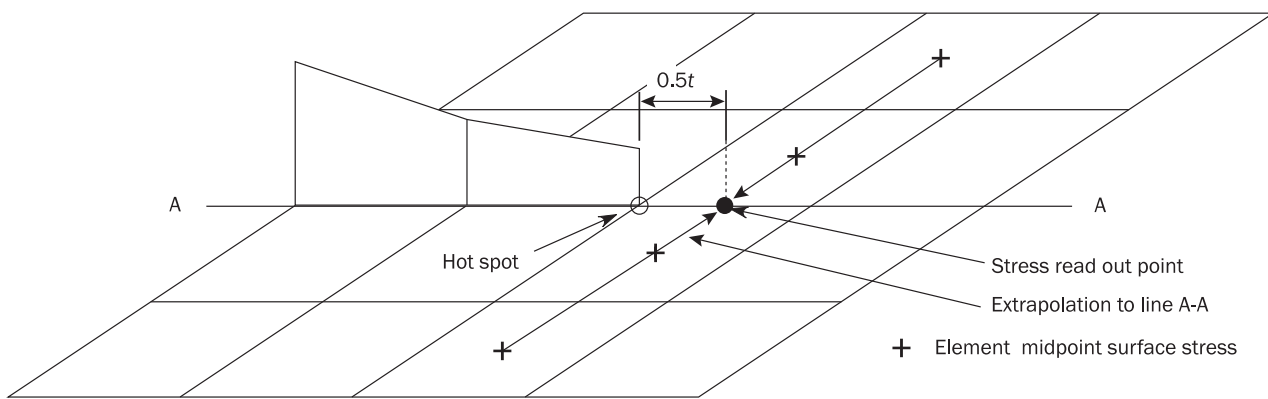


Figure 7 Determination of stress read out points and hot spot stress for 4-node element

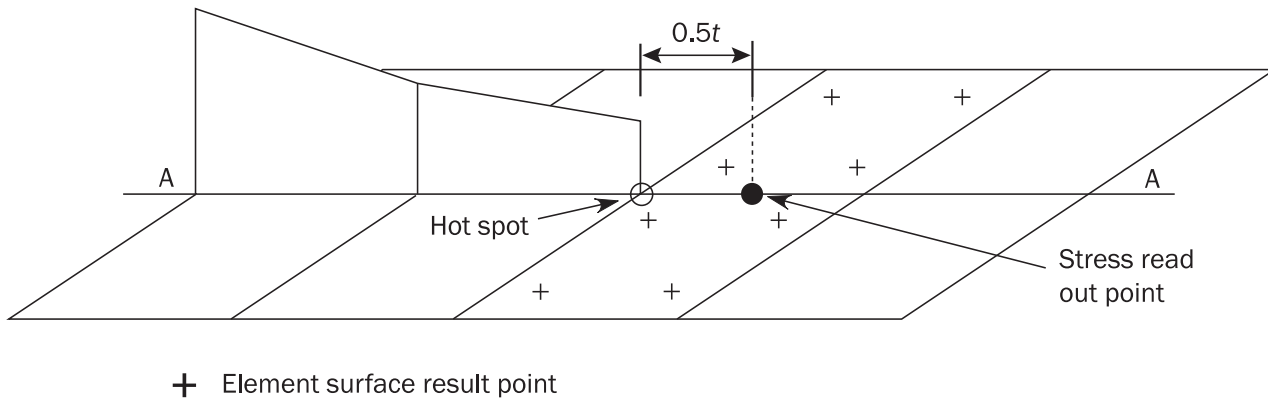


Figure 8 Determination of stress read out points and hot spot stress for 8-node element

3.4 Reduced hot spot stress for highly localized stress peaks with plate bending

At hot spots with significant plate bending in a local hot spot zone, an effective hot spot stress for fatigue assessment may be derived based on the following equation:

$$\Delta\sigma_{HS} = \Delta\sigma_{membrane} + 0.6\Delta\sigma_{bending}$$

$$\Delta\sigma_{bending} = \Delta\sigma_{surface} - \Delta\sigma_{membrane}$$

where:

- $\Delta\sigma_{membrane}$ = membrane stress, in N/mm², at hot spot
- $\Delta\sigma_{bending}$ = bending stress, in N/mm², at hot spot
- $\Delta\sigma_{surface}$ = surface stress, in N/mm², at hot spot taken from the FE analysis.

The reduction factor on the bending stress can be explained by redistribution of loads to other areas during crack growth, while the crack tip is growing into a region with reduced stress. The effect is limited to areas with a localised stress concentration, which occurs for example at a hopper knuckle.

However, in a case where the stress variation along the weld is small, e.g. when the effective flange effect is insignificant, the difference in fatigue life between axial loading and pure bending is also small. Therefore, it should be noted that it is not correct to generally reduce the bending part of the stress to 60%. This has to be restricted to cases with a pronounced stress concentration and where the stress distribution under fatigue crack development is more similar to a displacement controlled situation than that of a load controlled development. It can be applied to web-stiffened cruciform joints, while the effect on other details may need to be demonstrated.

4 Procedure for analysis of standard details

4.1 Procedure for analysis of hot spot stress at weld toe of welded details

For hot spot type 'a' and 'c', the structural hot spot stress, σ_{HS} , is calculated from a finite element analysis with $t \times t$ mesh density and is obtained by the following formula:

$$\sigma_{HS} = 1.12\sigma$$

where:

σ = surface principal stress, in N/mm², read out at a distance $t/2$ away from the intersection line
 t = plate thickness, in mm, in way of the weld toe.

At structural details where the hot spot type 'a' or 'c' are classified as a web-stiffened cruciform joint, the stress read out procedure of [5] should be applied. For hot spot type 'b', the stress distribution is not dependent on the plate thickness; the structural hot spot stress, σ_{HS} , is derived from a finite element analysis with mesh density 10 × 10 mm and is obtained by the following formula:

$$\sigma_{HS} = 1.12\sigma$$

where:

σ = surface principal stress at edge, in N/mm², read out at an absolute distance from the weld toe of 5 mm. The maximum of the surface principal stress from the two surfaces (edges) should be used.

4.2 Procedure for analysis of local stress of base material at free plate edge

For fatigue assessment at a free plate edge, a beam element should be used to obtain the fatigue stress range. The beam element should have the same depth as the connecting plate thickness while the in-plane width should be negligible. If the free plate edge is experiencing lateral bending, the beam should capture this bending and the worst surface should be considered.

5 Procedure for analysis of hot spot stress of web-stiffened cruciform joints

5.1 General

Different examples of web stiffened cruciform joints are illustrated in [Figure 9](#). Among the structural details which may be relevant, but not limited to, the following structural details are considered as a web-stiffened cruciform joints:

- welded hopper knuckle connections
- heel of horizontal stringers
- lower stool – inner bottom connection.

Two kinds of hot spots relative to the web-stiffened cruciform joints should be assessed:

- hot spots at the flange, see [\[5.2\]](#)
- hot spots in way of the web, see [\[5.3\]](#).

The hot spot stress for hopper knuckles of the bent type should be established by following the extrapolation procedure described in [App.E](#).

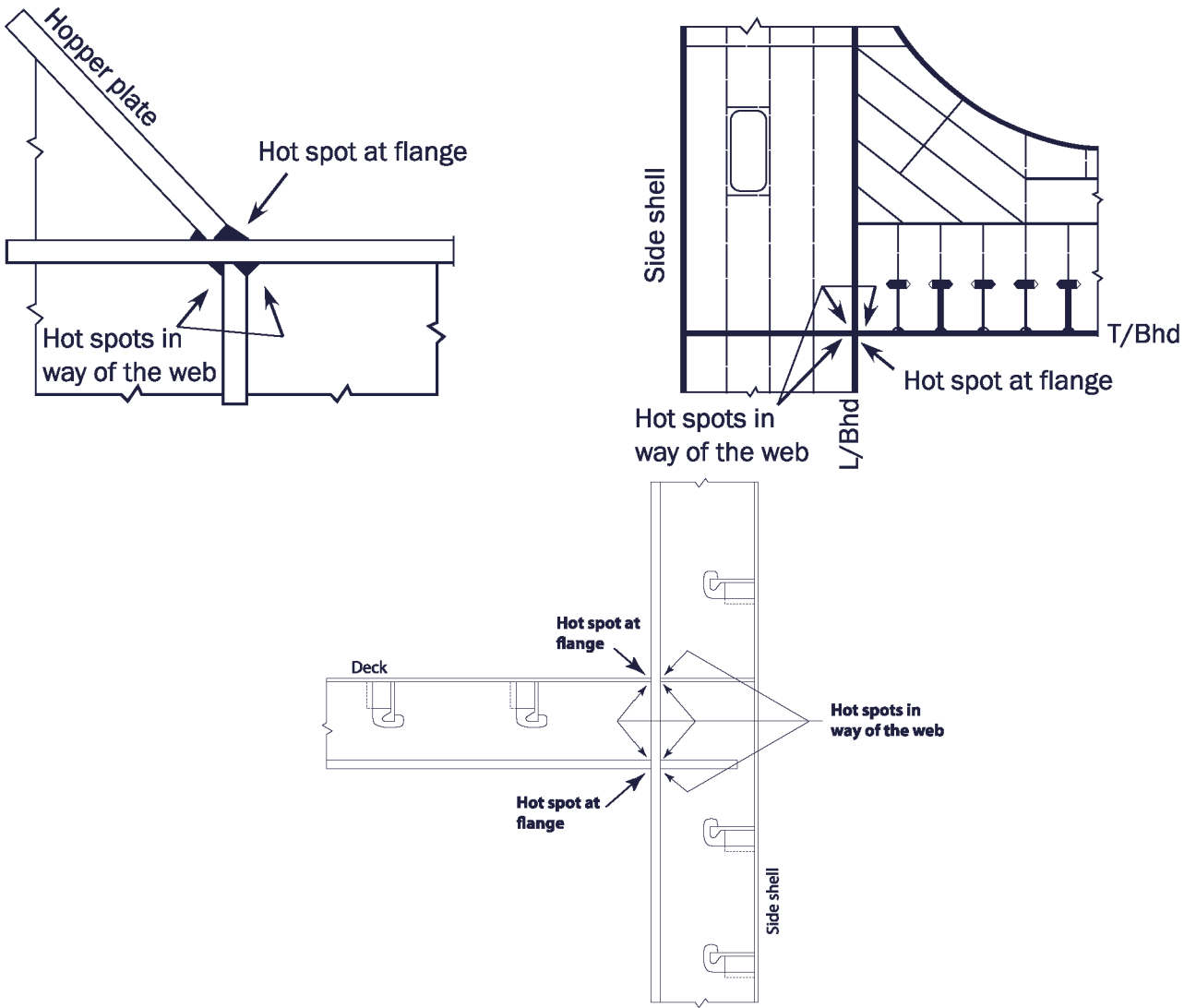


Figure 9 Web-stiffened cruciform joints; i.e. a 135° hopper knuckle, a 90° heel in a stringer and a connection between a deck web frame and a side web frame on a car carrier

5.2 Calculation of hot spot stress at the flange

For hot spot at the flange, the surface principal stress should be read out from a point shifted away from the intersection line between the considered member and the adjacent member to the position of the actual weld toe. The intersection line is taken at the mid-thickness of the cruciform joint assuming a median alignment. The hot spot stress, in N/mm², should be obtained as:

$$\sigma_{HS} = 1.12\sigma_{shift}$$

where:

σ_{shift} = surface principal stress, in N/mm², at shifted stress read out position.

The stress read out point shifted away from the intersection line is obtained as:

$$x_{shift} = \frac{t_1}{2} + x_{wt}$$

where:

- t_1 = plate thickness of the plate number 1, in mm, as shown in [Figure 10](#), associated with hot spot on plate number 1. For hot spot and read out position on plate number 2, t_1 should be replaced with t_2 in estimating X_{shift}
- x_{wt} = extended fillet weld leg length, in mm, as defined in [Figure 10](#), not taken larger than $t_1/2$ for plate number 1, or $t_2/2$ for plate number 2 (if the hot spot on the hopper tank plate is considered).

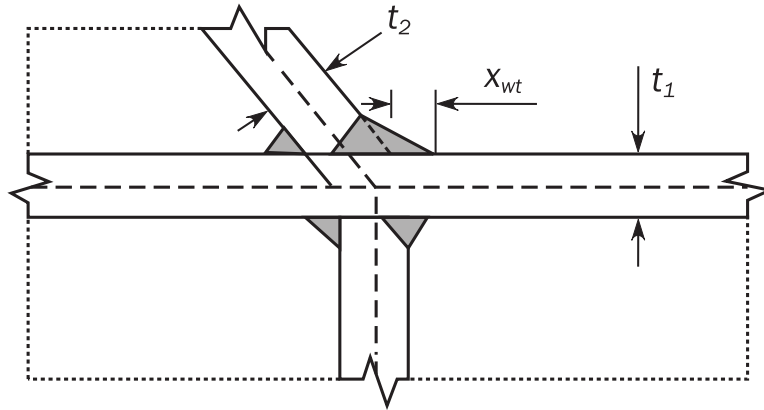


Figure 10 Geometrical parameters of web stiffened cruciform connections

The stress at the shifted position is derived according to the illustration in [Figure 11](#) where α is the angle, in degrees, between the plates forming the web-stiffened cruciform joint.

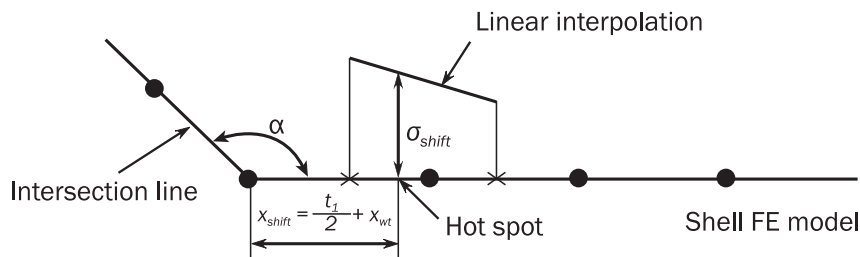


Figure 11 Procedure for calculation of hot spot stress at web stiffened cruciform connections

The stress at the shifted position, σ_{shift} , is derived as

$$\sigma_{shift} = (\sigma_{membrane}(x_{shift}) + 0.6 \cdot \sigma_{bending}(x_{shift})) \cdot \beta$$

$$\sigma_{bending}(x_{shift}) = \sigma_{surface}(x_{shift}) - \sigma_{membrane}(x_{shift})$$

where:

- β = plate angle hot spot stress correction factor
- $\sigma_{surface}(x_{shift})$ = total surface stress, in N/mm², at x_{shift} position (membrane stress and bending stress)
- $\sigma_{membrane}(x_{shift})$ = membrane stress, in N/mm², at x_{shift} position.

For $\alpha = 135^\circ$ connections the plate angle hot spot stress correction factor, β , is derived as:

$$\beta = 0.96 - 0.13 \frac{x_{wt}}{t_1} + 0.20 \left(\frac{x_{wt}}{t_1} \right)^2$$

For $\alpha = 120^\circ$ connections a correction factor is derived as:

$$\beta = 0.97 - 0.14 \frac{x_{wt}}{t_1} + 0.32 \left(\frac{x_{wt}}{t_1} \right)^2$$

For $\alpha = 90^\circ$ connections a correction factor is derived as:

$$\beta = 0.96 + 0.031 \frac{x_{wt}}{t_1} + 0.24 \left(\frac{x_{wt}}{t_1} \right)^2$$

The procedure is valid for $0 \leq x_{wt}/t_1 \leq 1.0$ and the β is adjusted based on experience.

Correction factors, β , for connections with plate angles, α , intermediate to those given should be derived based on a linear interpolation of the above values.

Considering [Figure 12](#), the surface stress components at the centre point of the two first elements (independent of 4- or 8-node elements) on left and right side of the line A-A are averaged and taken as the surface stress components in way of the web position (line A-A). For 8-node elements it may be sufficient to use the average of the element edge stress components from each element. The surface stress components are linearly interpolated along the line A-A in order to determine hot spot stress components at the stress read out point located at the x_{shift} position as shown in [Figure 12](#). Similar has to be done for the stress components, σ_x and σ_y , at the middle surface to obtain the membrane stress components, in order to estimate the stress components with reduced bending effect. The bending reduction effect with 0.6 factor is not applied to the shear stress.

In case of the EDW approach, the two principal hot spot stress ranges are determined based on the difference between the load case 'i1' and 'i2', e.g. $\sigma_x = \sigma_{x,i1} - \sigma_{x,i2}$, before the principal stresses in the two directions are calculated.

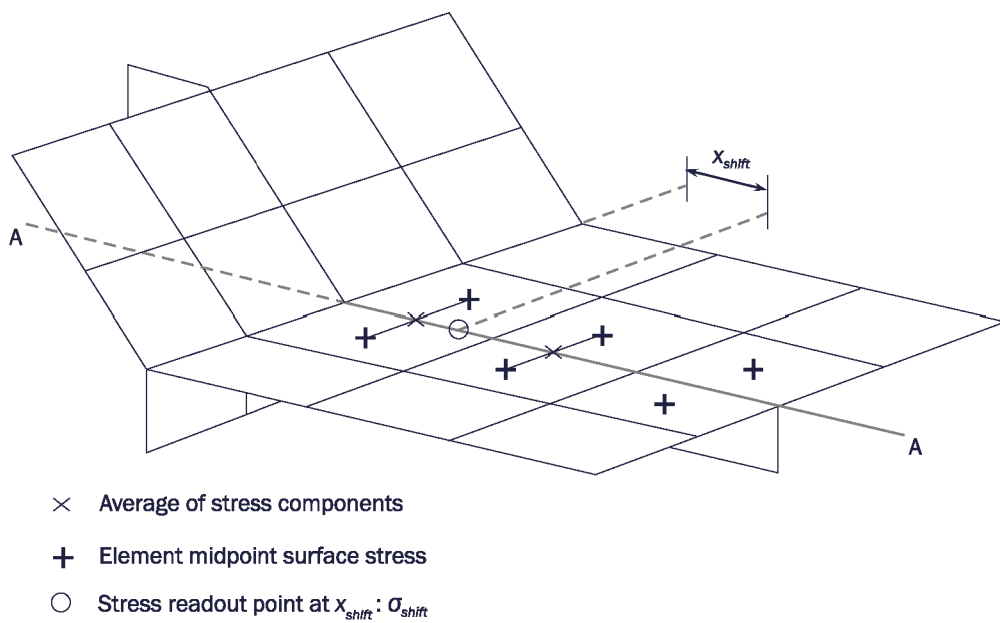


Figure 12 Determination of stress read out points for web-stiffened cruciform connections

5.3 Calculation of hot spot stress in way of the web

Hot spots located in way of the web as indicated in [Figure 13](#) and [App.E Figure 6](#) should be checked with the hot spot stress defined from the maximum principal surface stress at the intersection offset by the distance x_{shift} from the vertical and horizontal element intersection lines as illustrated in [Figure 13](#). The intersection line is taken at the mid thickness of the cruciform joint assuming a median alignment. The hot spot stress, in N/mm², should be obtained as:

$$\sigma_{HS} = \sigma_{shift}$$

where:

σ_{shift} = maximum principal surface stress, in N/mm², at the intersection offset by the distance x_{shift} .

The stress read out point at the intersection offset with reference to [Figure 13](#) is obtained as:

$$x_{shift} = \frac{t_3}{2} + x_{wt}$$

where:

t_3 = plate thickness of the web, in mm, as shown in [Figure 13](#)
 x_{wt} = extended fillet weld leg length, in mm, taken as:

$$x_{wt} = \min(\ell_{leg1}, \ell_{leg2})$$

where:

ℓ_{leg1}, ℓ_{leg2} = leg length, in mm, of the vertical and horizontal weld lines as shown in [Figure 13](#).

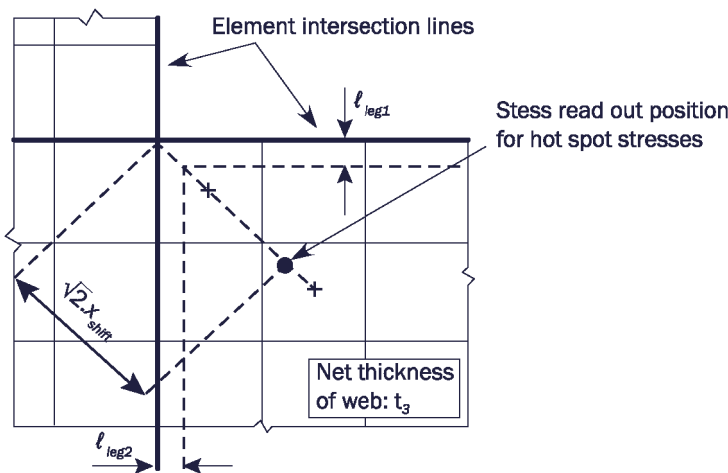


Figure 13 Hot spots in way of the web

6 Procedure for analysis of hot spot stress of simple cruciform joints

6.1 Limitation to hot spot stress approach

The definition of the stress field through the plate thickness in [Figure 4](#) implies that the described hot spot stress methodology is not recommended for simple cruciform joints, simple T-joints or simple butt joints. Analysing such connections with shell elements will result in a hot spot stress equal to the nominal stress. The hot spot stress approach is therefore not directly applicable when the stress flow in direction I, as shown in [Figure 14](#), is considered. For stresses in the direction normal to the weld at hot spot location c (direction I), there is no stress flow into the transverse plating as it is represented only by one plane in the shell model. However, it attracts stresses for in-plane direction (direction II) at hot spot location 'a'.

In situations where a bracket (or web) is fitted behind the transverse plate as shown in [Figure 1](#), acting with stiffness in the direction normal to the transverse plate, stresses flow also into the transverse plate, and the hot spot methodology is considered applicable.

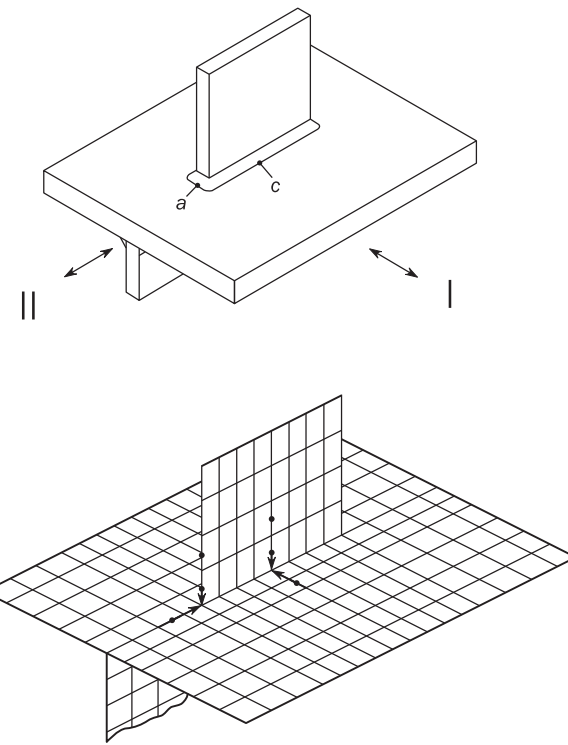


Figure 14 Illustration of difference to attract stresses normal to and in plane of a shell element model

6.2 Correction of hot spot stress approach for simple cruciform joints

For direction I at position c the calculated stress from FE analysis should be multiplied by a correction factor K/K_m .

The hot spot stress at position c should be determined by the stress read out procedure in [3] and is taken as:

$$\sigma_{HS} = \frac{K}{K_m} \cdot (1.12 \cdot \sigma)$$

where:

σ = stress read out at $t/2$ from the hot spot in N/mm^2

K = to be taken from [App.A Table 8](#).

K_m = stress concentration factor due to misalignment, see [App.A Table 3](#) and [App.A Table 8](#).

When considering the hot spot in [Figure 9](#) for web stiffened cruciform joints and the stress read out is taken adjacent to the centre of the web plane (where the critical hot spot is located), the detail goes from being a web stiffened cruciform joint to a simplified cruciform joint as represented by [App.A Table 8](#). It is then necessary to consider a sufficient transverse distance from the centre of the web plane to avoid the hot spot outside of the centre of the plane to become worse than at the centre of the plane, since the former is combined with the additional factors in [App.A Table 8](#). This could be relevant when determining the grinding extent.

SECTION 7 IMPROVEMENT OF FATIGUE LIFE BY FABRICATION

1 Introduction

1.1 General

The fatigue performance of structural details can be improved by adopting enhanced workmanship standards, which include building alignment and weld control. Building alignment below construction tolerance could introduce reduced stress concentration for structural details, increasing the fatigue performance. The shipbuilder is responsible to comply with the construction requirements given in the rules.

The detail design standard given in [Sec.8](#) and in relevant DNV GL class guideline for specific ship types may include workmanship and welding requirements.

Post-weld fatigue strength improvement methods may be considered as a supplementary means of achieving the required fatigue life. The limitations to post-weld improvement methods are given by the rules.

The post-weld improvement method by burr grinding is applied to the weld toe. Thus, it is intended to increase the fatigue life of the weld toe. If the risk of failure is shifted from the weld toe to the root by applying post-weld treatment, there may be no significant improvement in the overall fatigue performance. Improvements of the weld root cannot be expected from treatment applied to weld toe.

The weld notch stress concentration is a direct function of the weld flank angle and the weld toe radius. The validity of the S-N curves in [Sec.2 \[2\]](#) is based on a weld flank angle with a maximum mean value of 50°. Burr grinding will affect the weld toe radius, while weld profiling will affect the weld flank angle. Burr grinding is described in this section and weld profiling and other methods are given in the [App.F](#).

Experience indicates that it may be a good design practice to exclude post-weld improvement at the design stage. The designer is advised to improve the details locally by other means, or to reduce the stress range through design and keep the possibility of fatigue life improvement as a reserve to allow for possible increase in fatigue loading during the design and fabrication process.

2 Grinding

2.1 Weld toe burr grinding

The weld may be machined using a burr grinding tool to produce a favourable shape to reduce stress concentrations and remove defects at the weld toe, see [Figure 1](#). In order to eliminate defects, such as intrusions, undercuts and cold laps, the material in way of the weld toe shall be removed. To be efficient, grinding should extend below the plate surface in order to remove toe defects.

The total depth of the burr grinding should not exceed neither 2 mm nor 7% of the local gross thickness of the plate. Any initial undercut not complying with this requirement should be repaired by an approved method.

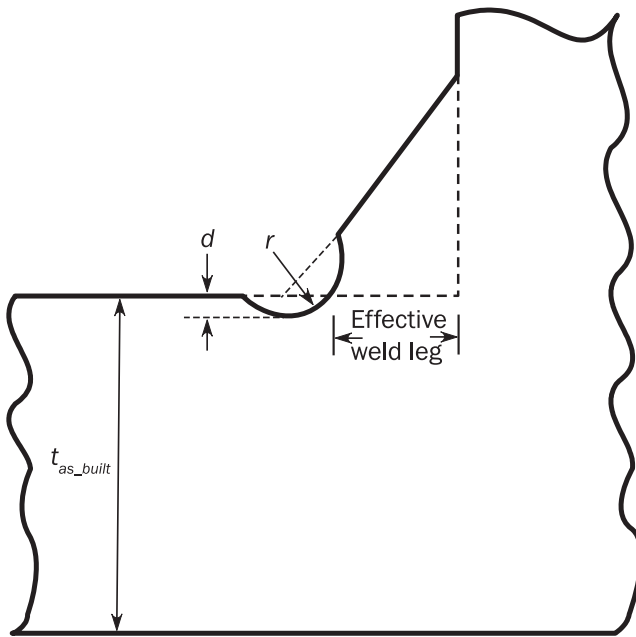


Figure 1 Details of ground weld toe geometry

To avoid introducing a detrimental notch effect by grinding, a sufficiently large burr diameter shall be used. The diameter should be between 10 and 25 mm for application to welded joints with plate thickness from 10 to 50 mm. The resulting root radius of the groove shall be no less than $0.25 t_{as_built}$. For thicker plates than 50 mm, the diameter should be agreed on a case by case basis. The weld throat thickness and leg length after burr grinding must comply with the rule requirements or any increased weld sizes as indicated on the approved drawings.

The treatment should produce a smooth concave profile at the weld toe with the depth of the depression penetrating into the plate surface to at least 0.5 mm below the bottom of any visible undercut.

Treatment of inter-bead toes should be carried out for large multi-pass welds as shown in Figure 2.

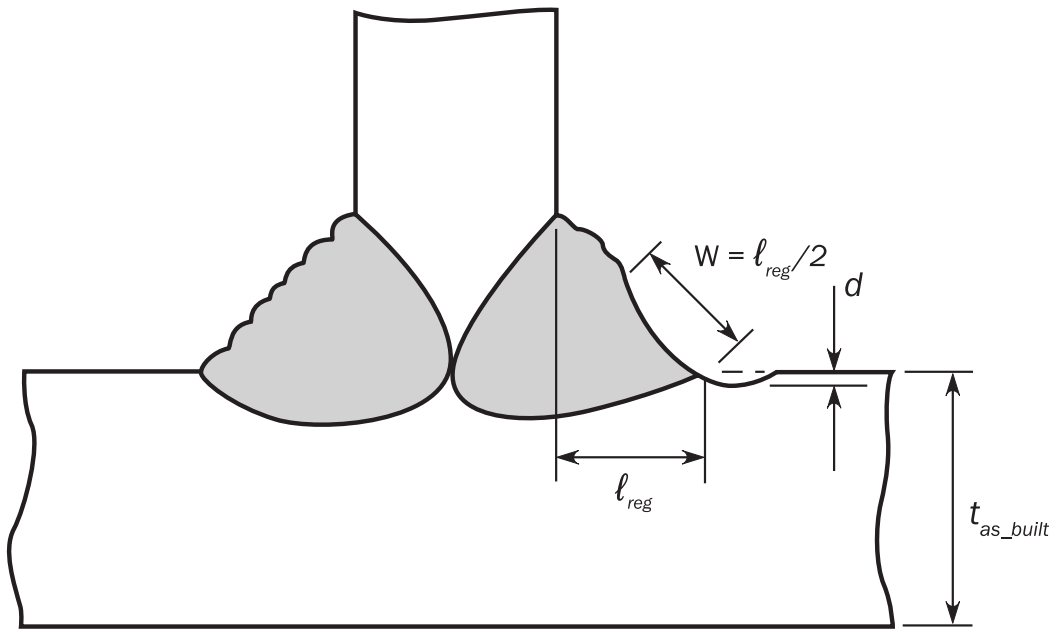


Figure 2 Extent of weld toe burr grinding to remove inter-bead toes on weld face; $\ell_{leg} = \ell_{reg}$: Weld leg length, W : Width of groove, d : Depth of grinding to be between 0.5 and 1 mm.

The inspection procedure should include a check of the weld toe radius, the depth of burr grinding, and confirmation that the weld toe undercut has been removed completely. Grinding also improves the reliability of inspection after fabrication and during service life.

If grinding is needed to achieve a specified fatigue life, the hot spot stress is rather high. Due to grinding a larger fraction of the fatigue life is spent during the initiation of fatigue cracks, and the crack grows faster after initiation. This may imply requirement for shorter inspection intervals during service life in order to detect the cracks before they affect the integrity of the structure.

2.2 Flush grinding of butt welds

Butt welds may be machined flush to achieve a better S-N curve with reference to [App.A](#). If a weld has been machined flush, it has to be documented that weld overfill has been removed by grinding and that the surface has been proven free from defects. The weld overfill may be removed by a coarse grinder tool such as a coarse grit flapper disk, grit size 40-60. The final surface should be achieved by fine grit grinding below that of weld toe defects. The surface should show a smooth or polished finish with no visible score marks. The roughness should correspond to $Ra = 3.2 \mu\text{m}$ or better. (It should be remembered that if the area is planned to be coated, a roughness around $Ra = 3.2 \mu\text{m}$ is often recommended). The surface should be checked by magnetic particle inspection. It is assumed that grinding is performed until all indications of defects are removed. Then possible presence of internal defects in the weld may be a limitation for use of a better S-N curve and it is important to perform a reliable non-destructive examination and use acceptance criteria that are in correspondence with the S-N classification that is used.

2.3 Fatigue life improvement factor for burr grinding

The full effect of burr grinding is shown in [Table 1](#). The fatigue life improvement for other methods of post-weld treatment is given in the [App.F](#). The post weld treatment factor, f_w , can be estimated based on the improvement factor, f_T , as described in [Sec.3 \[2.4\]](#).

Table 1 Improvement factor on fatigue life^{1, 2)}

<i>Improvement method</i>	<i>Minimum specified yield strength</i>	<i>Fatigue life improvement factor, f_T</i>
Burr grinding	Less than 350 N/mm ²	0.01 R_{eH}
	Higher than 350 N/mm ²	3.5

1) The improvement is only valid for high cycle fatigue where the slope m of the S-N curve is increased. This is represented by the improvement factor on the fatigue life. Alternatively, the fatigue life can be assessed by using S-N curves representing the improved state, when available.

2) The effect of burr grinding shall not be combined with the effect of improved S-N curve through flush grinding.

SECTION 8 DETAIL DESIGN STANDARD

1 Introduction

Detail design standards are provided to ensure improved fatigue performance of structural details. The design standard provides fatigue resistant detail design at an early stage in the structural design process based on the following considerations:

- application of fatigue design principles
- construction tolerances and other practical considerations
- in-service experience of fatigue performance.

The detail design standard may provide requirements in order to prevent the following types of fatigue cracks initiating from the:

- weld toe and propagating into the base material
- weld root and propagating into the plate section under the weld
- weld root and propagating through the weld throat
- surface irregularity or notch at the free plate edge and propagating into the base material.

The detail design standard may cover the following:

- highlighting potential critical areas within the ship structure
- identification of the fatigue hot spot locations for each of the critical structural details
- provision of a set of alternative improved configurations
- requirements on geometrical configurations, scantlings, welding and construction tolerances
- post fabrication method for improving fatigue life.

Alternative detail design configurations may be accepted if satisfactory fatigue performance, or equivalence to details in the design standard is demonstrated. For details covered by a given design standard, the Society may accept that fatigue assessment by FE hot spot or local stress analysis can be omitted.

2 Detail design standard for longitudinal end connections without top stiffener

2.1 Design standard A - slots with and without lug plate

This detail refers to detail 32 in [App.A Table 1](#) and represents a longitudinal stiffener without a top stiffener or collar plate. The critical hot spots may be located in the cut out.

Design standard 'A' as shown in [Table 1](#) or equivalent is recommended for locations in way of:

- side shell below $1.1T_{sc}$
- bottom.

The DNVGL CG for the specific ship types may also recommend design standard 'A' for locations in way of:

- inner hull longitudinal bulkhead below $1.1T_{sc}$
- topside tank sloping plating below $1.1T_{sc}$
- hopper
- inner bottom.

For designs that are different from those shown in [Table 1](#), satisfactory fatigue performance may be demonstrated by, e.g., using comparative FE analysis according to [\[2.3\]](#).

Table 1 Design standard A – slot/lug

Cut outs for longitudinals in transverse webs where web stiffeners are omitted or not connected to the longitudinal flange

Design standard A			
1	2	3	4
<p>Note 1: Soft toes marked '*' should be dimensioned to suit the weld leg length such that smooth transition from the weld to the curved part can be achieved. Maximum 15 mm or thickness of transverse web/collar plates/lug plates whichever is greater</p> <p>Note 2: Configurations 1 and 4 indicate acceptable lapped lug plate connections</p>			
Critical location	Locations around cut-out with high stress concentration and locations in way of weld terminations		

<i>Cut outs for longitudinals in transverse webs where web stiffeners are omitted or not connected to the longitudinal flange</i>	
<i>Design standard A</i>	
Detail design standard	Improved slot shape to avoid high stress concentrations in transverse webs due to shear loads and local pressure loads transmitted via welded joints
Building tolerances	Ensure alignment of all connecting members and accurate dimensional control of cut-outs according to IACS Recommendation No. 47
Welding requirements	A wraparound weld, free of undercut or notches, around the transverse web connection to longitudinal stiffener web

2.2 Design standard B - collar plate

This detail refers to detail 31 in [App.A Table 1](#) and represents a longitudinal stiffener without a top stiffener. The critical hot spots may be located in the cut out.

Design standard B as shown in [Figure 1](#) or equivalent is recommended for locations in way of:

- side shell below $1.1 T_{sc}$
- bottom.

The CG for the specific ship types may also recommend design standard 'B' for locations in way of:

- inner hull longitudinal bulkhead below $1.1 T_{sc}$
- hopper
- topside tank sloping plating below $1.1 T_{sc}$
- inner bottom.

For designs that are different from those shown in [Figure 1](#), satisfactory fatigue performance may be demonstrated by, e.g., using comparative FE analysis according to [\[2.3\]](#).

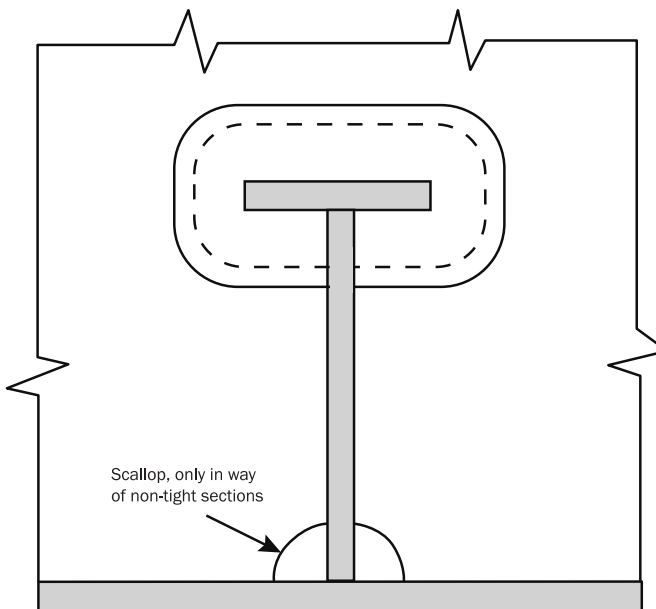


Figure 1 Complete collar fitted before the stiffener is pulled through the web frame

2.3 Equivalent design of longitudinal end connections without top stiffener

If the designs for longitudinal end connections in [2.1] and [2.2] are not used, the alternative design may be verified to have equivalent fatigue strength to the design standard A or B, or may be verified to have satisfactory fatigue performance. The alternative design may be verified according to the procedure described in the following.

The procedure is provided to verify the alternative design to have equivalent fatigue strength with respect to any position in the transverse cross section, i.e. double bottom and double side. The hot spot stress as well as the stress at the free plate edge of the alternative design and that of the design A should be compared to each other. The critical locations depend on the detail design and could be selected in agreement with the Society. The stress should be derived according to [Sec.6](#).

The FE models for verification of equivalence should have an transverse extent of 3 stiffeners, i.e. 4 stiffener spacings, and the longitudinal extent should be one half frame spacing in both forward and aft direction. A typical model is shown in [Figure 2](#). When extending this model in the longitudinal direction as in [\[6\]](#), the model can also be used to study longitudinal hot spots. No cut-outs for access openings should be included in the models. Connection between the lug or the web-frame to the longitudinal stiffener web, connections of the lug to the web-frame and free plate edges on lugs, and cut-outs in web-frame should be modelled with elements of plate thickness size ($t \times t$). The mesh with plate thickness size should extend at least five elements in all directions. Outside this area, the mesh size may gradually be increased in accordance with the requirements in [Sec.6](#). The eccentricity of the lapped lug plates should be included in the model. Transverse web and lug plates should be connected by eccentricity elements (transverse plate elements). The height of eccentricity elements should be the distance between mid-layers of transverse web and lug plates. The thickness of the eccentricity elements should be equal to two times the thickness of web-frame plate t_w . Eccentricity elements representing fillet welds are shown in [Figure 3](#).

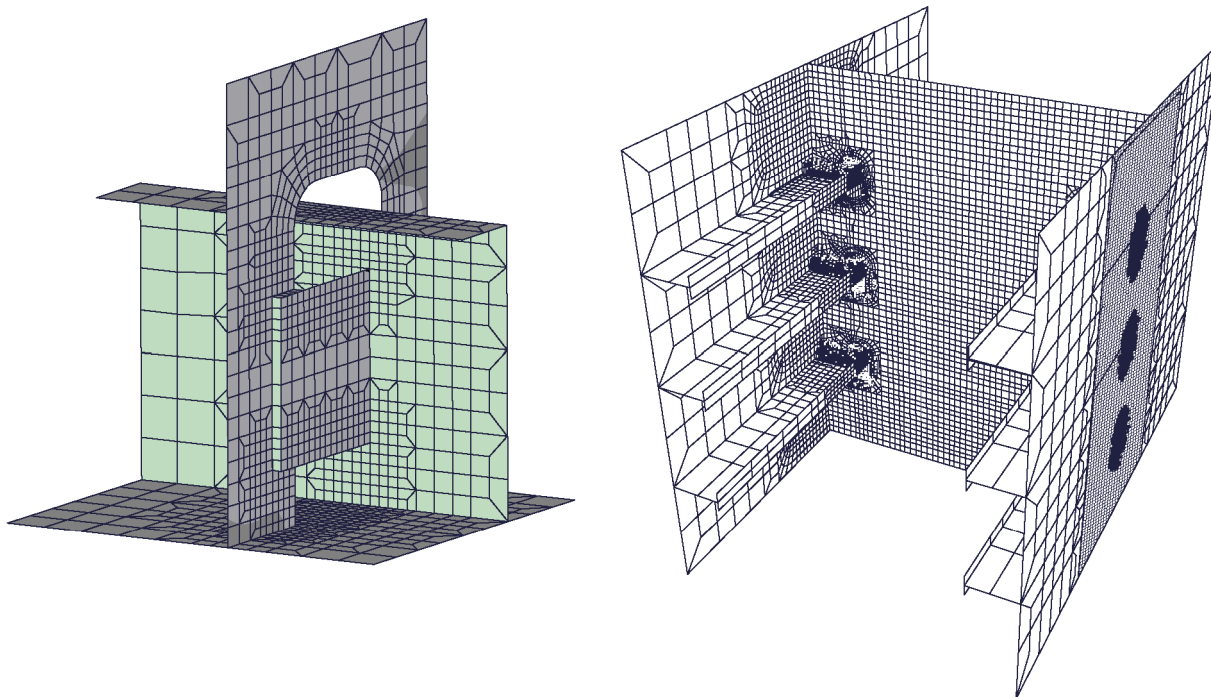


Figure 2 Finite element model for verification of equivalent design.

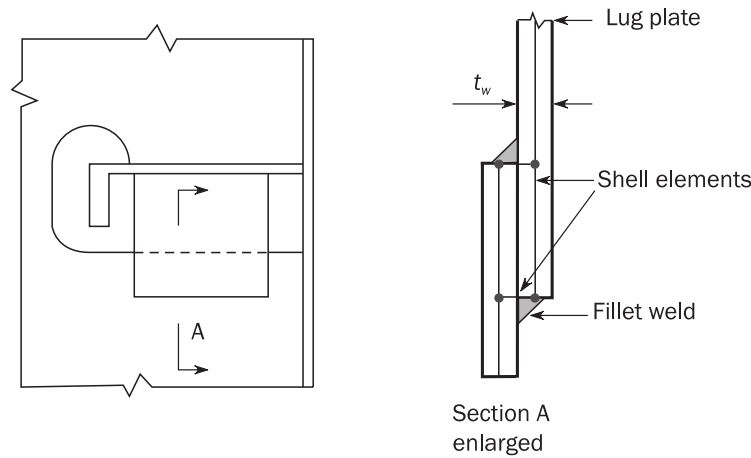


Figure 3 Modelling of eccentric lug plate by shell elements.

Three load cases should be applied to the models of the design standard and alternative designs:

- external pressure of unit value, fixed boundary conditions at top and bottom of model
- shear stress by prescribed unit displacement at the model top and fixed boundary conditions at the model bottom
- axial load by prescribed unit displacement at the model top and fixed boundary conditions at the model bottom.

The forward and aft part of the model should have symmetry condition describing the behaviour in a double hull structure. Load application and boundary conditions are provided in [Figure 4](#).

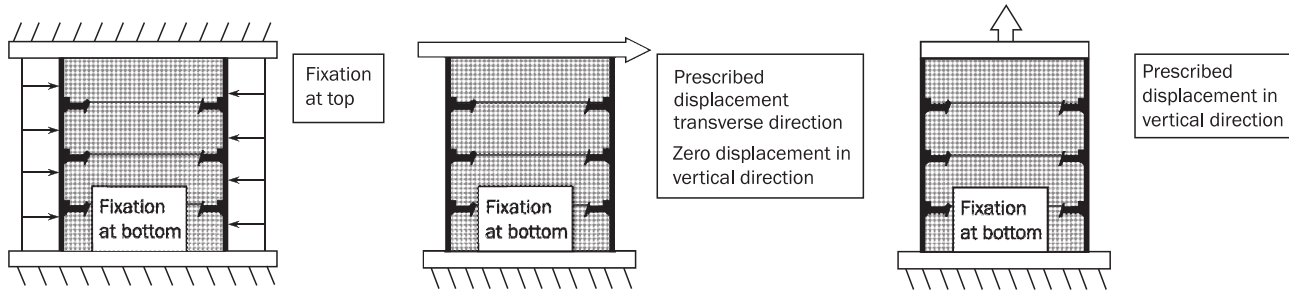


Figure 4 Load application and boundary conditions – FE model for verification of alternative design.

The alternative design may also be verified to have satisfactory fatigue performance using sub-modelling technique where a local model of the alternative design located at the actual position of the stiffener-frame connection is analysed. The alternative design is considered acceptable if the methodology and fatigue acceptance criterion of [Sec.6](#) is followed. The alternative design is considered acceptable only for the particular position where it is analysed.

3 Detail design standard for different ship types

The different ship types serve different functions, and the function of the vessel may define which structural details that are more susceptible to fatigue damage. Therefore, the detail design standard for specific ship types are given in the DNV GL class guideline relevant for the specific ship types.

SECTION 9 REFERENCES

1 References

- /1/ Det Norske Veritas, Rules for Classification of Ships, Part 3, Chapter 1, Hull Structural Design, Ships with Length 100 Meters and above, Høvik, January 2005.
- /2/ Hovem, L., Loads and Load Combinations for Fatigue Calculations - Background for the Wave Load Section for the DNVC Classification Note: Fatigue Assessment of Ships, DNVC Report No. 93-0314, Høvik, 1993.
- /3/ Cramer, E.H., Løseth, R. and Bitner-Gregersen, E., Fatigue in Side Shell Longitudinals due to External Wave Pressure, Proceedings OMAE conference, Glasgow, June 1993.
- /4/ Bergan, P. G., Lotsberg, I.: Advances in Fatigue Assessment of FPSOs. OMAE-FPSO'04-0012, Int. Conf. Houston 2004.
- /5/ Berge, S., Kihl, D., Lotsberg, I., Maherault, S., Mikkola, T. P. J., Nielsen, L. P., Paetzold, H., Shin, C.-H., Sun, H. -H and Tomita, Y.: Special Task Committee VI.2 Fatigue Strength Assessment. 15th ISSC, San Diego, 2003.
- /6/ British Maritime Technology, BMT, (Primary Contributors Hogben, H., Da Cunha, L.F. and Olliver, H.N), Global Wave Statistics, Unwin Brothers Limited, London, 1986.
- /7/ Doerk, O., Fricke, W., Weissenborn, C. (2003), "Comparison of Different Calculation Methods for Structural Stresses at Welded Joints". Int. J. of Fatigue 25, pp. 359-369.
- /8/ Fricke, W. (2001), "Recommended Hot Spot Analysis Procedure for Structural Details of FPSOs and Ships Based on Round-Robin FE Analyses". Proc. 11th ISOPE, Stavanger. Also Int. J. of Offshore and Polar Engineering. Vol. 12, No. 1, March 2002.
- /9/ Fricke, W., Doerk, O. and Gruenitz, L. (2004), "Fatigue Strength Investigation and Assessment of Fillet-Welds around Toes of Stiffeners and Brackets. OMAE-FPSO'04-0010. Int. Conf. Houston.
- /10/ Hobbacher, A. (1996), "Fatigue Design of Welded Joints and Components". IIW. XIII-1539-96/XV-845-96.
- /11/ Holtsmark, G. "The Bending Response of Laterally Loaded Panels with Unsymmetrical Stiffeners", DNVC Report No. 93-0152. Høvik, 1993.
- /12/ Holtsmark, G., Eimhjellen, R. and Dalsjø, P. "The Elastic Bending Response of Panel Stiffeners of Unsymmetrical Cross-section subjected to Uniform Lateral Pressure Loads". DNV Report No. 2004-1150. September 2004.
- /13/ Kim, W. S. and Lotsberg, I., "Fatigue Test Data for Welded Connections in Ship Shaped Structures". OMAE-FPSO'04-0018, Int. Conf. Houston 2004. Also Journal of Offshore and Arctic Engineering, Vol 127, Issue 4. November 2005, pp 359-365.
- /14/ Kuo, J.-F., Lacey, P. B., Zettlemoyer, N. and MacMillan, A. (2001), "Fatigue Methodology Specification for New-Built FPSO". OMAE Paper no 3016, Rio de Janeiro.
- /15/ Lotsberg, I., Cramer, E., Holtsmark, G., Løseth, R., Olaisen, K. and Valsgård, S.: Fatigue Assessment of Floating Production Vessels. BOSS'97, July 1997.
- /16/ Lotsberg, I., Nygård, M. and Thomsen, T.: Fatigue of Ship Shaped Production and Storage Units. OTC paper no 8775. Houston May 1998.
- /17/ Lotsberg, I., and Rove, H.: "Stress Concentration Factors for Butt Welds in Stiffened Plates". OMAE, ASME 2000.
- /18/ Lotsberg, I.: Overview of the FPSO Fatigue Capacity JIP. OMAE, Rio de Janeiro, June 2001.
- /19/ Lotsberg, I.: Design Recommendations from the FPSO Fatigue Capacity JIP. PRADS, Shanghai 2001.

- /20/ Lotsberg, I., "Fatigue Capacity of Fillet Welded Connections subjected to Axial and Shear Loading". IIW Document no XIII-2000-03 (XV-1146-03).
- /21/ Lotsberg, I., "Fatigue Design of Welded Pipe Penetrations in Plated Structures". Marine Structures, Vol 17/1 pp. 29-51, 2004.
- /22/ Lotsberg, I., "Recommended Methodology for Analysis of Structural Stress for Fatigue Assessment of Plated Structures". OMAE-FPSO'04-0013, Int. Conf. Houston 2004.
- Lotsberg, I. and Sigurdsson, G., "Hot Spot S-N Curve for Fatigue Analysis of Plated Structures".
- /23/ OMAE-FPSO'04-0014, Int. Conf. Houston 2004. Also Journal of Offshore and Arctic Engineering, Vol 128. November 2006, pp 330-336.
- /24/ Lotsberg, I and Landet, E. , "Fatigue Capacity of Side Longitudinals in Floating Structures". OMAE-FPSO'04-0015, Int. Conf. Houston 2004.
- /25/ Lotsberg, I. "Assessment of Fatigue Capacity in the New Bulk Carrier and Tanker Rules", Marine Structures, Vol 19, Issue 1. January 2006, pp 83-96.
- /26/ Lotsberg, I., Rundhaug, T. A, Thorkildsen, H. and Bøe, Å. (2005), "Fatigue Design of Web Stiffened Cruciform Connections", PRADS 2007, October 2007, Houston.
- Na, J. H., Lee, I. H., Sim, W. S. and Shin, H. S. (2003), "Full Stochastic Fatigue Analysis for Kizomba 'A' FPSO-Hull Interface Design". Proceedings 22nd Int. conf. on Offshore Mechanics and Arctic Engineering, Cancun Mexico.
- /28/ Polezhaeva, H. and Chung, H. (2001), "Effect of Misalignment on the Stress Concentration of a Welded Hopper Knuckle for a Typical FPSO". OMAE Rio de Janeiro.
- /29/ Sigurdsson, S., Landet, E. and Lotsberg, I. , "Inspection Planning of a Critical Block Weld in an FPSO". OMAE-FPSO'04-0032, Int. Conf. Houston, 2004.
- /30/ Storsul, R., Landet, E. and Lotsberg, I. , "Convergence Analysis for Welded Details in Ship Shaped Structures". OMAE-FPSO'04-0016, Int. Conf. Houston 2004.
- Storsul, R., Landet, E. and Lotsberg, I., "Calculated and Measured Stress at Welded Connections between Side Longitudinals and Transverse Frames in Ship Shaped Structures". OMAE-FPSO'04-0017, Int. Conf. Houston 2004.
- /32/ Urm, H. S., Yoo, I. S., Heo, J. H., Kim, S. C. and Lotsberg, I.: Low Cycle Fatigue Strength Assessment for Ship Structures. PRADS 2004.
- /33/ Witherby & Co. Ltd 1997: Guidance Manual for Tanker Structures.
- /34/ IIW Recommendations on Post Weld Improvement of Steel and Aluminium Structures. Document XIII-2200-07.
- /35/ Fricke, W. and Weissenborn, C, "Simplified stress concentration factors for fatigue-prone details in ship structures" (in German). Schiffbauforschung 43 (2004), pp. 39-50.
- /36/ Inge Lotsberg: "Assessment of the size effect for use in design standards for fatigue analysis", international journal of fatigue, Vol.66 March 2014, pp.86-100
- /37/ Schade, H.A., "Design curves for cross-stiffened plating under uniform bending load", Transactions, The society of naval architects and marine engineers, Volume 49, 1941, pp. 154-182.

APPENDIX A STRESS CONCENTRATION FACTORS AND FAT CLASSES

1 General

1.1 Definition of stress concentration factors

The fatigue life of a detail is governed by the hot spot stress range (or local stress for free plate edge). The hot spot stress, σ_{HS} , is obtained by multiplying the nominal stress, σ_n , by a stress concentration factor, K . The K factors in this document are thus defined as:

$$K = \frac{\sigma_{HS}}{\sigma_n}$$

The relation between the hot spot stress range, $\Delta\sigma_{HS}$, to be used together with the S-N curve, and the nominal stress range, $\Delta\sigma_n$, is:

$$\Delta\sigma_{HS} = K \cdot \Delta\sigma_n$$

The S-N curves in Sec.2 [2] are given for welded specimens, where the effect of the notch is included. All other stress risers have to be considered when evaluating the hot spot stress. This can be done by multiplication of K factors arising from different causes. The K factor to be used for calculation of the hot spot stress is derived as:

$$K = K_g \cdot K_m \cdot K_n = K_g \cdot (K_{me} + K_{ma} - 1) \cdot K_n$$

where:

- K_g = Stress concentration factor due to the gross geometry of the detail considered
- K_m = Stress concentration factor due to misalignment (eccentric and angular)
- K_{me} = Stress concentration factor due to misalignment from eccentricity (used for plate butt weld connections and cruciform joints)
- K_{ma} = Stress concentration factor due to misalignment from angular mismatch (used for plate butt weld connections only)
- K_n = Stress concentration factor for unsymmetrical stiffeners on laterally loaded panels; applicable when the nominal stress is derived from simple beam analyses.

For prescriptive analysis based on beam theory, all the K factors may be relevant. For hot spot analysis based on FE models, only K_m is regarded as additional. A K_g may, however, be relevant if the use of shell elements is not valid, see Sec.6 [6.2], e.g. for simplified cruciform joints.

1.2 Determination of stress concentration factors

The K factors may be determined based on FE hot spot analyses as described in Sec.6. Alternatively, K factors may be obtained from tabulated factors for typical details in ships. These tabulated factors can be found in [2].

1.3 Definition of FAT class

The FAT class refers to a detail categorization of S-N curves, where the FAT number refers to the stress range at $2 \cdot 10^6$ number of load cycles. For structural details where there is no difference between the stress concentration from axial and bending loads, or the loading is dominated by axial loads, FAT class curves can be used equivalently as K factors. The FAT number given in N/mm² is illustrated in [Sec.2 Figure 1](#).

1.4 Basis

The K factors and FAT classes presented in the following sections cover typical details in ships. Local stress concentration in way of welds depend on the level of workmanship. The default values given in the following tables are based workmanship tolerances according to normal shipbuilding practise. If greater tolerances are used, the K factors or FAT classes should be determined based on the actual tolerances, see also [App.F](#).

2 Longitudinal end connections

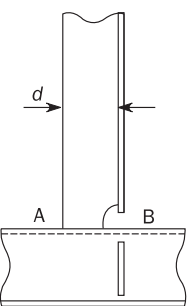
2.1 Tabulated K factors

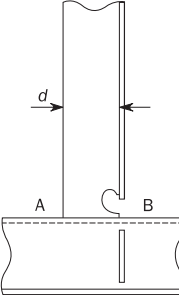
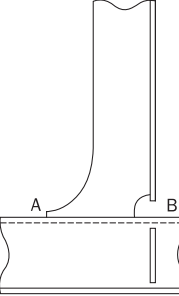
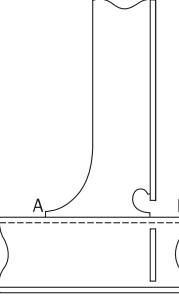
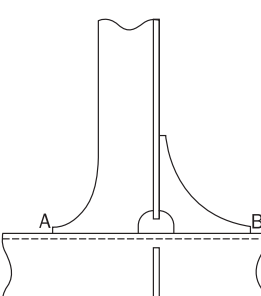
K_g factors for longitudinal end connections are given in [Table 1](#). For detail 1 to 31, the hot spot is located on the stiffener flange or top of the stiffener web in case of flat bars, while for detail 32 the hot spot is located at the stiffener web. These details are used in the prescriptive fatigue analysis in [Sec.4](#). The factors are applicable to stiffeners subject to axial and lateral loads.

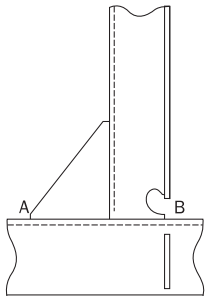
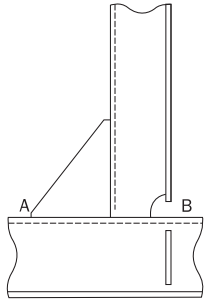
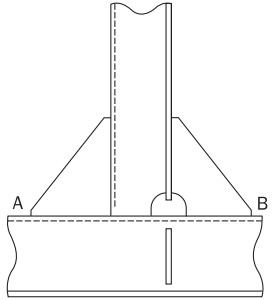
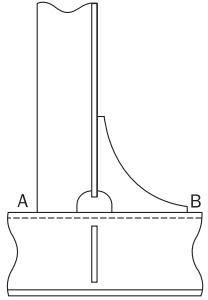
Where the longitudinal stiffener is a flat bar and there is a web stiffener/bracket welded to the flat bar, the stress concentration factor listed in [Table 1](#) (excluding detail 31 and 32) should be multiplied by a factor of 1.12 when there is less than 8 mm clearance between the edge of the flat bar stiffener and the attachment on either side of the attachment. This also applies to unsymmetrical profiles where there is less than 8 mm clearance between the edge of the stiffener flange and the attachment, e.g. bulb or angle profiles where the clearance of 8 mm cannot be achieved.

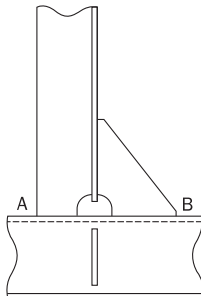
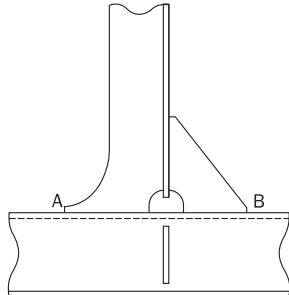
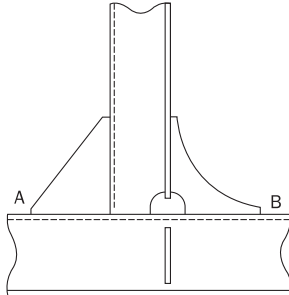
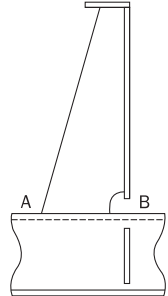
Designs with overlapped connection/attachments should be avoided in areas where fatigue might be critical. If overlap is used an additional factor of 1.15 should be used.

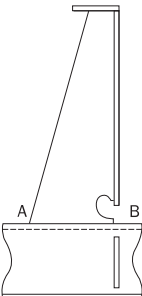
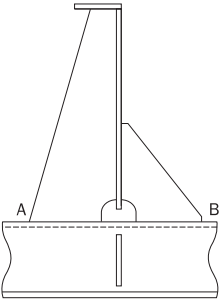
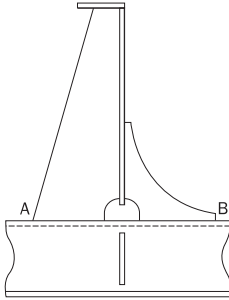
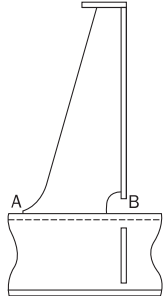
Table 1 K_g factors for stiffener supports

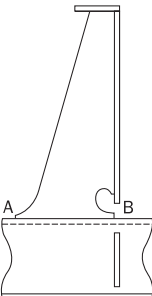
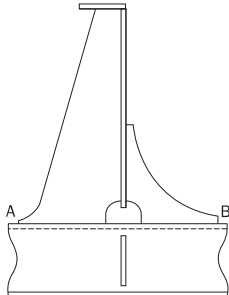
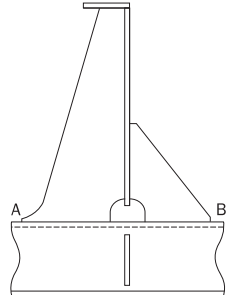
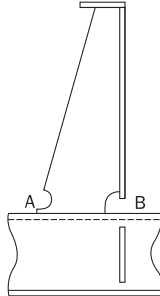
No.	Geometry Connection type	Point A		Point B	
		K_a	K_b	K_a	K_b
1 ⁽¹⁾		1.28 for $d \leq 150$ 1.36 for $150 < d < 250$ 1.45 for $d > 250$	1.40 for $d \leq 150$ 1.50 for $150 < d < 250$ 1.60 for $d > 250$	1.28 for $d \leq 150$ 1.36 for $150 < d \leq 250$ 1.45 for $d > 250$	1.60

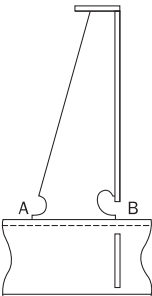
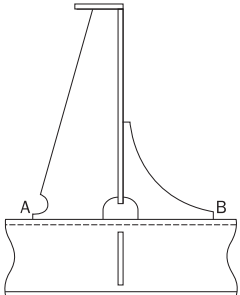
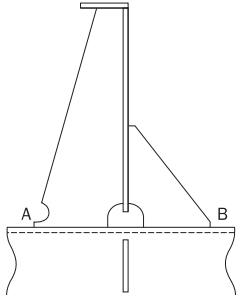
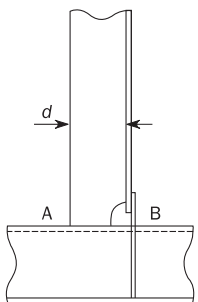
No.	Geometry Connection type	Point A		Point B	
		K_a	K_b	K_a	K_b
2 ⁽¹⁾		1.28 for $d \leq 150$ 1.36 for $150 < d < 250$ 1.45 for $d > 250$	1.40 for $d < 150$ 1.50 for $150 < d < 250$ 1.60 for $d > 250$	1.14 for $d \leq 150$ 1.24 for $150 < d \leq 250$ 1.34 for $d > 250$	1.27
3		1.28	1.34	1.52	1.67
4		1.28	1.34	1.34	1.34
5		1.28	1.34	1.28	1.34

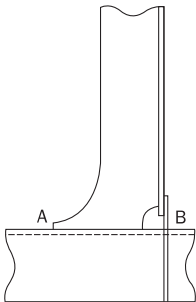
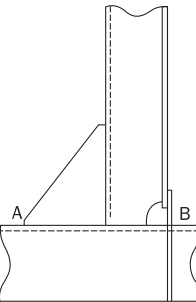
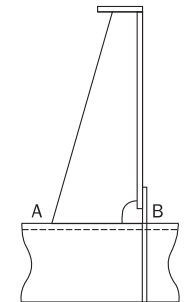
No.	Geometry Connection type	Point A		Point B	
		K_a	K_b	K_a	K_b
6		1.52	1.67	1.34	1.34
7		1.52	1.67	1.52	1.67
8		1.52	1.67	1.52	1.67
9		1.52	1.67	1.28	1.34

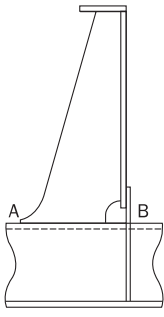
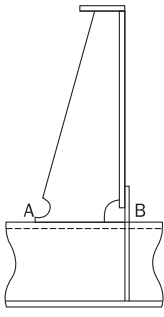
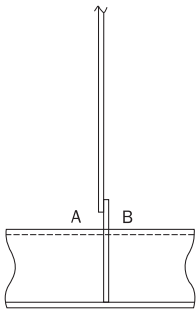
No.	Geometry Connection type	Point A		Point B	
		K_a	K_b	K_a	K_b
10		1.52	1.67	1.52	1.67
11		1.28	1.34	1.52	1.67
12		1.52	1.67	1.28	1.34
13		1.52	1.67	1.52	1.67

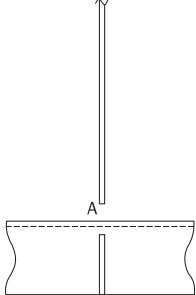
No.	Geometry Connection type	Point A		Point B	
		K_a	K_b	K_a	K_b
14		1.52	1.67	1.34	1.34
15		1.52	1.67	1.52	1.67
16		1.52	1.67	1.28	1.34
17		1.28	1.34	1.52	1.67

No.	Geometry Connection type	Point A		Point B	
		K_a	K_b	K_a	K_b
18		1.28	1.34	1.34	1.34
19		1.28	1.34	1.28	1.34
20		1.28	1.34	1.52	1.67
21		1.34	1.34	1.52	1.67

No.	Geometry Connection type	Point A		Point B	
		K_a	K_b	K_a	K_b
22		1.34	1.34	1.34	1.34
23		1.34	1.34	1.28	1.34
24		1.34	1.34	1.52	1.67
25 ⁽¹⁾		1.28 $d \leq 150$ 1.36 for $150 < d \leq 250$ 1.45 $d > 250$	1.40 $d \leq 150$ 1.50 for $150 < d \leq 250$ 1.60 $d > 250$	1.14 $d \leq 150$ 1.24 for $150 < d \leq 250$ 1.34 $d > 250$	1.25 $d \leq 150$ 1.36 for $150 < d \leq 250$ 1.47 $d > 250$

No.	Geometry Connection type	Point A		Point B	
		K_a	K_b	K_a	K_b
26		1.28	1.34	1.34	1.47
27		1.52	1.67	1.34	1.47
28		1.52	1.67	1.34	1.47

No.	Geometry Connection type	Point A		Point B	
		K_a	K_b	K_a	K_b
29		1.28	1.34	1.34	1.47
30		1.34	1.34	1.34	1.47
31 ⁽²⁾		1.13	1.20	1.13	1.20

No.	Geometry Connection type	Point A		Point B	
		K_a	K_b	K_a	K_b
32 ^(2,3)		1.13	1.14	1.13	1.14

1) The attachment length d , in mm, is defined as the length of the welded attachment on the longitudinal stiffener flange without deduction of the scallop
 2) ID. 31 and 32 refer to details where web stiffeners are omitted or not connected to the longitudinal stiffener flange. For detail 31, however, the collar is assumed welded to the stiffener flange. Reduction of the K_n factor for detail 32 for L and bulb profiles may be accepted based on verification by FE hot spot analysis
 3) For connection type ID. 32, with no collar and/or web plate welded to the flange, the stress concentration factors provided in this table should be used irrespective of the slot configuration. The fatigue assessment point 'A' is located at the connection between the stiffener web and the transverse web frame or lug plate. The stress concentration factor represents the hot spot related to the longitudinal stress.

For detail 32 in [Table 1](#), the hot spot stress is not located at the flange, but at the stiffener web. The bending stress can therefore be reduced compared to the bending stress in the flange by considering the hot spot to be located a height h_{HS} above the plate flange, corresponding to the upper connection between the stiffener web and the frame or the lug, as indicated in [Figure 1](#). The parameter h_{HS} should be estimated both for hot spot A and B separately. If no value is available, the default value of h_{HS} can be taken as the height of the stiffener, which would be conservative.

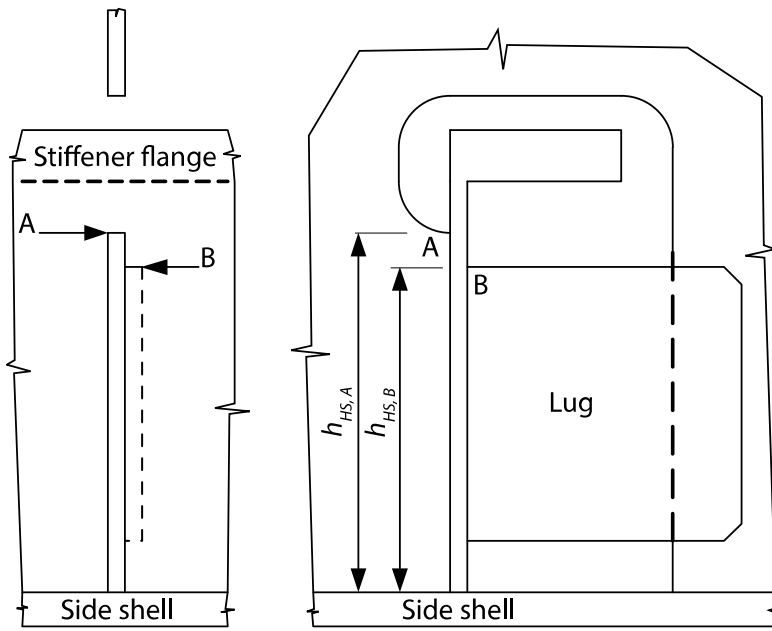


Figure 1 Illustration of detail 32 with hot spot A and B in the stiffener web. The arrows indicate the stress direction. A is taken at a distance h_{HS} from the plate flange.

To establish alternative K factors for actual geometries of stiffener supports, the procedure in [App.E \[6\]](#) should be followed.

2.2 Soft toe of web stiffener and backing bracket

Detail designs for longitudinal end connections with soft toes and backing brackets are given in [Figure 2](#). Soft toe geometry of end connection of web stiffener and backing bracket is defined as:

$$\theta \leq 20$$

$$h_{toe} \leq \max(t_{bkt-gr}, 15)$$

where:

- θ = Angle of the toe, in degrees, as shown in [Figure 2](#)
- h_{toe} = Height of the toe, in mm, as shown in [Figure 2](#)
- t_{bkt-gr} = Gross thickness of the bracket, in mm.

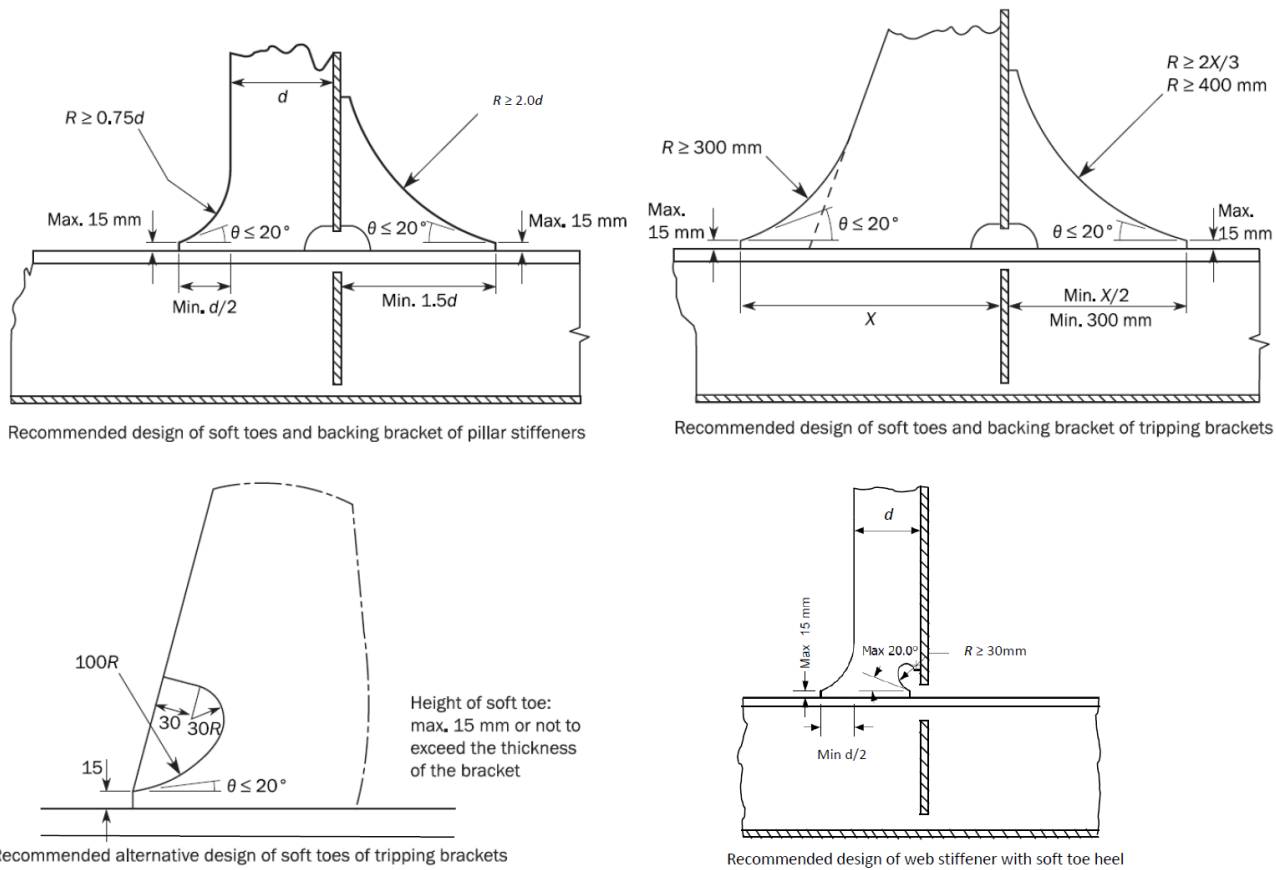


Figure 2 Detail design for soft toes and backing brackets

2.3 Unsymmetrical stiffener flange

The stress concentration factor K_n for unsymmetrical flange of built-up and rolled angle stiffeners under lateral load, calculated at the web's mid-thickness position, as shown in [Figure 3](#) and with parameters in [Figure 4](#), should be taken as:

$$K_n = 1 + (K_{n1} - 1) \cdot f_A$$

where:

$$K_{n1} = \frac{1 + \lambda \beta^2}{1 + \lambda \beta^2 \psi_z}$$

$$\lambda = \frac{3 \left(1 + \frac{\eta}{280} \right)}{1 + \frac{\eta}{40}}$$

$$\eta = \frac{\ell_{bdg}^4 10^{12}}{b_{f-n50}^3 \cdot t_{f-n50} \cdot h_{stf-n50}^2 \left(\frac{4 \cdot h_{stf-n50}}{t_{w-n50}^3} + \frac{s}{t_{p-n50}^3} \right)}$$

$$\beta = 1 - \frac{2b_{g-n50}}{b_{f-n50}} \quad \text{for built-up profiles}$$

$$\beta = 1 - \frac{t_{w-n50}}{b_{f-n50}} \quad \text{for rolled angle profiles}$$

$$\psi_z = \frac{h_{w-n50}^2 t_{w-n50}}{4 Z_{n50}} 10^{-3}$$

b_{g-n50}	= Eccentricity of the stiffener equal to the distance from the flange edge to the centre line of the web, in mm
b_{f-n50}	= Net breadth of flange, in mm
t_{f-n50}	= Net flange thickness, in mm
$h_{stf-n50}$	= Net stiffener height, including face plate, in mm
t_{w-n50}	= Net web thickness, in mm

h_{w-n50}	= Net height of stiffener web, in mm
t_{p-n50}	= Net thickness of attached plating, in mm
Z_{n50}	= Net section modulus, in cm^3 , of stiffener with an attached plating breadth equal to the stiffener spacing.
f_A	= Reduction factor
	= 0.5 for unsymmetrical profiles without weld at flange, i.e., hot spot located at stiffener web (detail No. 32 in Table 1)
	0.7 for rolled angle profiles in way of end connection of web stiffener (details No. 1 - 2 in Table 1) with offset equal or greater than 8 mm
	= 1.0 in other cases

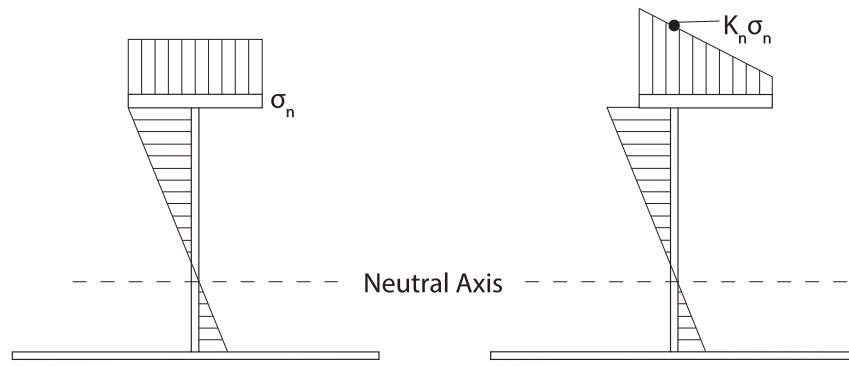


Figure 3 Bending stress in stiffener with symmetrical and unsymmetrical flange relative to nominal stress, σ_n

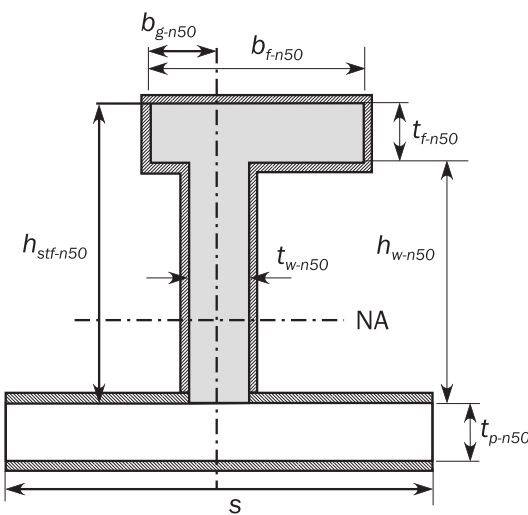


Figure 4 Stiffener - net scantling

For bulb profiles K_n factor should be calculated using the equivalent built-up profile as shown in [Figure 5](#). The flange of the equivalent built-up profile should have the same properties as the bulb flange, i.e. same cross sectional area and moment of inertia about the vertical axis and neutral axis position. For HP bulb profiles, examples of the equivalent built-up profile dimensions are listed in [Table 2](#).

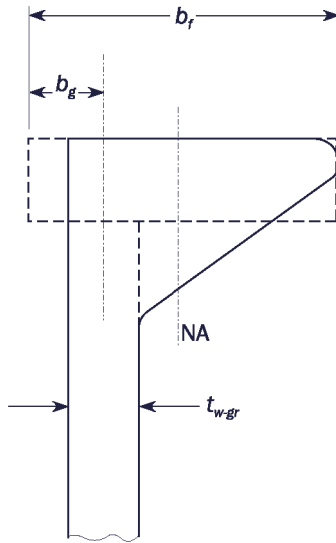


Figure 5 Bulb profile and equivalent built-up profile

Table 2 HP equivalent built-up profile dimensions (the last row represents an approximation for HP bulb profiles for sizes not listed)

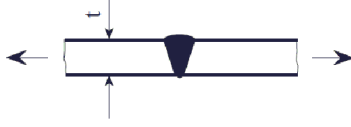
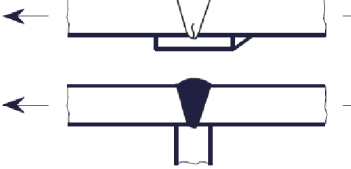
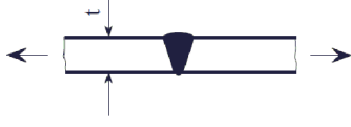
HP-bulb		Equivalent built-up flange in gross thickness		
Height (mm)	Gross web thickness, t_{w-gr} (mm)	b_f (mm)	t_{f-gr} (mm)	b_g (mm)
200	9 – 13	$t_{w-gr} + 24.5$	22.9	$(t_{w-gr} + 0.9)/2$
220	9 – 13	$t_{w-gr} + 27.6$	25.4	$(t_{w-gr} + 1.0)/2$
240	10 – 14	$t_{w-gr} + 30.3$	28.0	$(t_{w-gr} + 1.1)/2$
260	10 – 14	$t_{w-gr} + 33.0$	30.6	$(t_{w-gr} + 1.3)/2$
280	10 – 14	$t_{w-gr} + 35.4$	33.3	$(t_{w-gr} + 1.4)/2$
300	11 – 16	$t_{w-gr} + 38.4$	35.9	$(t_{w-gr} + 1.5)/2$
320	11 – 16	$t_{w-gr} + 41.0$	38.5	$(t_{w-gr} + 1.6)/2$
340	12 – 17	$t_{w-gr} + 43.3$	41.3	$(t_{w-gr} + 1.7)/2$
370	13 – 19	$t_{w-gr} + 47.5$	45.2	$(t_{w-gr} + 1.9)/2$
400	14 – 19	$t_{w-gr} + 51.7$	49.1	$(t_{w-gr} + 2.1)/2$
430	15 – 21	$t_{w-gr} + 55.8$	53.1	$(t_{w-gr} + 2.3)/2$
h_{stf}	t_{w-gr}	$t_{w-gr} + 0.1345 \cdot h_{stf} - 2.1216$	$0.1317 \cdot h_{stf} - 3.5726$	$(t_{w-gr} + 0.006 \cdot h_{stf} - 0.3139)/2$

3 Butt welds

K factors and FAT classes for butt welds are given in [Table 3](#). Default values are provided based on workmanship tolerances according to normal shipbuilding practise. If greater tolerances are used, the K factors or FAT classes should be determined based on the actual tolerances and the equations given in [Table 3](#). By the term "NDE" a method to detect surface cracks is meant, e.g. by liquid penetrant testing (PT) or magnetic particle testing (MT). The Society may accept on a case-by-case basis visual inspection for grinded surfaces. By the term "100% NDE", it is meant that NDE should be applied to all welds associated with the detail. In addition to surface methods, other methods such as radiographic testing (RT) or ultrasonic testing (UT) are relevant and may also detect internal defects. For "100% NDE", the Society may accept only surface methods as PT and MT on case-by-case basis, but visual inspections are not regarded sufficient.

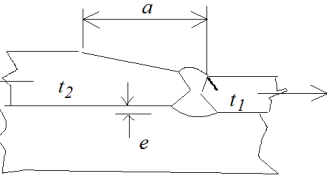
Table 3 K factors and FAT classes for butt welds

No.	Geometry connection	Description of joint	Included misalignment	K factor	FAT N/mm ²
1		Transverse butt weld, welded from both sides, ground flush to plate, 100% NDE	$K_m = 1.15$ from, e.g., axial misalignment of $0.05 \cdot t$ (may be limited to 2 mm provided that proper quality control is carried out ¹⁾)	0.80	112
2		Transverse butt weld, welded from both sides, made in shop in flat position, max. weld reinforcement 1 mm + $0.1 \cdot$ weld width, smooth transitions, NDE.	$K_m = 1.15$ from, e.g., axial misalignment of $0.05 \cdot t$ (may be limited to 2 mm provided that proper quality control is carried out ¹⁾)	1.00	90
3		Transverse butt weld welded from both sides and with max. weld reinforcement 1 mm + $0.15 \cdot$ weld width, NDE.	Quality level B ²⁾ : $K_m = 1.3$ from, e.g., axial misalignment of $0.1 \cdot t$ (may be limited to 3 mm provided that proper quality control is carried out ¹⁾) Quality level C ²⁾ : $K_m = 1.45$ from, e.g., axial misalignment of $0.15 \cdot t$ (may be limited to 4 mm provided that proper quality control is carried out ¹⁾)	1.13 1.25	80 72
4		Transverse butt weld, single side welding, welded on non-fusible temporary backing, root cracking	Quality level B ²⁾ : $K_m = 1.3$ from, e.g., axial misalignment of $0.1 \cdot t$ (may be limited to 3 mm provided that proper quality control is carried out ¹⁾) Quality level C ²⁾ : $K_m = 1.45$ from, e.g., axial misalignment of $0.15 \cdot t$ (may be limited to 4 mm provided that proper quality control is carried out ¹⁾)	1.13 1.25	80 72

No.	Geometry connection	Description of joint	Included misalignment	K factor	FAT N/mm ²
5		Laser ($t \leq 8\text{mm}$) and laser hybrid ($t \leq 12\text{mm}$) butt weld	$K_m = 1.3$ from, e.g., axial misalignment of $0.1 \cdot t$	1.13	80
6		Transverse butt weld with permanent backing strip or three plate connection, single side welding. These details are not recommended in areas prone to fatigue due to sensitivity of workmanship and fabrication	Quality level B ²⁾ : $K_m = 1.3$ from, e.g., axial misalignment of $0.1 \cdot t$ (may be limited to 3 mm provided that proper quality control is carried out ¹⁾) Quality level C ²⁾ : $K_m = 1.45$ from, e.g., axial misalignment of $0.15 \cdot t$ (may be limited to 4 mm provided that proper quality control is carried out ¹⁾)	1.27 1.42	71 63
7		Transverse butt weld without backing bar, single side welding. If root is checked by appropriate NDE, FAT class (K factors) may be improved by a factor 2. For tubular sections, FAT class (K factors) may be improved by a factor 1.125.	Quality level B ²⁾ : $K_m = 1.3$ from, e.g., axial misalignment of $0.1 \cdot t$ (may be limited to 3 mm provided that proper quality control is carried out ¹⁾) Quality level C ²⁾ : $K_m = 1.45$ from, e.g., axial misalignment of $0.15 \cdot t$ (may be limited to 4 mm provided that proper quality control is carried out ¹⁾)	2.48 2.78	36 32

No.	Geometry connection	Description of joint	Included misalignment	K factor	FAT N/mm ²
8		<p>Partial penetration butt weld.</p> <p>The stress should be related to the weld throat sectional area, and the weld overfill should not be taken into account</p>	<p>Quality level B²⁾: $K_m = 1.3$ from, e.g., axial misalignment of $0.1 \cdot t$ (may be limited to 3 mm provided that proper quality control is carried out¹⁾)</p> <p>Quality level C²⁾: $K_m = 1.45$ from, e.g., axial misalignment of $0.15 \cdot t$ (may be limited to 4 mm provided that proper quality control is carried out¹⁾)</p>	2.48 2.78	36 32

No.	Geometry connection	Description of joint	Included misalignment	K factor	FAT N/mm ²
9		<p>Transverse butt welds of plates with angular misalignment, unsupported.</p> <p>The formulation assumes zero mean stress, and in tension it will become conservative, but non-conservative in compression. The α is related to the deflection. For fixed ends the equation becomes equal to detail no. 10.</p>	$K_{m\alpha} = 1 + \frac{\lambda}{4} \cdot \alpha \cdot \frac{s}{t}$ <p>where: $\lambda = 6$ for pinned ends $\lambda = 3$ for fixed ends $\alpha = \text{angular misalignment, in radians}$ $s = \text{plate width, in mm}$ $t = \text{plate thickness, in mm}$ $e = \text{deflection, in mm}$</p>	For detail no. 1: 90/129 · $K_m^{3)}$ For details no. 2,3,4 & 5: 90/104 · $K_m^{3)}$	For detail no. 1: 129/ $K_m^{3)}$ For details no. 2,3,4 & 5: 104/ $K_m^{3)}$
10		<p>Transverse butt weld of plates or pipes with large radius, with axial misalignment, unsupported.</p>	$K_{me} = 1 + \frac{3e}{t}$ <p>where: $e = \text{eccentricity, in mm}$ $t = \text{plate thickness, in mm}$</p>	For details no. 6: 90/92 · $K_m^{3)}$	For details no. 6: 92/ $K_m^{3)}$
11	$a = \min 3(\Delta t + e)$ $\Delta t = t_2 - t_1$	<p>Transverse butt weld of plates or pipes with large radius, with different thickness and axial misalignment, sloped, unsupported.</p>	$K_{me} = 1 + \frac{6(e + e_t)}{t_1 \left[1 + \frac{t_2^{1.5}}{t_1^{1.5}} \right]}$ <p>where: $e = \text{max. misalignment}$ $e_t = \frac{1}{2} (t_2 - t_1) \text{ eccentricity due to change in thickness}$ $t_2 = \text{thickness of thicker plate}$ $t_1 = \text{thickness of thinner plate}$</p>	For details no. 7 & 8: 90/47 · $K_m^{3)}$	For details no. 7 & 8: 47/ $K_m^{3)}$

No.	Geometry connection	Description of joint	Included misalignment	K factor	FAT N/mm ²
12	$a = \min 3(\Delta t + e)$ $\Delta t = t_2 - t_1$ 	<p>Transverse butt weld of plates with different thickness and axial misalignment, sloped, supported.</p> <p>Within the transverse distance $2 \cdot t_2$ from the web. Outside this distance, detail no. 11 should be used.</p>	$K_{me} = 1.0$ $K_{ma} = 1.0$		

¹⁾ In case of limited axial misalignment, FAT X and K can be calculated by the relations for detail no. 10. However, the increased FAT class divided by f_{thick} is not to exceed the above tabulated FAT class and the reduced K factor times f_{thick} is not to be less than the above tabulated K factor, respectively.

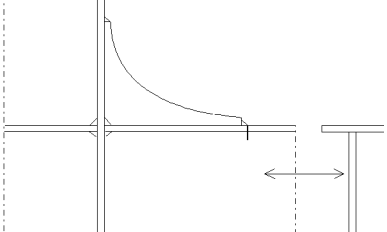
²⁾ Quality level refers to the EN ISO 5817 standard

³⁾ K_m should be calculated by $K_m = K_{ma} + K_{me} - 1$

4 Flange connections

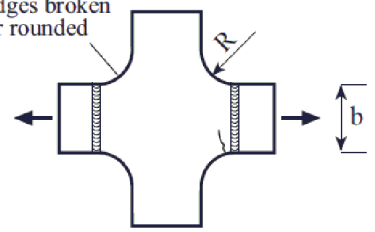
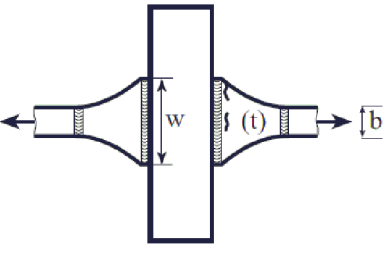
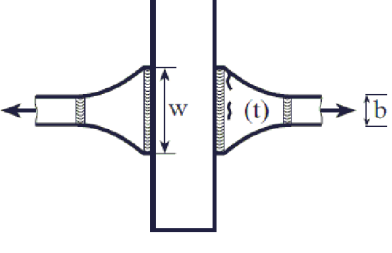
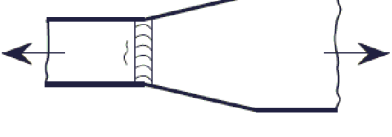
K factors and FAT classes for flange connections are given in [Table 4](#).

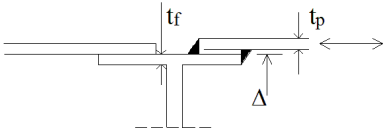
Table 4 K factors and FAT classes for flange connections

No.	Geometry	Description of joint	K factor	FAT N/mm ²
1		Flange connection with softening toe	1.47	61

No.	Geometry	Description of joint	K factor	FAT N/mm ²
2		<p>Attachment with smooth transition (sniped end or radius) welded on the beam flange, bulb or plate.</p> <p>$c < 2t_2$, max. 25 mm $r \geq 0.5h$ $r < 0.5h$ or $\varphi \leq 20^\circ$ $\varphi > 20^\circ$ see detail no.2 in Table 5</p> <p>For $t_2 \leq 0.5t_1$, the FAT class or K factor may be improved by a factor of 1.125, but not for bulb.</p> <p>When welding close to the edges of plates or profiles (distance less than 10mm), the FAT class and K factor should be downgraded by a factor of 1.125.</p>	1.27 1.43	71 63
3		<p>Longitudinal attachment welded on edge of plate or beam flange, with smooth transition (sniped end or radius)</p> <p>$c \leq 2 \cdot t_2$, max. 25 mm $r \geq 0.5h$ $r < 0.5h$ or $\varphi \leq 20^\circ$ $\varphi > 20^\circ$ see joint 5 in Table 5</p> <p>For $t_2 \leq 0.7 \cdot t_1$, the FAT class and K factor may be improved by a factor of 1.125.</p>	1.8 2.0	50 45
4		<p>Longitudinal attachment welded on edge of plate or beam flange, with smooth transition radius</p> <p>$r/h \geq 1/3$ or ($r \geq 150\text{mm}$) $1/6 \leq r/h < 1/3$ $r/h < 1/6$</p> <p>Smooth transition radius formed by grinding the full penetration weld area in order to achieve a notch-free transition area. Final grinding should be performed parallel to the stress direction.</p>	1.0 1.27 1.8	90 71 50

No.	Geometry	Description of joint	K factor	FAT N/mm ²
5		Crossing of flanges welded from both sides and where the radius R is ground $R \geq 1.25t$ where: t = thickness of flange	1.47	61
6		Crossing flanges with full penetration butt weld. $K_{me} = 1.30$	1.80	50
7		Crossing of flanges with transition radius R , crack at free plate edge. $R \geq 0.15b$ To be used together with S-N curve B to C2 dependent on surface condition. The reference stress is $1.9 \cdot \Delta\sigma_n$. The butt weld needs to be considered separately, see no. 8 or 9.	B-C2	150-100
8		Crossing flanged with transition radius R , full penetration butt weld, welded from both sides at flat position $R \geq b$ Welded reinforcement $\leq 1\text{mm} + 0.1 \cdot \text{weld width}$, smooth transitions, NDE, weld ends ground. $K_{me} = 1.15$. Cutting edges in the quality according to detail no. 2 or no. 3 in Sec.2 Table 2.	1.0	90

No.	Geometry	Description of joint	K factor	FAT N/mm ²
9		Crossing flanged with transition radius R , full penetration butt weld, welded from both sides, $R \geq b$ No misalignment, 100% NDE, weld ends ground, butt weld ground flush to surface. Cutting edges broken or rounded according to detail no. 2 in Sec.2 Table 2.	0.9	100
10		Crossing flanges with full penetration butt weld, welded from both sides. $K_{me} = 1.30$. Cutting edges in the quality according to detail no. 2 or 3 in Sec.2 Table 2. Connection length $w \geq 2 \cdot b$ Nominal stress $\sigma_n = \frac{F}{b \cdot t}$	1.43	63
11		Crossing flanges with full penetration butt weld, welded from both sides, NDE, weld ends ground, butt weld ground flush to surface. $K_{me} = 1.30$. Cutting edges in the quality according to detail no. 2 and 3 in Sec.2 Table 2. Connection length and nominal stress as in no. 10.	1.13	80
12		Transverse butt welds between plates of different widths, NDE slope 1:5 slope 1:3 slope 1:2 In case of thickness change, additional misalignment factor should be considered from [3]	1.13 1.27 1.43	80 71 63

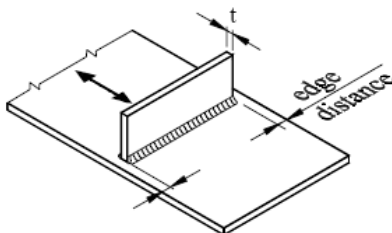
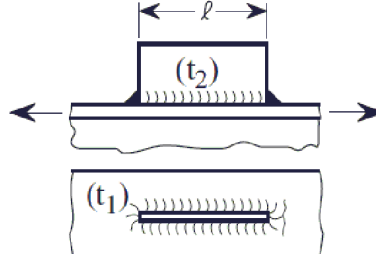
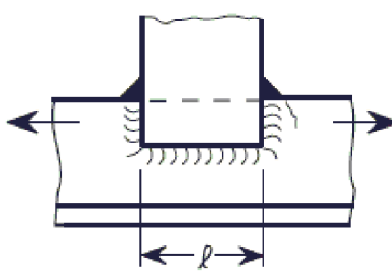
No.	Geometry	Description of joint	K factor	FAT N/mm ²
13		Overlap connection. If this detail is being used in an area with high axial stress and the K factor of 4 is resulting in fatigue life below the target, the actual K factor should be estimated based on FE analysis.	4.0	23

5 Welded attachments

5.1 Attachments welded to a plate or stiffener

K factors and FAT classes for attachments welded to a plate or stiffener are given in [Table 5](#).

Table 5 K factors and FAT classes for attachments welded to a plate

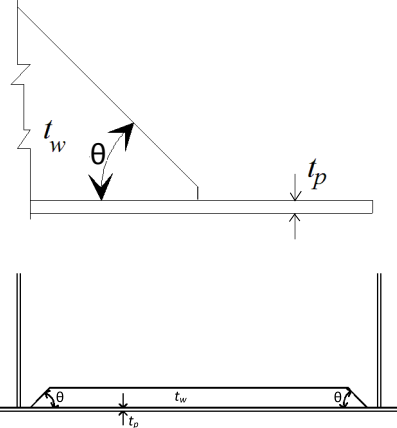
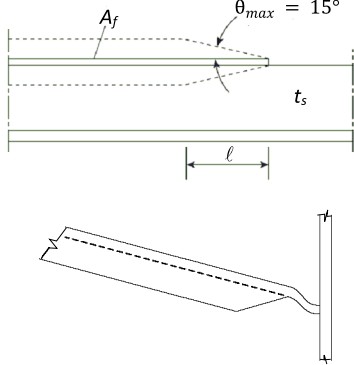
No.	Geometry	Description of joint	K factor	FAT N/mm ²
1		<p>Transverse attachment on unsupported plate. Edge distance, if any, to be minimum 10mm.</p> <p>$t \leq 25 \text{ mm}$ ($K_{ma} = 1.2$): $t > 25 \text{ mm}$ and $t_p > 25 \text{ mm}$ ($K_{ma} = 1.2$): $t_p > 50 \text{ mm}$ and $t_p > 2t$ ($K_{ma} = 1.12$):</p> <p>t_p = Base plate thickness For transverse attachment supported below, see detail no. 4 in Table 8</p>	1.13 1.27 1.19	80 71 76
2		<p>Longitudinal attachment welded on beam flange, bulb or supported plate:</p> <p>$\ell \leq 50 \text{ mm}$ $50 \text{ mm} < \ell \leq 150 \text{ mm}$ $150 \text{ mm} < \ell \leq 300 \text{ mm}$ $\ell > 300 \text{ mm}$</p> <p>For $t_2 \leq 0.5t_1$, FAT class (K factors) may be improved by a factor of 1.125, but not better than FAT 80 ($K = 1.13$) (not valid for bulb profiles)</p>	1.13 1.27 1.43 1.61	80 71 63 56
3		<p>Fillet welded non-load-carrying overlap joint at a axially loaded component:</p> <ul style="list-style-type: none"> — flat bar — bulb profile — angle profile <p>For $\ell > 150 \text{ mm}$, the FAT class (K factor) has to be downgraded by a factor of 1.125 while for $\ell \leq 50 \text{ mm}$, the FAT class (K factor) may be improved by a factor of 1.125. If the component is subject to bending the FAT class (K factor) has to be downgraded by a factor of 1.125.</p>	1.60 1.60 1.80	56 56 50

No.	Geometry	Description of joint	K factor	FAT N/mm ²
4		<p>Fillet welded overlap joint with smooth transition (sniped end with $\phi \leq 20$ deg or radius) welded to axially loaded component:</p> <ul style="list-style-type: none"> — flat bar — bulb profile — angle profile <p>$c \leq 2t$ max. 25 mm</p>	1.60 1.60 1.80	56 56 50
5		<p>Longitudinal attachment welded on edge of plate or beam flange:</p> <p>$\ell \leq 50\text{ mm}$</p> <p>$50\text{mm} < \ell \leq 150\text{mm}$</p> <p>$150\text{mm} < \ell \leq 300\text{mm}$</p> <p>$\ell > 300\text{mm}$</p> <p>For $t_2 \leq 0.7t_1$, FAT class (K factor) may be improved by a factor of 1.125, but not better than FAT 56 (K = 1.6). If the plate or beam flange is subjected to in-plane bending, the FAT class (K factor) has to be downgraded by a factor of 1.125.</p>	1.60 1.80 2.00 2.25	56 50 45 40
6		<p>Stud welding on a plate or bulb profile. For an adequate workmanship on bulb profile a centric connection is required.</p> <p>Non-load carrying</p> <p>Load carrying</p>	1.13 2.0	80 45

5.2 Termination of stiffeners

K factors and FAT classes for termination of stiffeners are given in [Table 6](#).

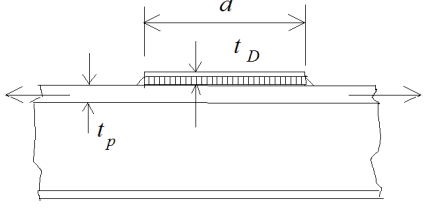
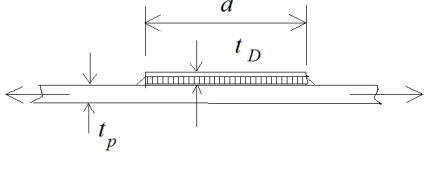
Table 6 K factors and FAT classes for termination of stiffeners

No.	Geometry	Description of joint	K factor	FAT N/mm ²
1		<p>Local attachments welded to unsupported plates, e.g. buckling stiffener. θ = angle in degrees of sloping termination</p>	$1.33 \left(1 + \frac{t_w \theta}{t_p 160} \right)$	$90/K$
2		<p>Sniped stiffener flange. The nominal stress at the hot spot should be considered. L profile should be considered with care due to twisting of the stiffener from lateral loading causing local bending stress in the web close to clamped ends (as illustrated based on a top view of a L profile).</p>	$\max \left\{ \frac{2A_f}{\ell t_s}, 2.0 \right\}$	$90/K$

5.3 Doubling plates

K factors and FAT classes for doubling plates are given in [Table 7](#).

Table 7 Doubling Plates

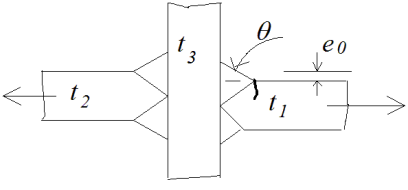
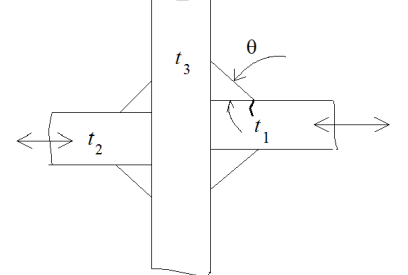
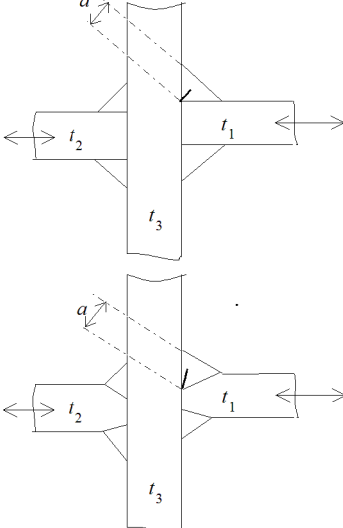
No.	Geometry	Description of joint	<i>K</i> factor	FAT N/mm ²
1		<p>End of doubling plate on beam, welded ends (based on stress range in flange at weld toe). The values are referring to and doubling plate thickness in the range of $0.8 t_p < t_D \leq 1.5 t_p$</p> <p> $d \leq 50$ $50 < d \leq 100$ $100 < d \leq 150$ $150 < d \leq 300$ $300 < d$ </p> <p>The following features improves the FAT class (<i>K</i> factor) by a factor of 1.125:</p> <ul style="list-style-type: none"> — reinforced ends or — weld toe angle $\leq 30^\circ$ <p>For $t_D \leq 0.8t_p$ the FAT class (and <i>K</i> factor) should be improved by a factor of 1.125</p> <p>For $t_D > 1.5t_p$ the FAT class (and <i>K</i> factor) should be downgraded by a factor of 1.125</p> <p>For all improvements, the FAT class is limited by 80 corresponding to a <i>K</i> factor of 1.13.</p>	1.20 1.27 1.33 1.47 1.80	75 71 68 61 50
2		<p>Doubling plates welded to unsupported plates</p> <p> $d \leq 50$ $50 < d \leq 100$ $100 < d \leq 150$ $150 < d \leq 300$ </p> <p>For doublers with $d > 300$, a more detailed analysis should be performed based on the actual geometry.</p>	1.27 1.32 1.43 1.61	71 68 63 56

If the welds of the doubling plates are placed closer to the free plate edges than 10 mm, the FAT classes and *K* factors should be downgraded by a factor 1.15

6 Simple cruciform joints

K factors and FAT classes for cruciform joints are given in [Table 8](#).

Table 8 K factors and FAT classes for cruciform joints

No.	Geometry	Description of joint	K factor	FAT N/mm ²
1	 $e = \frac{t_1}{2} + e_0 - \frac{t_2}{2}$ $t_1 \leq t_2$	<p>Cruciform or tee-joint K-butt welds with full penetration or defined incomplete root penetration. The effective weld thickness may be assumed as the thickness of the abutting plate t_1 minus f, where f is the incomplete root penetration of $0.2t_1$ with a maximum of 3 mm, which should be balanced by equally sized double fillet welds on each side. $e_0 \leq 0.3t_1$, $K_{ma} = 1.0^{(4)}$, $K_{me} = 1.45^{(3)}$, $\theta = 45^\circ$</p> <p>Cruciform joint:</p> <p>Tee-joint:</p>	1.27 1.13	71 80
2		<p>Cruciform or tee-joint with transverse fillet welds, toe failure (for root failure, in particular for throat thickness $a < 0.7t_1$ or $a < 0.7t_2$, see detail no. 3). e according to detail no. 1. $e_0 \leq 0.3t_1$, $K_{ma} = 1.0^{(4)}$, $K_{me} = 1.45^{(3)}$, $\theta = 45^\circ$</p> <p>Cruciform joint:</p> <p>Tee-joint:</p>	1.43 1.27	63 71
3		<p>Cruciform or tee-joint with transverse fillet or partial penetration welds, root failure based on stress range in weld throat (for toe failure, see detail no. 2). e according to detail no. 1. $e_0 \leq 0.3t_1$, $K_{ma} = 1.0^{(4)}$, $K_{me} = 1.45^{(3)}$</p> <p>The stress in the weld throat can be estimated based on the nominal stress in the member with thickness t_1:</p> $\sigma_a = \sigma_n \cdot t_1 / (2a)$ <p>$t_1/3 \leq a$</p> <p>$t_1/3 > a$</p> <p>$t_2 \geq t_1$</p>	2.5 2.25	36 40

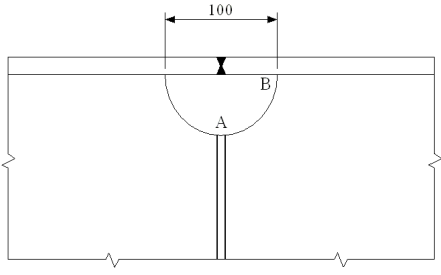
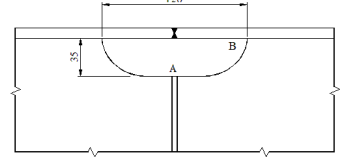
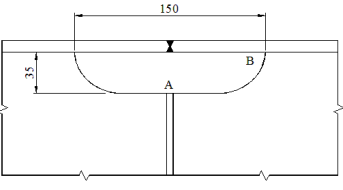
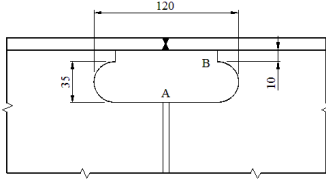
No.	Geometry	Description of joint	K factor	FAT N/mm ²
4		Cruciform joint or double sided transverse attachment with non-load carrying transverse attachment with thickness t . With full penetration or fillet weld. $K_{ma} = 1.12^{(4)}$, $K_{me} = 1.0$, $\theta = 45^\circ$ $t \leq 25 \text{ mm}$ $t > 25 \text{ mm}$	1.05 1.19	86 76
5		Simple (unsupported) cruciform joint with supports having no rotational fixation. e is the eccentricity of plates with thickness t_1 and t_2 . t is the thickness of the considered plate. In case the vertical plate is continuous $t_3 = t_4$.	Reference to detail no. 1 to 3.	Reference to detail no. 1 to 3.

1) For weld angle deviating from 45° the K should be multiplied by $c = 1/1.2 \cdot (0.6 + 0.6\tan(\theta))^{1/4}$. For correction of the FAT class, the FAT class should be multiplied with $1/c$.
2) For weld angle deviating from 45° the K should be multiplied by $c = 1/1.67 \cdot (0.8 + 0.87\tan(\theta))^{1/4}$. For correction of the FAT class, the FAT class should be multiplied with $1/c$.
3) If the misalignment is different than the default value for detail no. 1 to no. 3 then K factor can be multiplied with $K_{me,mod}/K_{me}$ and the FAT class can be multiplied with $K_{me}/K_{me,mod}$.
4) For angular misalignment reference is made to detail no. 9 in Table 3. If both angular misalignment and misalignment due to eccentricity is considered, then K_m should be calculated by $K_m = K_{ma} + K_{me} - 1$

7 Scallops and block joints

K factors and FAT classes for scallops are given in Table 9. The factors are applicable to stiffeners subjected to axial loads. For dynamic pressure loads on the plate, other design solutions may be necessary.

Table 9 K factors and FAT classes for scallops

No.	Geometry	Description of joint	K factor ^{1,2)}	FAT ^{1,2)} N/mm ²
1		Circular scallop with full penetration butt weld, welded from both sides, misalignment is not included (in Point A). Point A Point B	2.4 1.27	37.5 71
2		Scallop with full penetration butt weld, welded from both sides, misalignment is not included (in point A). Point A Point B	1.27 1.27	71 71
3		Scallop with full penetration butt weld, welded from both sides, misalignment is not included (in Point A). Point A Point B	1.17 1.27	77 71
4		Omega shaped scallop with full penetration butt weld, welded from both sides, misalignment is not included (in Point A). Point A Point B	1.17 1.27	77 71

Notes:

For scallops without transverse welds, the K_g at point B will be governing for the design.

For Ω shaped scallops with different shape than in no. 4, and assessment based on the hot spot analysis may be used to demonstrate value for point A, which may be worse than for no. 4.

¹⁾ If the scallop height is more than 40% of the web height, then FAT class and K factor should be downgraded by a factor of 1.125

²⁾ In the presence of shear stress, τ , in the web, the FAT class and K factor should be downgraded by the factor $1 - \Delta\tau/\Delta\sigma$, but not below FAT 36 or above K of 2.5.

8 Lower hopper knuckles

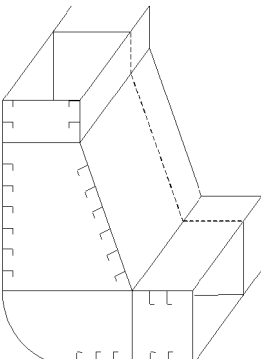
K factors and FAT classes for lower hopper knuckles, with angles (between inner bottom and hopper plate) between 30° and 75° , are given in [Table 10](#), and serves as references although they are regarded to depend on geometry and scantlings.

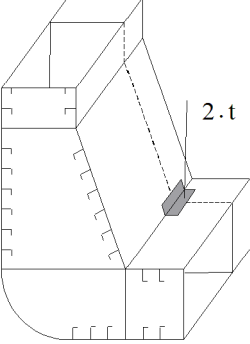
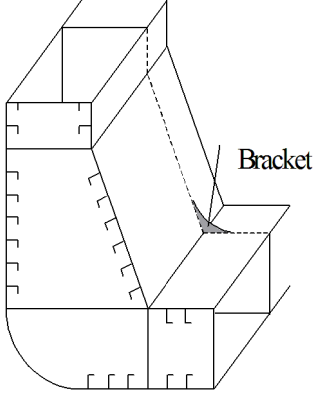
For the lower hopper knuckle, the nominal stress to be used with the K factors and FAT classes in [Table 10](#) should be taken as the transverse membrane stress. Its stress should be read out $1/2$ a stiffener spacing from the knuckle in the inner bottom plate. The stress should be taken as the averaged of the two stresses in the middle between the adjacent two floors. It is assumed that brackets (extension plate) are fitted in ballast tanks in line with inner bottom plate, and that a longitudinal girder (or similar brackets) are located beneath the lower hopper knuckle.

Geometrical eccentricity in the knuckle should be avoided or kept to a minimum.

For a yard standard geometry, a K factor related to nominal stress in a frame and girder model may alternatively be established using the hot spot model. A hot spot stress calculation of the panel knuckles may also be required by the rules.

Table 10 K factors and FAT classes for lower hopper knuckles

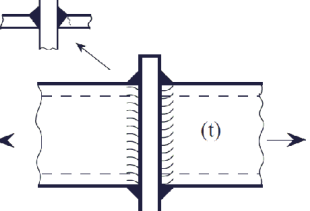
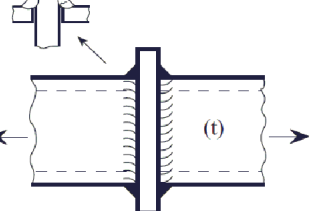
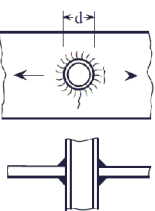
No.	Geometry	Description of joint	K factor	FAT N/mm ²
1		Lower hopper knuckle without insert plate or bracket and with transverse weld at the hot spot, which is caused by the high effective flange effect	7.0	13

No.	Geometry	Description of joint	K factor	FAT N/mm ²
2		Insert plate of two times the thickness normally required. Insert plates should be provided in inner bottom, hopper tank top, and web frame. The insert plates should extend approximately 400 mm along inner bottom and hopper plate, approximately 800 mm in longitudinal direction, and 400 mm in the depth of the web.	4.5	20
3		Bracket inside cargo tank. The bracket should extend approximately to the first longitudinals and the bracket toe should have a soft nose design.	2.5	36

9 Pipe connections

K factors and FAT classes for pipe connections are given in [Table 11](#).

Table 11 K factors and FAT classes for pipe connections

No.	Geometry	Description of joint	<i>K</i> factor	FAT N/mm ²
1		<p>Full penetration weld at the connection between a hollow section (e.g. pillar) and a plate.</p> <p>For tubular section</p> <p>For rectangular hollow section</p> <p>For $t \leq 8$ mm, the FAT class and <i>K</i> factor should be downgraded by a factor of 1.125</p>	1.61 1.80	56 50
2		<p>Fillet weld at the connection between a hollow section (e.g. pillar) and a plate:</p> <p>For tubular section</p> <p>For rectangular hollow section</p> <p>The stress should be related to the weld sectional area. For $t \leq 8$ mm, the FAT class and <i>K</i> factor should be downgraded by a factor of 1.125</p>	2.00 2.25	45 40
3		<p>Continuous butt or fillet weld connecting a pipe penetrating through a plate</p> <p>$d \leq 50$ mm</p> <p>$d > 50$ mm</p> <p>For large diameters an assessment based on local stress is recommended, or alternatively follow [10]</p>	1.27 1.43	71 63

10 Holes with edge reinforcements

K factors for holes with reinforcement are given for the following details:

- Holes in plates with inserted tubular are given in [Figure 7](#) to [Figure 18](#).
- Holes in plates with ring reinforcement are given in [Figure 19](#) to [Figure 23](#).
- Holes in plates with double ring reinforcement are given in [Figure 24](#) to [Figure 27](#).

For stresses parallel with the weld, the given stress concentration factors can be reduced according to [Sec.2 \[2.4\] Table 3](#).

At some locations of the welds there are stress in the plate transverse to the fillet weld, σ_w , and shear stress in the plate parallel with the weld τ_{\parallel} . Then the fillet weld is designed for a combined stress obtained as

$$\sigma_{comb} = \frac{t}{a} \sqrt{(1.80\sigma_w)^2 + (0.65\tau_{\parallel})^2}$$

where:

- t = plate thickness in mm
- a = throat thickness, in mm, for a double sided fillet weld.

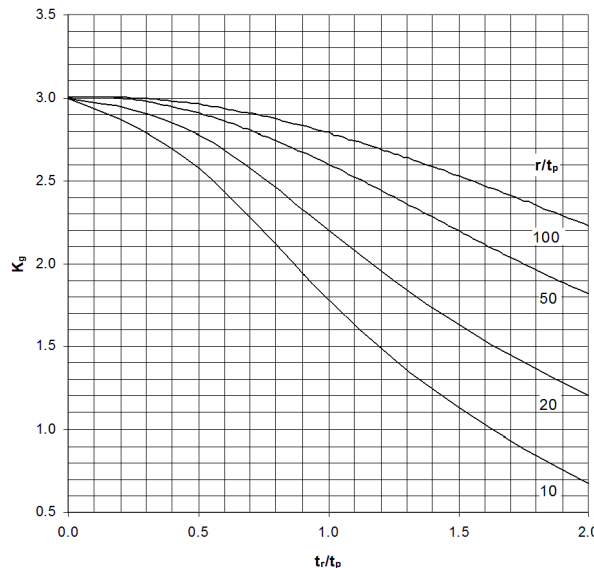
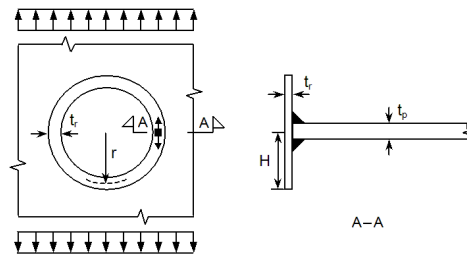


**Figure 6 K_g at hole with inserted tubular. Stress at outer surface of tubular, parallel with weld.
 $H/t_r = 2$**

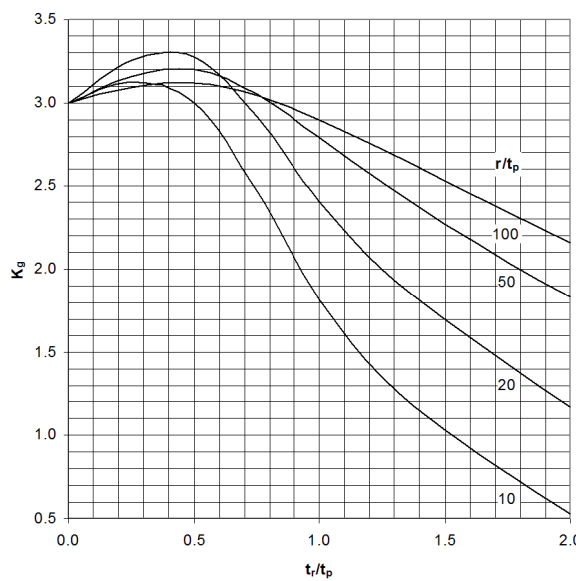
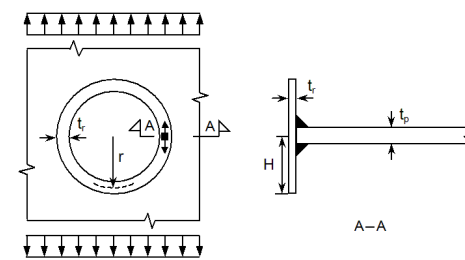


**Figure 7 K_g at hole with inserted tubular. Stress at outer surface of tubular, parallel with weld.
 $H/t_r = 5$**

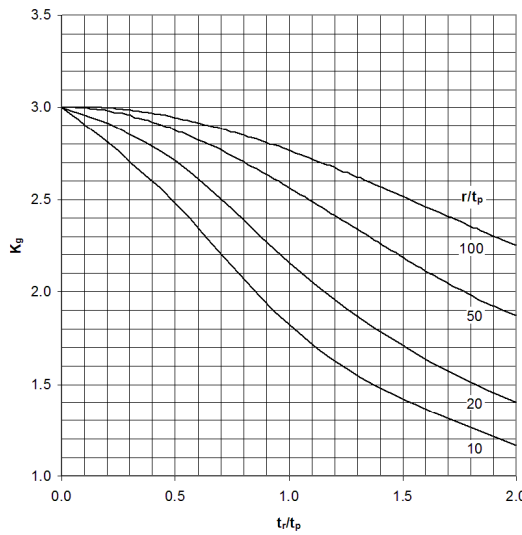
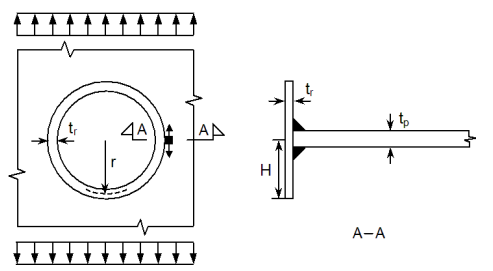


Figure 8 K_g at hole with inserted tubular. Stress in plate, parallel with weld. $H/t_r = 2$

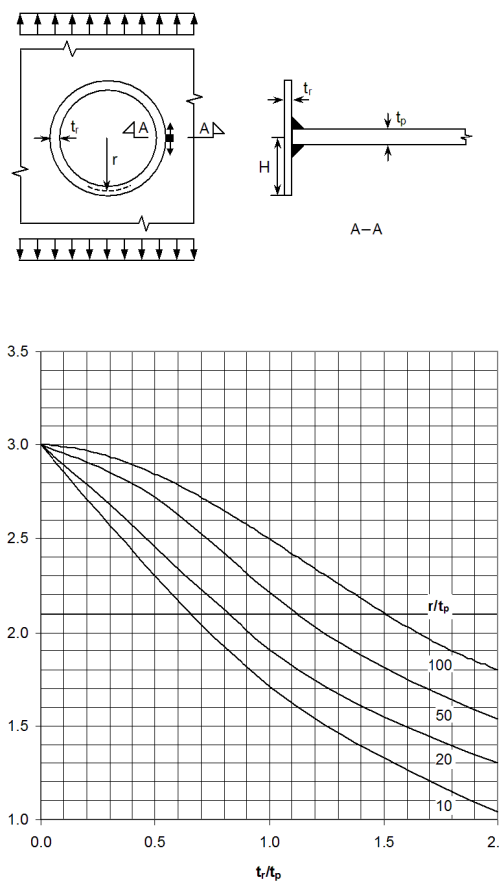


Figure 9 K_g at hole with inserted tubular. Stress in plate, parallel with weld. $H/t_r = 5$

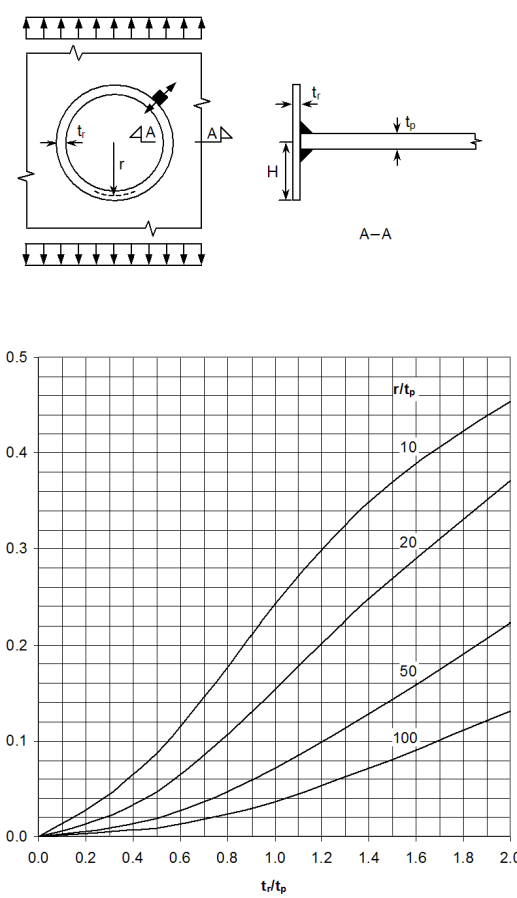


Figure 10 K_g at hole with inserted tubular. Stress in plate, normal to weld. $H/t_r = 2$

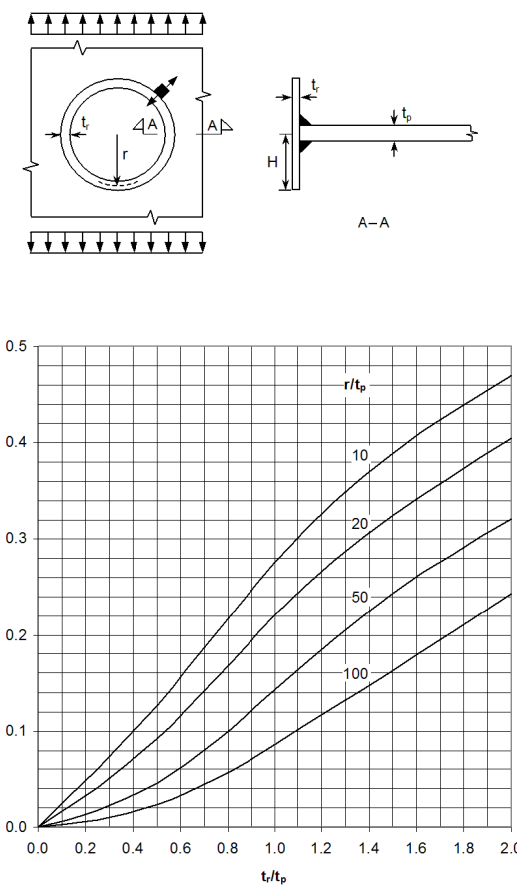


Figure 11 K_g at hole with inserted tubular. Stress in plate, normal to weld. $H/t_r = 5$

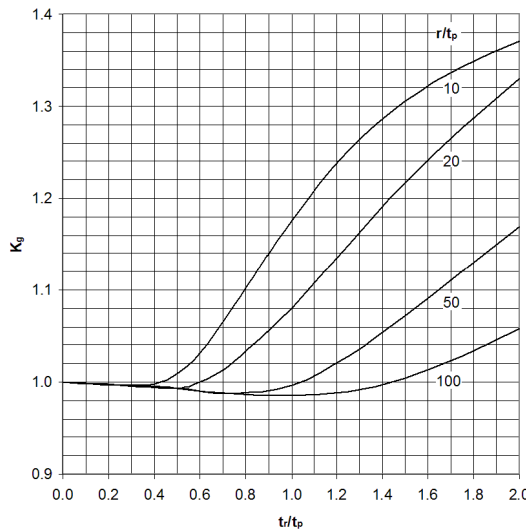
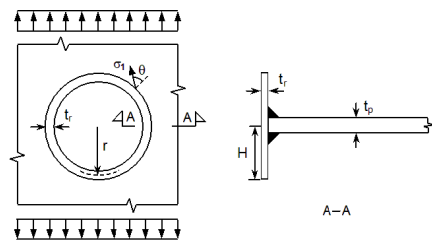


Figure 12 K_g at hole with inserted tubular. Principal stress in plate. $H/t_r = 2$

Table 12 Angle to principal stress. $H/t_r = 2$

t_r/t_p	$r/t_p = 10$	$r/t_p = 20$	$r/t_p = 50$	$r/t_p = 100$
0.0	90	90	90	90
0.5	72	80	86	88
1.0	56	63	75	82
1.5	50	54	64	73
2.0	46	50	57	66

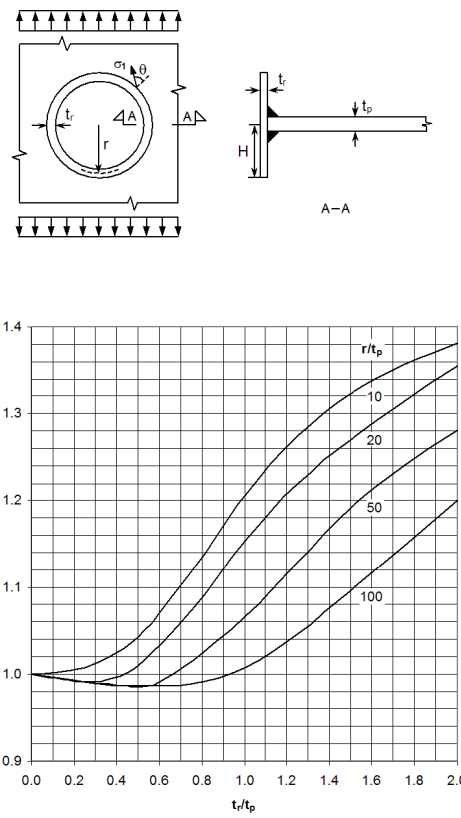


Figure 13 K_g at hole with inserted tubular. Principal stress in plate. $H/t_r = 5$

Table 13 Angle to principal stress. $H/t_r = 5$

t_r/t_p	$r/t_p = 10$	$r/t_p = 20$	$r/t_p = 50$	$r/t_p = 100$
0.0	90	90	90	90
0.5	66	72	80	85
1.0	54	58	65	72
1.5	49	52	56	62
2.0	46	48	52	56

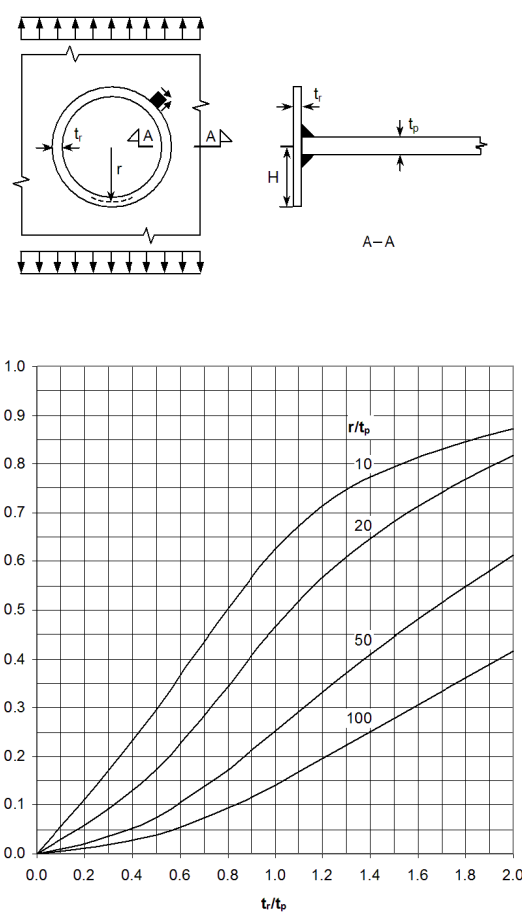


Figure 14 K_g at hole with inserted tubular. Shear stress in plate. $H/t_r = 2$

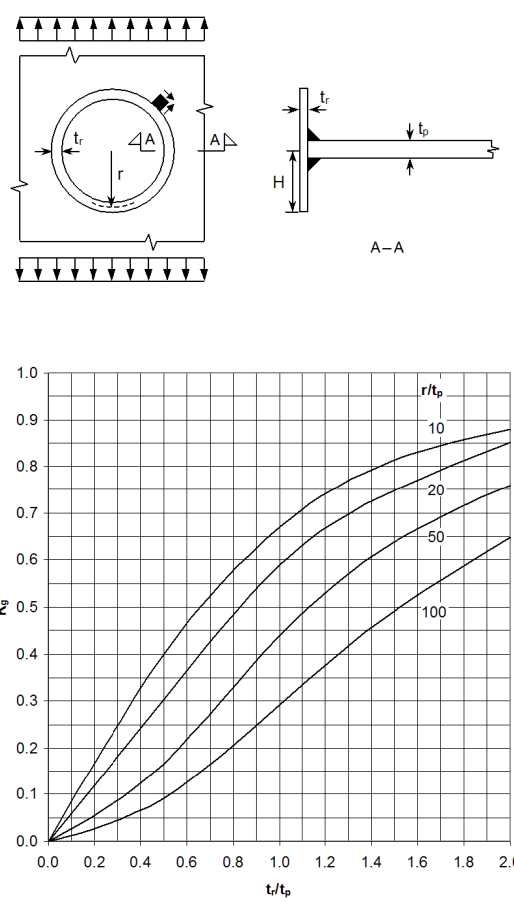


Figure 15 K_g at hole with inserted tubular. Shear stress in plate. $H/t_r = 5$

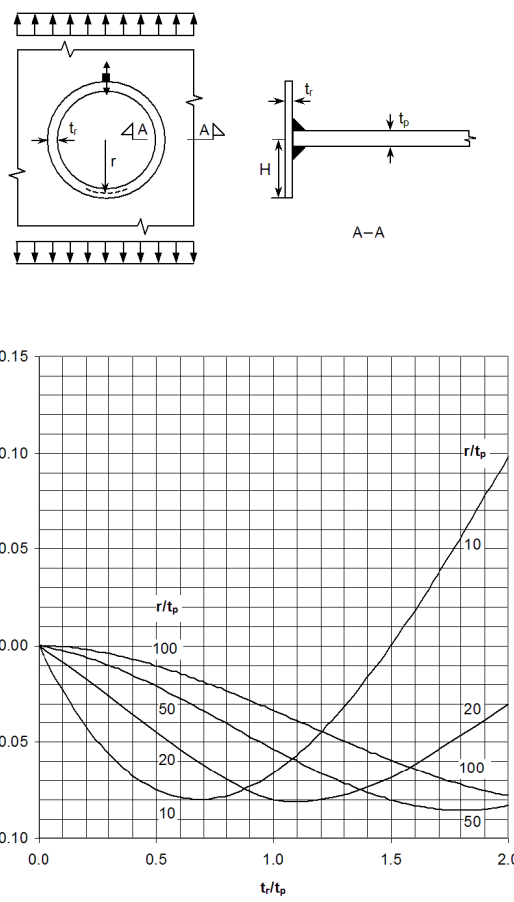


Figure 16 K_g at hole with inserted tubular. Stress in plate, normal to weld. $H/t_r = 2$

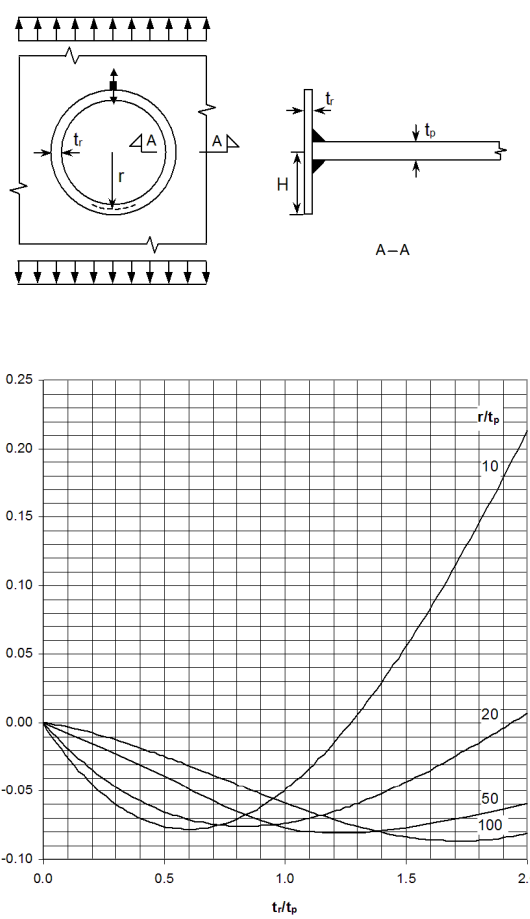


Figure 17 K_g at hole with inserted tubular. Stress in plate, normal to weld. $H/t_r = 5$

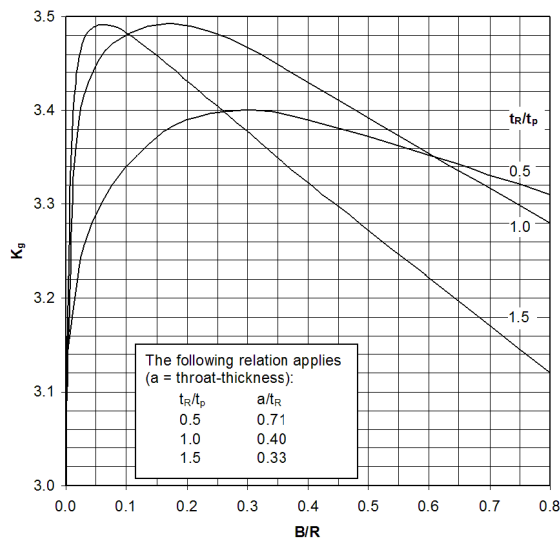
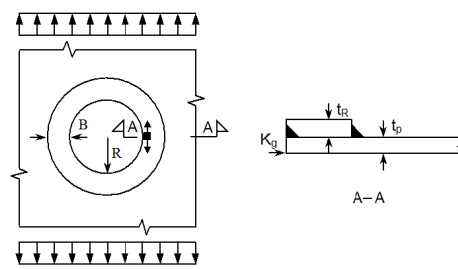


Figure 18 K_g at hole with ring reinforcement. Max stress concentration

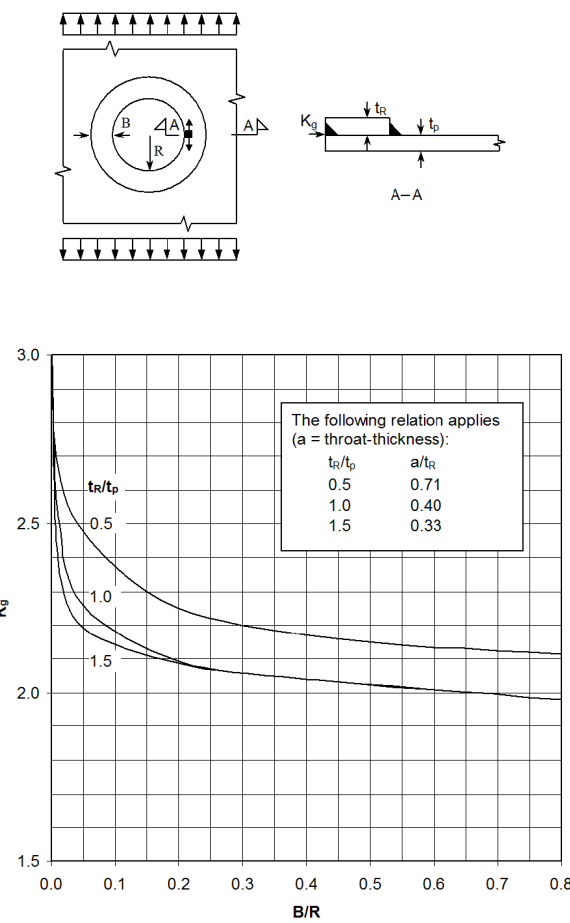


Figure 19 K_g at hole with ring reinforcement. Stress at inner edge of ring

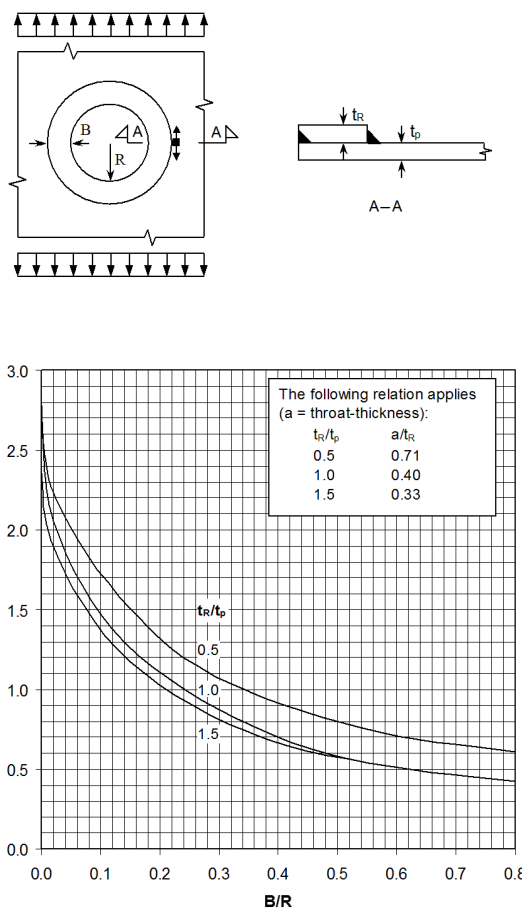


Figure 20 K_g at hole with ring reinforcement. Stress in plate, parallel with weld

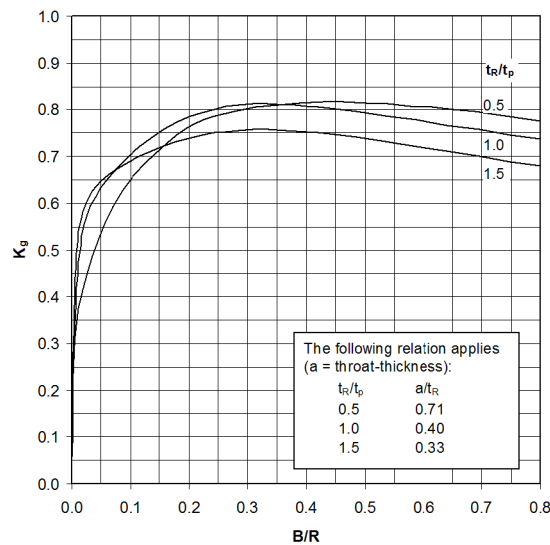
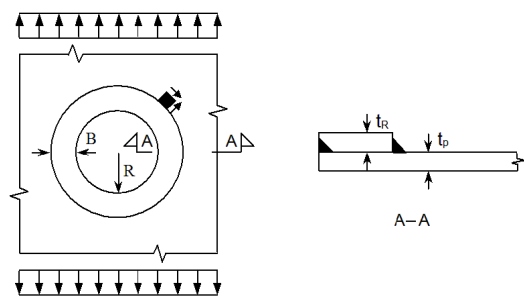


Figure 21 K_g at hole with ring reinforcement. Shear stress in weld

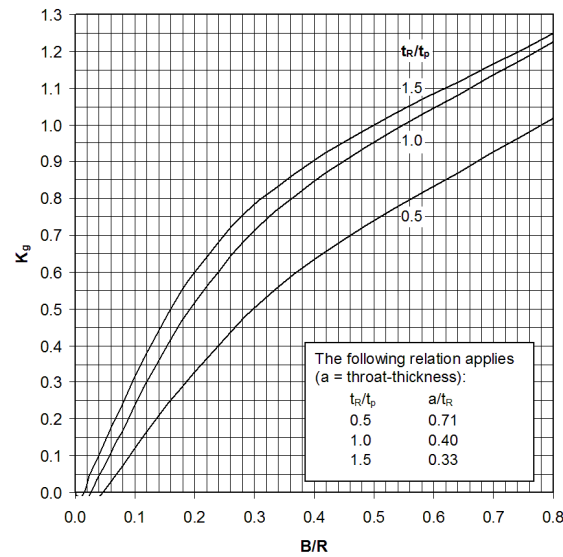
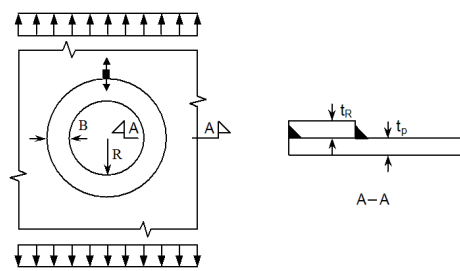


Figure 22 K_g at hole with ring reinforcement. Stress in plate, normal to weld

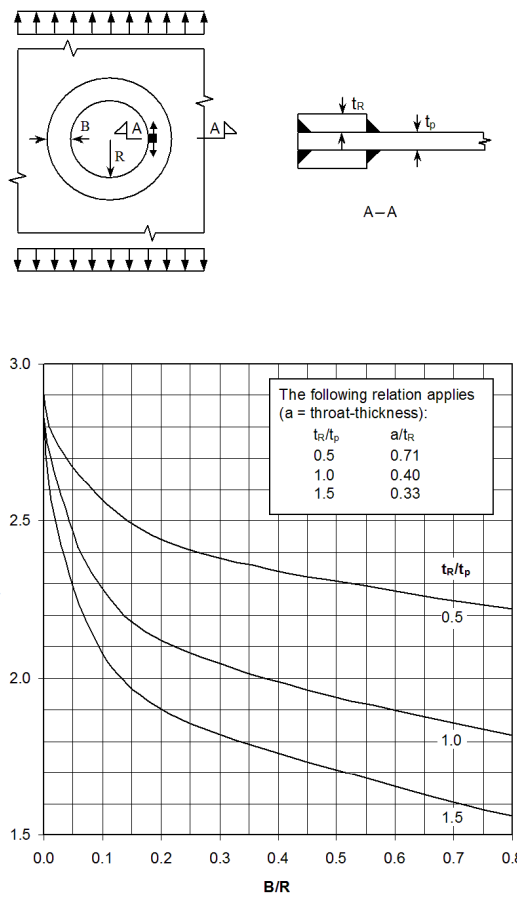


Figure 23 K_g at hole with double ring reinforcement. Stress at inner edge of ring

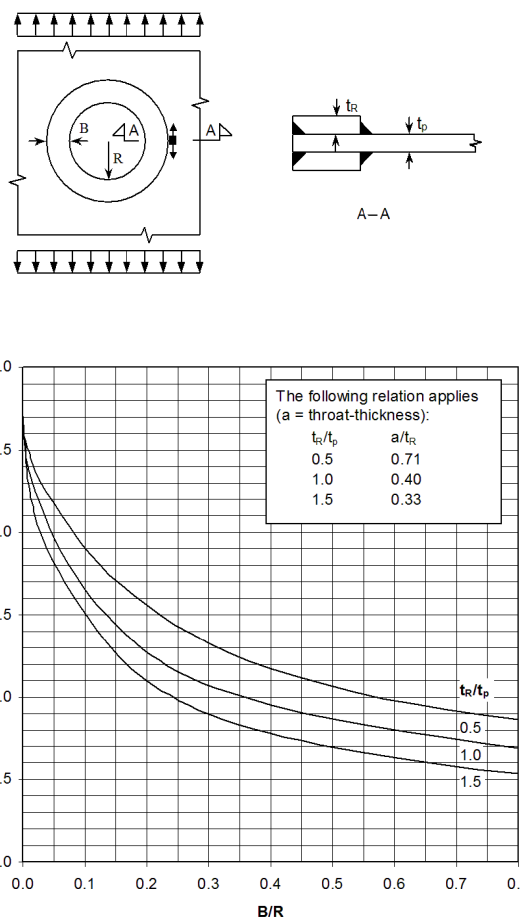


Figure 24 K_g at hole with double ring reinforcement. Stress in plate, parallel with weld

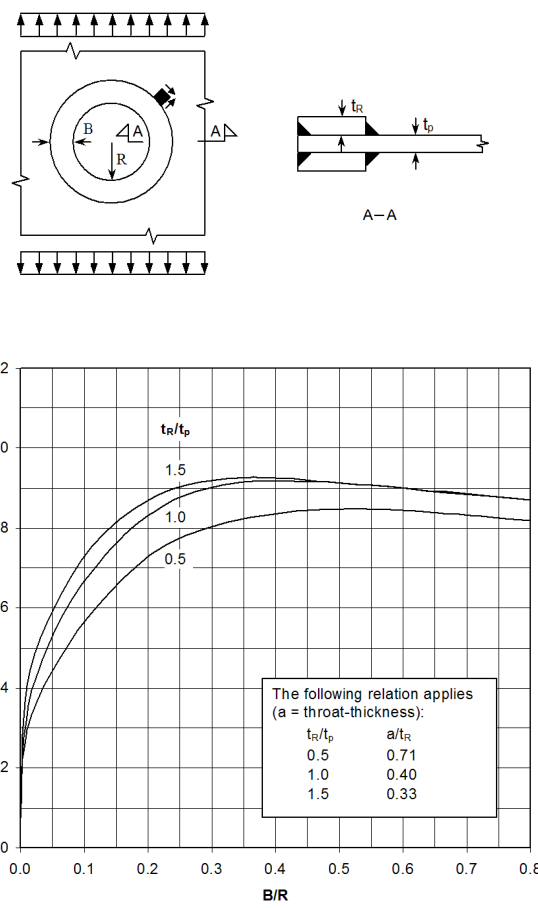


Figure 25 K_g at hole with double ring reinforcement. Shear stress in weld

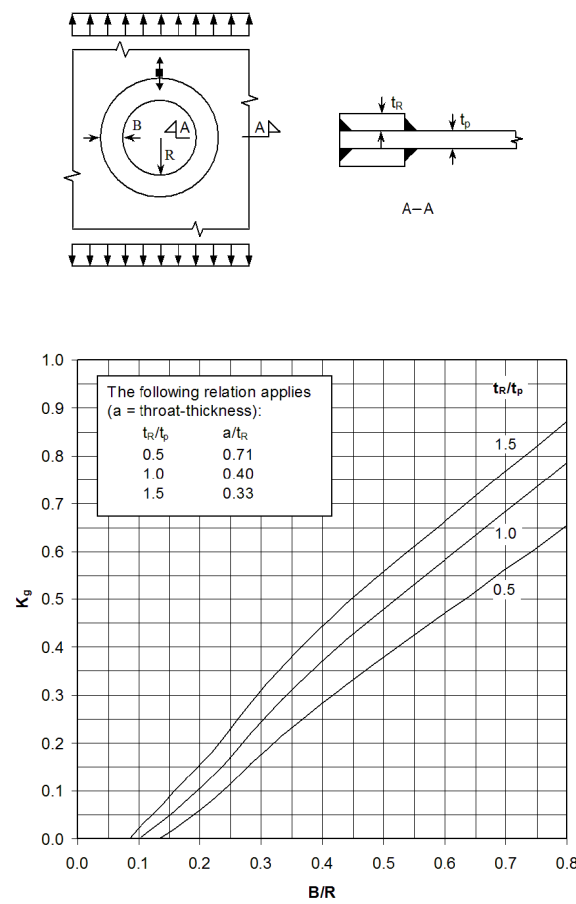


Figure 26 K_g at hole with double ring reinforcement. Stress in plate, normal to weld

11 Rounded rectangular, elliptical and oval holes

K factors for rounded rectangular holes are given in [Figure 27](#) and K factors for elliptical and oval holes are given in [Figure 28](#).

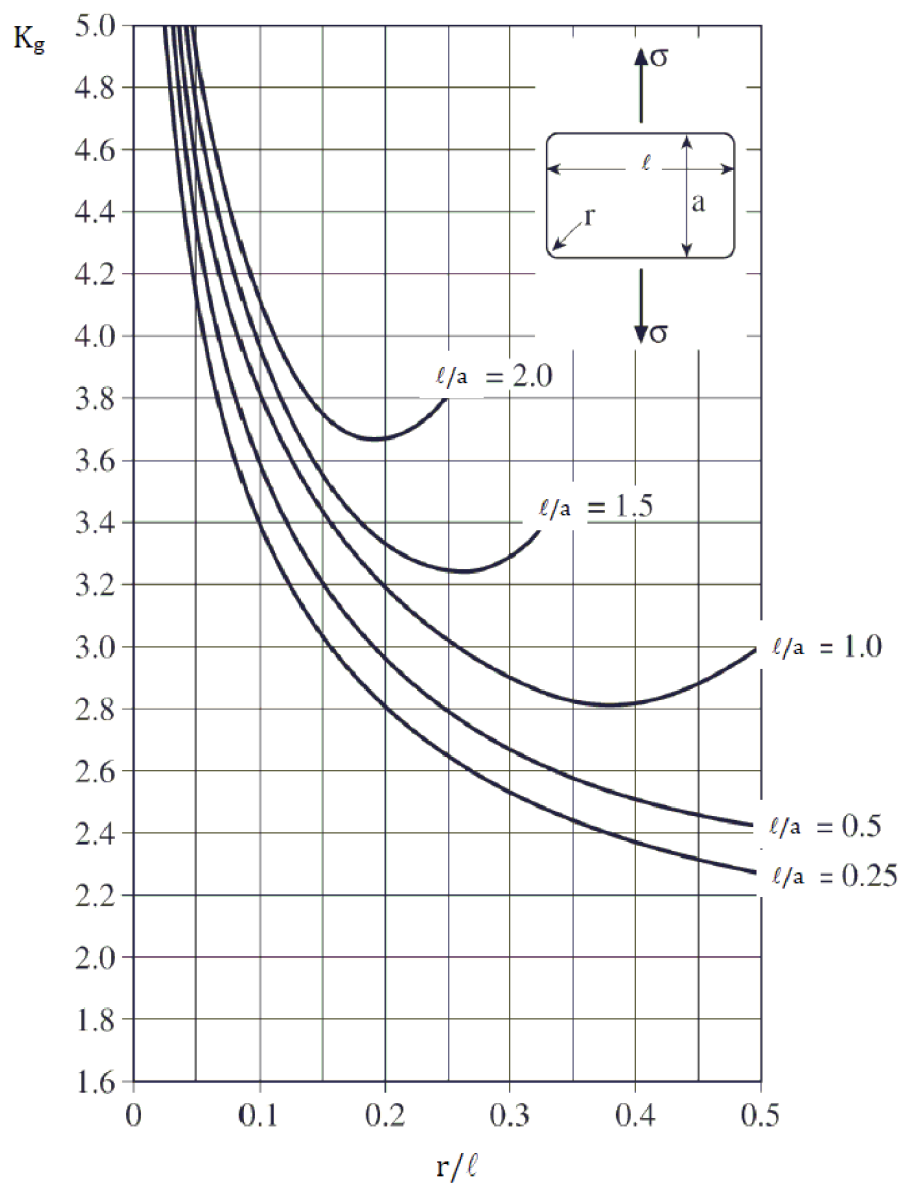


Figure 27 **K** factors for rounded rectangular holes

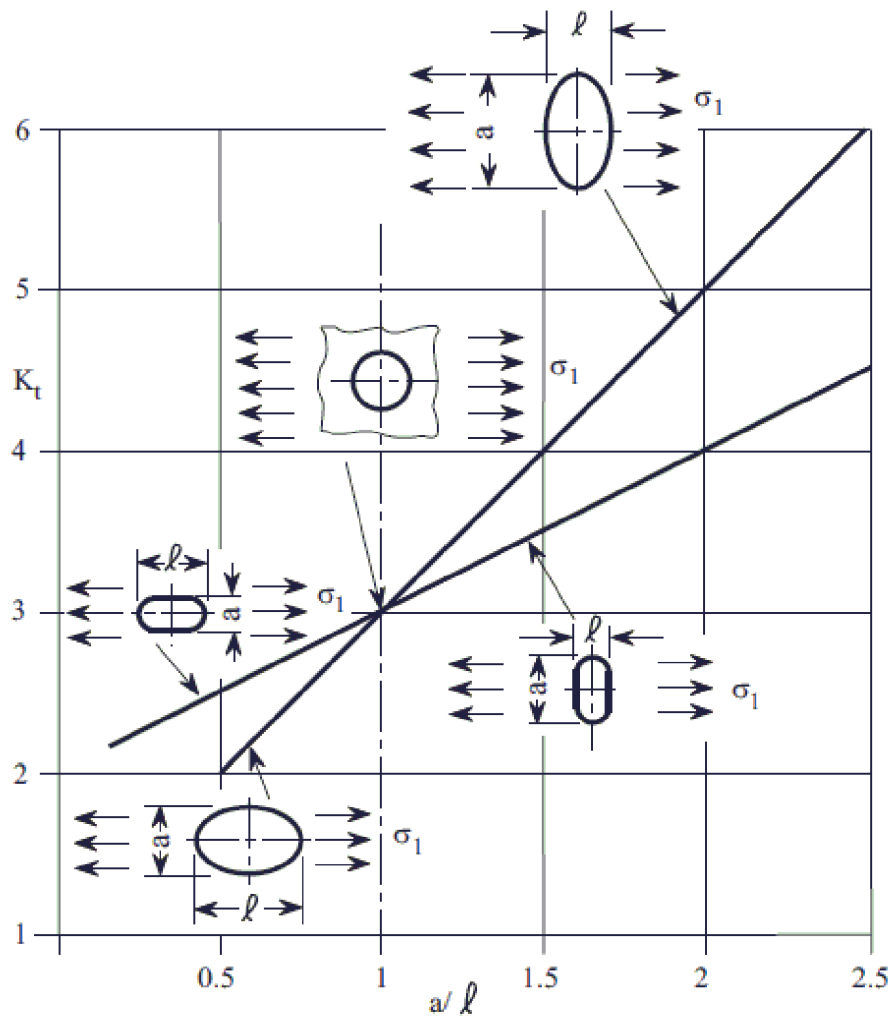


Figure 28 K factors for elliptical and oval holes

In case of superimposed stresses due to longitudinal and shear loads, the maximum local stress, σ_{loc} , in N/mm², of rectangular openings with rounded corners can approximately be calculated as follows:

$$\sigma_{loc} = K_t \cdot \sqrt{\sigma_1^2 + 3 \cdot \tau_1^2} \quad \text{for tensile stress}$$

$$\sigma_{loc} = -K_t \cdot \sqrt{\sigma_1^2 + 3 \cdot \tau_1^2} \quad \text{for compressive stress}$$

$$K_t = m \cdot \sqrt{\rho} + c$$

where:

m = Parameter according to [Figure 29](#)

K_t = Local stress factor for equivalent stress

c	= Parameter according to Figure 29
ρ	= Ratio of smaller length to radius of corner defined as $\rho = \ell/r$ or $\rho = a/r$ with $\rho \geq 3$
ℓ	= Length of opening, in m
a	= Height of opening, in m
τ_1	= Shear stress related to gross area of section, in N/mm ²
σ_1	= Longitudinal stress (in direction of length ℓ of opening) related to gross area of section, in N/mm ²
r	= Radius of rounded corner, in m.

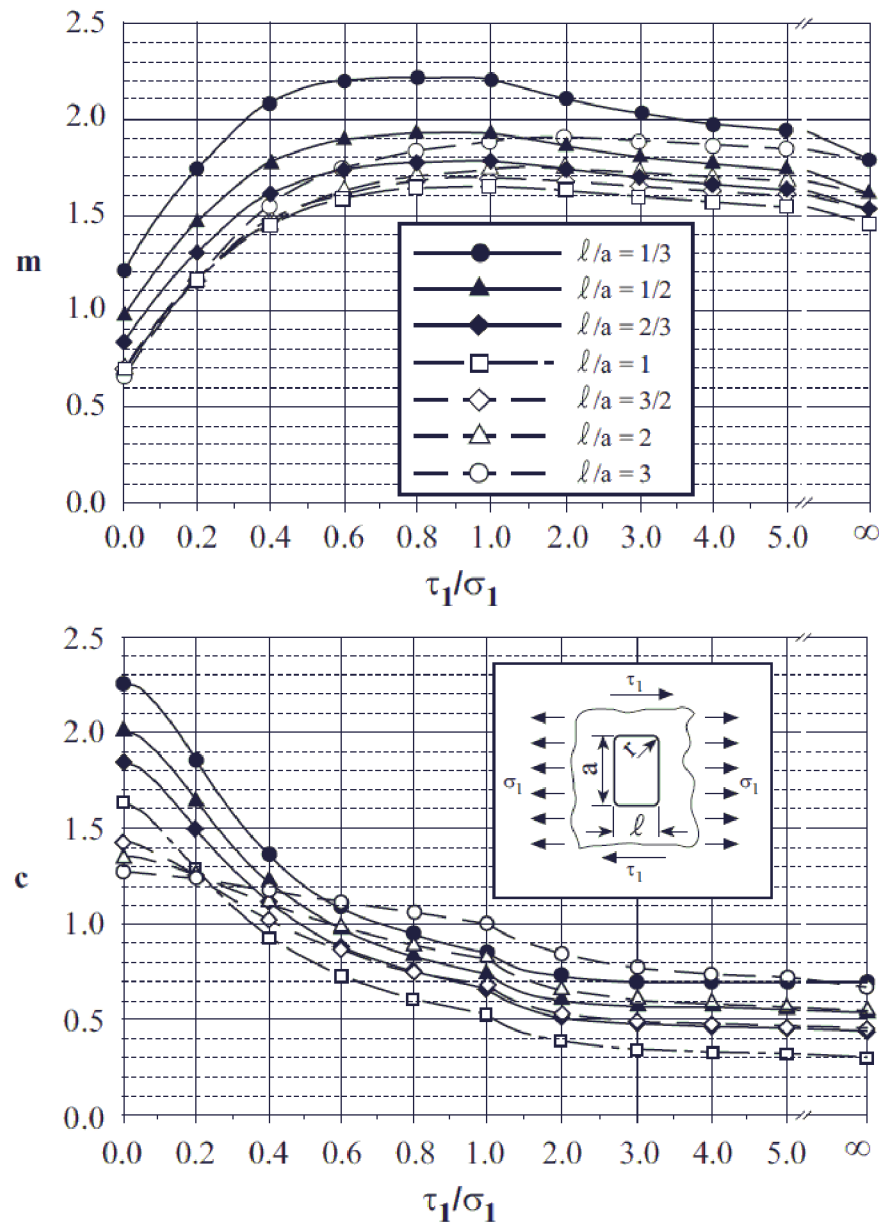


Figure 29 Parameters m and c to determine the local stress factors of rectangular openings loaded by superimposed longitudinal and shear stresses /35/

APPENDIX B FATIGUE CAPACITY

1 Failure criterion inherent in the S-N curves

Most S-N data are derived by fatigue testing of small specimens in test laboratories. For these specimens, the testing is performed until final fracture. In comparison to real ship structures, no redistribution of stresses occurs during crack growth. This means that most of the fatigue life is associated with growth of a small crack which grows faster as the crack size increases until fracture.

For details with the same calculated damage, the initiation period of a fatigue crack takes longer time for a rounded notch in base material than at the notch of a weld toe or a weld root (which are normally sharper). This also means that with a higher fatigue resistance of the base material as compared with welded details, the crack growth will be faster in the base material when fatigue cracks are growing as the stress range in the base material can be significantly higher than at the welds if they are designed with the same fatigue utilization.

For practical purpose one defines these failures as being crack growth through the thickness.

When this failure criterion is transferred into a crack size in a real structure where some redistribution of stress is more likely, this means that this failure criterion corresponds to a crack size that is somewhat less than the plate thickness.

2 Other S-N curves

2.1 S-N curves for base material of high strength steel above 500N/mm²

The fatigue capacity of the base material is depending on the surface finish of the material and the yield strength. For high strength steel, other than cast steel, with yield strength above 500 N/mm² and a surface roughness equal $R_a = 3.2\mu m$ or better, the following design S-N curve can be used for fatigue assessment of the base material:

$$\log N = 17.446 - 4.70 \log \Delta\sigma$$

The mean S-N curve is given by $\log N = 17.770 - 4.70 \log \Delta\sigma$. In air a fatigue limit at $2 \cdot 10^6$ cycles at a stress range equal 235 N/mm² can be used. For variable amplitude loading with one stress range larger than this fatigue limit, a constant slope S-N curve should be used. For seawater with cathodic protection a constant slope S-N curve should be used. (The same as for air to the left of $2 \cdot 10^6$ cycles, see [Figure 1](#)). If requirements to yield strength, surface finish and corrosion protection are not met, the S-N curves presented in [Sec.2 \[2.3\]](#) should be used. The thickness exponent is $n = 0$ for this S-N curve.

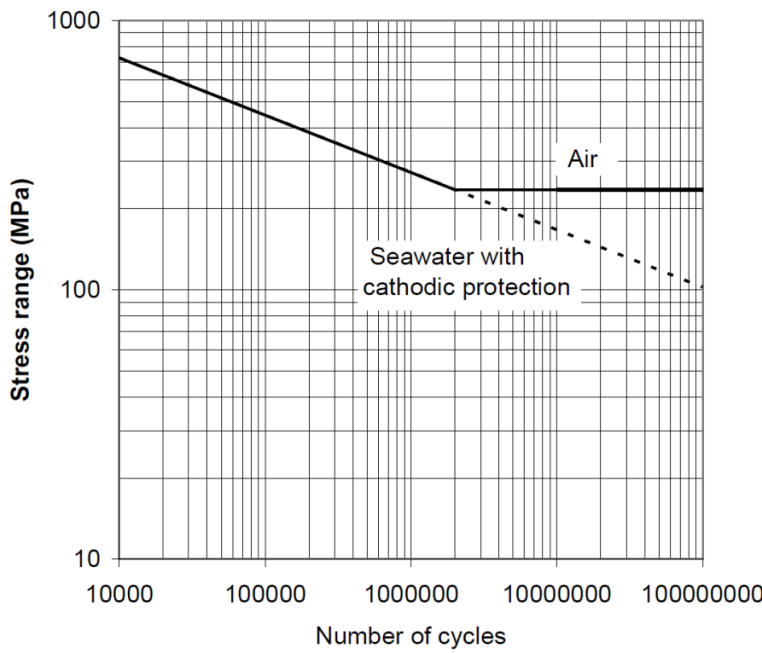


Figure 1 S-N curve for high strength steel (HS - curve)

2.2 Qualification of new S-N curves based on fatigue test data

Other S-N curves than given by this CG can be applied subject to the following conditions.

For qualification of new S-N data, it is important that the test specimens are representative for the actual fabrication and construction. This includes possibility for relevant production defects as well as fabrication tolerances. The sensitivity to defects may also be assessed by fracture mechanics.

For new types of connections, it is recommended to perform testing of at least 15 specimens in order to establish a new S-N curve. At least three different stress ranges should be selected in the relevant S-N region such that a representative slope of the S-N curve can be determined. Reference is made to the [DNVGL-RP-0005, Fatigue design of offshore steel structures; D.7](#) for a broader assessment of how to derive S-N curves from few fatigue test data.

Reference is also made to IIW document no IIW-XIII-WG1-114-03 for statistical analysis of the fatigue test data. Normally, fatigue test data are derived for number of cycles less than 10^7 . However, it should be noted that for ship structures significant fatigue damage occurs for $N > 10^7$ cycles. Thus, how to extrapolate the fatigue test data into this high cycle region is important in order to achieve a reliable assessment procedure. In addition to statistical analysis, engineering judgement based on experience is relevant for derivation of the S-N data in this region. Good details, where the fatigue initiation contributes significantly to the fatigue life, show a more horizontal S-N curve than for less good details where the fatigue life consists mainly of crack growth. Reference is also made to S-N curves with different slopes shown in [Sec.2 \[2\]](#).

The residual stresses of small scale test specimens are often small compared to residual stress in full size structures due to different restraints during fabrication. This is an item which is of importance when planning fatigue testing and for assessment of design S-N curves. Reference is made to the commentary section D.7 in [DNVGL-RP-0005 Fatigue design of offshore steel structures](#).

For $N > 10^7$ cycles there is additional uncertainty due to variable amplitude loading. This is an issue if it is desirable to establish a less conservative S-N curves than given in this CG.

The detection probability of defects during production should be considered. The defects with acceptable detection probability are normally larger in real structures than for test specimens.

3 Effect of fabrication tolerances

Larger fabrication tolerances are allowed in real structures than accounted for in the test specimens used to derive S-N data, see [DNVGL-OS-C401 Fabrication and Testing of Offshore Structures](#). Therefore, additional stresses resulting from normal fabrication tolerances should be included in the fatigue design. Special attention should be given to the fabrication tolerances for simple butt welds in plates and cruciform joints as these give the most significant contributions. Stress concentration factors for butt welds and cruciform joints are given in [App.A](#).

4 Design chart for fillet and partial penetration welds

Design should be performed such that fatigue cracking from the root is less likely than from the toe region. Fatigue crack at the toe can be found by in-service inspection, while a fatigue crack starting at the root can not be discovered before the crack has grown through the weld. Thus, the design of the weld geometry should be performed such that the fatigue life for cracks starting at the root is longer than the fatigue life of the toe. [Figure 3](#) can be used for evaluation of required weld penetration. The notation used is explained by [Figure 2](#). It is difficult to detect internal defects by NDE in fillet/partial penetration welds. Such connections should therefore not be used in structural connections of significant importance for the structural integrity.

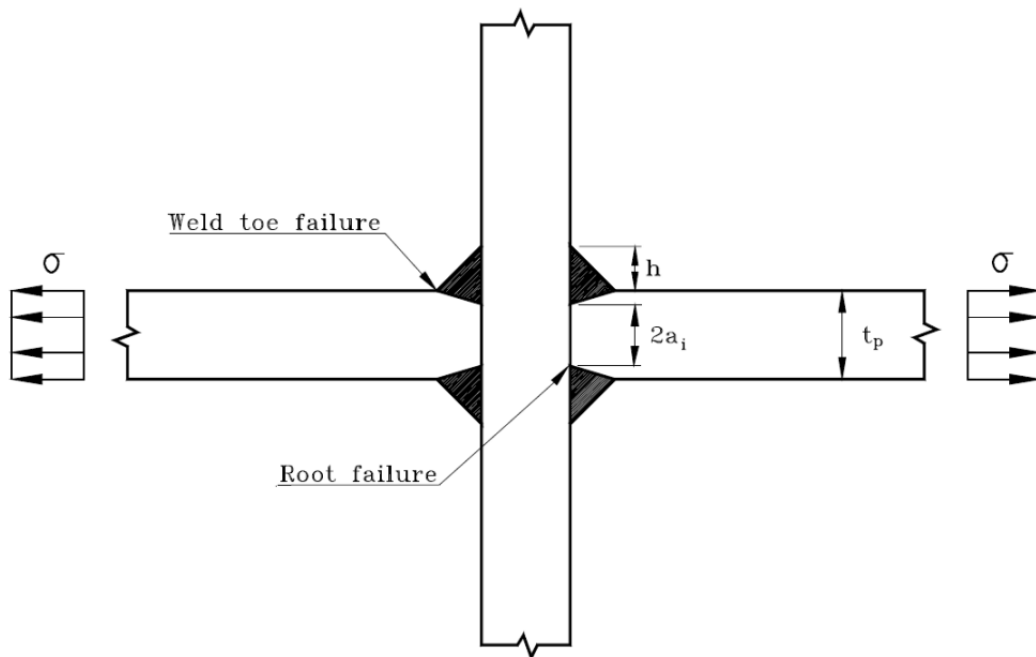


Figure 2 Welded connection with partial penetration weld

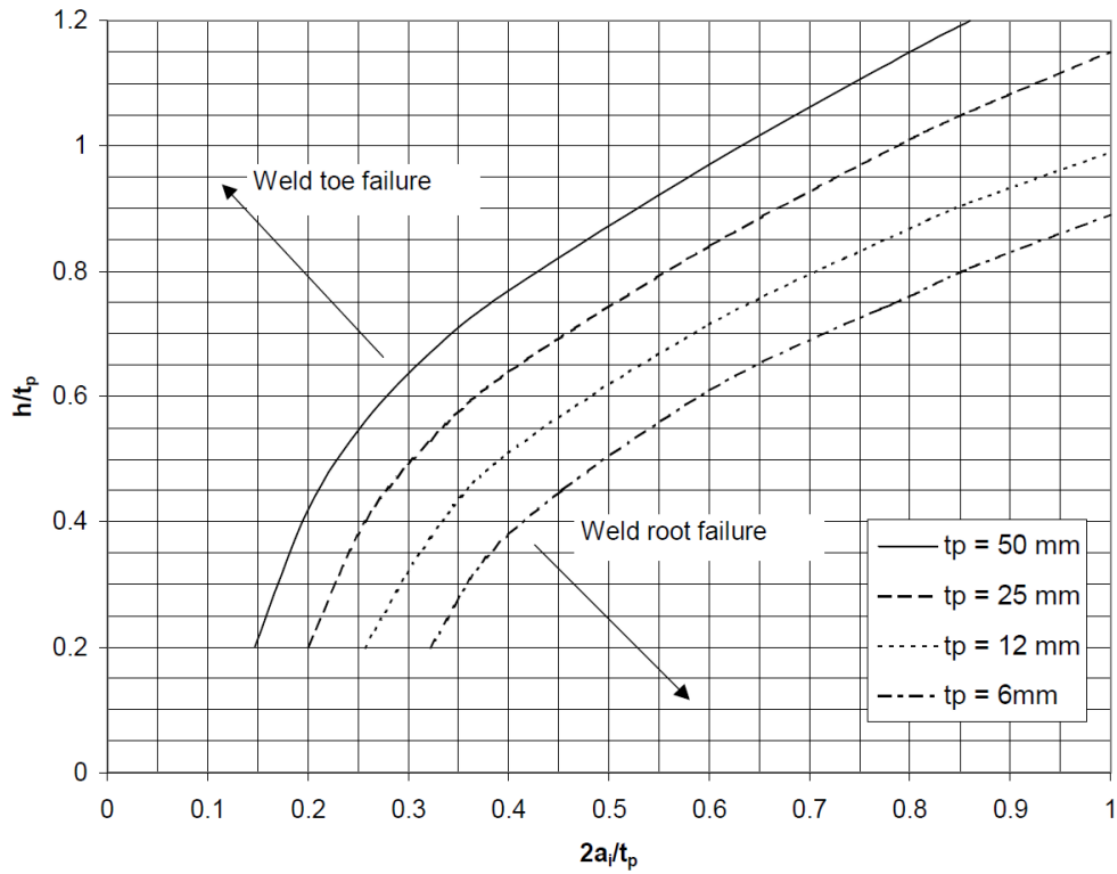


Figure 3 Weld geometry with probability of root failure equal toe failure

APPENDIX C FATIGUE DAMAGE CALCULATIONS AND FATIGUE STRESS DESIGN TABLES

1 Weibull long term stress distribution

The long term distribution of stress ranges may be described by the two-parameter Weibull distribution

$$Q(\Delta\sigma) = \exp\left[-\left(\frac{\Delta\sigma}{q}\right)^{\xi}\right]$$

$$q = \frac{\Delta\sigma_0}{(ln n_0)^{1/\xi}}$$

where:

Q = probability of exceeding the stress range $\Delta\sigma$

ξ = Weibull slope parameter

q = Weibull scale parameter.

The stress range distribution may also be expressed as

$$\Delta\sigma = \Delta\sigma_0 \left[\frac{ln n}{ln n_0} \right]^{1/\xi}$$

where:

$\Delta\sigma_0$ = reference (largest) stress range value at the local detail exceeded once out of n_0 cycles

n_0 = total number of cycles associated with the stress range level $\Delta\sigma_0$.

The Weibull slope parameter is established based on long term stress or wave load analysis. The Weibull distribution is a fit to the stress range distribution at different probability levels of exceedance. The Weibull slope depends on the location of the detail and the governing load components. The reference level for the stress is not significant if the Weibull slope and scale parameters are well established. Alternatively, the fatigue strength may be assessed by considering the different encountered sea states, and summarise the short term results from all the sea states.

2 Fatigue damage accumulation

2.1 Practical damage calculation with one slope S-N curve

The long term stress range distribution can be expressed by a stress histogram, consisting of a number of constant amplitude stress range blocks $\Delta\sigma_i$, each with a number of stress repetitions n_i . Based on this, the fatigue criterion reads:

$$D = \sum_{i=1}^{n_{tot}} \frac{n_i}{N_i} = \frac{1}{K_2} \sum_{i=1}^{n_{tot}} n_i (\Delta\sigma_i)^m \leq \eta$$

where:

- D = accumulated fatigue damage
- m, K_2 = S-N fatigue parameters
- n_{tot} = number of stress blocks
- n_i = number of stress cycles in stress block i
- N_i = number of cycles to failure at constant stress range $\Delta\sigma_i$
- η = Maximum acceptable usage factor.

2.2 Closed form damage estimate for one-slope S-N curves and Weibull distribution

The fatigue damage can be estimated based on the Weibull long term stress distribution and the one-slope S-N curve. For one loading condition, the fatigue damage is given by:

$$D = \frac{N_D}{K_2} q^m \Gamma\left(1 + \frac{m}{\xi}\right) \leq \eta$$

where:

- N_D = Total number of stress cycles experienced by ship during the design fatigue life, taken as: $N_D = 31.557 \times 10^6 (f_0 T_D) / (4 \log L)$
- f_0 = Factor taking into account time in seagoing operations
- T_D = Design life, in years
- v_0 = average zero-crossing frequency of the stress for the specific detail = $1/(4\log(L))$ based on wave bending moment
- $\Gamma(1+m/\xi)$ = Gamma function. Values of the gamma function are listed in [Table 1](#).

Use of one slope S-N curves give conservative estimates of the fatigue lives when using the slope at $N < 10^7$ cycles.

Table 1 Numerical values for $\Gamma(1+m/\xi)$

ξ	$m = 3.0$	ξ	$m = 3.0$	ξ	$m = 3.0$
0.60	120.000	0.77	20.548	0.94	7.671
0.61	104.403	0.78	19.087	0.95	7.342
0.62	91.350	0.79	17.772	0.96	7.035
0.63	80.358	0.80	16.586	0.97	6.750
0.64	71.048	0.81	15.514	0.98	6.483
0.65	63.119	0.82	14.542	0.99	6.234
0.66	56.331	0.83	13.658	1.00	6.000
0.67	50.491	0.84	12.853	1.01	5.781
0.68	45.442	0.85	12.118	1.02	5.575
0.69	41.058	0.86	11.446	1.03	5.382
0.70	37.234	0.87	10.829	1.04	5.200
0.71	33.886	0.88	10.263	1.05	5.029
0.72	30.942	0.89	9.741	1.06	4.868
0.73	28.344	0.90	9.261	1.07	4.715
0.74	26.044	0.91	8.816	1.08	4.571
0.75	24.000	0.92	8.405	1.09	4.435
0.76	22.178	0.93	8.024	1.10	4.306

2.3 Closed form damage estimate for two-slope S-N curves and Weibull distribution

The fatigue damage can be estimated based on the Weibull long term stress distribution and the two-slope (bi-linear) S-N curve. For one loading condition, the fatigue damage is given by:

$$D = N_D \left[\frac{q^m}{K_2} \Gamma \left(1 + \frac{m}{\xi}; \left(\frac{\Delta\sigma_q}{q} \right)^{\xi} \right) + \frac{q^{m+\Delta m}}{K_3} \gamma \left(1 + \frac{m+\Delta m}{\xi}; \left(\frac{\Delta\sigma_q}{q} \right)^{\xi} \right) \right] \leq \eta$$

where:

- $\Delta\sigma_q$ = Stress range in S-N curve, where the change of slope occurs
- K_2, m = S-N fatigue parameters for $N < 10^7$ cycles
- $K_3, m+\Delta m$ = S-N fatigue parameters for $N > 10^7$ cycles
- $\gamma(;)$ = Incomplete Gamma function, to be found in standard tables
- $\Gamma(;)$ = Complementary Incomplete Gamma function, to be found in standard tables.

2.4 Closed form damage estimate for one slope S-N curve and short term Rayleigh distribution

The fatigue damage can be estimated based on the one-slope S-N curve, short term Rayleigh distribution within each short term sea state, all sea states and all loading conditions, in the following way:

$$D = \frac{N_D}{K_2} \Gamma\left(1 + \frac{m}{2}\right) \cdot \sum_{j=1}^{n_{LC}} \alpha_j \sum_{i=1, n=1}^{all seastates, all headings} r_{inj} (2\sqrt{2m_{0inj}})^m \leq \eta$$

where:

- r_{inj} = the relative number of stress cycles in short term condition i , n for loading condition j
- α_j = Probability of loading condition j
- n_{LC} = Total number of loading conditions
- m_{0inj} = zero spectral moment of stress response process in short term condition i , n and loading condition j .

2.5 Closed form damage estimate for two-slope S-N curve and short term Rayleigh distribution

The fatigue damage can be estimated based on the two-slope S-N curve, short term Rayleigh distribution within each short term sea state, all sea states and one loading conditions, in the following way:

$$D = N_D \sum_{i=1, j=1}^{all seastates, all headings} r_{ij} \left(\frac{(2\sqrt{2m_{0ij}})^m}{K_2} \Gamma\left(1 + \frac{m}{2}, \left(\frac{\Delta\sigma_q}{2\sqrt{2m_{0ij}}}\right)^2\right) + \frac{(2\sqrt{2m_{0ij}})^{m+\Delta m}}{K_3} \gamma\left(1 + \frac{m+\Delta m}{2}, \left(\frac{\Delta\sigma_q}{2\sqrt{2m_{0ij}}}\right)^2\right) \right) \leq \eta$$

3 Maximum allowable stress range

The maximum allowable stress range, $\Delta\sigma_0$, results for different Weibull shape parameters ξ , S-N curves, two probabilities of exceedance (10^{-2} and 10^{-8}) and three design lives (given by $0.5 \cdot 10^8$, $0.7 \cdot 10^8$ and $1.0 \cdot 10^8$ cycles) are given in [Table 2](#) to [Table 4](#).

The maximum allowable stress range can be assumed to include K factors, referring to maximum allowable hot spot stress range or local stress range, but the maximum allowable nominal stress range can then be obtained by:

where K is the stress concentration factor.

Example:

- Weibull shape parameter $\xi = 1.0$
- total number of stress cycles = $0.7 \cdot 10^8$
- welded joint, in-air environment

It follows from [Table 2](#) to [Table 4](#) that the maximum allowable stress range is:

- 75 N/mm^2 at 10^{-2} probability level of exceedance,
- 300 N/mm^2 at 10^{-8} probability level of exceedance.

If the stress concentration factor is $K = 1.5$, then the maximum nominal stress range at a probability level of exceedance of 10^{-2} is 51 N/mm^2 .

In lieu of more accurate calculations, the slope parameter, ξ , for vertical wave bending moment may be taken as:

$$\begin{aligned}\xi &= \text{Weibull slope parameter for wave bending moment} \\ &= 2.21 - 0.54\log_{10}(L)\end{aligned}$$

As another example, the vertical bending is a crucial design load for cruise vessels. For a vessel rule length, L , between 250 and 350m, the Weibull slope parameter is between 0.92 and 0.84. The corresponding zero up-crossing period is between 9.6 to 10.2 sec. For a life time of 25 years, this gives $0.78 \cdot 10^8$ to $0.82 \cdot 10^8$ cycles. Based on a probability level of 10^{-2} , $1.0 \cdot 10^8$ cycles and a free plate edge with normal workmanship (C/FAT class 125), Table 2 gives the rule of thumb value of 100 N/mm^2 for the stress range.

In Table 5 the maximum allowable stress range is estimated for all the S-N curves listed in Sec.2 Table 1. The maximum allowable stress range is based on a 10^{-2} probability level of exceedance and a Weibull slope of $\xi = 1.0$.

Table 2 Maximum allowable stress range in N/mm² at a probability of exceedance 10⁻² giving a fatigue damage of 1.0 for different design life cycles.

Weibull Shape-parameter ξ	Welded joint, D (FAT 90) In-Air $\Delta\sigma_0$			Free plate edge, C (FAT125) and B2 (FAT 140) In-air $\Delta\sigma_0$		
	Design life cycles			Design life cycles		
	$0.5 \cdot 10^8$ cycles	$0.7 \cdot 10^8$ cycles	$1.0 \cdot 10^8$ cycles	$0.5 \cdot 10^8$ cycles	$0.7 \cdot 10^8$ cycles	$1.0 \cdot 10^8$ cycles
0.60	82	73	66	107/113	98/104	89/95
0.70	84	76	68	115/124	105/114	95/105
0.80	85	77	69	118/130	108/120	98/110
0.90	84	76	69	119/133	109/122	99/113
1.00	83	75	68	118/133	108/123	99/114
1.10	81	74	67	117/133	107/123	98/114
1.20	79	72	66	115/132	106/123	97/113
1.30	77	71	64	113/131	104/122	96/113

Table 3 Maximum allowable stress range in N/mm² at a probability of exceedance 10⁻⁸ giving a fatigue damage of 1.0 for different design life cycles.

Weibull Shape-parameter ξ	Welded joint, D (FAT 90) In-Air $\Delta\sigma_0$			Free plate edge, C (FAT 125) and B2 (FAT 140) In-air $\Delta\sigma_0$		
	Design life cycles			Design life cycles		
	$0.5 \cdot 10^8$ cycles	$0.7 \cdot 10^8$ cycles	$1.0 \cdot 10^8$ cycles	$0.5 \cdot 10^8$ cycles	$0.7 \cdot 10^8$ cycles	$1.0 \cdot 10^8$ cycles
0.60	822	740	662	1083/1138	987/1047	895/960
0.70	612	552	495	831/897	758/827	690/759
0.80	480	434	391	667/734	609/677	555/623
0.9	392	355	321	554/618	507/571	463/526
1.00	331	300	272	472/534	433/494	396/455

Weibull Shape-parameter ξ	Welded joint, D (FAT 90) In-Air $\Delta\sigma_0$			Free plate edge, C (FAT 125) and B2 (FAT 140) In-air $\Delta\sigma_0$		
	Design life cycles			Design life cycles		
	$0.5 \cdot 10^8$ cycles	$0.7 \cdot 10^8$ cycles	$1.0 \cdot 10^8$ cycles	$0.5 \cdot 10^8$ cycles	$0.7 \cdot 10^8$ cycles	$1.0 \cdot 10^8$ cycles
1.10	285	259	235	412/470	378/435	347/402
1.20	251	229	208	366/420	336/389	308/360
1.30	225	205	187	329/381	303/353	279/327

Table 4 Maximum allowable stress range in N/mm² at a probability of exceedance 10⁻² and 10⁻⁸ giving a fatigue damage of 1.0 for different design life cycles.

Weibull shape-parameter ξ	Free plate edge, C1 (FAT 112) and B (FAT 150) In-Air $\Delta\sigma_0$, 10 ⁻² level			Free plate edge, C1 (FAT 112) and B (FAT 150) In-Air $\Delta\sigma_0$, 10 ⁻⁸ level		
	Design life cycles			Design life cycles		
	0.5·10 ⁸ cycles	0.7·10 ⁸ cycles	1.0·10 ⁸ cycles	0.5·10 ⁸ cycles	0.7·10 ⁸ cycles	1.0·10 ⁸ cycles
0.60	96/121	88/111	80/102	970/1217	884/1122	802/1029
0.70	103/133	94/122	85/112	744/960	680/885	618/813
0.80	106/139	97/128	88/118	597/786	546/725	497/667
0.90	106/142	97/131	89/121	496/662	454/612	414/564
1.00	106/143	97/132	89/122	423/572	388/529	355/488
1.10	105/143	96/132	88/122	369/503	339/466	310/430
1.20	103/142	95/131	87/121	327/450	301/417	276/386
1.30	101/140	93/130	86/121	295/407	271/378	250/350

Table 5 Maximum allowable stress range in N/mm² at a probability of exceedance 10⁻² and for Weibull shape parameter $\xi = 1.0$ giving a fatigue damage of 1.0 for different design life cycles and S-N curves.

S-N curves	In-Air			Corrosive		
	$\Delta\sigma_0$			$\Delta\sigma_0$		
	Design life cycles			Design life cycles		
	$0.5 \cdot 10^8$ cycles	$0.7 \cdot 10^8$ cycles	$1.0 \cdot 10^8$ cycles	$0.5 \cdot 10^8$ cycles	$0.7 \cdot 10^8$ cycles	$1.0 \cdot 10^8$ cycles
B1	153	141	130	130	121	112
B	143	132	122	122	113	105
B2	133	123	114	114	106	98
C	118	108	99	99	91	84
C1	106	97	89	89	82	75
C2	94	87	79	79	73	67
D	83	75	68	68	62	56
E	73	67	60	60	55	50
F	65	59	54	54	49	45

4 Guidance for omission of fatigue analysis

A detailed fatigue analysis can be omitted if the largest hot spot stress range or local stress range for actual details in air or cathodic protected environment is less than the fatigue limit at 10⁷ cycles.

The use of the fatigue limit is illustrated in [Figure 1](#). A detailed fatigue assessment can be omitted if the largest stress cycle is below the fatigue limit. However, in the example in [Figure 2](#), there is one stress cycle $\Delta\sigma_1$ above the fatigue limit. This means that a further fatigue assessment is required. This also means that the fatigue damage from the stress cycle $\Delta\sigma_2$ has to be included in the fatigue assessment and the summation of fatigue damage presented in this document should be used.

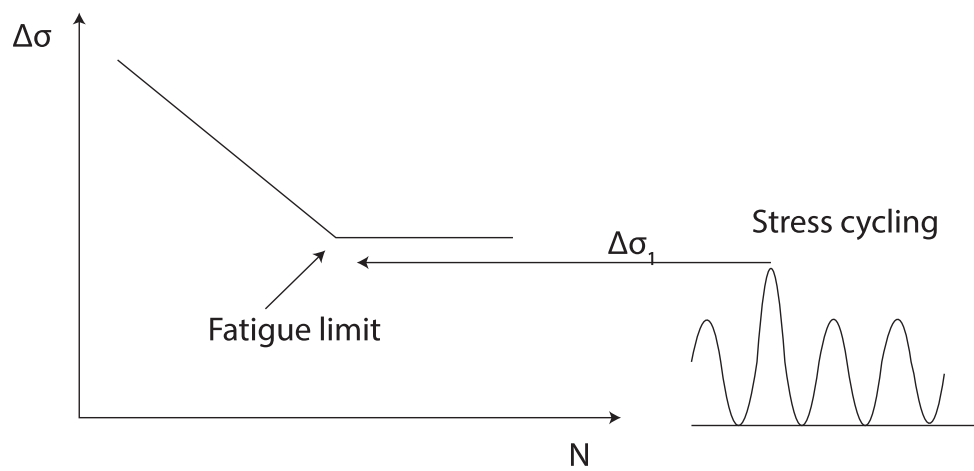


Figure 1 Stress cycling where further fatigue assessment can be omitted

APPENDIX D PRESCRIPTIVE FATIGUE STRENGTH ASSESSMENT

1 Bending stress of PSM

1.1 Prescriptive double hull bending stress at transverse bulkhead

When relative deflection (see [2]) contributes, then also double hull bending stress may contribute. Double hull bending contributes when the double hull is represented by a grillage system with longitudinal girders (stringers). The following prescriptive estimates serve as an alternative to more advanced FE analysis. [Figure 1](#) gives an illustration of the main dimensions of the grillage model with longitudinal stress due to double hull bending. In [Figure 2](#) the girder system with longitudinal stiffening is illustrated. The stiffeners are smeared out in the prescriptive model to contribute to the flange area of the longitudinal girders (stringers).

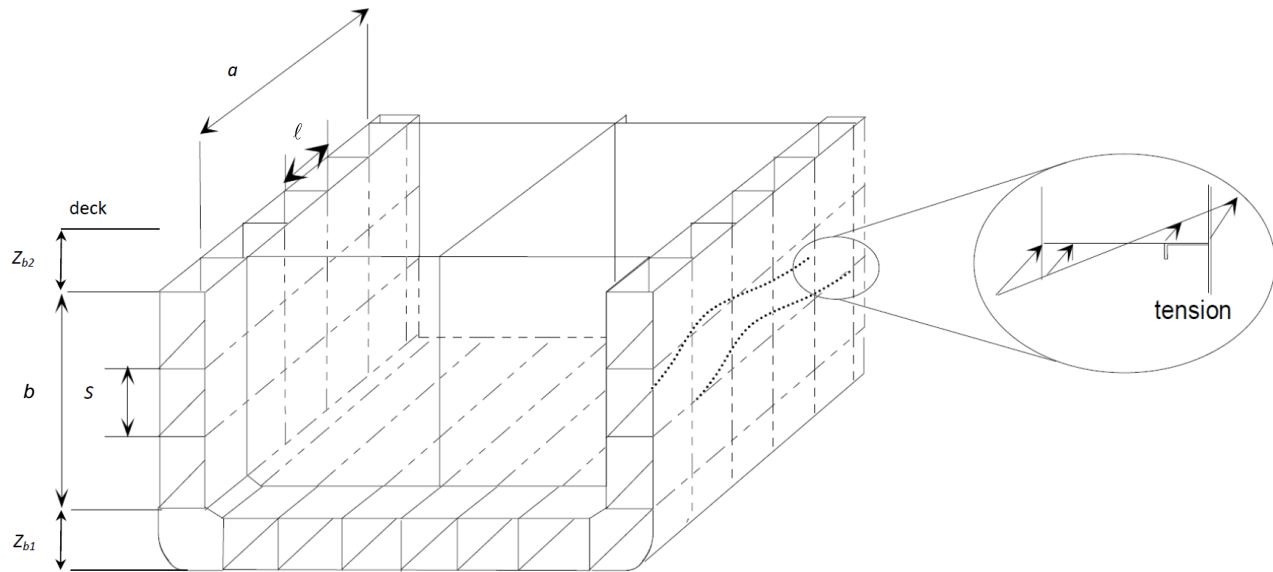


Figure 1 Double hull configuration with illustration of double hull bending stress.

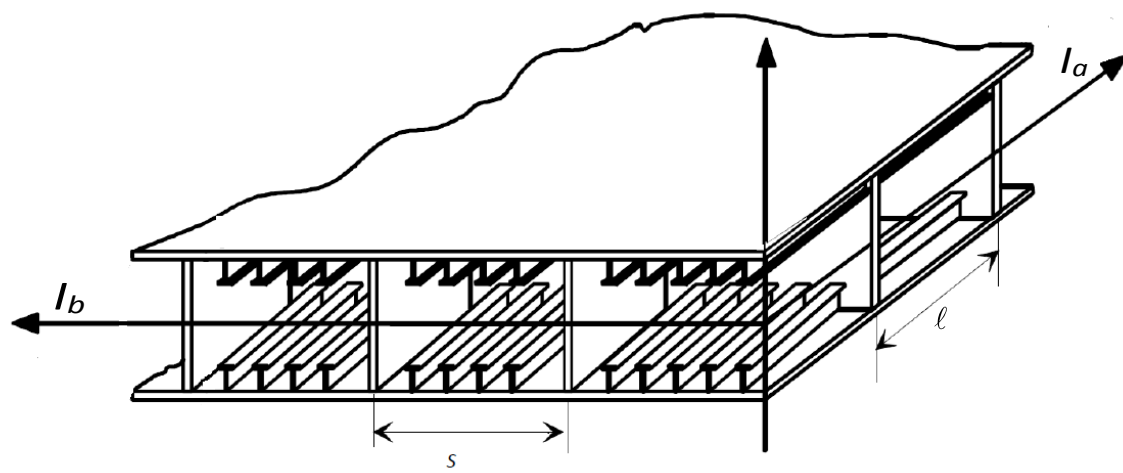


Figure 2 Double hull configuration with distances between girders

1.2 Prescriptive wave induced double side bending stress at the transverse bulkhead

The longitudinal double side hot spot stress (or nominal stress with $K_a = 1$), $\sigma_{dhD,ik(j)}$, in N/mm², is given as:

$$\sigma_{dhD,ik(j)} = K_a \frac{K_{c1} b^2 r_a}{\sqrt{i_a i_b}} (K_d P_{W,ik(j)} - K_e P_{ld,ik(j)}) \cdot K_i \cdot 10^{-3} \rho = \frac{a}{b} \cdot \sqrt[4]{\frac{i_b}{i_a}} \text{ when } a > b$$

$$\sigma_{dhD,ik(j)} = K_a \frac{K_{c2} a^2 r_a}{i_a} (K_d P_{W,ik(j)} - K_e P_{ld,ik(j)}) \cdot K_i \cdot 10^{-3} \rho = \frac{b}{a} \cdot \sqrt[4]{\frac{i_a}{i_b}} \text{ when } b > a$$

$$K_i = \begin{cases} 0 & \text{when } z \leq z_{b1} \\ 0 & \text{when } z \geq D - z_{b2} \\ 1 - \left(1 - 2 \frac{(z - z_{b1})}{b}\right)^2 & \text{when } z_{b1} < z < D - z_{b2} \end{cases}$$

where:

- K_a = Axial stress concentration factor from App.A for the respective detail
- K_{c1}, K_{c2} = Coefficients dependent on aspect ratio, ρ
- K_e = Coefficient for loading area; $K_e = 1.0$ for double side
- r_a = Distance from neutral axis of the double hull panel to the point considered, in mm, defined as positive outwards towards the outer shell
- K_d = Coefficient for loading area; $K_d = T_{LC}/D$ for double side_d

a	= Longitudinal length of double hull panel, in mm
b	= Height of double hull panel, in mm.
i_a	= Average moment of inertia per longitudinal double panel girder about transverse neutral axis of the girder; taken as $i_a = I_a/S$, in mm^3
i_b	= Average moment of inertia per transverse double panel girder about longitudinal neutral axis of the girder; taken as $i_b = I_b/\ell$, in mm^3
I_a, I_b	Longitudinal and transverse moment of inertia about the double hull neutral axis in transverse and longitudinal axes respectively, in mm^4 , per girder including effective flange. In the computation of I_a , the area of the longitudinal stiffeners may be added to the plate as a smeared out thickness
S, ℓ	= Spacing between girders in longitudinal and transverse direction, respectively, in mm.
$P_{W,ik(j)}$	= Dynamic pressure, in kN/m^2 , for external pressure at T_{LC} for double side. The pressure should be taken at a global x-position corresponding to the bulkhead considered Dynamic internal pressure (from the cargo tank), in kN/m^2 , on the longitudinal bulkhead. If the cargo tank is not carrying fluid, the internal pressure should be neglected. The pressure should be taken at a global x-position corresponding to the longitudinal centre of the tank
$P_{ld,ik(j)}$	= located on the same side of the transverse bulkhead as the detail considered, at a transverse position corresponding to the longitudinal bulkhead and at a vertical position corresponding to the vertical centre of the tank
z	= Vertical distance from base line, in m, to the considered detail
D	= Depth moulded, in m.
z_{b1}	= vertical distance from base line, in m, to top of inner bottom or top of hopper tank in case it has a hopper tank
z_{b2}	= vertical distance in mm from top of b to deck. Top of b should correspond to the lower part of the transverse deck frame or lower part of topside tank in case it has an topside tank = $D - b - z_{b1}$

It is assumed that the grillage is clamped at the ends (due to symmetry) and simply supported at the longitudinal edges. The K_{c1} and K_{c2} can then be estimated as:

$$K_{c1} = -0.0663 + 0.2042\rho - 0.067\rho^2 + 0.0072\rho^3$$

$$K_{c2} = 0.0589 + 0.0243\rho - 0.0041\rho^2$$

1.3 Prescriptive still water double side bending stress at the transverse bulkhead

The longitudinal double side hot spot stress (or nominal stress with $K_a = 1$), $\sigma_{dhS,(j)}$, in N/mm^2 , can be given as:

$$\sigma_{dhS,(j)} = K_a \frac{K_{c1} b^2 r_a}{\sqrt{i_a i_b}} (K_d P_{S,(j)} - K_e P_{ls,(j)}) \cdot K_i \cdot 10^{-3} \quad \rho = \frac{a}{b} \cdot \sqrt[4]{\frac{i_b}{i_a}} \quad \text{when } a > b$$

$$\sigma_{dhS,(j)} = K_a \frac{K_{c2} d^2 r_a}{i_a} (K_d P_{S,(j)} - K_e P_{ls,(j)}) \cdot K_i \cdot 10^{-3} \quad \rho = \frac{b}{a} \cdot \sqrt[4]{\frac{i_a}{i_b}} \quad \text{when } b > a$$

where:

- K_d = Coefficient for loading area; $K_d = 0.5T_{LC}/D$ for double side
- K_e = Coefficient for loading area; $K_e = 1/2$ for double side
- $P_{S, (j)}$ = Static external pressure, in kN/m^2 , in loading condition (j) and taken at $z = 0$, i.e. at the base line. The pressure should be taken at a global x-position corresponding to the bulkhead considered
- $P_{IS, (j)}$ = Static internal pressure (from the cargo tank), in kN/m^2 , in loading condition (j). If the cargo tank is not carrying fluid, the internal pressure should be neglected. The pressure should be taken at a global x-position corresponding to the longitudinal centre of the tank located on the same side of the transverse bulkhead as the detail considered, and at a vertical position corresponding to the tank top.

2 Local relative displacement stress

2.1 Prescriptive wave induced relative deflection for double hull vessels

As an alternative to relative deflection estimated by FE analysis, the wave induced relative deflection hot spot stress amplitude, $\sigma_{dD,ik(j)}$, in N/mm^2 , for load case ik and loading condition (j) may be estimated as follows:

$$\begin{aligned}\sigma_{dD,ik(j)} &= K_b \cdot \frac{4.4 \cdot Ez_{01}}{(1000 \cdot \ell_{bdg})^2} \cdot r_\delta \cdot \delta_{ik(j)} \\ r_\delta &= 1 - 2\left(\frac{x_e}{\ell_{bdg}}\right) \quad 0 \leq x_e \leq \ell_{bdg} \\ z_{01} &= \frac{I_{n50}}{Z_{n50}}\end{aligned}$$

where:

- x_e = Distance, in m, to the hot spot from the closest end of the span ℓ_{bdg} , as defined in [Sec.4 Figure 3](#)
- z_{01} = Distance from neutral axis of the stiffener/plate to stiffener flange, in mm
- Z_{n50} = Net section modulus for the stiffener/plate, in mm^3 , referring to the stiffener between the transverse bulkhead and the adjacent frame, on which the hot spot is located
- ℓ_{bdg} = The effective length of the stiffener, in m
- E = Young's Modulus, in N/mm^2
- I_{n50} = Net moment of inertia, in mm^4 , for the stiffener/plate, referring to the stiffener between the transverse bulkhead and adjacent frame, on which the hot spot is located
- $\delta_{ik(j)}$ = Relative deflection, in mm, for load case ik and loading condition j.

The formulation is regarded applicable for transverse bulkheads without transverse stringers restraining the adjacent frame. An illustration of the relative deflection for the adjacent frame is given in [Figure 3](#). The relative deflection, $d_{ik(j)}$, in mm, for the side shell can be estimated as:

$$\delta_{ik(j)} = K_i \cdot \delta_{m,ik(j)}$$

where:

- $d_{m,ik(j)}$ = Maximum relative deflection, in mm, over the height of the web frame for load case ik and loading condition j
- z = Vertical distance from base line, in m, to the considered detail
- D = Depth moulded, in m.

The maximum relative deflection is estimated as:

$$\delta_{m,ik(j)} = -\eta_1 \frac{0.3S \ell^2 b}{E \sqrt{i_a i_b} \sqrt{1 + N_s}} (P_{W,ik(j)} - P_{ld,ik(j)}) \text{ for designs with stringers}$$

$$\delta_{m,ik(j)} = -\eta_1 \frac{110 \ell^3 b^2}{EI_b \sqrt{1 + N_s}} (P_{W,ik(j)} - P_{ld,ik(j)}) \text{ for designs without stringers}$$

where:

- S = Sum of half plate flange width on each side of the horizontal stringer closest to $D/2$, in mm
- η_1 = Sign factor being 1 for stiffener in outer shell and -1 for stiffener in inner side
- ℓ = Frame spacing, in mm
- I_a = Moment of inertia for the longitudinal stringer, in mm^4
- I_b = Moment of inertia for the transverse frame, in mm^4
- N_s = Number of cross ties
- i_a, i_b = $I_a/S, I_b/\ell$
- $P_{W,ik(j)}$ = Dynamic external pressure, in kN/m^2 , at T_{LC} . The pressure should be taken at a global x-position corresponding to the bulkhead considered
Dynamic internal pressure (from the cargo tank), in kN/m^2 , on the longitudinal bulkhead.
If the cargo tank is not carrying fluid, the internal pressure should be neglected. The pressure should be taken at a global x-position corresponding to the longitudinal centre of the tank located on the same side of the transverse bulkhead as the detail considered, at a transverse position corresponding to the longitudinal bulkhead and a vertical position corresponding to the $z = D/2$.
- $P_{ld,ik(j)}$

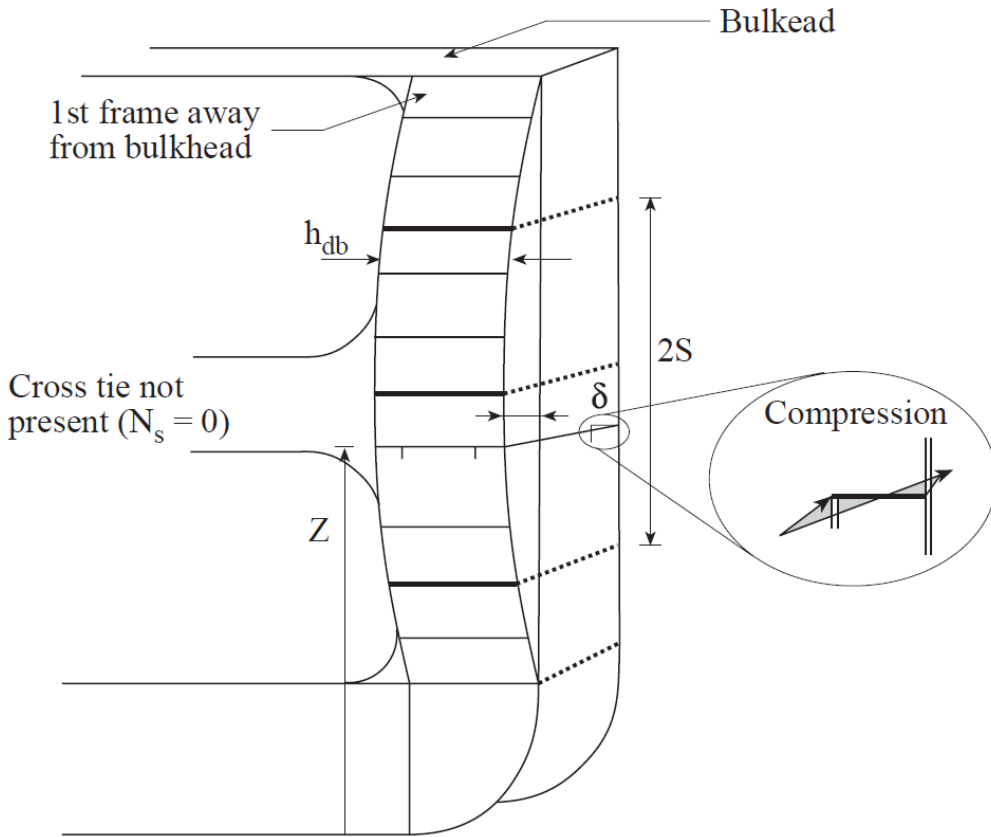


Figure 3 Illustration of stress due to relative deflection between a transverse bulkhead and the adjacent frame

2.2 Prescriptive relative deflection for double hull vessels due to static pressure

The static hot spot stress amplitude for relative deflection, $\sigma_{dS,(j)}$, in N/mm², is given as:

$$\sigma_{dS,(j)} = K_b \cdot \frac{4.4 \cdot EZ_{01}}{(1000 \cdot \ell_{bdg})^2} \cdot r_\delta \cdot \delta_{ik(j)}$$

$$r_\delta = 1 - 2\left(\frac{x_e}{\ell_{bdg}}\right) \quad 0 \leq x_e \leq \ell_{bdg}$$

$$\delta_{ik(j)} = K_i \cdot \delta_{m,ik(j)}$$

$$\delta_{m, ik(j)} = -\eta_1 \frac{0.3S \ell^2 b}{E \sqrt{i_a i_b} \sqrt{1 + N_s}} (K_d P_{S, (j)} - K_e P_{ls, (j)}) \text{ for designs with stringers}$$

$$\delta_{m, ik(j)} = -\eta_1 \frac{110 \ell^3 b^2}{EI_b \sqrt{1 + N_s}} (K_d P_{S, (j)} - K_e P_{ls, (j)}) \text{ for designs without stringers}$$

where:

- $P_{S, (j)}$ = Static external pressure, in kN/m², in loading condition (j) and taken at z = 0, i.e. at the base line. The pressure should be taken at a global x-position corresponding to the bulkhead considered.
- K_d = Coefficient for loading area; $K_d = T_{LC}/D/2$ for double side
- $P_{ls, (j)}$ = Static internal pressure (from the cargo tank), in kN/m², in loading condition (j). If the cargo tank is not carrying fluid, the internal pressure should be neglected. The pressure should be taken at a global x-position corresponding to the longitudinal centre of the tank located on the same side of the transverse bulkhead as the detail considered, at a transverse position corresponding to the longitudinal bulkhead and a vertical position corresponding to the tank top.
- K_e = Coefficient from loading area; $K_e = 1/2$ for double side .

3 Local plate bending stress

3.1 Wave induced plate bending stress

The longitudinal plate bending stress at the plate short edge, σ_{PLD} , is located at the weld of the plate/transverse frame/bulkhead intersection midway between the longitudinals. The wave induced hot spot stress amplitude (or nominal stress with $K=1$) in load case i1 and i2 for loading condition (j), $\sigma_{PLD, ik(j)}$, in N/mm², is given by:

$$\sigma_{PLD, ik(j)} = -0.343 (\eta_W f_{NL} P_{W, ik(j)} + \eta_{ld} P_{ld, ik(j)} + \eta_{bd} P_{bd, ik(j)}) \left(\frac{s}{t_{n50}} \right)^2 K$$

where:

- K = Stress concentration factor, which depends on the plate thickness in App.A. If nothing else is specified K can be taken as 1.13 for fillet welds.
- s = Stiffener spacing, in mm
- t_{n50} = Net plate thickness, in mm.

The transverse plate bending stress at the plate long edge, σ_{PTD} , is located at the weld at the stiffener mid-length. The wave induced hot spot stress amplitude (or nominal stress with $K = 1$) in load case i1 and i2 for loading condition (j), $\sigma_{PTD, ik(j)}$, in N/mm², is given by:

$$\sigma_{PTD, ik(j)} = -0.5 (\eta_W f_{NL} P_{W, ik(j)} + \eta_{ld} P_{ld, ik(j)} + \eta_{bd} P_{bd, ik(j)}) \left(\frac{s}{t_{n50}} \right)^2 K$$

For local plate bending due to local pressures the following sign conventions apply:

- Positive for pressure acting on the welded side of the plate (tension at hot spot)
- Negative for pressure acting on the non-welded side of the plate (compression at hot spot).

3.2 Still water plate bending stress

The longitudinal and transverse static stress depends on the loading condition (j). The longitudinal static hot spot stress amplitude (or nominal stress with $K = 1$) for loading condition (j), $\sigma_{PLS,(j)}$, in N/mm², is given by:

$$\sigma_{PLS,(j)} = -0.343(\eta_s P_{S,(j)} + \eta_{ls} P_{ls,(j)} + \eta_{bs} P_{bs,(j)})\left(\frac{s}{t_{n50}}\right)^2 K$$

The transverse static hot spot stress (or nominal stress with $K = 1$) for loading condition (j), $\sigma_{PTS,(j)}$, in N/mm², is given by:

$$\sigma_{PTS,(j)} = -0.5(\eta_s P_{S,(j)} + \eta_{ls} P_{ls,(j)} + \eta_{bs} P_{bs,(j)})\left(\frac{s}{t_{n50}}\right)^2 K$$

APPENDIX E FINITE ELEMENT ANALYSIS

1 FE modelling

1.1 Mesh size

For 8-node shell elements and 4-node shell elements with additional internal degrees of freedom for improved in-plane bending behaviour, a mesh size from $t/2$ up to $2t$ may be used. For conventional 4-node elements, a mesh size from $t/2$ to t may be used. Larger mesh sizes at the hot spot region may provide non-conservative results.

1.2 Solid elements

An alternative, particularly for complex cases, is offered by solid elements. These need to have a displacement function capturing steep stress gradients, e.g. by using linear plate bending stress distribution in the plate thickness direction. This is offered, e.g. by iso-parametric 20-node elements (with mid-side nodes at the edges), which mean that only one element in plate thickness direction is required. An easy evaluation of the membrane and bending stress components is then possible if a reduced integration order with only two integration points in the thickness direction is chosen. A finer mesh sub-division is necessary particularly if 8-node solid elements are selected. Here, at least four elements are recommended in the thickness direction. Modelling of the welds is generally recommended as shown in [Figure 1](#).

For modelling with solid elements, the dimensions of the first two or three elements in front of the weld toe should be chosen as follows. The element length may be selected to correspond to the plate thickness. In the transverse direction, the plate thickness may be chosen again for the breadth of the plate elements. However, the breadth should not exceed the attachment width, i.e. the thickness of the attached plate plus two times the weld leg length (in case of type c in [Figure 1](#): The thickness of the web plate behind plus two times the weld leg length). The length of the elements should be limited to $2 \cdot t$. It is recommended that also the fillet weld is modelled to achieve proper local stiffness and geometry.

In order to capture the properties of bulb sections with respect to St. Venant torsion, it is recommended to use several solid elements for modelling of the bulb section. The meshing of the bulb however has to be adopted to the meshing at the relevant hot spots, which are located at the end connection in way if the frame.

2 Derivation of hot spot stress

2.1 Extrapolation from $t/2$ and $3t/2$

Recommended stress evaluation points are located at distances $t/2$ and $3t/2$ away from the hot spot, where t is the plate thickness at the weld toe. These locations are also denoted as stress read out points. The extrapolation method is regarded as the basic method, but read out at $t/2$ with stress correction is regarded more convenient for many standard details.

For modelling with shell elements without any weld considered, the following procedures can be used:

- A linear extrapolation of the stresses to the intersection line based on read out points at $t/2$ and $3t/2$ from the intersection line. The principal stress at the hot spot is calculated from the extrapolated component values (principal stress within an angle $\pm 45^\circ$ to the normal to the weld).

For modelling with solid elements with the weld included, the following procedures can be used:

- A linear extrapolation of the stresses to the weld toe based on read out points at $t/2$ and $3t/2$ from the weld toe. The principal stress at the hot spot is calculated from the extrapolated component values (principal stress within an angle $\pm 45^\circ$ to the normal to the weld).

The stress components on the plate surface should be evaluated along the paths shown in Sec.6 Figure 14 and Figure 1 and extrapolated to the hot spot. The average stress components between adjacent elements are used for the extrapolation.

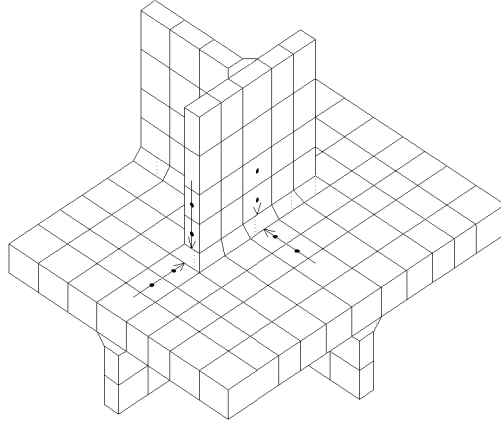


Figure 1 A FE model with solid elements with stress extrapolation to the weld toe

2.2 Derivation of effective hot spot stress considering principal stress directions

The S-N curves defined in Sec.2 [2] are derived based on stress range normal to the weld. As the angle between the principal stress direction and the normal to the weld is increased, it becomes conservative to use the principal stress range. An alternative method for deriving the hot spot stress is described below and can replace the procedure described in Sec.6 [3.2].

Two alternative methods can be used for hot spot stress derivation: Method A and method B.

Method A

The linear extrapolation for shell and solid elements are according to [2.1]. The notations for stress components are shown in Figure 2 and Figure 3. The effective hot spot stress, σ_{Eff} , in N/mm², to be used together with the hot spot S-N curve is derived as:

$$\sigma_{Eff} = \left(c \cdot \max \left(\begin{array}{l} \sqrt{\Delta\sigma_{\perp}^2 + 0.81\Delta\tau_{||}^2} \\ K_p \cdot \Delta\sigma_1 \\ K_p \cdot |\Delta\sigma_2| \end{array} \right) \right)$$

where the principal stresses are calculated as

$$\Delta\sigma_1 = \frac{\Delta\sigma_{\perp} + \Delta\sigma_{||}}{2} + \frac{1}{2}\sqrt{(\Delta\sigma_{\perp} - \Delta\sigma_{||})^2 + 4\Delta\tau_{||}^2}$$

$$\Delta\sigma_2 = \frac{\Delta\sigma_{\perp} + \Delta\sigma_{||}}{2} - \frac{1}{2}\sqrt{(\Delta\sigma_{\perp} - \Delta\sigma_{||})^2 + 4\Delta\tau_{||}^2}$$

where:

$K_p = 0.90$ if manual fillet or butt welds are carried out

$K_p = 0.80$ if automatic fillet or butt welds are carried out from both sides with stop and start positions.
 $K_p = 0.72$ if automatic fillet or butt welds are carried out from both sides without stop and start positions
 $c = 1.0$

The equation for effective stress accounts for the situation with fatigue cracking along a weld toe, as shown in [Figure 2](#), and fatigue cracking when the principal stress direction is more parallel with the weld toe, as shown in [Figure 3](#). This is then a refinement compared to [Sec.6 \[1.4\]](#) where only the principal stress more parallel to the weld included a K_p factor. The relation above is more cumbersome as also the weld type need to be identified.

Method B

For modelling with shell elements without any weld, the hot spot stress is taken as the stress at the read out point $t/2$ from the intersection line. For modelling with solid elements with the weld included in the model, the hot spot stress is taken as the stress at the read out point $t/2$ from the weld toe.

The effective hot spot stress is derived as in Method A, but with the parameter $c = 1.12$.

3 Derivation of stress at read out points

3.1 Derivation of stress at read out points $t/2$ and $3t/2$

The stress at the read out points is established as described in the following. Alternatively, the nodal stresses may be used provided that they are derived directly from the calculated element stresses within each element. When referring to hot spot 'a' and 'c' in [Figure 1](#) $t/2$ and $3t/2$ are used, but when considering hot spot 'b' 5 and 15 mm are used as basis.

4-node shell elements $t/2 \leq$ element size $\leq t$:

- element surface stress at the centre points are used as illustrated in [Figure 2 a\)](#)
- the stress at the element centre points are extrapolated to the line A-A as shown in [Figure 2 b\)](#) to determine the stress at read out points
- if the mesh density differs from $t \times t$, the stresses at the stress read out points are determined by 2nd order interpolation as shown in [Figure 2 c\).](#)

8-node shell elements $t/2 \leq$ element size $\leq t$:

- element edge surface stress points can be used as stress read out points as illustrated in [Figure 3 a\) and b\)](#)
- if the mesh density differs from $t \times t$, the stresses at the read out points are determined by 2nd order interpolation as shown in [Figure 3 b\).](#)

8-node shell elements $t \leq$ element size $\leq 2t$:

- element surface result point stress is used as illustrated in [Figure 4 a\)](#)
- the stress at the surface result points are extrapolated to the line A-A by 2nd order interpolation as shown in [Figure 4 b\)](#)
- the stress at the read out points are determined by 2nd order interpolation as shown in [Figure 4 c\).](#)

Solid elements:

- in case of solid elements the stress may first be extrapolated from the Gaussian points to the surface. Then these stresses can be interpolated linearly to the surface centre or extrapolated to the edge of the elements, if this is the line with the hot spot stress derivation to determine the stress read out points.

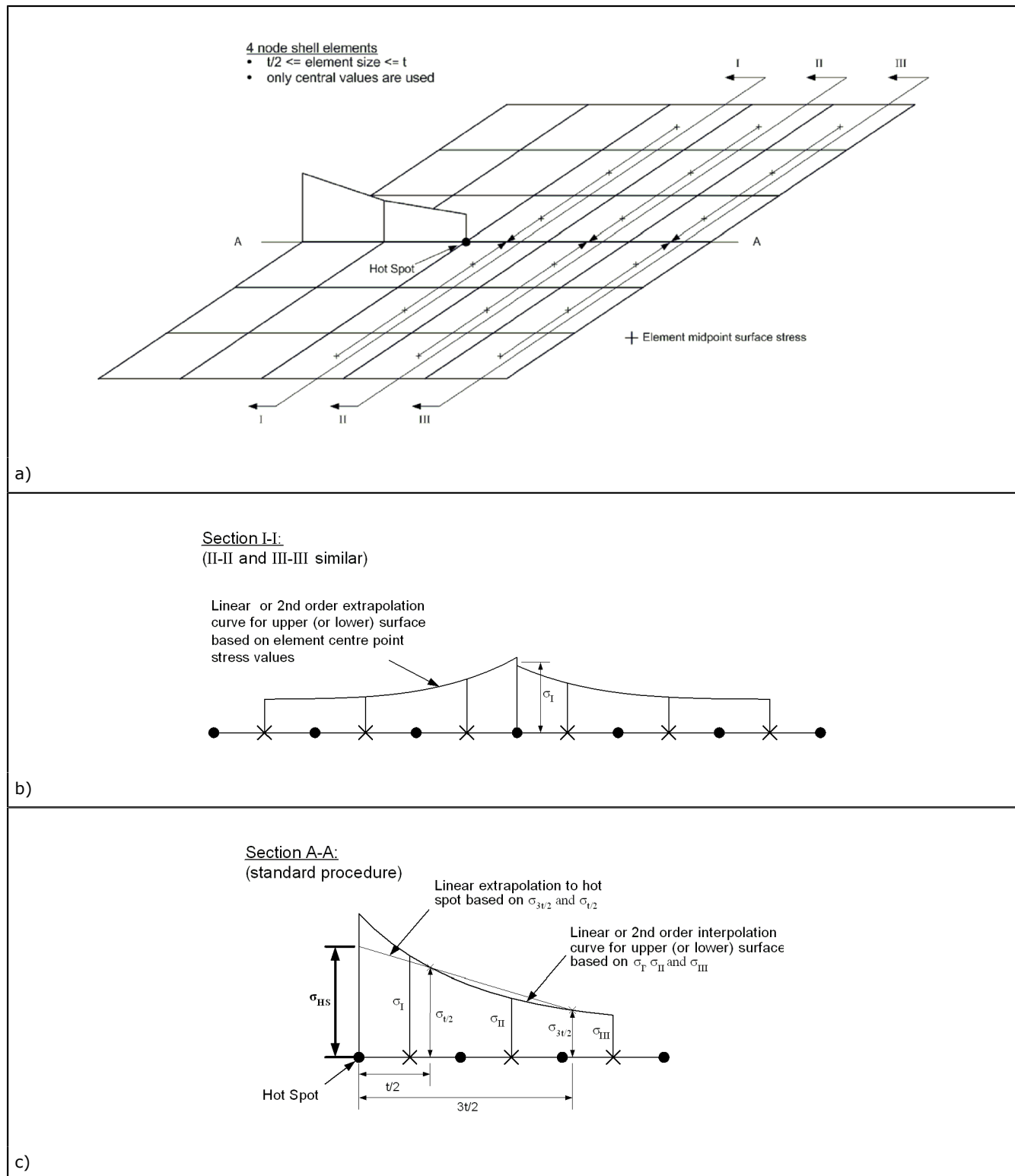


Figure 2 Determination of stress read out points and hot spot stress for 4-node shell elements

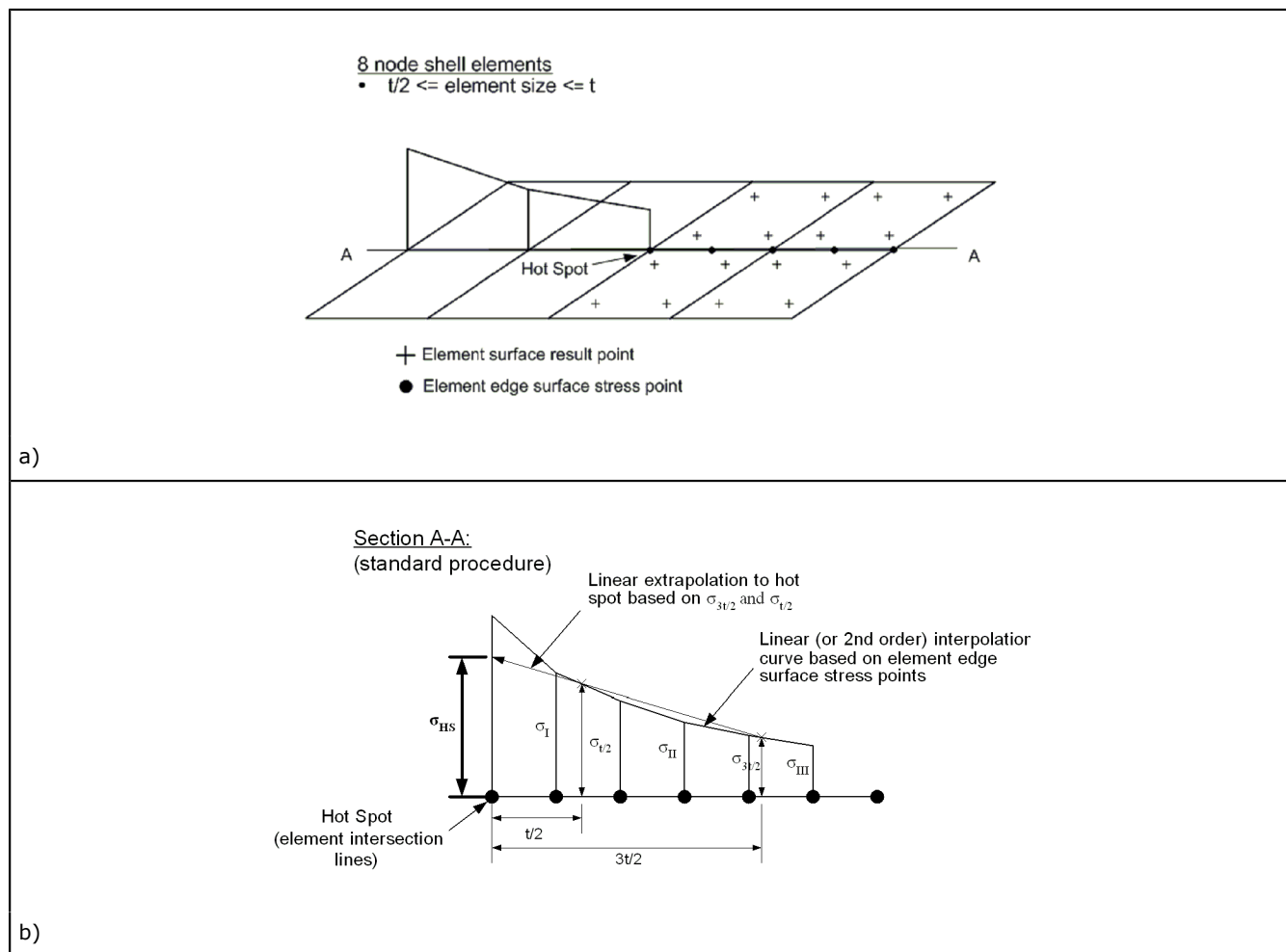


Figure 3 Determination of stress read out points and hot spot stress for 8-node shell elements $t/2 \leq \text{element size} \leq t$

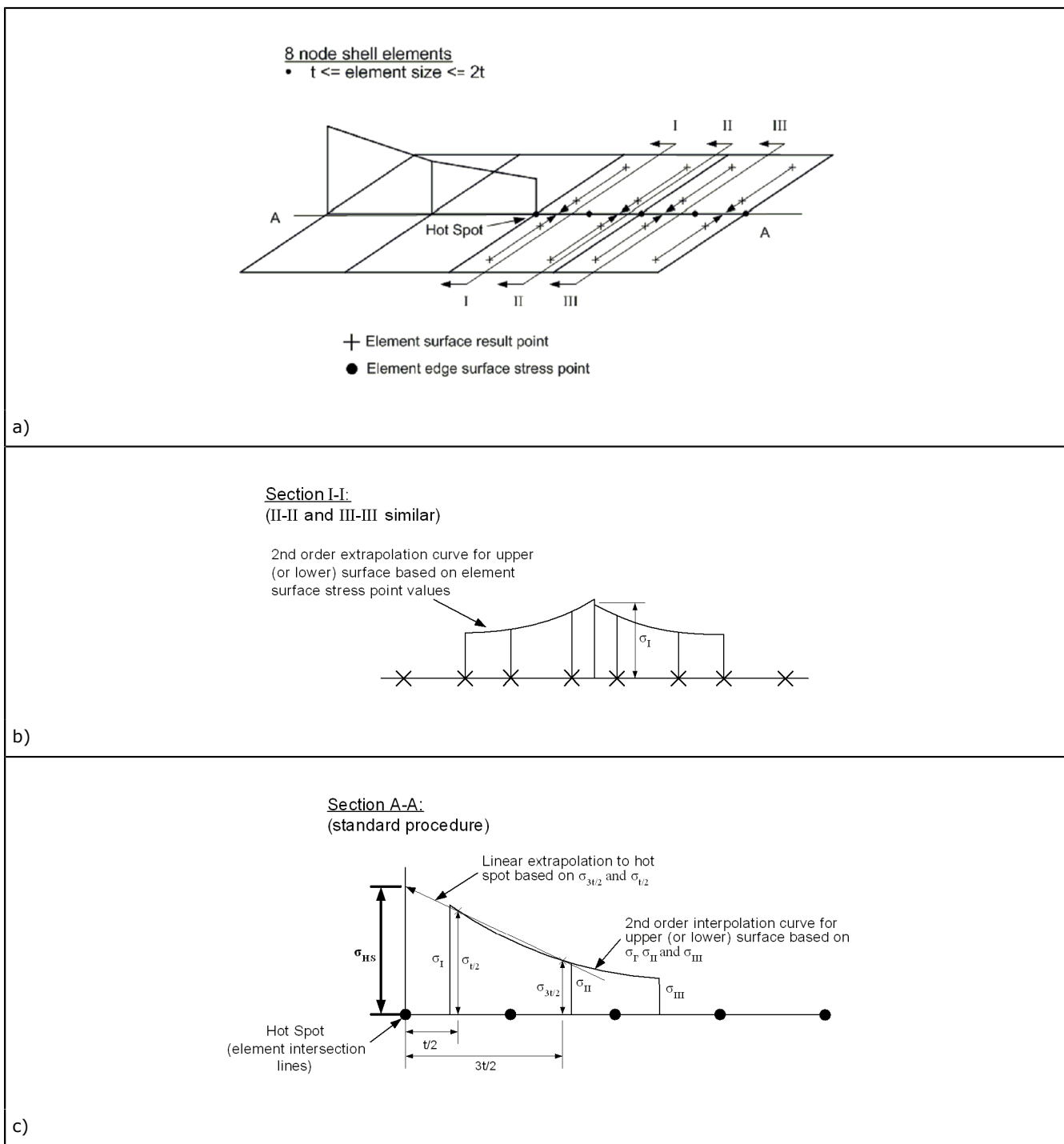


Figure 4 Determination of stress read out points and hot spot stress for 8-node shell elements $t \leq \text{element size} \leq 2t$

4 Procedure for analysis of hot spot stress for tuned details

4.1 Bent hopper tank knuckles

The hot spots at the inner bottom/hopper sloping plate in transverse and longitudinal directions are referred to as hot spot 1, 2 and 3 on the ballast tank side in [Figure 5](#). The hot spot stress of a bent hopper knuckle should be taken as the surface principal stress, read out from a point shifted from the intersection line. The shifted read out position is defined in [Sec.6 \[5.2\]](#). The hot spot stress, σ_{HS} , in N/mm², is obtained as:

$$\begin{aligned}\sigma_{HS} &= \sigma_{shift}(x_{shift}) \\ \sigma_{shift}(x_{shift}) &= \sigma_{membrane}(x_{shift}) + \sigma_{bending}(x_{shift})\end{aligned}$$

where:

$$\begin{aligned}\sigma_{bending}(x_{shift}) &= \text{Bending stress, in N/mm}^2, \text{ at } x_{shift} \text{ position} \\ \sigma_{membrane}(x_{shift}) &= \text{Membrane stress, in N/mm}^2, \text{ at } x_{shift} \text{ position.}\end{aligned}$$

The procedure that applies for hot spots on the ballast tank side of the inner bottom/hopper plate in way of a bent hopper knuckle is in principle the same as that applied on the cargo tank side of the inner bottom plate for welded knuckle in [Figure 10](#) and [Figure 12](#) in [Sec.6 \[5.2\]](#). The intersection line is taken at the mid-thickness of the joint assuming median alignment. The plate angle correction factor and the reduction of bending stress as applied for a web-stiffened cruciform joint in [Sec.6 \[5.2\]](#) are not to be applied for the bent hopper knuckle type.

The stress at hot spots located in way of the transverse web and side girder, i.e. hot spots 4, 5 and 6 defined in [Figure 6](#), of a bent hopper knuckle type should be derived as described for web-stiffened cruciform joints in [Sec.6 \[5.3\]](#).

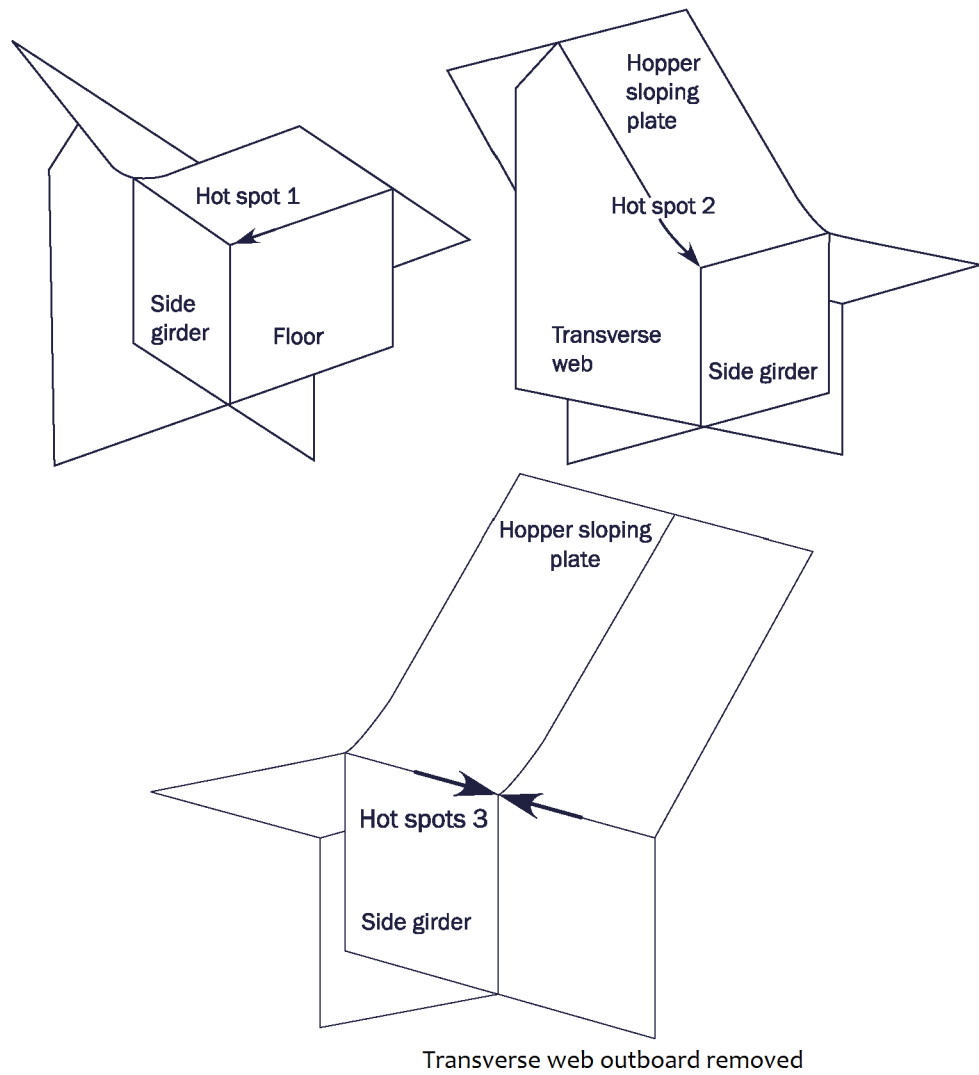


Figure 5 Hot spots for inner bottom plate of bent lower hopper tank knuckle

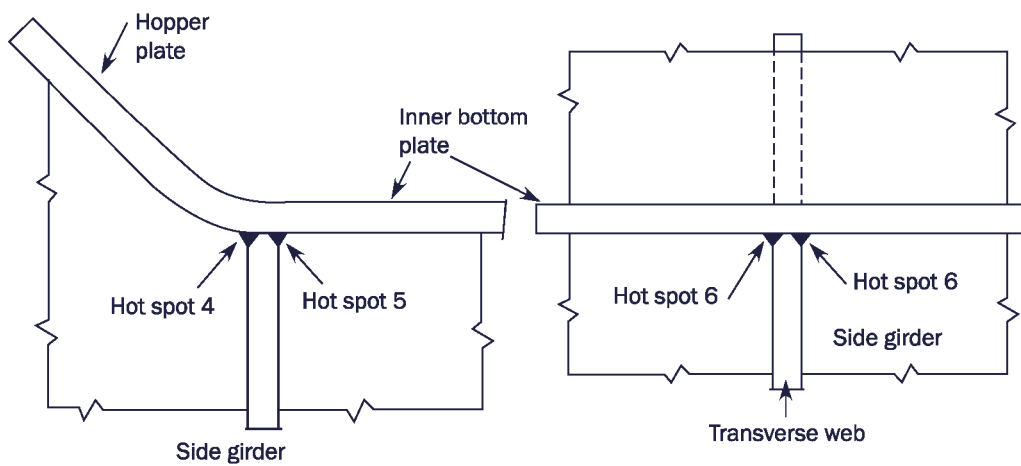


Figure 6 Hot spots for attached supporting girders of bent lower hopper tank knuckle

5 Derivation of stress concentration factors for alternative end connection designs

The structural stress concentration factors for alternative designs should be calculated by a FE hot spot model analysis according to [Sec.6](#). Additional procedure for derivation of geometrical stress concentration factors for stiffener end connections using FE hot spot model analysis are given below:

- a) FE model extent: The FE model, as shown in [Figure 10](#), should cover at least four web frame spacings in the longitudinal stiffener direction, and the considered detail should be located at the middle frame. The same type of end connection should be modelled at all the web frames. In the transverse direction, the model may be limited to one stiffener spacing (half stiffener spacing on each side). For L profiles, three stiffener spacings is regarded necessary to limit twisting, or alternatively coupling where the two longitudinal free plate edges should have the same rotation and displacement.
- b) Load application: In general, two loading cases should be considered:
 - axial loading by enforced displacement applied to the model ends
 - lateral loading by unit pressure load applied to the shell plating.
- c) Boundary conditions:
 - Symmetry conditions are applied along the longitudinal cut of the plate flange (T profiles and flat bars), and symmetry conditions along transverse and vertical cuts on web frames and on top of the web stiffener.
 - For lateral pressure loading: the model should be fixed in all degrees of freedom at both forward and aft ends as well as at the transverse cut at the top of the three web frames.
 - For axial loading: the model should be fixed for displacement in the longitudinal direction at the aft end of the model while enforced axial displacement is applied at the forward end, or vice versa.
- d) FE mesh density: At the location of the hot spots under consideration, the element size should be in the order of the thickness of the stiffener flange. In the remaining part of the model, the element size shall be in the order of $s/10$, where s is the stiffener spacing.

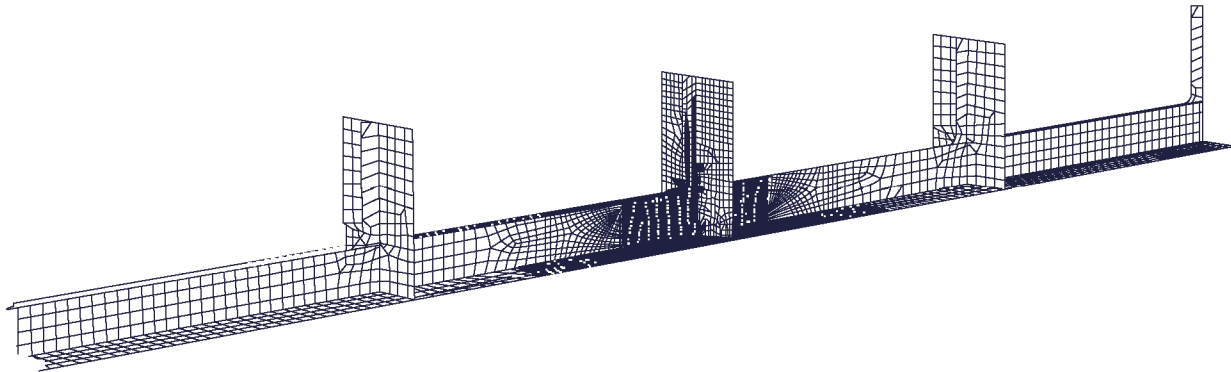


Figure 7 Fine mesh finite element model for derivation of geometrical stress concentration factors

For the two loading cases, the stress concentration factors are determined as follows:

$$K_a = \frac{\sigma_{HS,a}}{\sigma_{n,a}} \quad \text{for the axial loading case}$$

$$K_b = \frac{\sigma_{HS,b}}{\sigma_{n,b}} \quad \text{for the bending loading case}$$

- $\sigma_{HS,a}$ = Hot spot stress, in N/mm², determined at the stiffener flange for the axial displacement
- $\sigma_{n,a}$ = Nominal axial stress, in N/mm², calculated at the stiffener flange, based on a unit axial displacement applied at one end of the FE model
- $\sigma_{HS,b}$ = Hot spot stress, in N/mm², determined at the stiffener flange for the unit pressure load
- $\sigma_{n,b}$ = Nominal bending stress, in N/mm², calculated at the stiffener flange according to Sec.4 [6] in way of the hot spot for the unit pressure load applied to the FE model.

The nominal stress should be determined consistently with the expressions used to derive the nominal stress from beam theory to ensure consistency between the stress concentration factor and the prescriptive approach.

6 Verification of analysis methodology

The verification of the hot spot stress methodology based on hot spot FE models may be carried out for specific details with already derived target hot spot stress. Such details with target hot spot stress are shown in the commentary section of DNVGL RP 0005, *Fatigue design of offshore steel structures*.

APPENDIX F WORKMANSHIP AND LINK TO ANALYSIS PROCEDURES

1 Tolerance limits

The fatigue life of a detail depends on the workmanship in terms of geometrical imperfections, internal defects and external defects due to the welding process and surface preparation of base material and free plate edges.

Internal and external defects are weld toe undercuts, cracks, overlaps, porosity, slag inclusions and incomplete penetration. Geometrical imperfections are defined as axial misalignment (eccentricity), angular distortion, excessive weld reinforcement and otherwise poor weld shapes.

Following common workmanship practise, embedded internal defects like porosity and slag inclusion are less harmful for the fatigue strength compared to external defects.

[App.A](#) gives equations for calculation of K factors and FAT classes due to fabrication tolerances for misalignment of butt welds and cruciform joints, as well as effects of the local weld geometry. The default values for K factors and FAT classes including misalignments according to common workmanship standard are given in [App.A](#). Some default values are given in [Table 1](#). The S-N curves given in [Sec.2 \[2\]](#) include the effect of the notch at the weld or free plate edge as well as internal and external defects according to common workmanship standard.

If the fabrication tolerances, related to equations for misalignment in [App.A](#), are exceeded by poor workmanship or a higher workmanship standard is followed, modified K factors and FAT classes can be estimated. A higher workmanship standard may be difficult to achieve and follow up during production, and the Society may require additional documentation for acceptance of such a standard.

Table 1 Default fabrication tolerances

Type of imperfection	Type of imperfection	Embedded imperfection	Surface imperfection
Porosity, isolated ²⁾ max. pore diameter, d :min. distance to adjacent pore:	Internal and external defects	$t/4$, max. 4 mm $2.5d$	3 mm $2.5d$
Porosity, clustered ¹⁾ Max. pore diameter, d :max. length of cluster:	Internal defects	3 mm 25 mm	Not applicable
Slag inclusions ¹⁾⁽²⁾⁽³⁾ max. width: max. length:	Weld discontinuities	3.0 mm t , max. 25 mm	Not applicable
Undercut max. depth:(Smooth transition required)	Weld discontinuities	Not applicable	0.6 mm
Underfill ¹⁾⁽²⁾ max. depth: max. length:	Weld discontinuities	Not applicable	1.5 mm $t/2$
Excessive weld reinforcement ²⁾⁽⁴⁾ max. height:	Geometrical imperfections	Not applicable	$b/5$, max. 6 mm
Overlap ¹⁾⁽²⁾ max. length	Weld discontinuities	Not applicable	t
Cracks	Weld discontinuities	Not accepted	Not accepted
Lack of fusion	Weld discontinuities	Not accepted	Not accepted
Linear misalignment max. eccentricity, butt joints: max. eccentricity, cruciform joints:	Geometrical imperfections	Not applicable	See App.A Table 3 and App.A Table 8

Type of imperfection	Type of imperfection	Embedded imperfection	Surface imperfection
Angular misalignment max. distortion:	Geometrical imperfections	Not applicable	See App.A Table 3 and App.A Table 8
Incomplete penetration ¹⁾²⁾ max. length:max. height:	Weld discontinuities	t 1.5 mm	t $t/10$, max. 1.5 mm
<p>1) Defects on a line, where the distance between the defects is shorter than the longest defect, should be regarded as one continuous defect.</p> <p>2) t: Plate thickness of the thinnest plate in the weld connection.</p> <p>3) If the distance between parallel slag inclusions, measured in the transverse direction of the welding, is less than 3 times the width of the largest slag inclusion, the slag inclusions are regarded as one defect.</p> <p>4) b: Width of weld reinforcement.</p> <p>5) See ACS Rec. No. 47.</p> <p>6) See ISO 5817.</p>			

2 Weld profiling by machining and grinding

Weld profiling is referred to as profiling by machining or grinding. Profiling by welding is not considered efficient to improve the fatigue strength.

In design calculations, the thickness effect for cruciform joints, T-joints and transverse attachments may be reduced to an exponent $n = 0.15$, provided that the weld is profiled by either machining or grinding to a radius, R , of approximately half the plate thickness, $t/2$, with stress direction as shown in Figure 1.

When weld profiling is performed with geometric parameters are given in Figure 1, a reduced hot spot stress (or nominal stress at hot spot), σ_r , in N/mm², due to reduced notch stress can be calculated as:

$$\begin{aligned}\sigma_r &= \sigma_{membrane} \alpha + \sigma_{bending} \beta \\ \alpha &= 0.47 + 0.17(\tan\varphi)^{0.25} \left(\frac{t}{R}\right)^{0.5} \\ \beta &= 0.60 + 0.13(0.17)(\tan\varphi)^{0.25} \left(\frac{t}{R}\right)^{0.5}\end{aligned}$$

The local stress (hot spot stress or nominal stress at hot spot) should be separated into a membrane part and a bending part:

$$\sigma_{bending} = \sigma_{local} - \sigma_{membrane}$$

where:

- $\sigma_{membrane}$ = Stress in N/mm² at middle surface at location of the hot spot
- $\sigma_{bending}$ = Deduced bending stress component, in N/mm², at upper surface at location of the hot spot
- σ_{local} = Hot spot stress (or nominal stress at hot spot), in N/mm², at upper surface at location of hot spot.

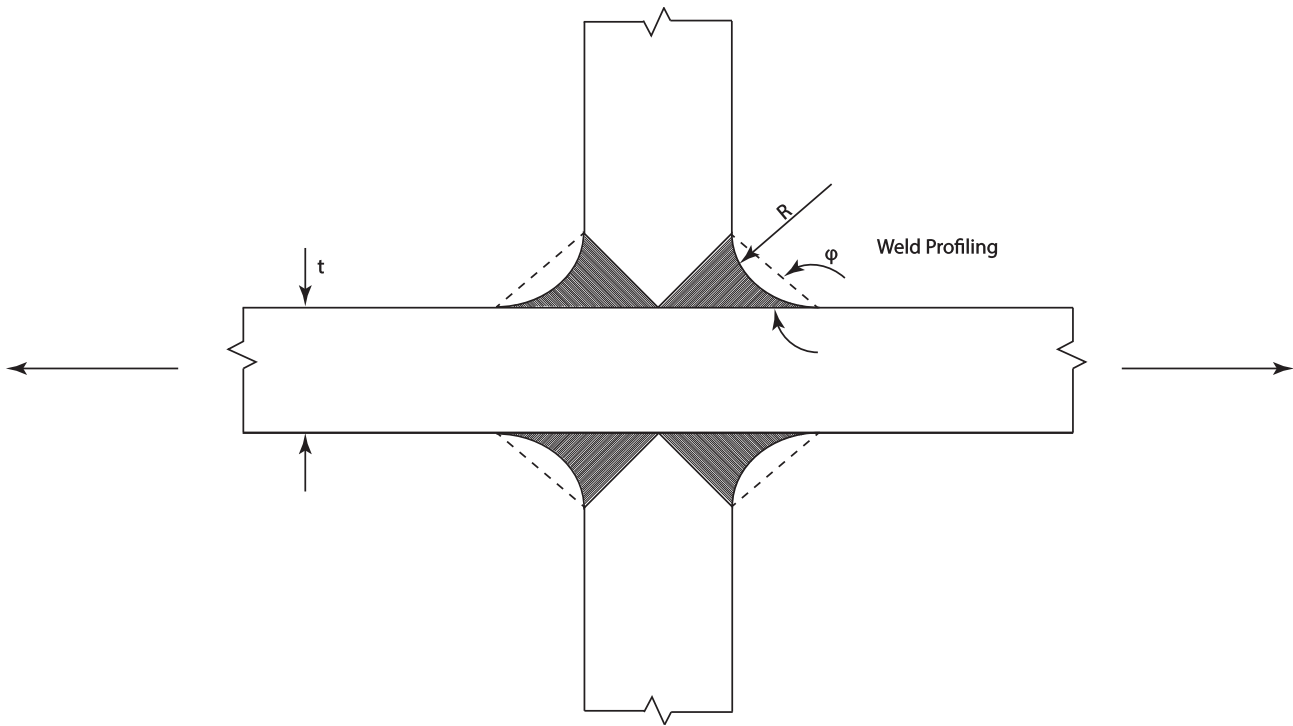


Figure 1 Weld profiling of load carrying and non-load carrying cruciform joints

3 TIG dressing

The fatigue life may be improved by TIG dressing as given in [Table 2](#). Due to uncertainties regarding quality assurance of the welding process, this method may not be recommended for general use at the design stage.

4 Hammer peening

The fatigue life may be improved by means of hammer peening as given in [Table 2](#). However, the following limitations apply:

- Hammer peening should only be used on members where failure will be without substantial consequences
- Overload in compression must be avoided, because the residual stress set up by hammer peening will be destroyed
- It is recommended to grind a steering groove by means of a rotary burr of a diameter suitable for the hammer head to be used for the peening. The peening tip must be small enough to reach weld toe.

Due to uncertainties regarding quality assurance of the process, this method is not recommended for use at the design stage.

5 Improvement factors for TIG dressing and Hammer peening

Improvement factor for toe grinding is given in [Sec.7 \[2\]](#), while improvement factors for TIG dressing and hammer peening are given in [Table 2](#). The factor assumes full effect of the post weld treatment method, but the acceptance of considering the full effect depends on agreement by the Society. The post weld treatment factor, f_w , can be estimated based on the improvement factor, f_T , as described in [Sec.3 \[2.4\]](#).

Table 2 Improvement factor on fatigue life^{1, 3, 4)}

<i>Improvement method</i>	<i>Minimum specified yield strength</i>	<i>Fatigue life improvement factor, f_T</i>
TIG dressing	Less than 350 N/mm ²	0.01 R_{eH}
	Higher than 350 N/mm ²	3.5
Hammer peening ²⁾	Less than 350 N/mm ²	0.011 R_{eH} for constant amplitude loading
	Higher than 350 N/mm ²	4.0

1) The improvement is only valid for high cycle fatigue where the slope m of the S-N curve is increased. This is represented by the improvement factor on the fatigue life. Alternatively, the fatigue life can be assessed by using S-N curves representing the improved state, when available.

2) The improvement effect depends on the tool used and workmanship. If lacking experience with respect to hammer peening, it is recommended to perform fatigue testing of relevant detail (with and without hammer peening) before a factor on improvement is decided

3) The technique are normally not accepted for ships

4) The improvement factor can not be claimed in addition to improvement factor for any form of grinding

APPENDIX G UNCERTAINTIES IN FATIGUE LIFE PREDICTIONS

1 Introduction

There are a number of uncertainties associated with fatigue life predictions. These uncertainties are related to both the wave loading and to the fatigue capacity.

Fatigue damage is proportional to stress raised to the power of the inverse slope, m , of the S-N curve, i.e. a small change in the stress results in a much greater change in the fatigue life. Special attention should therefore be given both to stress raisers from workmanship and to the loading.

There is a large uncertainty associated with the determination of S-N curves. The scatter in the test results, which form the basis for the S-N curves, is related to the variation of the fabrication quality. The ratio between calculated fatigue lives based on the mean S-N curve and the mean minus two standard deviations S-N curve is significant as shown in [Figure 1](#). The latter is used for design.

There is also uncertainty associated with the determination of the stress concentration factor. The error introduced in the calculated fatigue life by wrong selection of the stress concentration factor is indicated in [Figure 2](#).

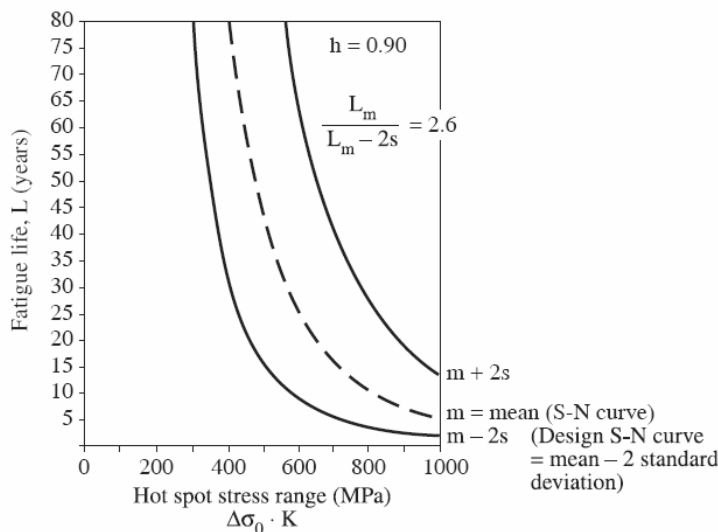


Figure 1 Fatigue life influence of stress level and S-N data for welded connections

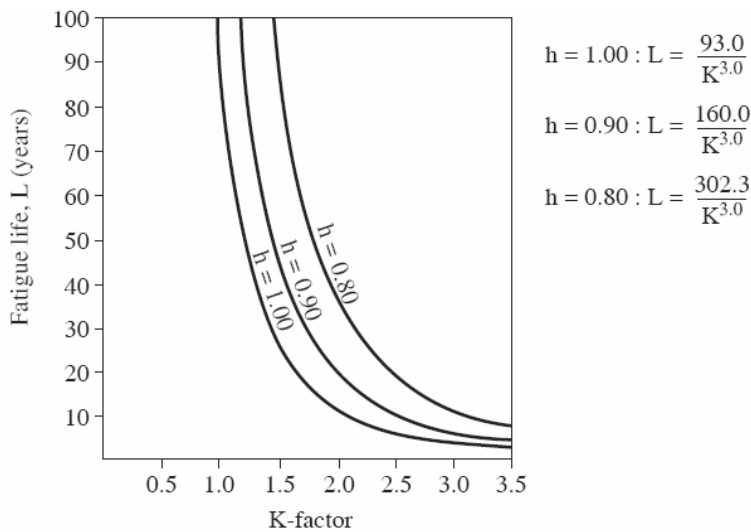


Figure 2 Fatigue life sensitivity to stress concentration factor K and Weibull shape factor ξ

2 Probability of fatigue failure

A high predicted fatigue life is associated with a reduced probability of fatigue failure, see [Figure 3](#). It may reduce the need for in-service inspection. A high calculated fatigue life means that the accumulated fatigue damage occurring during the service life is in the left part of [Figure 3](#).

Reliability methods may be used to illustrate the effect of uncertainties on the probability of a fatigue failure. Reference is made to [Figure 4](#), which shows accumulated probability of a fatigue failure as function of years in service for different assumptions of uncertainty in the input parameters. The left part of [Figure 4](#) corresponding to the first 20 years service life is shown in [Figure 5](#).

[Figure 3](#) and [Figure 4](#) shows accumulated probability of fatigue failure for uncertainty in S-N data corresponding to a standard deviation of 0.20 in log N scale. A normal distribution in logarithmic scale is assumed. The uncertainty in the Miner summation assumed log-normal distributed with median 1.0 and CoV (Coefficient of Variance) equal to 0.3 (30%). Uncertainties to the load and response are assumed normal distributed with CoV_{nom} equal 15-20%, and hot spot stress derivation is assumed normal distributed with CoV_{hs} equal 5-10%.

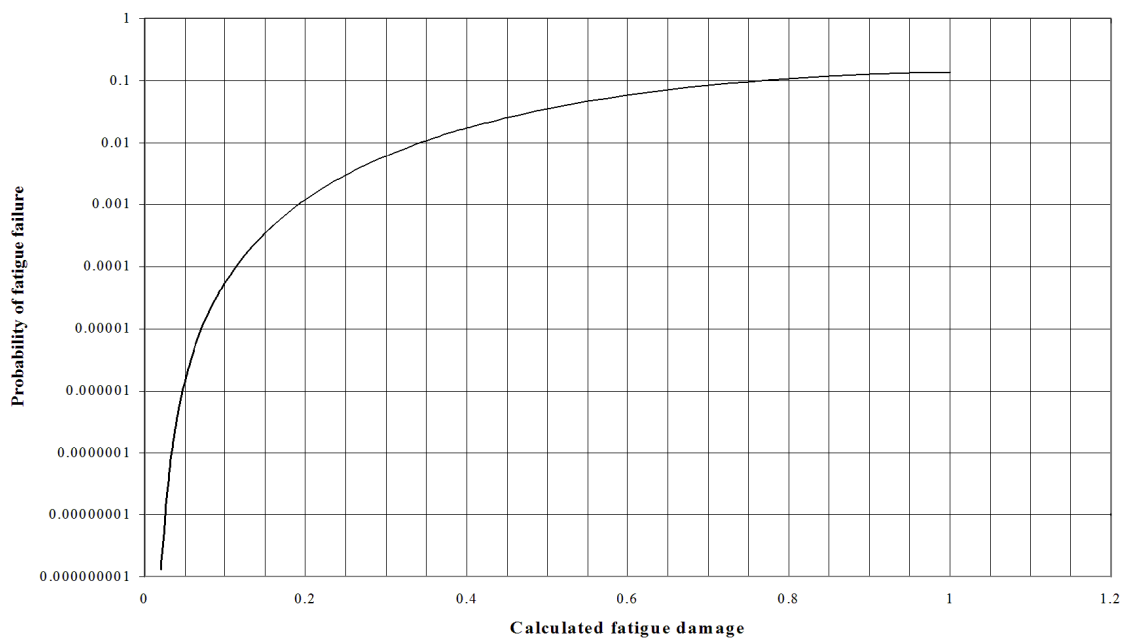


Figure 3 Calculated probability of fatigue failure as function of calculated damage

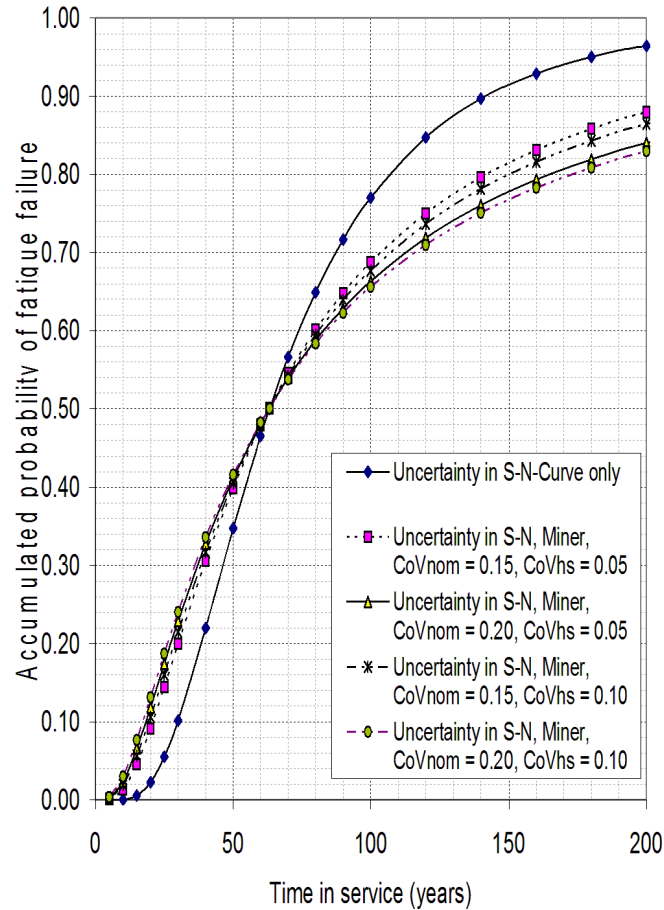


Figure 4 Accumulated probability of fatigue crack as function of service life for 20 years design life

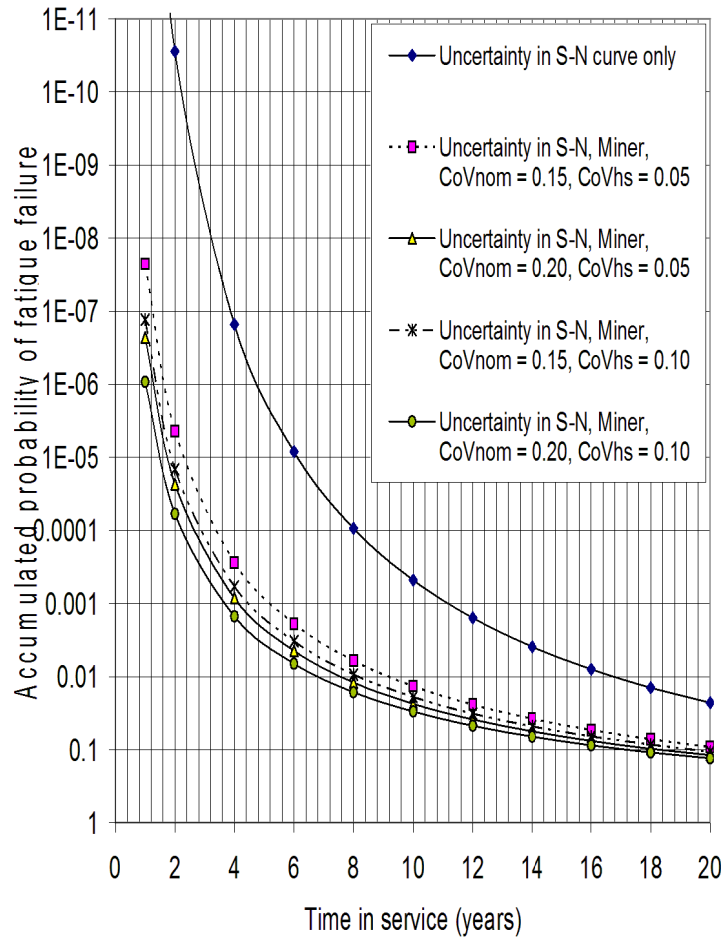


Figure 5 Accumulated probability of fatigue crack as function of service life for 20 years design life (left part from Figure 3)

3 Size of defects inherent in S-N data and requirements to non-destructive examination

Most fatigue cracks are initiated from undercuts at weld toes. There can be different reasons for undercuts. It is recommended to prepare a good welding procedure to avoid large undercuts during production welding. No undercut is included in S-N curves better than D (FAT 90) or where the hot spot curve D is associated with a K factor less than 1.0. Maximum allowable size of undercuts equal to 0.5 mm in depth may be considered inherent in the different design S-N classes D, E and F (FAT 90 to FAT 71). For stricter S-N curves (FAT below 71) an undercut equal to 1.0 mm may be accepted.

The weld details can be subjected to larger stress ranges when better S-N curves are used. Butt welds with lower K factors (higher FAT classes) are more critical with respect to internal defects than many other details. Planar defects like cracks and lack of fusion are not allowed. It should be noted that use of S-N curves better than D (K factor below 1 or FAT class above 90) imply special consideration with respect to requirements to NDE and acceptance criteria. Thus, the requirements in ISO 5817 are not strict enough for details belonging

to S-N class better than D. Reference is made to NORSO M-101 and ISO 5817 regarding requirements to volumetric defects like porosity and slag inclusions.

An example of crack growth through a plate thickness of 25 mm based on an initial maximum surface defects are shown in [Figure 6](#) based on different S-N curves. A semi-elliptic surface defect is assumed with half axes $a/c = 0.2$ (a = crack depth, c = crack half width). This calculation is based on a Weibull long term stress range distribution with 10^8 cycles during a life time of 20 years. The shape parameter is $\xi = 1.0$ and the scale parameter is determined such that the accumulated Miner damage is equal 1.0 during the life time of the structure. It is observed that larger surface defects can be accepted for S-N curve F ($K = 1.27/\text{FAT 71}$) as compared with that of D ($K = 1.0/\text{FAT 90}$) and C ($K = 0.8/\text{FAT 112}$). In [Figure 6](#) the initial crack depths are estimated to 1.28 mm for F, 0.23 mm for D and 0.37 mm for C. The reason for the low value for the S-N curve D as compared with C, is the notch effect at the weld toe which is not present for a machined ground flush surface, C. The situation becomes different for internal defects where only very small defects are acceptable for a C class due to high stresses inside the weld.

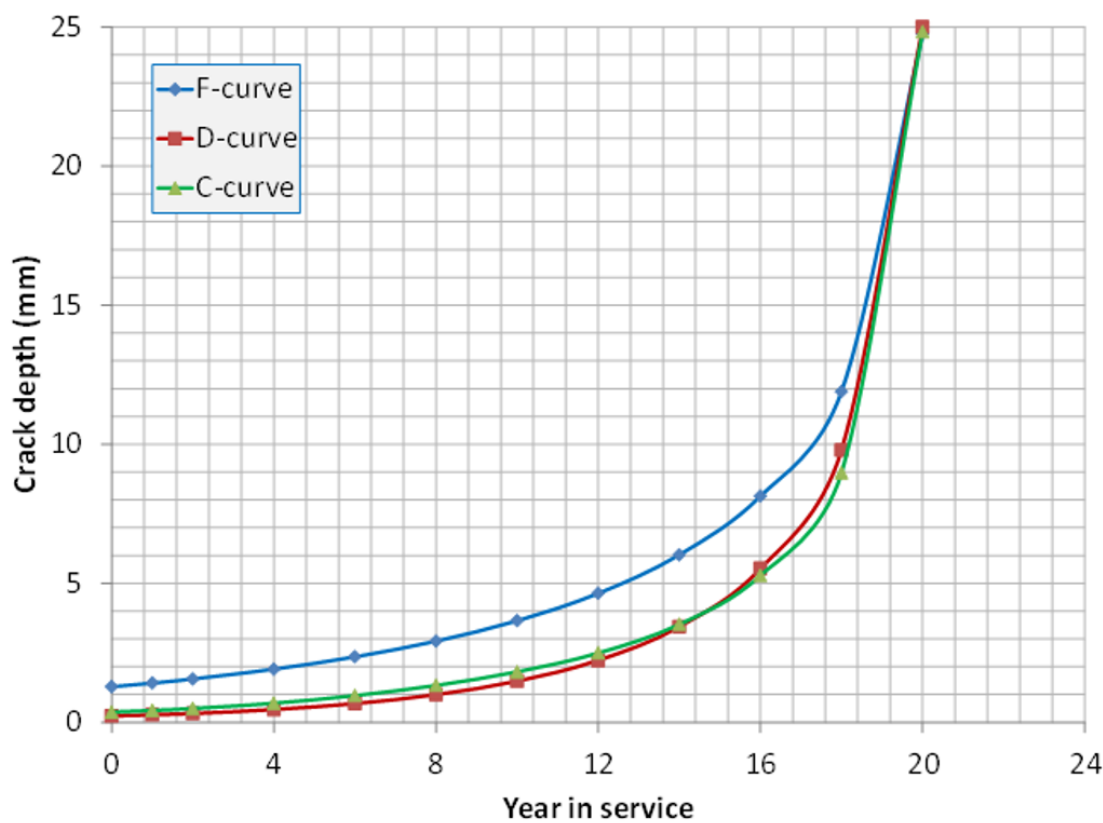


Figure 6 Crack growth development from maximum surface defects in some different S-N classes

APPENDIX H LOW CYCLE FATIGUE

1 General

The low cycle fatigue (LCF) procedure is based on frequent loading and unloading cycles. The procedure is based on the required design life, T_D . If extended design fatigue life, T_{DF} , is required, the number of static cycles and dynamic cycles, inducing high cycle fatigue (HCF), should be adjusted accordingly.

Details will experience static and dynamic loads during their life time. Fatigue strength of details may be required based on HCF loads. Even though HCF has been checked at the design stage, some cracks have been reported within few years of operation. For such cases, LCF due to repeated yielding in compression and tension have been the cause.

LCF strength should be assessed for highly stressed locations under cyclic static loads, as repeated yielding can cause cracks and/or paint cracks at hot spots even though the dynamic stress is low.

A fatigue life in low cycle high stress region is expressed in terms of the total strain range, rather than the stress range. An approach based on the pseudo-elastic hot spot stress range is adopted. This approach is compatible with the hot spot strain range approach, as total strain is converted to pseudo-elastic stress range by using a plasticity correction factor.

An S-N curve approach in the LCF region, below 10000 design cycles is used.

The following locations may be vulnerable in view of LCF.

- Web stiffener on top of inner bottom longitudinal and hopper slope longitudinals when wide frame space is employed
- Web-frame hotspots at the stiffener-frame connections in areas of high girder shear stress or where web stiffener is not fitted on top of longitudinal flange
- Heel and toe of horizontal stringer of transverse bulkhead for frequent alternate loading
- Inner bottom connection to transverse bulkhead for frequent alternate loading
- Lower stool connection to inner bottom for a loading condition with one side tank empty and the other tank full
- Any other locations under repeated high static stress ranges.

The procedure is developed for the LCF assessment with the following limitations:

- new building of steel ship structures
- steel materials with yield stress less than 355 N/mm^2
- same LCF performance for base metal and welded joints
- the maximum principal stress direction does not change for a load condition.

The procedure describes how to calculate combined fatigue damage due to LCF and HCF for free plate edges and welded details. The combined fatigue damage due to HCF and LCF should be below acceptable limits. The simplified LCF procedure is shown in [Figure 1](#).

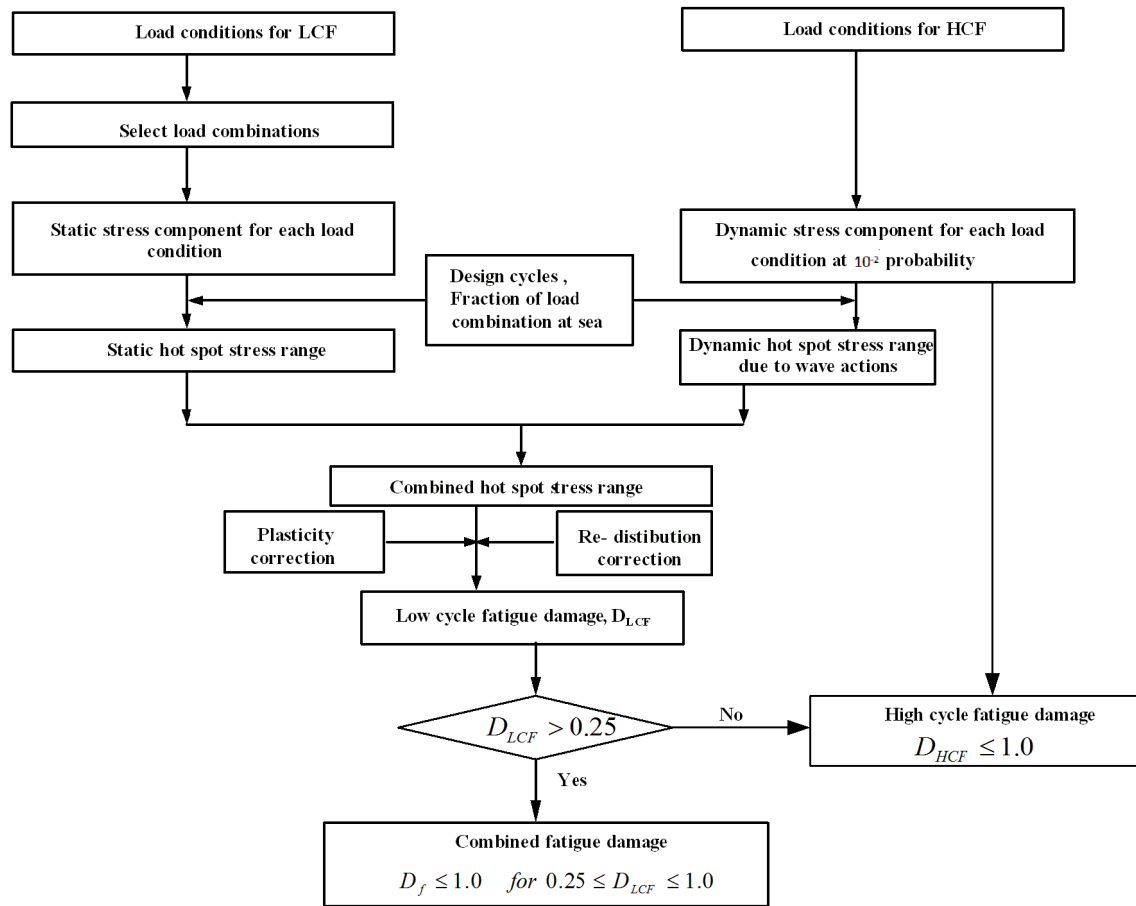


Figure 1 Assessment procedure for low cycle fatigue

Stress components for LCF can be obtained from beam theory with known K factors or by hot spot FE analysis for welded details or local FE analysis for free plate edges according to [Sec.6](#). The calculated stress ranges for LCF should be corrected by using a plasticity correction factor in order to employ S-N curves instead of a strain-cycle curve.

2 Number of static design cycles and fraction in different loading conditions

The number of design cycles depends on the ship type, trade and design fatigue life, T_{DF} . The design cycles in [Table 1](#) should be used unless otherwise described, and is referring to $T_D = 25$ years.

Table 1 Design cycles for low cycle fatigue, n_{LCF}

Ship type	Design cycle, n_{LCF}
Tankers over 120 000 TDW	500
Tankers below 120 000 TDW	600
Chemical tankers	1000

<i>Ship type</i>	<i>Design cycle, n_{LCF}</i>
LNG carriers	1000
LPG carriers	1000
Over Panamax bulk carriers	500
Panamax bulk carriers	800
Handymax bulk carriers, about 45 000 TDW or smaller	1000
Shuttle tankers	1200

For vessels to be operated with frequent loading and unloading cycles, the design cycle may be increased, but need not be greater than 1 500 cycles for shuttle tankers, chemical tankers and Handymax bulk carriers, and 1 000 cycles for the other vessel types, respectively.

The fraction, α_k , of load combination at sea is given in [Table 2](#).

Table 2 Fraction of load combination at sea for low cycle fatigue

<i>Ship type</i>	<i>Fraction of load combinations, α_k</i>	
	<i>Full load-Ballast, L₁</i>	<i>Alternate LCs, L₂</i>
Tankers over 120 000 TDW	0.90	0.10
Tankers below 120 000 TDW	0.85	0.15
Chemical tankers	0.80	0.20
LNG carriers	1.00	0.00
LPG carriers	0.85	0.15
Over Panamax bulk carriers	0.90	0.10
Panamax bulk carriers and smaller	0.85	0.15
Ore carriers	0.85	0.15
Shuttle tankers	1.00	0.00

3 Loading conditions

3.1 Combination of static stress

Load conditions should be selected to obtain the static stress for each load condition and the stress range from combination of those. [Figure 2](#) and [Figure 3](#) show possible loading and unloading scenarios of a vessel during a round trip. The following two stress ranges should be taken into account at the design stage:

$$\Delta\sigma_{LCF}^1 = |\sigma^{full} - \sigma^{ballast}| \quad \text{for full load and ballast}$$

$$\Delta\sigma_{LCF}^2 = |\sigma^{alt1} - \sigma^{alt2}| \quad \text{for alternate conditions}$$

Other possible load combinations, e.g. full load to alternate or ballast to alternate, can be disregarded.

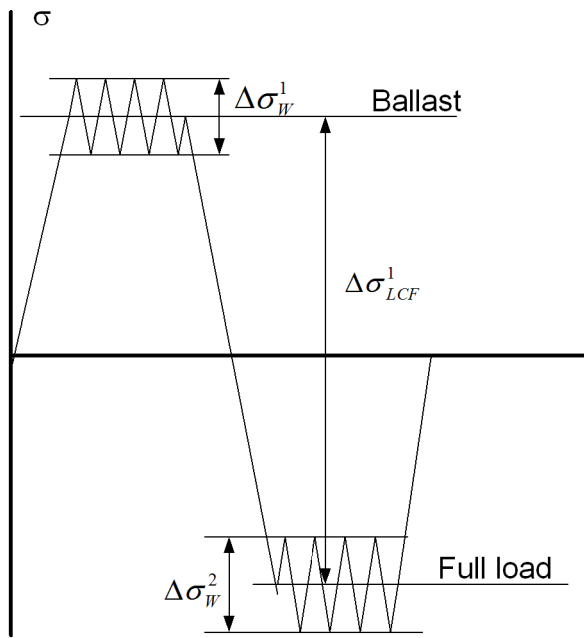


Figure 2 Operation scenarios, full load - ballast

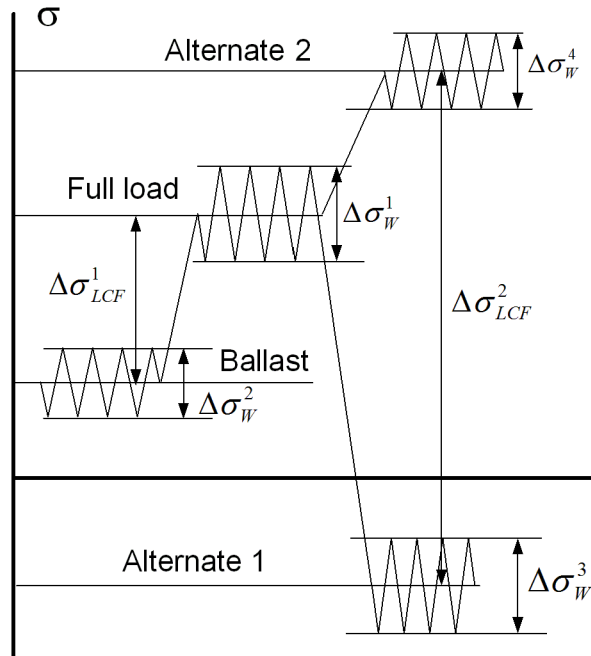


Figure 3 Operation scenarios, ballast - full load - alternate load conditions

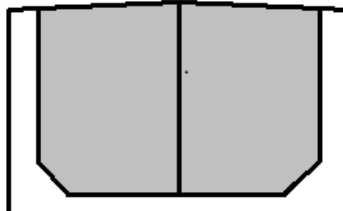
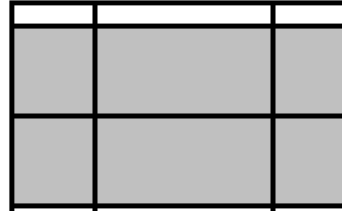
The static hot spot surface stress range or local stress range for free plate edge for low cycle fatigue should be obtained from a combination of load conditions as shown in [Table 3](#), [Table 4](#) and [Table 5](#).

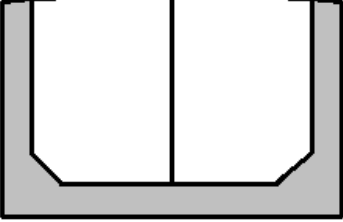
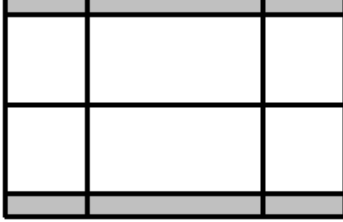
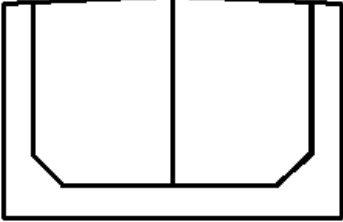
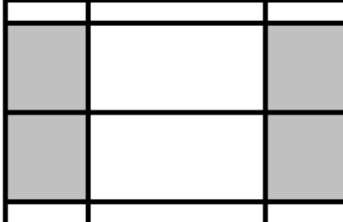
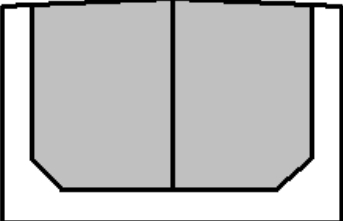
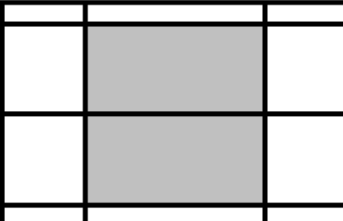
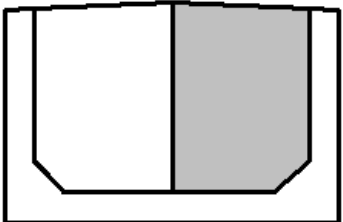
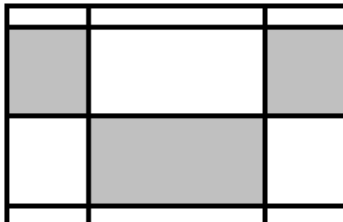
Table 3 Load combination for calculation of low cycle fatigue stress range, $\Delta\sigma_{LCF}$

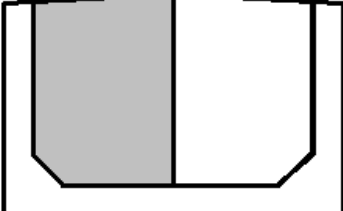
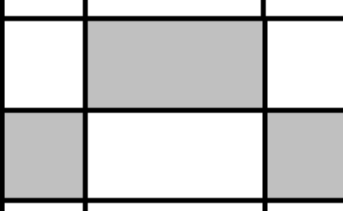
Location	Load conditions	Tankers with centreline longitudinal bulkhead	Tankers with two longitudinal bulkheads	Vessels without longitudinal bulkhead
Longitudinal flange connections *)	Full load -ballast	$ \sigma_{LC1}-\sigma_{LC2} $	$ \sigma_{LC7}-\sigma_{LC8} $	$ \sigma_{LC13}-\sigma_{LC14} $
Web stiffener on top of longitudinal stiffener	Full load -ballast	$ \sigma_{LC1}-\sigma_{LC2} $	$ \sigma_{LC7}-\sigma_{LC8} $	$ \sigma_{LC13}-\sigma_{LC14} $
Transverse members welded to longitudinals in water ballast tanks, i.e. web stiffener, cut out, lug plate	Full load -ballast	$ \sigma_{LC1}-\sigma_{LC2} $	$ \sigma_{LC7}-\sigma_{LC8} $	$ \sigma_{LC13}-\sigma_{LC14} $
Lower and upper hopper knuckles, lower and upper chamfers ¹⁾	Full load -ballast	$ \sigma_{LC1}-\sigma_{LC2} $	$ \sigma_{LC7}-\sigma_{LC8} $	$ \sigma_{LC13}-\sigma_{LC14} $
Horizontal stringer at inner side longitudinal bulkhead ¹⁾	Full load -ballast	$ \sigma_{LC1}-\sigma_{LC2} $	$ \sigma_{LC7}-\sigma_{LC8} $	$ \sigma_{LC13}-\sigma_{LC14} $
	Alternate load	$ \sigma_{LC3}-\sigma_{LC4} $	$ \sigma_{LC9}-\sigma_{LC10} $	$ \sigma_{LC15}-\sigma_{LC16} $
Girder connection to transverse bulkhead, inner bottom to lower stool, inner bottom to cofferdam bulkhead ¹⁾	Full load -ballast	$ \sigma_{LC1}-\sigma_{LC2} $	$ \sigma_{LC7}-\sigma_{LC8} $	$ \sigma_{LC13}-\sigma_{LC14} $
	Alternate LCs 1 -2	$ \sigma_{LC3}-\sigma_{LC4} $	$ \sigma_{LC9}-\sigma_{LC10} $	$ \sigma_{LC15}-\sigma_{LC16} $
¹⁾ hull girder stress should be added to the local bending stress for the corresponding load condition in the trim and stability booklet.				

The load conditions in [Table 4](#) may be applied to vessels with a centreline bulkhead. Normal ballast condition shall be used for ballast condition. Actual draft for the alternate conditions, T_{act} , shall be obtained from the loading manual.

Table 4 Load conditions for vessels with a centreline bulkhead

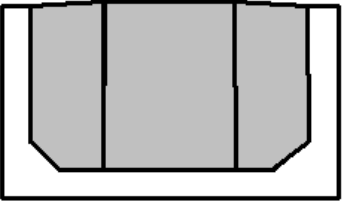
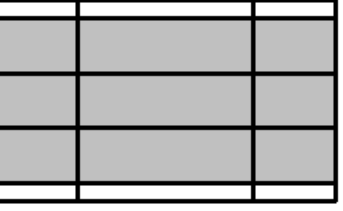
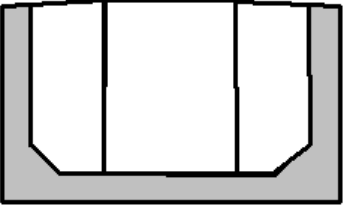
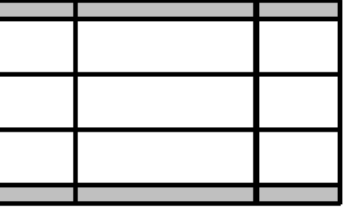
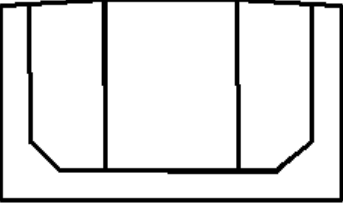
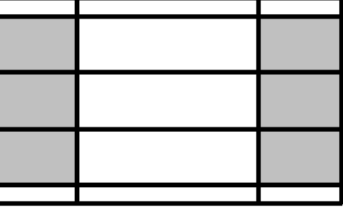
Load case	Stress component	Midship section view	Plan view
LC1	Full load, T_{SC} , σ_{LC1}		

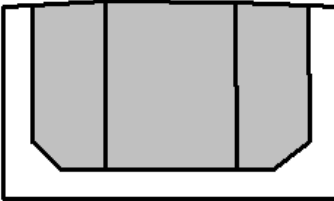
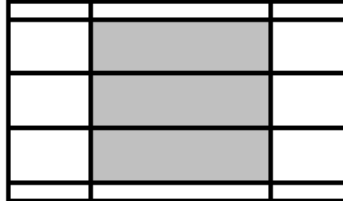
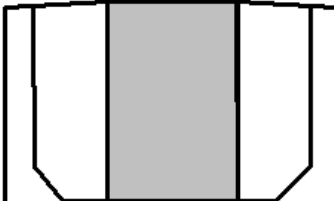
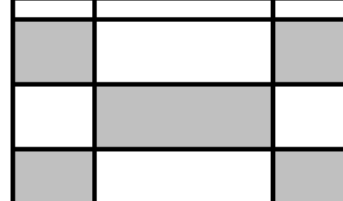
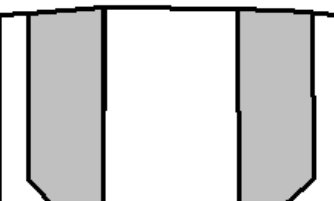
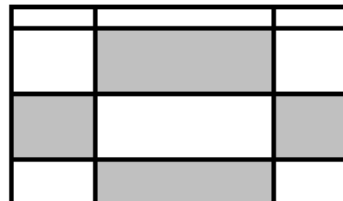
<i>Load case</i>	<i>Stress component</i>	<i>Midship section view</i>	<i>Plan view</i>
LC2	Ballast, T_{BAL} , $\sigma_{LC\ 2}$		
LC3	Alternate 1, T_{act} , $\sigma_{LC\ 3}$		
LC4	Alternate 2, T_{act} , $\sigma_{LC\ 4}$		
LC5	Alternate 3, T_{act} , $\sigma_{LC\ 5}$		

Load case	Stress component	Midship section view	Plan view
LC6	Alternate 4, $T_{act}, \sigma_{LC\ 6}$		

The load conditions in [Table 5](#) may be applied to vessels with two longitudinal bulkheads. As the load combination between load conditions LC5 and LC6 and between load conditions LC11 and LC12 is not common, the combinations are neglected at the design stage.

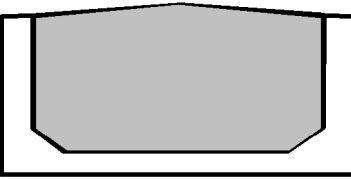
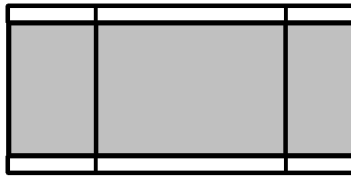
Table 5 Load conditions for vessels with two longitudinal bulkheads

Load case	Stress component	Midship section view	Plan view
LC7	Full load, T_{SC} , $\sigma_{LC\ 7}$		
LC8	Ballast, T_{BAL} $\sigma_{LC\ 8}$		
LC9	$T_{act}, \sigma_{LC\ 9}$		

LC10	$T_{act}, \sigma_{LC\ 10}$		
LC11	$T_{act}, \sigma_{LC\ 11}$		
LC12	$T_{act}, \sigma_{LC\ 12}$		

The load conditions in [Table 6](#) may be applied to vessels without longitudinal bulkhead, e.g. LNG carriers, bulk carriers, ore carriers, etc.

Table 6 Load conditions for vessels without longitudinal bulkhead

Load case	Stress component	Midship section view	Plan view
LC13	Full load, T_s $\sigma_{LC\ 13}$		

LC14	Ballast, T_{ball} , $\sigma_{LC\ 14}$		
LC15	T_{actr} , $\sigma_{LC\ 15}$		
LC16	T_{actr} , $\sigma_{LC\ 16}$		

3.2 Pressure loads

Stresses contributed from both external pressure from sea water and internal pressure from both cargo and ballast water should be considered. The calculation and establishment of external and internal dynamic pressures on 10^{-2} probability level of exceedance are given by the rules.

The static external pressure is calculated based on the draft as specified in [Table 4](#) to [Table 6](#) and according to the loading manual. The static internal pressure is calculated based on actual filling height and cargo density, which can be obtained from the loading manual and the rules. The static internal pressure should be established according to the loading conditions defined in [Table 4](#) to [Table 6](#).

4 Simplified calculations of stresses

4.1 Hot spot stress range due to wave loading

Where the principal stress direction for LCF is the same as for HCF, the following procedure may be used. The maximum expected stress range from the wave loading in the period between the loading and unloading operations should be added to the low cycle stress range before the fatigue damage from LCF is calculated.

The hot spot stress range or local stress at free edge plate, $\Delta\sigma_j$, in N/mm², at a probability of exceedance of $n_{LCF}/10^8$ from the wave loading can be calculated as:

$$\Delta\sigma_j = \Delta\sigma_{HCF,j} \cdot \left(\frac{\log n_0}{\log 100} \right)^{1/\xi} \left(1 - \frac{\log n_{LCF}}{\log n_0} \right)^{1/\xi} \quad (1)$$

where:

- $\Delta\sigma_{HCF,j}$ = High cycle fatigue stress range for hot spot or local stress at free plate edge corresponding to 10^{-2} probability level for the loading condition j
 n_0 = number of cycles, 10^8 .

4.2 Hot spot stress range for low cycle fatigue

The static elastic hot spot stress range (or local stress for free plate edge) for the load combination k for LCF calculations is the difference between the hot spot stress (or local stress for free plate edge) components for loading condition i and j .

$$\Delta\sigma_{LCF}^k = |\sigma_s^i - \sigma_s^j|$$

where:

- $\Delta\sigma_{LCF}^k$ = static hot spot stress range for the load combination k given in Table 3
 σ_s^i = static hot spot stress amplitude for loading condition i
 σ_s^j = static hot spot stress amplitude for loading condition j.

4.3 Combined hot spot stress range

The combined stress range for LCF, representing a peak to peak stress due to loading and unloading and wave loading, is given as:

$$\Delta\sigma_{comb}^k = \Delta\sigma_{LCF}^k + 0.5 \cdot (\Delta\sigma_i + \Delta\sigma_j)$$

where:

- $\Delta\sigma_i$ = Wave stress range at probability of $n_{LCF}/10^8$ for loading condition i
 $\Delta\sigma_j$ = Wave stress range at probability of $n_{LCF}/10^8$ for loading condition j.

The effective pseudo stress range for calculation of LCF damage for the loading combination k can be obtained as:

$$\begin{aligned}\Delta\sigma_{eff}^k &= \lambda_n \cdot \Delta\sigma_{comb}^k \\ \lambda_n &= k_e \cdot \psi\end{aligned}$$

where:

λ_n = Non-linearity correction factor

k_e = Plasticity correction factor

= 1.0

for

$$\frac{\Delta\sigma_{comb}}{R_{eH}} \leq 2.0$$

$$= \max \left\{ \begin{array}{l} 1.0; \\ a \cdot \Delta\sigma_{comb} \cdot 10^{-3} + b \end{array} \right\} \quad \text{for} \quad \frac{\Delta\sigma_{comb}}{R_{eH}} > 2.0$$

Ψ = Factor due to stress redistribution

$$\begin{aligned} &= 1.0 && \text{if} && \frac{\Delta\sigma_{comb}}{R_{eH}} \leq 2.0 \\ &= 0.9 && \text{for VL A-E if} && \frac{\Delta\sigma_{comb}}{R_{eH}} > 2.0 \\ &= 0.8 && \text{for VL A-E32 or VL A-E36 steel} && \frac{\Delta\sigma_{comb}}{R_{eH}} > 2.0 \\ &&& \text{if} && \end{aligned}$$

Coefficients for the plasticity correction factor, a and b are given in [Table 7](#).

Table 7 Plasticity correction factor, k_e

Stress range	$\frac{\Delta\sigma_{comb}}{R_{eH}} > 2.0$
VL A-E steel	$a = 1.16$ $b = 0.524$
VL A-E32 and VL A-E36 steels	$a = 1.0$ $b = 0.53$

The combined stress ranges should be derived from the linear elastic analysis. The hot spot stress range (or local stress range at free plate edge) contributing to LCF is large and implies local yielding. Thus, a correction of the elastic stress range is needed in order to derive a stress range that is representative for the actual strain range taking the non-linear material behaviour into account.

4.4 Plasticity correction factor

The plasticity correction factor can be obtained from an actual cyclic stress-strain curve and Neuber's rules or non-linear FE analysis, as shown in [Figure 4](#).

$$k_e = \frac{\sigma_{pseudo}}{\sigma_{elastic}}$$

where:

- $\sigma_{elastic}$ = Elastic hot spot stress (or local stress at free plate edge), in N/mm², obtained from linear elastic FE analysis or a beam theory
- σ_{pseudo} = Pseudo linear elastic hot spot (or local stress at free plate edge), in N/mm²
- = $E \cdot \epsilon_{hs}$

For more complex structural connections only part of the region around the hot spot (or local stress area at the free plate edge) will be yielding when subjected to large dynamic loads. This can be accounted for by a

factor accounting for redistribution of stress and strain. Based on non-linear FE analysis of actual connections a redistribution factor may be introduced.

In order to obtain the plasticity correction factor, a cyclic stress-strain curve for materials should be obtained from tests.

If the cyclic stress-strain relation is combined with the Neuber's rule, the Neuber's formula is given using the Ramberg-Osgood relation as:

$$\frac{\sigma_n^2 \cdot K^2}{E} = \frac{\sigma_{hs}^2}{E} + \sigma_{hs} \cdot \left(\frac{\sigma_{hs}}{K} \right)^{1/n}$$

where:

K = stress concentration factor

σ_{hs} = the actual stress in the hot spot (or local stress at free plate edge), in N/mm², to be based on non-linear FE analysis (hence, it should not be based on nominal stress from linear FE times a K factor, but taken from a curve as illustrated in [Figure 4](#))

ε_{hs} = the actual strain in the hot spot (or local stress at free plated edge)

E = Young's modulus, in N/mm²

n, K' = material coefficients.

K depends on the magnitude of the load and the sharpness of the notch. Coefficients n and K' are given in [Table 8](#) for different steel grades used for derivation of the plasticity correction factors.

Neuber's rule is widely used to obtain the plasticity correction factor, since it may give conservative results. If the plane strain behaviour is relevant, the Glinka rule may be used for derivation of the plasticity correction factor instead of the Neuber's rule.

Table 8 Material properties for cyclic stress-strain curves

Material	VL A-E	VL A-E32	VL A-E36
K' , in N/mm ²	602.8	678.3	689.4
n	0.117	0.111	0.115

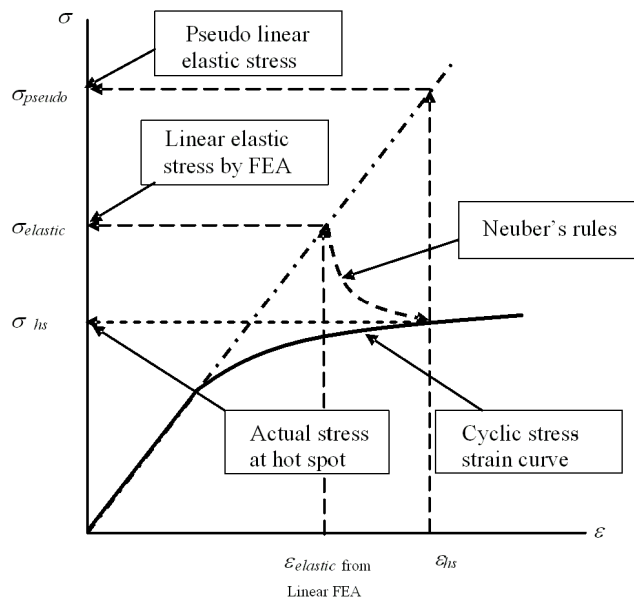


Figure 4 Definition of stresses and strains

4.5 Total elastic stress component

The elastic static hot spot stress amplitude due to static hull girder and pressure loads, [4.2], and the elastic dynamic hot spot stress amplitude at $n_{LCF}/10^8$ probability level due to wave actions during loading and unloading, [4.1], are established by use of beam theory or FE analysis, as listed in Table 9. The relevant pressure and girder loads are given in the rules. The dynamic stress components due to local and global loads should be combined to a total dynamic stress range.

Table 9 Stress models for elastic hotspot stress at LCF vulnerable location

Location	Stress approach
Longitudinal flange connection	Prescriptive stress analysis according to Sec.4
Web stiffener on top of longitudinal stiffener	Semi-nominal stress model according to DNVGL-CG-0152 Plus - Extended fatigue analysis of ship details
Transverse members welded to longitudinals in water ballast tanks, i.e. cut-outs, lug plate	Semi-nominal stress model according to DNVGL-CG-01520152 Plus - Extended fatigue analysis of ship details
Lower and upper hopper knuckles, lower and upper chamfers	Hot spot or local stress model according to Sec.6.
Horizontal stringer at inner side longitudinal bulkhead	Hot spot or local stress model according to Sec.6.
Girder connection to transverse bulkhead, inner bottom to lower stool, inner bottom to cofferdam bulkhead	Hot spot or local stress model according to Sec.6.

5 Fatigue damage calculations for low cycle fatigue

A one-slope S-N curve (upper part of two slope S-N curves) for LCF strength is given as follows:

$$\log N_k = \log \bar{\alpha} - m \cdot \log \Delta\sigma_{eff}^k$$

N_k = Number of cycles to failure for LCF stress range

$\Delta\sigma_{eff}^k$ = Effective stress range, in N/mm², for the loading combination k.

The basic S-N curve for low cycle fatigue assessment is given in [Table 10](#). This design S-N curve is applicable to both welded joints and free plate edges for the LCF region. The damage due to the LCF is calculated as:

$$D_{LCF} = \sum_1^{n_{LC}} \alpha_k \cdot D_{LCF}^k = \sum_1^{n_{LC}} \alpha_k \cdot \frac{n_{LCF}}{N_k}$$

where:

n_{LC} = Total number of design load condition

α_k = Fraction of load combinations, see [Table 2](#).

If a non-linear FE analysis is carried out directly, the effective pseudo-elastic hot spot stress amplitude can be obtained by multiplying the Young's modulus by the calculated notch strain amplitude.

Table 10 Low cycle fatigue S-N curve

Material	$10^2 \leq N < 10^4$	
	$\log K_2$	m
Welded joints & free plate edge	12.164	3.0

6 Correction of the damage or stress

Net or gross scantlings, t , should be used according to the rules for the specific ship type with the consistent scantlings approach factor, f_c , when based on FE analysis.

S-N curve in air should be used for the entire design fatigue life.

The thickness effect is not accounted for when evaluating the LCF damage.

No mean stress effect should be considered for free plate edges and welded details for the LCF damage.

No environmental reduction factor, f_e , should be considered for evaluation of the LCF damage.

Benefit of weld improvement methods like grinding, hammer-peening and TIG-dressing should not be applied.

The fabrication tolerances given in [App.A](#) are assumed applicable.

7 Combined fatigue damage due to high and low cycle fatigue

When $D_{LCF} \geq 0.25$, the combined damage ratio due to HCF and LCF is compared to the acceptance criteria as:

$$D_f = \sqrt{D_{HCF}^2 + \left(\frac{D_{LCF} - 0.25}{0.75} \right)^2} \leq 1.0 \quad \text{for } 0.25 \leq D_{LCF} \leq 1.0$$

where:

D_{HCF} = Damage due to HCF for the design life = 25 years

D_{LCF} = Damage due to LCF based on the design cycles, not to be taken greater than the maximum design cycles in [2].

Note that the HCF damage contribution to the combined fatigue damage should be based on 25 years, even if an extended fatigue design life is required for the HCF calculations.

For $D_{LCF} < 0.25$, the fatigue damage is represented by the HCF damage with the acceptance criteria given as:

$$D_{HCF} \leq 1.0 \quad \text{for } D_{LCF} < 0.25$$

Figure 5 shows the requirements for the combined fatigue damages.

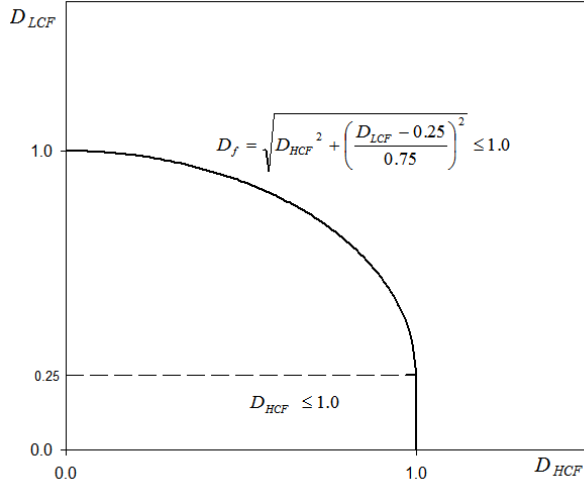


Figure 5 The combined fatigue criteria

8 Example of application

An example of LCF strength assessment of a VLCC is illustrated. Figure 6 shows a hot spot to be checked at an inner bottom longitudinal.

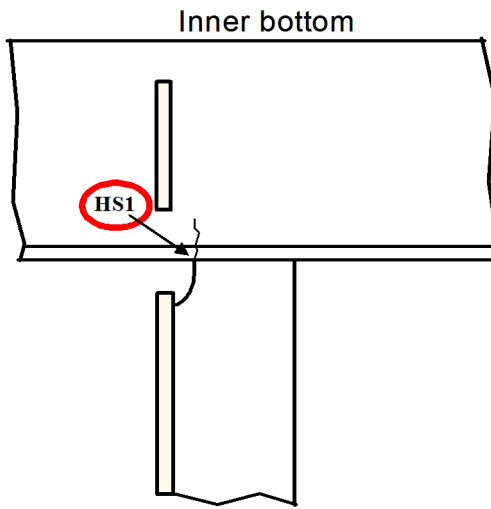


Figure 6 Hot spot to be checked

The design condition and scantlings are given in [Table 11](#).

Table 11 Location to be checked

Item	Requirements	Remark
Design cycle, n_{LCF}	600 cycles	From Table 1
Dimension of longitudinal	$645 \times 12 + 175 \times 20$ mm (T), VL A-E32 steel	Net or gross scantling depending on the rules for the specific ship type

From FE analysis, the assumed hot spot stress components are obtained at HS1 and given in [Table 12](#).

Table 12 Hot spot stress components at HS1, N/mm²

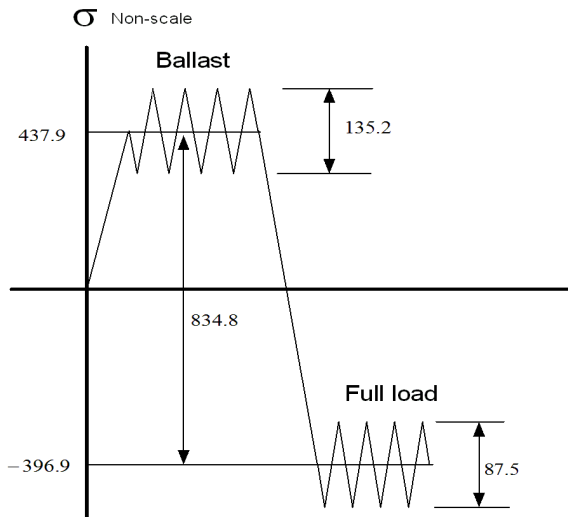
Stress components	Full load	Ballast
Hot spot stress due to still water vertical bending moment	-126.9	126.9
Hot spot stress due to local bending of stiffener	-270	311.0
Total static hot spot stress, σ_s^i	-396.9	437.9
Dynamic stress range at 10^{-2} probability level, σ_{HCF}^i	32.35	50.3
Dynamic stress range due to wave actions, $\Delta\sigma_i$	87.5	135.2

Thus, the stress range for LCF is obtained as given in [Table 13](#).

Table 13 Combined stress range for low cycle fatigue strength assessment, N/mm²

<i>Stress component</i>	<i>Full load-Ballast</i>
Static hot spot stress range for low cycle fatigue, Ds_{LCF}^k	$437.9 - (-396.9) = 834.8$
Combined stress range, Ds_{Comb}^k	$834.8 + 0.5 (87.5 + 135.2) = 946.2$

Figure 7 shows the hot spot stress components from loading and unloading and wave loading.

**Figure 7 Hot spot stress components, N/mm²**

The fatigue damage due to LCF is calculated in Table 14.

Table 14 Low cycle fatigue strength assessment

	<i>Full load-Ballast</i>
Plasticity correction k_e ,	$1.0 \cdot 946.2 \cdot 10^{-3} + 0.53 = 1.48$
Effective pseudo stress range, $\Delta\sigma_{eff}^k$, N/mm ²	$0.8 \cdot 1.48 \cdot 946.2 = 1120.3$
The number of cycles, N_k	$10^{12.164-3\log 1120.3} = 1038$
Damage ratio due to HCF, D_{HCF}	0.24
Damage ratio due to LCF, D_{LCF}	$\frac{600}{1038} = 0.58$

Since the LCF damage is greater than 0.25, a combined damage due to HCF and LCF is calculated as:

$$D_f = \sqrt{D_{HCF}^2 + \left(\frac{D_{LCF} - 0.25}{0.75}\right)^2} = \sqrt{0.24^2 + 0.44^2} = 0.50 \leq 1.0$$

The current detail is acceptable in view of the combined fatigue due to LCF and HCF.

APPENDIX I WAVE INDUCED VIBRATIONS FOR BLUNT VESSELS

1 Introduction

The target vessels for this appendix are blunt vessels as oil tankers, bulk carriers and ore carriers with block coefficient in the order of 0.8 or more.

In fatigue assessment of ship structures, the waves induce

- quasi static stresses in the ship structure, referred to as wave stress
- dynamic vibrations of the hull girder, referred to as vibration stress.

The vibration stress comes from springing (resonance) and whipping (transient), and their relative importance depends on design (flexibility and shape), loading condition (ballast and cargo) and wave condition (speed, sea state and heading).

Springing is caused by linear and non-linear excitation, where the encounter frequency or the sum of two encounter frequencies coincides with the natural frequency of the hull girder. Whipping is caused by non-linear excitation, like wave impact or slamming in the bow flare, stem flare, bottom and stern area. The two phenomena occur more or less continuously and simultaneously and may be difficult to distinguish due to low vibration damping. Therefore, they are commonly referred to as wave induced vibrations from a fatigue consequence point of view.

The governing vibration shape, as shown in [Figure 1](#), is the two-node vertical mode, which is associated with the lowest natural vibration frequency. It is most easily excited and gives the largest vertical bending stress amidships.

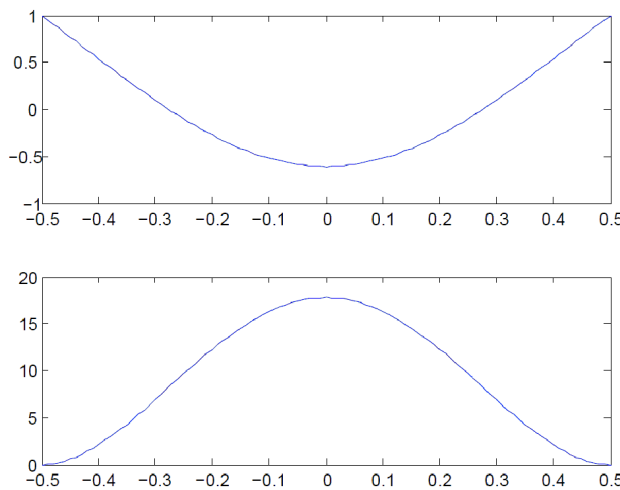


Figure 1 Upper is 2-node vertical bending moment and lower plot is associated vertical bending moment distribution for a normalised homogeneous ship.

The damping is an important parameter, which affects the vibration level of springing and the decay of the springing and whipping in lack of excitation. The damping is low for the governing vibration modes.

The period of the vibration stress (0.25-3 seconds) is an order of magnitude lower than the periods of the wave stress (5-20 seconds). The vibration stress combined with the wave stress makes up a broad band process, and Rainflow counting is then the recognised approach to establish the loading history. First the fatigue damage is calculated for the total stress (wave stress + vibration stress), which defines the total damage. Secondly, the fatigue damage is estimated for the wave stress referred to as the wave damage. The difference between the total and wave damage makes up the vibration damage. In practise it is the vibration on top of the wave frequency loading that makes up the significant part of the vibration damage for ocean

going vessels. The vibration damage has been of comparable magnitude as the wave damage for all full scale measurements and model tests that have been assessed, but the relative magnitude depends on ship type and trade.

2 How to include the effect of vibration

The effect of vibration should be applied to the simplified fatigue assessment.

It is assumed that the vibration stress is put on top of the wave stress from the vertical wave bending moment only. The vertical wave stress to be used in the fatigue assessment is then adjusted by

$$\sigma_v = f_{vib} \cdot \sigma_{vw}$$

where:

f_{vib} = vibration factor, which represents a correction of the wave stress consistent with the additional vibration damage (from whipping and springing) for the intended design area, e.g. North Atlantic or world wide. The correction factor assumes all wave headings of equal probability.

σ_{vw} = denotes the wave stress σ_v from vertical bending moment, which can be derived from the first component of the global hull girder bending stress in Sec.4 [4].

The vibration factor f_{vib} is given as $f_{vib} = f_{vib,j}$ where the subscript j refers to the loading condition j. It can be estimated as:

$$f_{vib,j} = \sqrt[m]{\frac{D_{w,j} + D_{vib,j}}{D_{w,j}}} \geq 1.0$$

where:

$D_{w,j}$ = Wave damage in loading condition j

$D_{vib,j}$ = Vibration damage in loading condition j

m = Inverse slope of the SN-curve consistent with the estimate of the damages.

The ship specific estimate of f_{vib} can replace the same factor in the rules (RU SHIP Pt.3 Ch.4 Sec.4 [3.1.1]).

3 Vibration factor for blunt vessels

Blunt vessels are vessels with high block coefficients like ore carriers. Empirical vibration factor is based mainly on full scale measurement data with some correction from model tests for ships with block coefficient of about 0.8 and with design speeds of about 15 knots. It is supposed to cover a size range from about 170 to 350 meters in length. The correction factor is estimated as:

$$f_{vib,j} = \sqrt[m]{\frac{F_w^4 + F_{vib}^{3.7}}{F_w^4}} \quad (1)$$

where:

$$F_w = 18.5 \cdot 10^{-6} \frac{B(C_B + 0.7)L_{pp}^{1.9}}{Z}$$

- B = Moulded hull breadth (m)
 C_B = Block coefficient at scantling draught
 L_{pp} = Length between perpendiculars (m)
 Z = Hull girder section modulus, gross scantlings (m^3)
 m = 3 for welded material, and 4 for base material assumed protected from corrosive environment.

$$F_{vib,c} = 6.55 \cdot 10^{-7} \frac{R V B (C_B + 0.7) L_{pp}^{1.9}}{(T_c / L_{pp})^{0.2} Z}$$

$$F_{vib,b} = 1.82 \cdot 10^{-7} \frac{R V B (C_B + 0.7) L_{pp}^{1.9}}{(T_b / L_{pp})^{0.6} Z}$$

- R = route factor
= 0.937 for North Atlantic operation
= 1.0 for World Wide operation
 T_i = forward draught, in m, in loading condition i , $i = c$ for cargo and $i = b$ for ballast. It is recommended to use draft related to heavy ballast condition or gale ballast draft.
 V = contract speed at design draft at 85% MCR and 20% sea margin, in knots.

If the contract speed, V_d , is specified at another x% MCR and y% sea margin, it can be converted by the following formula (simplistic)

$$V = 0.891 \cdot V_d \cdot \left(\frac{1+y/100}{x/100} \right)^{1/3}$$

For hatch corners (where $m = 4$ is relevant), the vibration factor is only applied as a correction to wave stress from vertical bending moment.

4 Application of the vibration factor f_{vib}

In the most simplified approach, useful for early design, the f_{vib} is replacing f_{vib} in the rules, related to the downscaling of the wave bending moment to a 10^{-2} probability level of exceedance as shown in [DNVGL-RU-SHIP Pt.3 Ch.4 Sec.4 \[3.1.1\]](#). This implies that the fatigue vertical bending moment is multiplied with f_{vib} .

It is however convenient to utilize the directly calculated vertical wave bending moment towards the forward and aft part of the cargo area. A reduction factor, $f_d(x)$, can be established based on the directly calculated fatigue moment distribution along the hull

$$f_{d,j}(x) = \frac{M_{wv-LC,j}(x)}{\max(M_{wv-LC,j}(x))}$$

where:

$M_{wv-LC,j}$ = Directly calculated wave bending moment for position x from AP for loading condition j . The moment is taken out at a probability level of exceedance of 10^{-2} .

The $f_d(x)$ is applied as a reduction factor to the maximum vertical wave bending moment amidships. It thereby replaces the moment distribution factor f_m in the rules (however f_m may be used in the software, and then this need to be accounted for). The $f_d(x)$, i.e. the normalised bending moment distributions for ballast and cargo condition, is illustrated Figure 2.

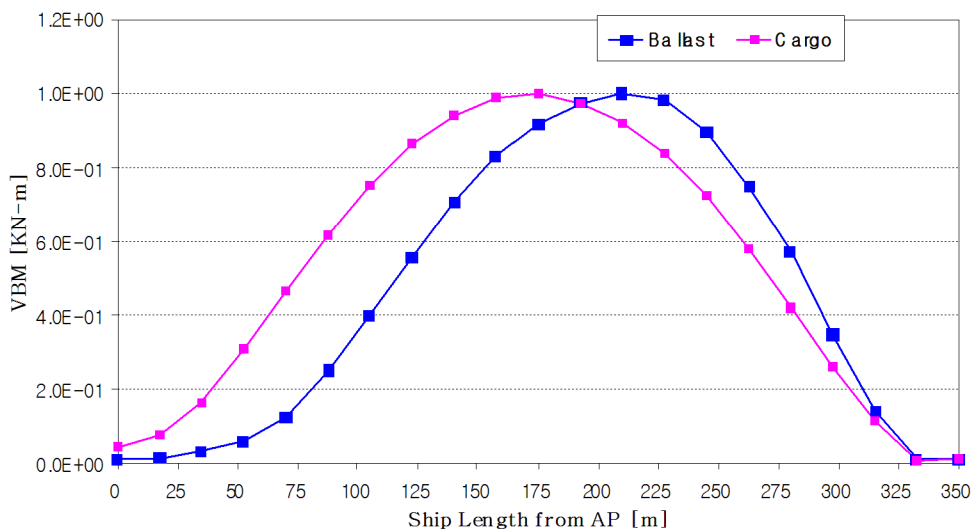


Figure 2 Reduction factor, $f_d(x)$, as a function of length in ballast and cargo condition (an example).

The stress from the vertical bending moment is now calculated as

$$\sigma_v = f_d \cdot f_{vib} \cdot \sigma_{vw}$$

Where σ_{vw} denotes the wave stress σ_v as determined from the first component of the global hull girder bending stress in [4], but where $f_m = 1.0$, consistent with the maximum moments amidships.

5 Effect of the trade

Standard design trades are the North Atlantic or World Wide. If another specific trade is specified by the owner/yard in agreement with the Society, the environmental factor, f_e , can be estimated. This can also be useful if another wave source than global wave statistics should be used or small vessels are intended for harsh design trade, since the relation between World Wide and North Atlantic may differ from large vessels.

The environmental factor f_e is established for the vessel or for a similar vessel by component stochastic fatigue analysis. For convenience it is sufficient to consider only the vertical wave bending moment. The fatigue damage is calculated for the North Atlantic and the actual scatter diagram for a life time of 25 years,

and for both loading conditions (as the route specific scatter diagram may also differ for the two loading conditions due to sailing restrictions). This gives the following damages:

- $D_{b,a}$ = Damage for ballast condition in actual trade
- $D_{c,a}$ = Damage for cargo condition in actual trade
- $D_{b,WW}$ = Damage for ballast condition in North Atlantic
- $D_{c,WW}$ = Damage for cargo condition in North Atlantic.

The part time in the different conditions is denoted α_j , where $j = b$ for ballast and $j = c$ for cargo. The part time is taken from the rules or as specified. The environmental factor is estimated in the following principle way:

$$f_e = \left(\frac{D_{b,a} \cdot \alpha_b + D_{c,a} \cdot \alpha_c}{D_{b,NA} \cdot \alpha_b + D_{c,NA} \cdot \alpha_c} \right)^{\frac{1}{m}}$$

Where m can be taken as 3, and represents most of the fatigue sensitive welded details.

6 Model tests procedure

While empirical relations are useful in early design, the most accurate way of establishing f_{vib} , is by model tests. This assumes that the state-of-the-art procedure is followed.

Another benefit of model tests is that the vibration factor f_{vib} can be estimated along the vessel, while the empirical relations assume a constant value in the cargo area.

In agreement with the owner/yard, the model test procedure should be submitted for approval.

7 Numerical calculation procedure

Numerical analysis can replace model tests. It is regarded less accurate than model tests, but can still be a useful alternative in order to estimate ship specific f_{vib} factors. This assumes that the state-of-the-art procedure is followed and that the numerical tool is tuned for the particular vessel design.

The state-of-the-art hydroelastic tools today are regarded more useful for container vessels with dominating whipping impacts than blunt vessels with dominating non-linear springing excitation.

In agreement with the owner/yard, the model test procedure should be submitted for approval.

8 Full scale measurements.

The uncertainties in the encountered wave environment in different trades are considerable in model tests and numerical analysis. Full scale measurements of similar ships on similar trades can also be basis for estimation of f_{vib} factors for sister vessels or future similar designs.

The full scale measurements for obtaining useful data in decision support should preferably be carried out using approved hull monitoring system according to the rules for Hull monitoring systems (class notation **HMON**). Systems approved according to 2005 revision or later include fatigue and extreme loading with and without the effect of vibration included, but it should also be ensured that measured raw and statistical data is stored and can be submitted to shore for further assessment.

In agreement with the owner/yard, the documentation should be submitted for approval.

APPENDIX J CONSIDERATIONS OF SPECIAL DETAILS

1 Crane foundations and foundations for heavy top side loads

1.1 Introduction

Crane foundations, permanent foundations for top side equipment and preliminary foundations for cargo are integrated into to the hull structure. The foundations may be exposed to high loads from the top side equipment and cargo, but also to hull girder wave loads. When these foundations are located close to midship, the nominal stress from the hull girder wave loads in way of the foundation may be significant. If the foundation is not designed with due consideration to the risk of fatigue damage, cracks may appear in operation.

It may be sufficient to consider the fatigue damage from the top side loads and the hull girder wave loads separately, but for some designs it is necessary to assess the combined effect of the two main load effects. For cranes, the specific operation of the crane may also need to be considered, and for optimized designs even low cycle fatigue assessment may be necessary. This is however regarded as outside the scope of the hull girder fatigue assessment and subject to requirements for lifting appliances.

A brief guidance is given in the following.

1.2 Fatigue assessment based on wave induced loads

The support details exposed to longitudinal (axial) stresses from the global hull girder loads should be considered.

For support details located in the shadow zone from global hull girder loads, aft or forward of large deck openings, fatigue assessment based on hull girder wave loads may be neglected.

Unless the support details are covered by standard details in App.A, the support details should be assessed by FE analysis using the hot spot stress approach.

For the foundations, nominal stress level for the top side loads at the deck level should be estimated based on inertia loads caused by ship motions. When the largest dynamic vertical nominal stress exceed

- the dynamic nominal longitudinal stress at the deck corner, even though the foundation is located in the shadow zone, the foundation should be assessed by FE analysis due to the top side loads
- half the dynamic nominal longitudinal stress at the deck level where the foundation is located, the interaction between the longitudinal hull girder stress and the vertical stress from the top side loads should be considered. The loads should be assumed to be simultaneously acting.

If the vertical dynamic nominal stress is less or equal to half of the longitudinal stress from the hull girder wave loads at deck corner, the foundation can be assessed as if the top side loads are not present.

Both the top side loads and the hull girder wave loads should be based on the same probability level of exceedance (10^{-2}). If the top side loads can vary due to different possible arrangements, the most unfavourable realistic arrangement should serve as basis for the estimate of the vertical nominal stress.

CHANGES – HISTORIC

October 2015 edition

This is a new document.

About DNV GL

Driven by our purpose of safeguarding life, property and the environment, DNV GL enables organizations to advance the safety and sustainability of their business. We provide classification, technical assurance, software and independent expert advisory services to the maritime, oil & gas and energy industries. We also provide certification services to customers across a wide range of industries. Operating in more than 100 countries, our experts are dedicated to helping our customers make the world safer, smarter and greener.